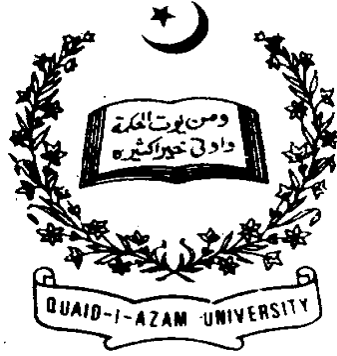


Interaction of heat transfer and variable viscosity with peristaltic motion



By

Fahad Munir Abbasi

**Department of Mathematics
Quaid-i-Azam University
Islamabad, Pakistan
2014**

Interaction of heat transfer and variable viscosity with peristaltic motion



By

Fahad Munir Abbasi

Supervised By

Prof. Dr. Tasawar Hayat

Department of Mathematics
Quaid-i-Azam University
Islamabad, Pakistan
2014

Interaction of heat transfer and variable viscosity with peristaltic motion



By

Fahad Munir Abbasi

A THESIS SUBMITTED IN THE PARTIAL FULFILLMENT OF THE REQUIREMENT
FOR THE DEGREE OF
DOCTOR OF PHILOSOPHY
IN
MATHEMATICS

Supervised By

Prof. Dr. Tasawar Hayat

Department of Mathematics
Quaid-i-Azam University
Islamabad, Pakistan
2014

Interaction of heat transfer and variable viscosity with peristaltic motion

By

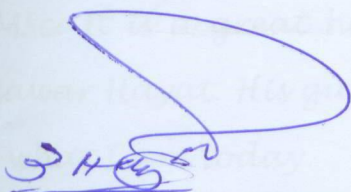
Fahad Munir Abbasi

CERTIFICATE

A THESIS SUBMITTED IN THE PARTIAL FULFILLMENT OF THE
REQUIREMENTS FOR THE DEGREE OF THE DOCTOR OF
PHILOSOPHY

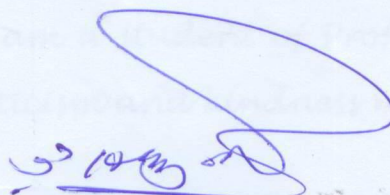
We accept this dissertation as conforming to the required standard

1.



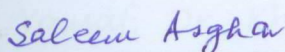
Prof. Dr. Tasawar Hayat
(Supervisor)

2.



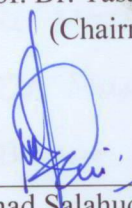
Prof. Dr. Tasawar Hayat
(Chairman)

3.



Prof. Dr. Saleem Asghar
(External Examiner)

4.



Dr. Muhammad Salahuddin
(External Examiner)

Department of Mathematics
Quaid-i-Azam University
Islamabad, Pakistan
2014

Acknowledgement

Allah Almighty, the merciful, the beneficent, the praise-worthy, has given me the strength to complete this thesis. The sense of He being with me has been the sole reason of my strength throughout the time of hardships. O my Lord I can never thank you for what you have blessed me with. Countless Darood O Salam for the "Most Praised One" (P.B.U.H), mercy for all the worlds, his off springs and his companions.

My love and respect for Prof. Dr. Tasawar Hayat is beyond the grasp of words. He has been a great inspiration for me right from day one of MSc. It is a great honor for me that I am a student of Prof. Dr. Tasawar Hayat. His guidance, creative criticism and kindness made me what I am today.

I am grateful to all my teachers in Q.A.U Math department, particularly Dr. M. Ayub, Dr. Sohail Nadeem, Dr. Masood Khan, Dr. M. Yousaf, Dr. Khalid Saif ullah and Dr. Babur Majeed. I am thankful to Mr. Safdar, Mr. Bilal, Mr. Zahoor, Mr. Sheraaz, Mr. Sajid and all others for their cooperation throughout my tenure in this department.

I also acknowledge the Higher Education Commission (H.E.C) of Pakistan for their financial support through PhD Indigenous program.

What I actually want to say about my family perhaps can't be said. Continuous struggle and untiring hard work of my father Mr. Gul Munir Abbasi is the prime reason behind every success I had. It is a greatest blessing of Almighty to have a father like him. Throughout his life he stood up and battled through hardships with pride and honor. I always wish I can be like him, the most hard working man I have ever seen in my life, a man full of honor and pride. I never said so but I Love you, you are my proud and I can do anything for a single smile of yours. For my mother, I only can say, Maa g, main kuch na hota agr main roz ap k paon na choomta. Ap ko bhi pata hai k how much I love u, ap jaan ho mere, mere zindagi ho. My brother, Farhan (fani) (he is more a friend to me than a brother) is another precious gift Almighty has blessed me with. He is the love of my life. Special thanks to my sisters as their care, love and prayers played key role in my success. Lots of love for Moon, Areeba and my little angels Aarsal and Salaar.

This PhD started with a phone call from Sabir Ali (Dr. S. A. Shehzad) on a hazy morning of December 2011. From then onwards it has been a pleasure to have him as a friend of mine. Sabir Ali has always been helpful to me during research. Bilal (Dr. M. B. Ashraf) has been with me from past 10 years. He has always given me strength and motivation. Shani (Dr. Zeeshan Asghar) is a vital part of our company. The love and respect he gave me is unforgettable. Hasan Shah (shah saab) and Adnan Bhai (Peer saab) are two most beautiful persons I have ever known. I have enjoyed every minute of their company. I pay special gratitude to all other friends of mine,

Shehzad, Babar, Zafar, Atif, Malik Shehzad, Rashid, Danish, Riazwan, Tayyab, Waqar, Afzal and Farrukh. I also want to acknowledge my seniors, Dr. Qasim, Dr. Nawaz, Dr. Zahid, Dr. Rahila, Dr. Awaiz, Dr. Mariyam and Nazim bhai for the guidance they provided me. I am thankful to my juniors Waqar, Waqas, Farooq, Zahid, Imdad, Anum Shafique, Sadia Asad, Humaira Yasmin and all others for the respect they gave me.

At the end, I would like to pay my gratitude to all others whose names are not mentioned above and have prayed for my success.

Fahad Munir Abbasi

August 7, 2014

Preface

It is commonly accepted now that peristaltic flows are caused by the propagation of waves along the flexible boundaries of channel or tube. Such flows in physiology are represented by food movement in the digestive tract, urine transport from kidney to bladder, semen movement in vas deferens, movement of lymphatic fluids in lymph vessels, bile flow from the gall bladder into the duodenum, vasomotion of blood cells, movement of ovum in the female fallopian tube, transport of spermatozoa in the ductus efferents etc. Peristaltic motion in the industrial applications are employed in the transport of corrosive and noxious fluids, roller and finger pumps, hose pumps, tube pumps, dialysis machines and heart-lung machines. The concept of heat transfer has key role in the analysis of tissues, hemodialysis and oxygenation. The recent progress in the application of heat (hyperthermia), radiation (laser therapy) and coldness (cryosurgery), as means to destroy undesirable tissues including cancer have stimulated much interest in mathematical modeling for properties of tissue. Moreover, radiofrequency therapy has significance in the treatment of diseases like tissue coagulation, the liver cancer, the lung cancer and reflux of stomach acid. Moreover the energy flux is not only induced due to temperature gradient but by compositions gradient as well. Phenomena of heat and mass transfer taking place simultaneously can perturb each other's efficiency by producing the Soret and Dufour effects. Such effects are especially significant in chemical engineering and geosciences. Specifically the Soret effect is useful for isotope separation and in mixtures between gases having light and medium molecular weights, the Dufour effect is very significant. The concept of variable viscosity of fluid is now very well recognized. Some of the processes in which viscosity of the fluids depends on temperature include nuclear power plants, pumps operated at high temperatures, in turbines, rockets, missile technologies and space vehicles. Even in blood, the

living ingredient for animals is very sensitive to temperature changes and slight change in temperature may cause irreversible damage during dialysis or in heart lung machines. Magnetohydrodynamic (MHD) flow in channels/tubes has wide applications in purification of crude oil, petroleum industry, fluid droplets sprays, electrostatic precipitation, designing cooling systems, magnetic resonance imaging (MRI), blood pumps etc. Inability of the Newtonian fluid model to predict the viscoelastic behavior of several fluids in industry and physiology lead to the development of several non-Newtonian models. Third order fluid model is one of such models which can easily describe both the shear thickening and shear thinning properties even in the steady flows. The present thesis in view of afore mentioned facts is arranged as follows:

Review of available literature on peristalsis under various flow configurations is included in Chapter one. The fundamental equations are also presented here. The MHD mixed convection peristaltic flow with variable viscosity and thermal conductivity is analyzed in chapter two. Joule heating effect here is also taken into account. Viscosity and thermal conductivity of fluid vary linearly with temperature. Resulting nonlinear system is solved numerically. Velocity, pressure gradient, temperature and streamlines are examined through graphs. Numerical values of heat transfer rate at the wall are computed and analyzed for variation in certain embedded parameters. The main observations of this chapter are summarized at the end of chapter. Material of this chapter is accepted for publication in **“Sains Malaysiana”**.

Hydromagnetic peristaltic transport of fluid with variable viscosity is studied in chapter three. Here fluid fills the porous space in a channel. Heat transfer analysis is carried out in the presence of viscous dissipation and Joule heating. Viscosity of the fluid is taken temperature dependent. Both channel and magnetic field have the inclined considerations. The resulting problems are solved numerically. A parametric study is performed to predict the impact of embedded

variables. Results of this chapter are compiled in the Key findings of this chapter. The main observations of this chapter have been submitted for publication in **Journal of Mechanical Engineering Science**.

Impact of convective boundary conditions on the peristaltic transport in an asymmetric channel is examined in chapter four. Joule heating effect is included in the analysis of heat transfer. Cases of hydrodynamic and magnetohydrodynamic (MHD) fluids are considered separately. Analytic solutions for stream function and temperature are constructed. Numerical integration is carried out for pressure rise per wavelength. Effects of influential flow parameters are pointed out through graphs. Findings of this study are accepted for publication in **Journal of Central South University, 21 (2014) 1411-1416**”.

Simultaneous effects of heat and mass transfer on the peristaltic transport of viscous fluid are examined in chapter five. The channel is assumed to be axially symmetric. Soret and Dufour effects along with Ohmic heating are considered. Closed form solutions for temperature and concentration are analyzed by plots for variation of embedded parameters. Numerical values of heat and mass transfer rates at the wall are also tabulated. Material of this study is published in **Magnetohydrodynamics, 47 (2011) 295-302**.

Effects of heat and mass transfer on the peristaltic transport of variable viscosity fluid are studied in chapter six. The fluid viscosity is considered space dependent. Thermo-diffusion and diffusion-thermo effects are taken into account. Series solutions for the nonlinear equations are obtained using the perturbation technique. Results for the stream function, temperature and concentration are constructed. The variations of sundry parameters are analyzed. Results of this chapter are published in **Applied Mathematics and Information Sciences, 8 (2014) 211-219**.

Influences of velocity, thermal and concentration slips on the peristaltic transport in an asymmetric channel are analyzed in chapter seven. Fluid is electrically conducting under the effect of a constant applied magnetic field. Soret, Dufour and Joule heating effects are taken into account. Close form solutions for stream function, temperature, concentration and heat transfer coefficient are obtained. Plots of physical quantities of interest are given and explored. Research presented in this chapter is accepted for publication in **Arabian Journal for Science and Engineering**, 39 (2014) 4341–4349.

MHD mixed convective peristaltic transport in a vertical channel is studied in chapter eight. Simultaneous effects of heat and mass transfer for peristaltic transport of viscous fluid are addressed in presence of Joule heating and Soret and Dufour effects. Perturbation solution is prepared for small Brinkman number. Flow quantities of interest are plotted and analyzed. Material of this chapter is accepted for publication in **Applied Mechanics and Technical Physics**.

Mixed convective heat and mass transfer analysis for peristaltic transport in an asymmetric channel has been carried out in chapter nine. Mathematical modeling and analysis is presented in presence of Soret and Dufour effects. The convective conditions for both temperature and concentration are used in the analysis of heat and mass transfer. Resulting problems are solved for the series solutions. Numerical values of heat and mass transfer rates are displayed and studied. Main observations of this chapter are accepted for publication in **Journal of Central South University**.

The effect of variable viscosity on the peristaltic motion of MHD third order fluid in a channel is studied in chapter ten. Mathematical formulation includes the concept of slip condition. Both the governing equations and boundary conditions are nonlinear even after long wavelength and low

Reynolds number assumptions. The series solutions of stream function, longitudinal velocity and pressure gradient are first derived and then discussed in detail. The pressure rise and frictional forces are monitored through numerical integration. This material is published in **International Journal for Numerical Methods in Fluids**, 67 (2011) 1500-1515.

Heat transfer analysis for the peristaltic transport of third order fluid is carried out in chapter eleven. Viscosity of third order fluid is considered space dependent. The fluid is electrically conducting in the presence of uniform applied magnetic field. Analysis is performed when no-slip condition at the boundaries does not hold. The velocity and thermal slip effects are thus taken into account. Perturbation solution is discussed and a comparative study between the cases of constant and variable viscosities is presented and analyzed. The observations of this study are published in **Chinese Physics Letters**, 28 (2011) 044701.

Soret and Dufour effects on peristaltic transport of third order fluid in a symmetric channel are reported in chapter twelve. Joule heating effect is also taken in to account. The governing nonlinear problem is solved using perturbation approach. Graphical results are reported and discussed for various parameters of interest entering into the problem. Findings of this chapter are accepted for publication in **Heat Transfer Research**, 45 (2014) 589-603.

Contents

1	Introduction	4
1.1	Peristaltic transport	4
1.2	Literature review	4
1.3	Fundamental laws	9
1.3.1	Law of conservation of mass	9
1.3.2	Law of conservation of linear momentum	9
1.3.3	First law of thermodynamics	10
1.3.4	Advection diffusion equation	11
1.3.5	Dufour and Soret effects	11
1.3.6	Maxwell's equations	11
1.4	Constitutive equations of a third order fluid	12
2	MHD mixed convection peristaltic flow with variable viscosity and thermal conductivity	13
2.1	Mathematical formulation	13
2.2	Heat transfer analysis	17
2.3	Graphical analysis	18
2.4	Main points	20
3	Hydromagnetic peristaltic transport of variable viscosity fluid with heat transfer and porous medium	29
3.1	Mathematical analysis	29
3.2	Solution and analysis	34

3.3	Key findings	35
4	Peristaltic flow in an asymmetric channel with convective boundary conditions and Joule heating	48
4.1	Mathematical analysis	48
4.2	Solution expressions	52
4.3	Graphical analysis	54
4.4	Concluding remarks	55
5	Peristaltic motion with Soret and Dufour effects	61
5.1	Mathematical analysis	61
5.2	Solutions expressions	64
5.3	Discussion	65
6	Soret and Dufour effects on peristaltic transport of MHD fluid with variable viscosity	72
6.1	Mathematical analysis	72
6.2	Discussion	77
7	Soret and Dufour effects on peristaltic flow in an asymmetric channel	87
7.1	Mathematical analysis	87
7.2	Discussion	90
7.3	Main points	91
8	Peristaltic transport in a vertical channel subject to Soret and Dufour effects	99
8.1	Mathematical formulation	99
8.2	Series expressions	103
8.3	Graphical results and analysis	107
9	Mixed convective heat and mass transfer for peristaltic transport in an asymmetric channel with Soret and Dufour effects	119
9.1	Mathematical analysis	119
9.2	Solution of the problem	123

9.3 Graphical analysis	125
10 Variable viscosity effects on the peristaltic motion of a third-order fluid	134
10.1 Governing problem	134
10.2 Series expressions	138
10.3 Results and discussion	143
11 Heat transfer analysis for peristaltic mechanism in variable viscosity fluid	157
11.1 Statement of the problem	157
11.2 Solution expressions	159
11.3 Graphical analysis and key points	162
12 Soret and Dufour effects on peristaltic transport of a third order fluid	167
12.1 Mathematical formulation	167
12.2 Solution expressions	171
12.3 Discussion	174

Chapter 1

Introduction

The aim of this chapter is to provide a material for the better understanding of the subsequent chapters. Here the literature review about peristaltic flows, and some definitions and fundamental equations are presented.

1.1 Peristaltic transport

The peristaltic transport of fluid is caused by a progressive wave of area contraction/expansion travelling along the length of a distensible tube. Such wave in turn propels the fluid in the direction of propagation of wave. This type of transport mechanism finds its application in the physiological and industrial processes. These include the locomotion of worms, urine passage from kidney to bladder, food swallowing by the esophagus, vasomotion of small blood vessels, sanitary and corrosive fluids transport, movement of bio fluids (chyme in gastrointestinal tract, bile in the bile duct, ovum in the fallopian tube and spermatozoa in cervical canal), in heart lung machine and roller and finger pumps.

1.2 Literature review

Despite of the fact that the mechanism of peristalsis was known to the physiologist since long, mechanical analysis of peristalsis begin in later half of the twentieth century. Initial investigation of peristaltic pumping was inspired by its application in human ureter system. Studies of

Kiil [1] and Boyarsky [2] are fundamentals in this direction. Latham [3] in his MS thesis carried out the experimental investigation of peristaltic pump. Shapiro [4] discussed the inertia free two-dimensional peristaltic transport when the wavelength of peristaltic wave is large compared to the half channel width. Under these assumptions there is a steady flow in a wave frame. Later on these two considerations (the long wavelength and low Reynolds number approximation) were widely utilized by the researchers in the analysis of peristaltic flows. The theoretical investigation of Shapiro [4] was found in good agreement with the experimental work of Latham [3]. These pioneering studies of Latham [3] and Shapiro [4] were first precise efforts to mechanically investigate peristaltic flows and triggered extensive interest in peristaltic flows. Later on several investigations were made to study peristaltic flows under different flow configurations. More realistic models for the ureteral waves were proposed by Lykoudis [5] and Weinberg et al. [6]. Time elapsed during the chyme motion through small intestine was calculated by Barton and Raynor [7] using the concept of peristaltic motion. Inertia free peristaltic flow in a roller pump was studied by Maginniss [8]. Shapiro et al. [9] examined the peristaltic flow of Newtonian fluid in a planar channel and circular tube. Long wavelength and low Reynolds number approximations were used in this investigation. In continuation Jaffrin [10] studied the effects of inertia and streamline curvature on peristaltic pumping. Yin and Fung [11] and Fung and Yih [12] studied the peristaltic flow for arbitrary Reynolds and wave numbers in axisymmetric tube and planar channel respectively. In these studies the authors performed the analysis for small amplitude ratio. Jaffrin and Shapiro [13] made review for studies available on peristaltic pumping. Mittra and Prasad [14] studied the interaction of peristalsis with poiseuille flow. Wilson and Perel [15] analyzed the interaction of peristalsis with pulsatile flow. Brown and Hung [16] compiled the computational and experimental investigations on two-dimensional peristaltic flows up to 1977. Srivastava and Srivastava [17] discussed the interaction of peristalsis with pulsatile flow in a cylindrical tube by assuming that the flow is generated by an arbitrary pressure gradient and peristaltic waves. Peristaltic transport of blood was seen by Srivastava and Srivastava [18]. In this study they used the Casson fluid model to describe the non-Newtonian properties of blood. Numerical solutions of two-dimensional peristaltic flow problem were obtained by Takabatake and Ayukawa [19]. Takabatake et al. [20] studied the peristaltic pumping in circular cylindrical tubes. They obtained the numerical solutions of the

problem and discussed the efficiency of such flow. Fluid mechanics of gastrointestinal tract was studied by Mishra and Rao [21]. They considered the peristaltic transport in a channel with porous peripheral layer analogous to the flow in gastrointestinal tract.

The magnetohydrodynamic character of fluid has a pivotal role in solidification processes of metals and metal alloys, study of nuclear fuel debris, control of underground spreading of chemical wastes and pollution control, design of MHD power generators, blood pump machines, diagnose and treatment of cancer tumors. Interaction of peristaltic flow with pulsatile magneto-fluid through a porous medium was analyzed by Afifi and Gad [22]. Elshehawey et al. [23] examined the effects of inclined magnetic field on magneto fluid flow between two inclined wavy plates. In this study they further assumed the boundaries to be porous. Peristaltic flow of blood through a non-uniform channel was inspected by Mekheimer [24]. Blood was assumed to flow under the influence of a uniform applied magnetic field. Mekheimer [25] carried out the study of magnetohydrodynamic nonlinear peristaltic transport in an inclined planar channel. Magnetic fluid model induced by peristaltic waves was proposed by Siddiqui et al. [26]. Hayat and Ali [27] investigated the peristaltically induced motion of MHD third grade fluid in a deformable tube. Abd El Naby et al. [28] analyzed the effects of magnetic field on trapping while studying peristaltic motion of a generalized Newtonian fluid. Nonlinear peristaltic transport in a planar channel under the influence of applied magnetic field was studied by Hayat et al. [29]. Hayat and Ali [30] provided the mathematical description of peristaltic hydromagnetic flow in a tube. Effect of applied magnetic field on the peristaltic transport of micropolar fluid was discussed by Wang et al. [31]. Hayat et al. [32] studied the influence of inclined magnetic field on peristaltic transport of fourth grade fluid in an inclined asymmetric channel.

In several physical situations, the no-slip condition between the fluid and solid boundary is not valid. Such situation arises in fluid mechanics within the body of living beings where the internal linings of the tubular organs are coated with mucus/secretions. Also in the case of artificial heart the no-slip condition is no longer effective. In such situations one may take into account the slip effects while analyzing the flow phenomena. Mandiwilla and Archer [33] inspected the effects of velocity slip on the peristaltic pumping in a rectangular channel. Hayat et al. [34] studied the peristaltic transport through a porous medium under the influence of partial slip. Hayat et al. [35] studied the peristaltic transport with simultaneous effects of

heat transfer and velocity slip. Effects of partial slip and heat transfer on the peristaltic flow of MHD Newtonian fluid in an asymmetric channel were examined by Yildirim and Sezer [36]. Kumari and Radhakrishnamacharya [37] studied the effects of slip on heat transfer for peristaltic transport in the presence of magnetic field.

Processes that take place at high temperature e.g. in nuclear reactors, turbines, rockets, missile technologies, pumps operated at high temperatures and space vehicles may face variation in fluid viscosity with temperature. Moreover the dependence of fluid viscosity is justified physiologically because normal person or animal of similar size takes 1-2L of the fluid every day. Also 6-7L of the fluid is received by the small intestine as secretions from salivary glands, stomach, pancreas, liver and small intestine itself. Ali et al. [38] carried out the study to examine the influence of velocity slip on the peristaltic transport in a planar channel. Fluid viscosity was assumed to be space dependent and a uniform magnetic field was also taken into account. El Naby et al. [39] studied the effects of an endoscope and variable viscosity on peristaltic motion. Elshehawey and Gharseldien [40] examined the peristaltic transport of three-layered flow with variable viscosity. Hayat and Ali [41] examined the effect of variable viscosity on the peristaltic transport of Newtonian fluid in an asymmetric channel. Ebaid [42] computed numerical solution for the MHD peristaltic flow of bio-fluid with variable viscosity in a circular cylindrical tube via Adomian decomposition method. Effects of heat transfer on the MHD peristaltic transport of a variable viscosity fluid were studied by Nadeem and Akbar [43]. The fluid viscosity in this study was considered to vary linearly with temperature and Adomian decomposition Method (ADM) was used to obtain the solution of the coupled equations. Nadeem et al. [44] discussed the influence of heat transfer on the peristaltic transport of fluid with variable viscosity. Nadeem and Akbar [45] presented the study for the effects of temperature dependent viscosity on peristaltic flow of Jeffrey-six constant fluid in a non-uniform vertical tube. Nadeem and Akbar [46] examined the influence of temperature dependent viscosity on peristaltic transport of a Newtonian fluid.

The concept of heat transfer has a key role in the analysis of tissues, hemodialysis and oxygenation. Radhakrishnamacharya and Murty [47] studied influence of heat transfer on peristaltic transport in a non-uniform channel. Vajravelu et al [48] performed the heat transfer analysis of the peristaltic transport in a vertical porous annulus under the long wavelength consideration.

Simultaneous effects of heat transfer and applied magnetic field on the peristaltic transport in a vertical annulus were studied by Mekheimer and Elmaboud [49]. Srinivas and Kothandapani [50] examined the peristaltic transport in an asymmetric channel with heat transfer. Hayat et al. [51] performed the heat transfer analysis for the peristaltic transport of an electrically conducting fluid in porous space. Srinivas and Kothandapani [52] studied the impact of heat and mass transfer on the MHD peristaltic motion with compliant walls. Hayat and Hina [53] investigated the heat and mass transfer effects on the peristaltic motion of Maxwell fluid. Mekheimer et al. [54] analyzed the peristaltic transport under the influence of heat transfer and space porosity. Nadeem and Akbar [55] analyzed the effect of radially varying MHD on the peristaltic flow in an annulus with heat and mass transfer. Ali et al. [56] studied the heat transfer effect on peristaltic transport in a curved channel. Hayat and Noreen [57] examined the peristaltic transport of fourth grade fluid with heat transfer and induced magnetic field. Effects of thermal radiation and space porosity on MHD mixed convection flow in a vertical channel were analyzed by Srinivas and Muthuraj [58]. Vajravelu et al. [59] discussed the influence of heat transfer on peristaltic transport of Jeffrey fluid in a vertical porous stratum. Hayat et al. [60] analyzed the heat transfer effects on the peristaltic transport in a curved channel with compliant walls. Mixed convection heat and mass transfer in an asymmetric channel with peristalsis was discussed by Srinivas et al. [61]. Effects of heat and mass transfer on the peristaltic flow of Johnson Segalman fluid in a vertical asymmetric channel with induced MHD was examined by Nadeem and Akbar [62]. Tripathi [63] proposed a mathematical model for swallowing of food bolus through the oesophagus under the influence of heat transfer. Akbar et al. [64] computed the effects of heat and mass transfer on the peristaltic transport of hyperbolic tangent fluid. Akbar and Nadeem [65] investigated the heat and mass transfer effects in the peristaltic transport of Johnson-Segalman fluid. Effects of induced magnetic field were also taken into account in this study. Effects of induced magnetic field and heat transfer on peristaltic transport were also discussed by Hayat et al. [66]. This study was performed for the Carreau fluid model. Peristaltic transport of third order fluid under the effect of applied magnetic field was studied by Hayat et al. [67]. Hayat et al. [68] also analyzed the peristaltic flow of a third order fluid in an asymmetric channel with slip effects. Heat and mass transfer analysis for the peristaltic transport of third order fluid in a diverging tube was carried out by Nadeem et al. [69]. Akbar

et al. [70] studied the effects of slip and heat transfer on the peristaltic flow of third order fluid in an inclined asymmetric channel.

1.3 Fundamental laws

1.3.1 Law of conservation of mass

Mathematical form of law of conservation of mass is known as continuity equation which for unsteady flow is given by

$$\frac{\partial \rho}{\partial t} + \nabla \cdot (\rho \mathbf{V}) = 0, \quad (1.1)$$

in which ρ denotes the density of the fluid and \mathbf{V} the velocity. Eq. (1.1) for an incompressible fluid is

$$\nabla \cdot \mathbf{V} = 0. \quad (1.2)$$

1.3.2 Law of conservation of linear momentum

Newton's second law of motion states that time rate of change of linear momentum is equal to the total force acting on the fluid element. Mathematically it is expressed as

$$\rho \frac{d\mathbf{V}}{dt} = \nabla \cdot \boldsymbol{\tau} + \rho \mathbf{b}, \quad (1.3)$$

for an incompressible flow. Here $\boldsymbol{\tau}$ is the Cauchy stress tensor which is different for different fluids, $\nabla \cdot \boldsymbol{\tau}$ the surface force and $\rho \mathbf{b}$ the body force. The body force $\rho \mathbf{b}$ is different for different flow situations. For instance the expression of body force $\rho \mathbf{b}$ for the flow of an electrically conducting fluid in the presence of magnetic field and buoyancy effects is

$$\rho \mathbf{b} = \rho \mathbf{g} [\beta_T (T - T_0) + \beta_c (C - C_0)] + \mathbf{J} \times \mathbf{B} \quad (1.4)$$

where \mathbf{g} is the gravitational acceleration, T and T_0 the temperatures of fluid and boundary respectively, C and C_0 the concentrations of fluid and boundary respectively, β_T and β_c the

volumetric expansion coefficients, \mathbf{J} the current density and \mathbf{B} the applied magnetic field. Furthermore first two terms on the right hand side of Eq. (1.4) represent the body force due to density differences caused by temperature difference and composition difference. The last term of Eq. (1.4) is the Lorentz force.

The Cauchy stress tensor $\boldsymbol{\tau}$ is expressed as

$$\boldsymbol{\tau} = \begin{bmatrix} \sigma_{xx} & \tau_{xy} & \tau_{xz} \\ \tau_{yx} & \sigma_{yy} & \tau_{yz} \\ \tau_{zx} & \tau_{zy} & \sigma_{zz} \end{bmatrix} \text{ or } \boldsymbol{\tau} = \begin{bmatrix} \sigma_{rr} & \tau_{r\theta} & \tau_{rz} \\ \tau_{\theta r} & \sigma_{\theta\theta} & \tau_{\theta z} \\ \tau_{zr} & \tau_{z\theta} & \sigma_{zz} \end{bmatrix}, \quad (1.5)$$

where σ_{xx} (σ_{rr}), σ_{yy} ($\sigma_{\theta\theta}$) and σ_{zz} are the normal stresses while all others are shear stresses.

In cartesian coordinates (x, y, z) Eq. (1.3) can be written as

$$\rho \left(\frac{\partial u}{\partial t} + u \frac{\partial u}{\partial x} + v \frac{\partial u}{\partial y} + w \frac{\partial u}{\partial z} \right) = \frac{\partial (\sigma_{xx})}{\partial x} + \frac{\partial (\tau_{xy})}{\partial y} + \frac{\partial (\tau_{xz})}{\partial z} + \rho b_x, \quad (1.6)$$

$$\rho \left(\frac{\partial v}{\partial t} + u \frac{\partial v}{\partial x} + v \frac{\partial v}{\partial y} + w \frac{\partial v}{\partial z} \right) = \frac{\partial (\tau_{yx})}{\partial x} + \frac{\partial (\sigma_{yy})}{\partial y} + \frac{\partial (\tau_{yz})}{\partial z} + \rho b_y, \quad (1.7)$$

$$\rho \left(\frac{\partial w}{\partial t} + u \frac{\partial w}{\partial x} + v \frac{\partial w}{\partial y} + w \frac{\partial w}{\partial z} \right) = \frac{\partial (\tau_{zx})}{\partial x} + \frac{\partial (\tau_{zy})}{\partial y} + \frac{\partial (\sigma_{zz})}{\partial z} + \rho b_z. \quad (1.8)$$

1.3.3 First law of thermodynamics

The law of conservation of energy is also known as first law of thermodynamics and can be expressed as

$$\rho \frac{d(C_p T)}{dt} = \boldsymbol{\tau} \cdot \nabla \mathbf{V} - \nabla \cdot (-K \nabla T) + \frac{1}{\sigma} \mathbf{J} \cdot \mathbf{J}. \quad (1.9)$$

Here C_p is the internal energy, $\boldsymbol{\tau} \cdot \nabla \mathbf{V}$ the viscous dissipation, $K \nabla T$ the heat flux, T the temperature field, C_p the specific heat, σ the electrical conductivity of fluid, K the thermal conductivity, D the diffusion coefficient and the last term on RHS of Eq. (1.9) is due to the Joule heating.

1.3.4 Advection diffusion equation

The diffusion of chemically reacting species is governed by Fick's second law. It is given by

$$\frac{dC}{dt} = D\nabla^2 C - K_n(C - C_0)^n, \quad (1.10)$$

where C is the concentration field of the diffusing species, n the order of chemical reaction, D the diffusion coefficient and K_n the reaction rate.

1.3.5 Dufour and Soret effects

It has been experimentally verified that the diffusion of energy can be caused by a composition gradient. This fact is known as Dufour effect or diffusion-thermo effect. The diffusion of diffusing species by temperature gradient is termed as Soret effect or thermal diffusion effect. In most of the studies dealing with the transfer of heat and mass, Dufour and Soret effects are neglected under the assumptions that these effects have smaller order of magnitude when compared to the effects described by Fourier's and Fick's laws. However recent developments show that these effects are significant when transfer of heat and mass occur in the flow of mixture of gases with very light molecular weight (H_2 , He) and gases with medium molecular weight (N_2 , air). Eqs. (1.9) and (1.10) can be modified to make them capable of describing Dufour and Soret effects as follows:

$$\rho c_p \frac{dT}{dt} = K_c \nabla^2 T + \bar{\tau} \cdot \bar{L} + \frac{DK_T}{C_s} \nabla^2 C + \frac{1}{\sigma} \mathbf{J} \cdot \mathbf{J}, \quad (1.11)$$

$$\frac{dC}{dt} = D \nabla^2 C + \frac{DK_T}{T_m} \nabla^2 T, \quad (1.12)$$

where $\bar{\tau} \cdot \bar{L}$ is the viscous dissipation term, $\bar{\tau}$ the stress tensor, \bar{L} the velocity gradient, C_s the concentration susceptibility, K_T the thermal-diffusion ratio and T_m the mean fluid temperature.

1.3.6 Maxwell's equations

Equations which mathematically state a set of laws namely Gauss' law of electricity, Gauss' law of magnetism, Faraday's law and Ampere-Maxwell law are known as Maxwell equations after

the name of James Clerk Maxwell. These equations are

$$\nabla \cdot \mathbf{E} = \frac{\rho_c}{\varepsilon_0}, \quad (\text{Gauss' law for electricity}), \quad (1.13)$$

$$\nabla \cdot \mathbf{B} = 0, \quad (\text{Gauss' law for magnetism}), \quad (1.14)$$

$$\nabla \times \mathbf{E} = -\frac{\partial \mathbf{B}}{\partial t}, \quad (\text{Faraday's law}), \quad (1.15)$$

$$\nabla \times \mathbf{B} = \mu_0 \mathbf{J} + \mu_e \varepsilon_0 \frac{\partial \mathbf{E}}{\partial t}, \quad (\text{Ampere-Maxwell law}). \quad (1.16)$$

Here ρ_c indicates the charge density, ε_0 the permittivity of free space, \mathbf{B} the magnetic field, \mathbf{E} the electric field, \mathbf{J} the current density and μ_e the electric constant.

1.4 Constitutive equations of a third order fluid

The Cauchy stress tensor $\boldsymbol{\tau}$ in an incompressible homogeneous third order fluid is [67-70]:

$$\boldsymbol{\tau} = -p\mathbf{I} + \left(\mu + \beta_3 \text{tr} \overline{\mathbf{A}}_1^2 \right) \mathbf{A}_1 + \alpha_1 \overline{\mathbf{A}}_2 + \alpha_2 \overline{\mathbf{A}}_1^2 + \beta_1 \overline{\mathbf{A}}_3 + \beta_2 (\overline{\mathbf{A}}_1 \overline{\mathbf{A}}_2 + \overline{\mathbf{A}}_2 \overline{\mathbf{A}}_1), \quad (1.17)$$

in which μ , α_i ($i = 1, 2$) and β_i ($i = 1, 2, 3$) are the material constants. The Rivlin-Ericksen tensors can be represented as follows

$$\overline{\mathbf{A}}_1 = \overline{\mathbf{L}} + \overline{\mathbf{L}}^t, \quad (1.18)$$

$$\overline{\mathbf{A}}_{n+1} = \frac{d\overline{\mathbf{A}}_n}{dt} + \overline{\mathbf{A}}_n \overline{\mathbf{L}} + \overline{\mathbf{L}}^t \overline{\mathbf{A}}_n \quad n = 1, 2. \quad (1.19)$$

Chapter 2

MHD mixed convection peristaltic flow with variable viscosity and thermal conductivity

This chapter concerns with mixed convection peristaltic flow of an electrically conducting fluid in an inclined channel. Analysis has been carried out in the presence of Joule heating. The fluid viscosity and thermal conductivity are assumed to vary with respect to temperature. A nonlinear coupled governing system is computed. Numerical results are presented for the velocity, pressure gradient, temperature and streamlines. Heat transfer rate at the wall is computed and analyzed. Graphs reflecting the contributions of embedded parameters are discussed.

2.1 Mathematical formulation

We examine the peristaltic transport of viscous fluid in an inclined asymmetric channel of width $(d_1 + d_2)$. The channel is inclined at an angle α_1 . The \overline{X} -axis is chosen along the length of the channel and \overline{Y} -axis is taken normal to the \overline{X} -axis. A uniform magnetic field of strength B_0 acts parallel to the \overline{Y} -axis. Effects of induced magnetic and electric fields are ignored. The viscosity and thermal conductivity are temperature dependent. The following forms of waves propagate along the channel walls

$$\begin{aligned}\overline{H}_1(\overline{X}, \overline{t}) &= d_1 + \xi_1, \\ \overline{H}_2(\overline{X}, \overline{t}) &= -d_2 - \xi_2,\end{aligned}$$

$$\begin{aligned}\xi_1 &= a_1 \cos \left(\frac{2\pi}{\lambda} (\overline{X} - c\overline{t}) \right), \\ \xi_2 &= b_1 \cos \left(\frac{2\pi}{\lambda} (\overline{X} - c\overline{t}) + \gamma \right),\end{aligned}$$

in which \overline{t} is time, \overline{H}_1 and \overline{H}_2 represent the upper and lower walls of channel, a_1 and b_1 are the amplitude of the waves at respective walls, γ the phase difference of two waves and c and λ are the speed and wavelength of the waves respectively. Appropriate velocity field for this problem is $\overline{V} = [\overline{U}(\overline{X}, \overline{Y}, \overline{t}), \overline{V}(\overline{X}, \overline{Y}, \overline{t}), 0]$. Laws of conservation of mass and linear momentum give

$$\frac{\partial \overline{U}}{\partial \overline{X}} + \frac{\partial \overline{V}}{\partial \overline{Y}} = 0, \quad (2.1)$$

$$\begin{aligned}\rho \left(\frac{\partial}{\partial \overline{t}} + \overline{U} \frac{\partial}{\partial \overline{X}} + \overline{V} \frac{\partial}{\partial \overline{Y}} \right) \overline{U} &= -\frac{\partial \overline{P}}{\partial \overline{X}} + 2 \frac{\partial}{\partial \overline{X}} \left(\overline{\mu}(T) \frac{\partial \overline{U}}{\partial \overline{X}} \right) + \frac{\partial}{\partial \overline{Y}} \left[\overline{\mu}(T) \left(\frac{\partial \overline{V}}{\partial \overline{X}} + \frac{\partial \overline{U}}{\partial \overline{Y}} \right) \right] \\ &\quad - \sigma B_0^2 \overline{U} + \rho g \alpha^* (T - T_m) \sin \alpha_1 + \rho g \sin \alpha_1,\end{aligned} \quad (2.2)$$

$$\begin{aligned}\rho \left(\frac{\partial}{\partial \overline{t}} + \overline{U} \frac{\partial}{\partial \overline{X}} + \overline{V} \frac{\partial}{\partial \overline{Y}} \right) \overline{V} &= -\frac{\partial \overline{P}}{\partial \overline{Y}} + 2 \frac{\partial}{\partial \overline{Y}} \left(\overline{\mu}(T) \frac{\partial \overline{V}}{\partial \overline{Y}} \right) + \frac{\partial}{\partial \overline{X}} \left[\overline{\mu}(T) \left(\frac{\partial \overline{V}}{\partial \overline{X}} + \frac{\partial \overline{U}}{\partial \overline{Y}} \right) \right] \\ &\quad - \rho g \alpha^* (T - T_m) \cos \alpha_1 - \rho g \cos \alpha_1.\end{aligned} \quad (2.3)$$

In above equations ρ is the density of fluid, σ the electric conductivity, $\overline{\mu}(T)$ the temperature dependent dynamic viscosity, g the acceleration due to gravity, T_m the mean value of temperature of both the channel walls and α^* the thermal expansion coefficient. We consider $(\overline{u}, \overline{v})$ and \overline{p} as the velocity components and pressure in the wave frame $(\overline{x}, \overline{y})$. The transformations between laboratory and wave frames are

$$\overline{x} = \overline{X} - c\overline{t}, \quad \overline{y} = \overline{Y}, \quad \overline{u} = \overline{U} - c, \quad \overline{v} = \overline{V}, \quad \overline{p}(\overline{x}, \overline{y}) = \overline{P}(\overline{X}, \overline{Y}, \overline{t}), \quad (2.4)$$

where (\bar{U}, \bar{V}) and \bar{P} are the velocity components and pressure in the laboratory frame. The conservation laws of mass and momentum in wave frame can be expressed as

$$\frac{\partial \bar{u}}{\partial \bar{x}} + \frac{\partial \bar{v}}{\partial \bar{y}} = 0, \quad (2.5)$$

$$\begin{aligned} \rho \left((\bar{u} + c) \frac{\partial}{\partial \bar{x}} + \bar{v} \frac{\partial}{\partial \bar{y}} \right) (\bar{u} + c) = & -\frac{\partial \bar{P}}{\partial \bar{x}} + 2 \frac{\partial}{\partial \bar{x}} \left(\bar{\mu}(T) \frac{\partial \bar{u}}{\partial \bar{x}} \right) + \frac{\partial}{\partial \bar{y}} \left[\bar{\mu}(T) \left(\frac{\partial \bar{v}}{\partial \bar{x}} + \frac{\partial \bar{u}}{\partial \bar{y}} \right) \right] \\ & -\sigma B_0^2 (\bar{u} + c) + \rho g \alpha^* (T - T_m) \sin \alpha_1 + \rho g \sin \alpha_1, \end{aligned} \quad (2.6)$$

$$\begin{aligned} \rho \left((\bar{u} + c) \frac{\partial}{\partial \bar{x}} + \bar{v} \frac{\partial}{\partial \bar{y}} \right) (\bar{v}) = & -\frac{\partial \bar{P}}{\partial \bar{y}} + 2 \frac{\partial}{\partial \bar{y}} \left(\bar{\mu}(T) \frac{\partial \bar{v}}{\partial \bar{y}} \right) + \frac{\partial}{\partial \bar{x}} \left[\bar{\mu}(T) \left(\frac{\partial \bar{v}}{\partial \bar{x}} + \frac{\partial \bar{u}}{\partial \bar{y}} \right) \right] \\ & -\rho g \alpha^* (T - T_m) \cos \alpha_1 - \rho g \cos \alpha_1. \end{aligned} \quad (2.7)$$

Defining the dimensionless quantities

$$\begin{aligned} x &= \frac{\bar{x}}{\lambda}, \quad y = \frac{\bar{y}}{d_1}, \quad u = \frac{\bar{u}}{c}, \quad v = \frac{\bar{v}}{c\delta}, \quad \delta = \frac{d_1}{\lambda}, \quad h_1 = \frac{\bar{H}_1}{d_1}, \quad h_2 = \frac{\bar{H}_2}{d_1}, \quad d = \frac{d_2}{d_1}, \quad p = \frac{d_1^2 \bar{P}}{c\lambda\mu_0}, \\ v &= \frac{\mu_0}{\rho}, \quad \mu(\theta) = \frac{\bar{\mu}(T)}{\mu_0}, \quad M^2 = \left(\frac{\sigma}{\mu_0} \right)^2 B_0^2 d_1^2, \quad t = \frac{c\bar{t}}{\lambda}, \quad G_t = \frac{\rho g \alpha^* (T_1 - T_0) d_1^2}{\mu_0 c}, \quad \theta = \frac{T - T_m}{T_1 - T_0}, \\ Re &= \frac{\rho c d_1}{\mu_0}, \quad Fr = \frac{c^2}{g d_1}, \quad u = \psi_y, \quad v = -\psi_x \end{aligned} \quad (2.8)$$

and adopting long wavelength and low Reynolds number approach we have in terms of stream function ψ the following equations

$$\begin{aligned} p_x &= \frac{\partial}{\partial y} \left[\mu(\theta) \frac{\partial^2 \psi}{\partial y^2} \right] - M^2 \left(\frac{\partial \psi}{\partial y} + 1 \right) \\ &+ G_t \theta \sin \alpha_1 + \frac{\text{Re} \sin \alpha_1}{Fr}, \end{aligned} \quad (2.9)$$

$$p_y = 0, \quad (2.10)$$

and the continuity equation is identically satisfied. Here, $h_{1,2}$ are the dimensionless wall shapes, M the Hartman number, G_t the Grashoff number, Re the Reynolds number, Fr the Froud number and ψ the stream function. Equation (2.10) indicates that $p \neq p(y)$ and compatibility

equation from Eqs. (2.9) and (2.10) has the form

$$0 = \frac{\partial^2}{\partial y^2} \left[\mu(\theta) \frac{\partial^2 \psi}{\partial y^2} \right] - M^2 \left(\frac{\partial^2 \psi}{\partial y^2} \right) + G_t \frac{\partial \theta}{\partial y} \sin \alpha. \quad (2.11)$$

The volume flow rate in fixed frame is defined as

$$Q = \int_{\bar{H}_2}^{\bar{H}_1} \bar{U}(\bar{X}, \bar{Y}, \bar{t}) dY \quad (2.12)$$

and in wave frame we have

$$q = \int_{h_2}^{h_1} \bar{u}(x, y) dy, \quad (2.13)$$

in which $h_{1,2}$ are functions of x alone. From Eqs. (2.12), (2.13) and (2.8) one has

$$Q = q + ch_1(x) - ch_2(x).$$

The time averaged flow over a period T_f is

$$\bar{Q} = \frac{1}{T} \int_0^{T_f} Q dt,$$

which implies that

$$\bar{Q} = q + cd_1 + cd_2.$$

Defining η and F as the dimensionless mean flows in laboratory and wave frames by

$$\eta = \frac{\bar{Q}}{cd_1}, \quad F = \frac{q}{cd_1}$$

one can write

$$\eta = F + 1 + d, \quad (2.14)$$

where

$$F = \int_{h_2}^{h_1} \frac{\partial \psi}{\partial y} dy = \psi(h_1) - \psi(h_2). \quad (2.15)$$

Dimensionless boundary conditions in terms of stream function are

$$\begin{aligned}\psi &= \frac{F}{2}, \quad \psi_y = -1 \text{ at } y = h_1, \\ \psi &= -\frac{F}{2}, \quad \psi_y = -1 \text{ at } y = h_2.\end{aligned}\tag{2.16}$$

2.2 Heat transfer analysis

We have assumed that the walls at h_1 and h_2 have temperature T_0 and T_1 respectively. Energy equation in presence of viscous dissipation and Joule heating effects in laboratory frame is

$$\begin{aligned}\rho C_p (T_t + \bar{U} T_{\bar{X}} + \bar{V} T_{\bar{Y}}) &= \bar{\nabla} \cdot [\bar{K}(T) (\nabla T)] + \bar{\mu}(T) \left[2 \left\{ \left(\frac{\partial \bar{U}}{\partial \bar{X}} \right)^2 + \left(\frac{\partial \bar{V}}{\partial \bar{Y}} \right)^2 \right\} + \left(\frac{\partial \bar{V}}{\partial \bar{X}} + \frac{\partial \bar{U}}{\partial \bar{Y}} \right)^2 \right] \\ &\quad + \sigma B_0^2 \bar{U}^2.\end{aligned}\tag{2.17}$$

In wave frame above equation takes the form

$$\begin{aligned}\rho C_p ((\bar{u} + c) T_{\bar{x}} + \bar{v} T_{\bar{y}}) &= \bar{\nabla} \cdot [\bar{K}(T) (\nabla T)] + \bar{\mu}(T) \left[2 \left\{ \left(\frac{\partial \bar{u}}{\partial \bar{x}} \right)^2 + \left(\frac{\partial \bar{v}}{\partial \bar{y}} \right)^2 \right\} + \left(\frac{\partial \bar{v}}{\partial \bar{x}} + \frac{\partial \bar{u}}{\partial \bar{y}} \right)^2 \right] \\ &\quad + \sigma B_0^2 (\bar{u} + c)^2,\end{aligned}\tag{2.18}$$

in which T is the fluid temperature, C_p the specific heat, $K(T)$ the dimensional temperature dependent thermal conductivity and $\bar{\mu}(T)$ is the temperature dependent viscosity. The dimensionless energy equation in view of afore mentioned approximations becomes

$$\frac{\partial}{\partial y} \{K(\theta) \theta_y\} + Br \mu(\theta) (\psi_{yy})^2 + Br M^2 \left(\frac{\partial \psi}{\partial y} + 1 \right)^2 = 0,\tag{2.19}$$

where Br is the Brinkman number, $K(\theta)$ the dimensionless temperature dependent thermal conductivity, θ the dimensionless temperature, Pr the Prandtl number and E the Eckert number. These involved quantities are defined as follows:

$$\theta = \frac{T - T_m}{T_1 - T_0}, \quad K(\theta) = \frac{\bar{K}(T)}{K_0}, \quad Br = Pr E, \quad Pr = \frac{\mu_0 C_p}{K_0}, \quad E = \frac{c^2}{C_p (T_1 - T_0)}.\tag{2.20}$$

Dimensionless boundary conditions for the temperature are given by

$$\theta = -\frac{1}{2} \text{ at } y = h_1 \text{ and } \theta = \frac{1}{2} \text{ at } y = h_2. \quad (2.21)$$

Temperature dependent viscosity and thermal conductivity are taken in the form

$$\mu(\theta) = 1 - \alpha\theta, \quad K(\theta) = 1 + \epsilon\theta, \quad (\alpha, \epsilon) \ll 1. \quad (2.22)$$

Note that μ_0 and K_0 are the viscosity and thermal conductivity of the fluid when the temperature of the fluid approaches the mean temperature. Also the cases of constant viscosity and thermal conductivity can be recovered by choosing α and ϵ equal to zero. The values of h_1 and h_2 are

$$h_1(x) = 1 + a \cos(2\pi x), \quad h_2(x) = -d - b \cos(2\pi x + \gamma). \quad (2.23)$$

We note that Eq. (2.19) is nonlinear in the present analysis. Hence in this study we have nonlinear coupled system. Analytic solution of the resulting nonlinear coupled system seems difficult. Hence the numerical solution through **Mathematica** is preferred here. The step sizes for x and y are chosen 0.01. The flow quantities of interest will be analyzed in the next section.

2.3 Graphical analysis

This section aims to analyze the numerical results for influential parameters. Plots of pressure gradient, axial velocity, temperature and stream function are obtained and examined. Numerical values of the heat transfer rate are given in Table 2.1.

It is obvious from Figs. 2.1 that pressure gradient for constant viscosity fluid is less when compared with variable viscosity fluid. Temperature dependent thermal conductivity also increases the value of pressure gradient. Such results are obvious from the Figs. 2.1a-b. An increase in α and ϵ also increases the pressure gradient. Pressure gradient decreases by increasing Hartman and Froud numbers. However this change in pressure gradient due to M and Fr is sufficiently large when compared with that of α and ϵ (see Figs. 2.1d and f). As the value of α_1 is varied from 0 to $\pi/2$ the pressure gradient tends to attain significantly large value which highlights the fact that pressure gradient is higher in a vertical channel when compared

to horizontal channel (Fig. 2.1 c). For assisting flow (+ve value of acceleration due to gravity g) pressure gradient is large than that of opposing flow (see Fig. 2.1e).

Plots of axial velocity are given in Figs. 2.2 a-d. These Figs. showed that velocity tends to follow parabolic path with maximum value occurring near the center of the channel. Fig. 2.1a shows that when the viscosity parameter α is taken zero i.e. the velocity for constant viscosity fluid is seen to have maximum value near the center of the channel whereas it tends to shift towards the lower wall for non zero values of the viscosity parameter. Moreover a slight increase in the maximum value of velocity is observed when α increases. Channel inclination angle α_1 is seen to have almost similar effect on the velocity as that of α (see Fig. 2.2b). Maximum value of velocity in inclined channel is shifted towards the lower wall. Increase in the strength of applied magnetic field decreases the velocity. This change in velocity is maximum when the Hartman number is taken between 1 and 2 (see Fig. 2.2c). Change in the value of Grashoff number varies the symmetry of the velocity profile relative to the channel i.e. velocity has maximum value near the center for opposing flow and this change occurs when G_t has +ve value. Effect of Grashoff number on the velocity also depends on the channel inclination which is well justified physically (see Fig. 2.2d). It is further noted that ϵ has no effect on the axial velocity.

Behavior of the dimensionless temperature through α , ϵ , M , α_1 , G_t and Br are examined in the Figs. 2.3 a-f. Fig. 2.3a depicts that an increase in the viscosity parameter decreases the temperature. This decrease in temperature subject to decrease in α is uniform throughout the channel. Fig. 2.3 b analyzes the impact of variable thermal conductivity parameter ϵ on the temperature. Effect of ϵ on the temperature is noteworthy in the sense that it is not uniform throughout the channel. It means that near the lower wall (h_2) an increase in the value of ϵ decreases the value of temperature of the fluid whereas near the upper wall (h_1) it increases the value of θ . Since ϵ yields the perturbation in the thermal conductivity of the fluid so increase in this parameter gives rise to increase in the ability of the fluid to dissipate or absorb heat. Hence when temperature of the fluid is higher than the temperature of the boundary then increase in ϵ results in reduction of the temperature of fluid and vice versa.

Increase in the Hartman number increases the value of θ . This fact is primarily due to consideration of Joule heating (see Fig. 2.3c). Channel inclination also has non-uniform effect on the temperature. Increase in α_1 near the lower wall increases the temperature but such

increase although is not very significant. Similarly the Grashoff number also has very less and non-uniform effect on the temperature (see Figs. 2.3d and e). Fig. 2.3 f shows that an increase in Br increases the temperature θ significantly. Also when Br is increased then the temperature plots become non-linear. Streamlines for α and ϵ are plotted in the Figs. 2.4 and 2.5. It is seen that the size of trapped bolus decreases with an increase in α . However ϵ has no significant effect on the size of the bolus.

Table 2.1 gives the numerical values of heat transfer rate at the wall $\theta'(h_1)$ for different values of the embedded parameters. Results showed that an increase in the value of viscosity parameter α reduces the transfer rate but heat transfer rate increases through increase in ϵ . The transfer rate decreases via inclined nature of channel. Further an increase in Hartman number increases the transfer rate.

2.4 Main points

Effects of variable viscosity and thermal conductivity on the MHD peristaltic transport of fluid in an inclined asymmetric channel are analyzed. Mixed convection and Joule heating effects are present. Main results are reported below.

- Variable viscosity and thermal conductivity tend to increase the pressure gradient.
- Viscosity parameter, Grashoff number and inclination angle have similar effects on the velocity. However velocity is unperturbed due to change in thermal conductivity parameter.
- Variable thermal conductivity has no significant change on the bolus size.
- Variable viscosity tends to reduce the temperature of fluid.
- Viscosity parameter and inclination angle have similar effects on heat transfer rate at the wall.

The following values are used in the plots

Figs. 2.1 (a-g), $\alpha = 0.1$, $\alpha_1 = \pi/6$, $\epsilon = 0.1$, $Re = 3$, $Fr = 2$, $Br = 0.2$, $M = 0.5$, $G_t = 2$, $Pr = 0.5$, $a = 0.4$, $b = 0.3$, $\gamma = \pi/4$, $d = 0.7$ and $\eta = 0.7$.

Figs. 2.2 (a-d), $\alpha = 0.1$, $\alpha_1 = \pi/6$, $\epsilon = 0.1$, $x = 0$, $Re = 3$, $Fr = 2$, $Br = 0.4$, $M = 0.5$, $G_t = 2$, $Pr = 0.5$, $a = 0.4$, $b = 0.3$, $\gamma = \pi/4$, $d = 0.7$ and $\eta = 0.9$.

Figs. 2.3 (a-f), $\alpha = 0.1$, $\alpha_1 = \pi/6$, $\epsilon = 0.1$, $x = 0$, $Re = 5$, $Fr = 2$, $Br = 0.5$, $M = 1$, $G_t = 1$, $Pr = 0.5$, $a = 0.4$, $b = 0.3$, $\gamma = \pi/4$, $d = 0.7$ and $\eta = 1.5$.

Figs. 2.4 and 2.5, $\alpha = 0.1$, $\alpha_1 = \pi/6$, $\epsilon = 0.1$, $Re = 3$, $Fr = 2$, $Br = 0.2$, $M = 0.5$, $G_t = 2$, $Pr = 0.5$, $a = 0.4$, $b = 0.3$, $\gamma = \pi/4$, $d = 0.7$ and $\eta = 1.2$.

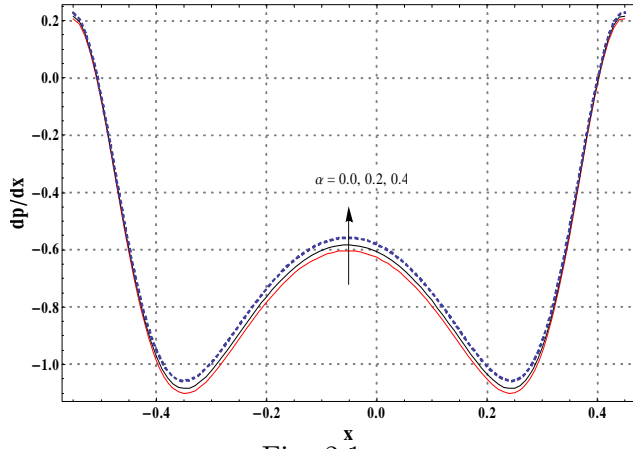


Fig. 2.1 a

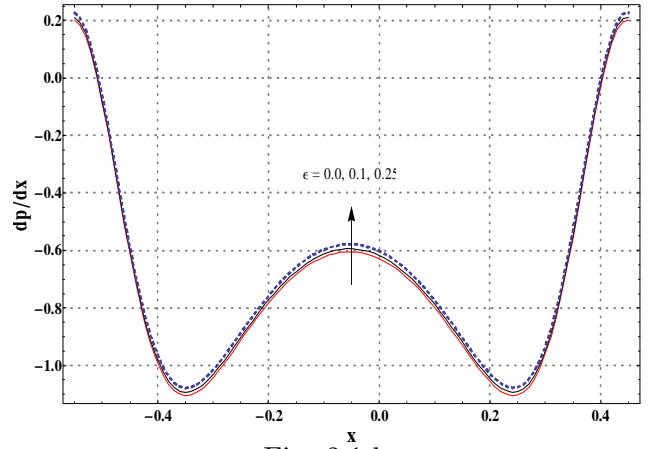


Fig. 2.1 b

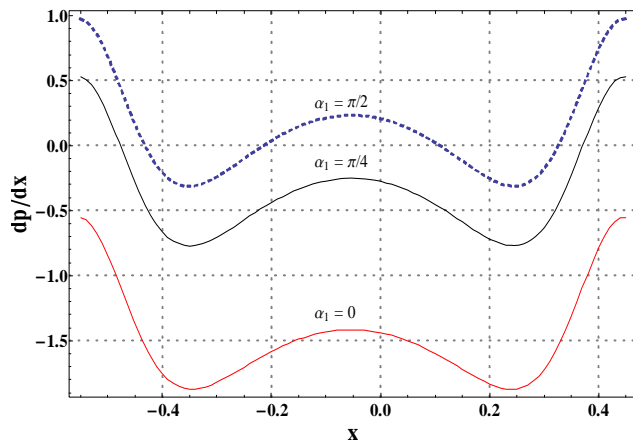


Fig. 2.1 c

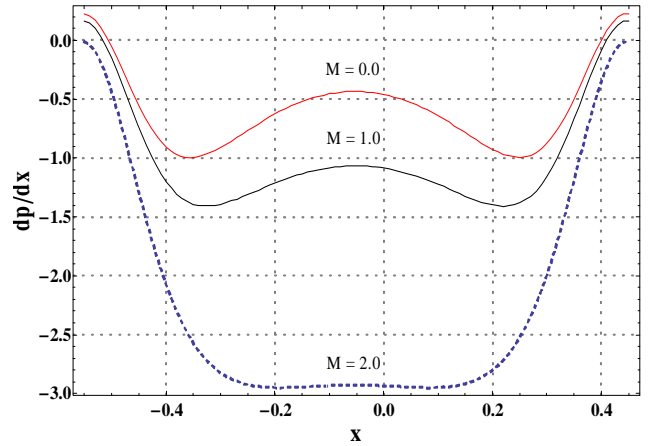
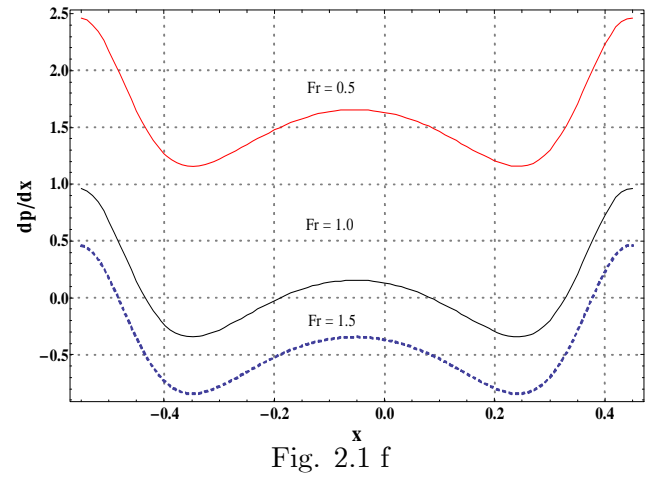
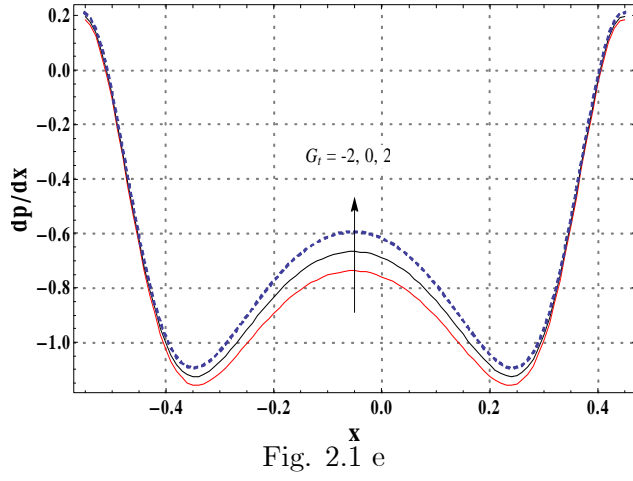


Fig. 2.1 d



Figs. 2.1 a-f. Development of pressure gradient in the axial direction.

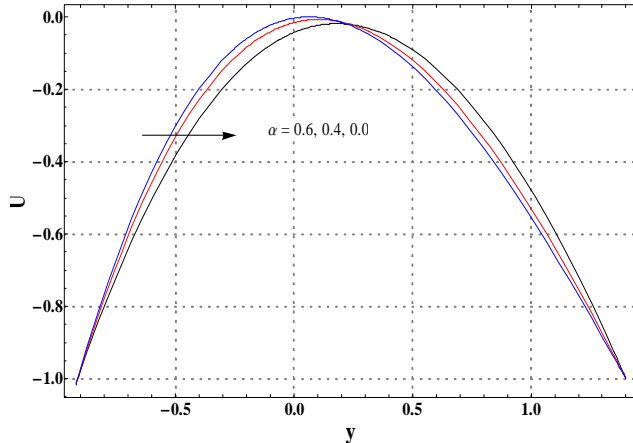


Fig. 2.2 a

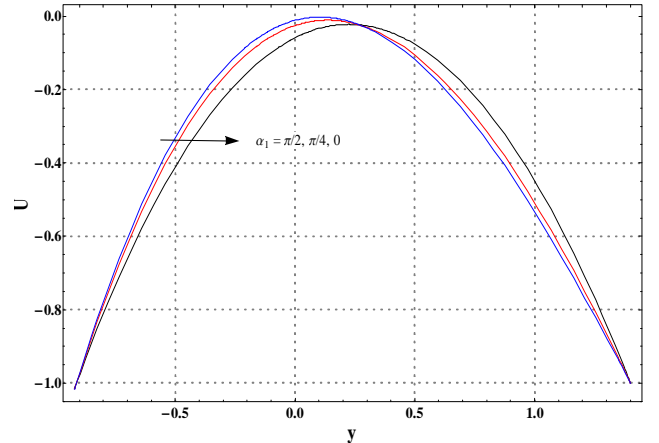


Fig. 2.2 b

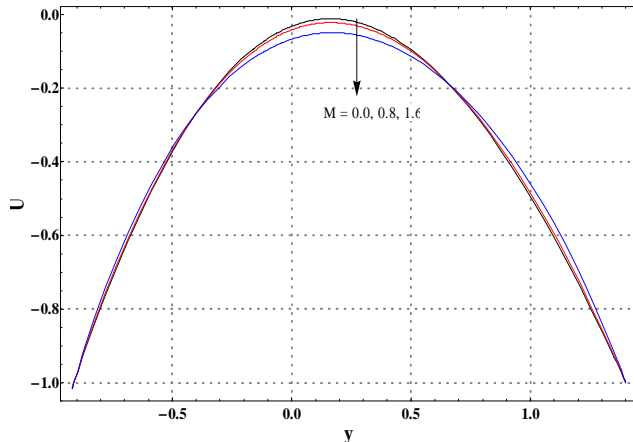


Fig. 2.2 c

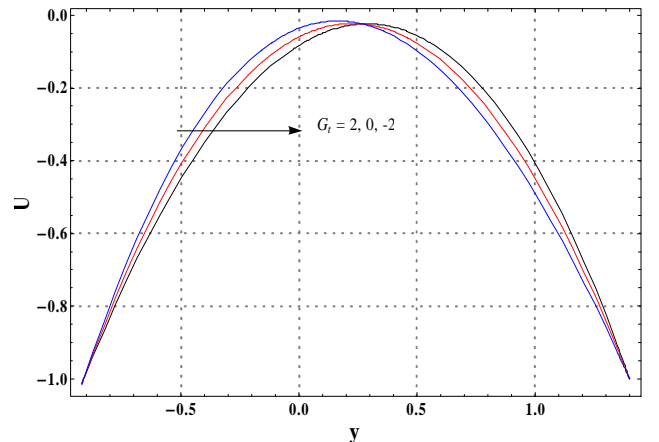


Fig. 2.2 d

Fig. 2.2 a-d Axial velocity for different parameters.

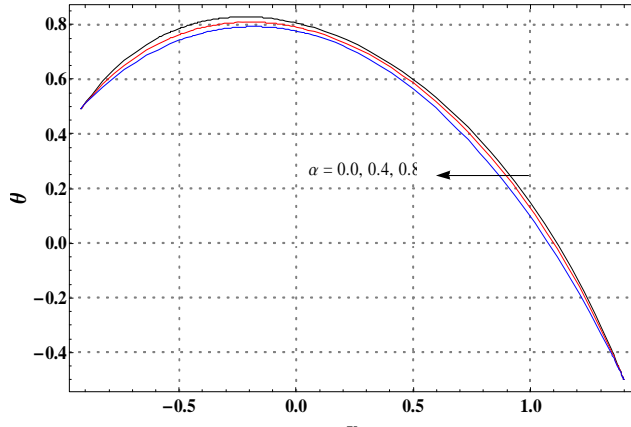


Fig. 2.3 a

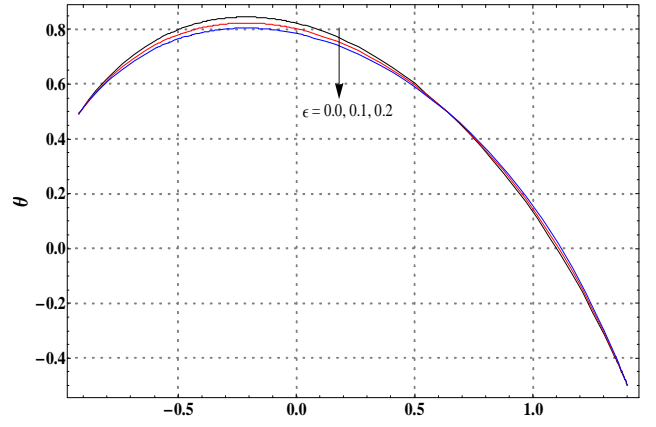


Fig. 2.3 b

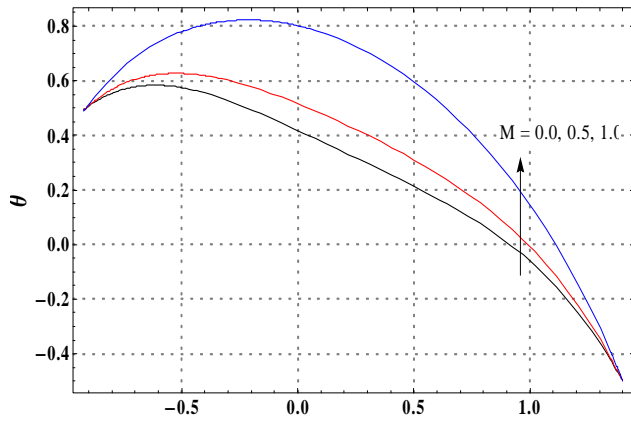


Fig. 2.3 c

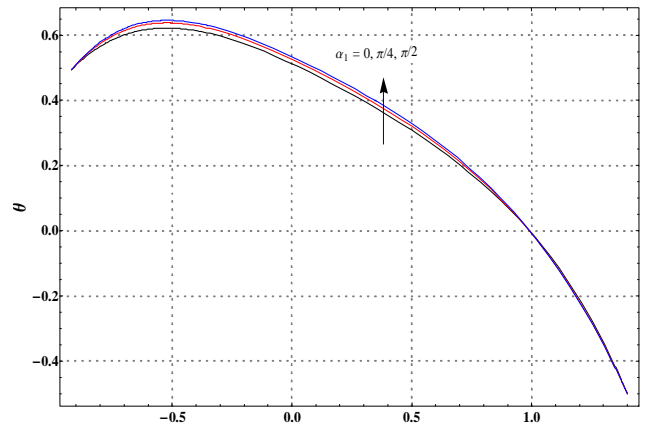
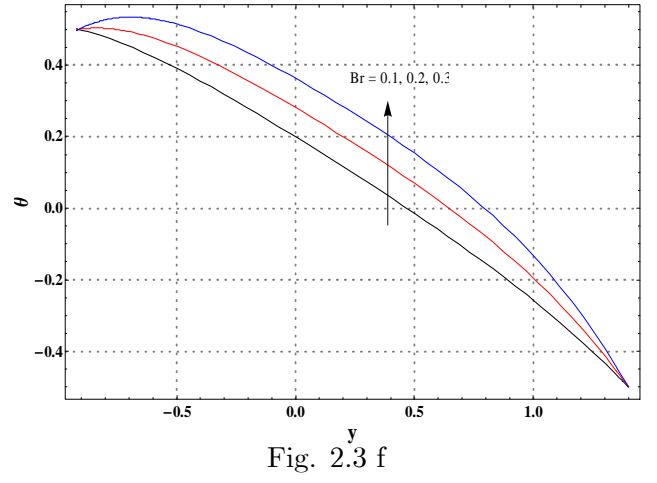
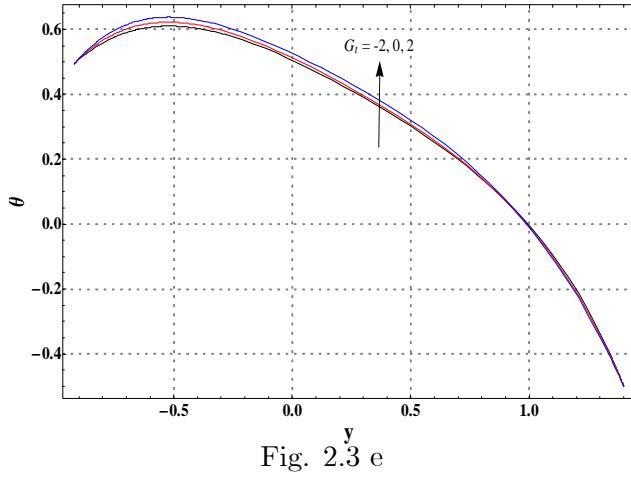


Fig. 2.3 d



Figs. 2.3 a-f. Dimensionless temperature for various parameters.

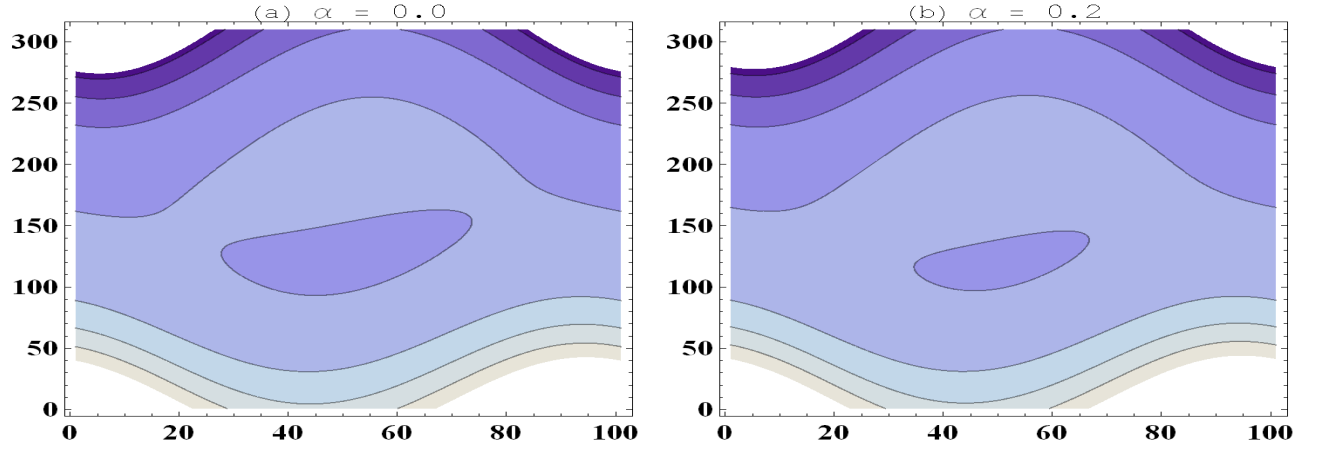


Fig. 2.4 Streamlines for viscosity parameter α .

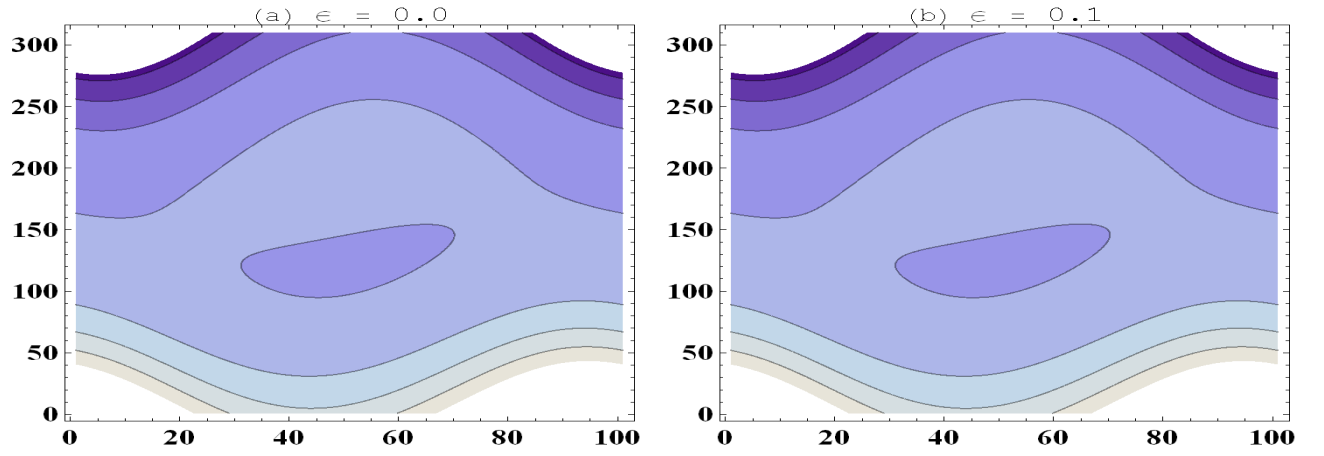


Fig. 2.5 Streamlines for thermal conductivity parameter ϵ .

α	ϵ	α_1	M	$-\theta'(h_1)$
0.0	0.1	$\pi/6$	0.5	1.0603
0.4				1.0257
0.6				1.0051
0.1	0.0			0.9893
	0.1			1.0524
	0.2			1.1258
	0.1	0		1.1278
		$\pi/4$		1.0247
		$\pi/2$		0.9892
		$\pi/6$	0.0	0.9857
			0.4	1.0284
			0.8	1.1567

Table 2.1. Numerical values of heat transfer rate at the wall (h_1) when $Re = 3$, $Fr = 2$, $Br = 0.2$, $x = 0$, $G_t = 2$, $Pr = 0.5$, $a = 0.4$, $b = 0.3$, $\gamma = \pi/4$, $d = 0.7$ and $\eta = 1.2$.

Chapter 3

Hydromagnetic peristaltic transport of variable viscosity fluid with heat transfer and porous medium

This chapter examines the peristaltic transport of variable viscosity fluid in a planar channel with heat transfer. The fluid viscosity is taken temperature dependent. The fluid is electrically conducting in the presence of a constant applied magnetic field. Both channel and magnetic field are considered inclined. An incompressible fluid saturates the porous space. Heat transfer analysis is carried out in the presence of viscous dissipation and Joule heating. The resulting problems are solved numerically. A parametric study is performed to predict the impact of embedded parameters. Important results have been pointed out in the key findings.

3.1 Mathematical analysis

Let us examine the peristaltic transport of an incompressible viscous fluid in a symmetric channel. The channel is taken inclined at an angle α_1 to the vertical. The fluid is electrically conducting in the presence of an inclined magnetic field with constant strength \mathbf{B}_0 . The flow generated is due to peristaltic waves travelling along the channel walls. The wall geometry is chosen in the form

$$\overline{H}(\overline{X}, \overline{t}) = d_1 + \xi,$$

where d_1 is the half channel width and ξ is the disturbance produced due to propagation of peristaltic waves at the walls. This disturbance can be written in the form

$$\xi = a_1 \cos \left(\frac{2\pi}{\lambda} (\overline{X} - c\overline{t}) \right),$$

in which \overline{t} is time, a_1 is the amplitude of the peristaltic wave, c and λ are the speed and wavelength of the waves respectively. Appropriate velocity field for this problem is $\overline{V} = [U(\overline{X}, \overline{Y}, \overline{t}), V(\overline{X}, \overline{Y}, \overline{t}), 0]$. Laws of conservation of mass, momentum and energy can be represented as follows:

$$\frac{\partial \overline{U}}{\partial \overline{X}} + \frac{\partial \overline{V}}{\partial \overline{Y}} = 0, \quad (3.1)$$

$$\begin{aligned} \rho \left(\frac{\partial}{\partial \overline{t}} + \overline{U} \frac{\partial}{\partial \overline{X}} + \overline{V} \frac{\partial}{\partial \overline{Y}} \right) \overline{U} = & -\frac{\partial \overline{P}}{\partial \overline{X}} + 2 \frac{\partial}{\partial \overline{X}} \left(\overline{\mu}(T) \frac{\partial \overline{U}}{\partial \overline{X}} \right) + \frac{\partial}{\partial \overline{Y}} \left[\overline{\mu}(T) \left(\frac{\partial \overline{V}}{\partial \overline{X}} + \frac{\partial \overline{U}}{\partial \overline{Y}} \right) \right] \\ & -\sigma B_0^2 \cos \beta (\overline{U} \cos \beta - \overline{V} \sin \beta) + \rho g \alpha^* (T - T_0) \sin \alpha_1 + \rho g \sin \alpha_1 - \frac{\overline{\mu}(T) \overline{U}}{\overline{k}}, \end{aligned} \quad (3.2)$$

$$\begin{aligned} \rho \left(\frac{\partial}{\partial \overline{t}} + \overline{U} \frac{\partial}{\partial \overline{X}} + \overline{V} \frac{\partial}{\partial \overline{Y}} \right) \overline{V} = & -\frac{\partial \overline{P}}{\partial \overline{Y}} + 2 \frac{\partial}{\partial \overline{Y}} \left(\overline{\mu}(T) \frac{\partial \overline{V}}{\partial \overline{Y}} \right) + \frac{\partial}{\partial \overline{X}} \left[\overline{\mu}(T) \left(\frac{\partial \overline{V}}{\partial \overline{X}} + \frac{\partial \overline{U}}{\partial \overline{Y}} \right) \right] \\ & -\sigma B_0^2 \sin \beta (\overline{U} \cos \beta - \overline{V} \sin \beta) - \rho g \alpha^* (T - T_0) \cos \alpha_1 - \rho g \cos \alpha_1 - \frac{\overline{\mu}(T) \overline{V}}{\overline{k}}, \end{aligned} \quad (3.3)$$

$$\begin{aligned} \rho C_p (T_{\overline{t}} + \overline{U} T_{\overline{X}} + \overline{V} T_{\overline{Y}}) = & K [T_{\overline{X}\overline{X}} + T_{\overline{Y}\overline{Y}}] + \overline{\mu}(T) \left[2 \left\{ \left(\frac{\partial \overline{U}}{\partial \overline{X}} \right)^2 + \left(\frac{\partial \overline{V}}{\partial \overline{Y}} \right)^2 \right\} + \left(\frac{\partial \overline{V}}{\partial \overline{X}} + \frac{\partial \overline{U}}{\partial \overline{Y}} \right)^2 \right] \\ & + \sigma B_0^2 (\overline{U} \cos \beta - \overline{V} \sin \beta)^2 + \frac{\overline{\mu}(T) \overline{U}^2}{\overline{k}}. \end{aligned} \quad (3.4)$$

Here \overline{U} , \overline{V} and \overline{P} are the velocity components and pressure in the laboratory frame $(\overline{X}, \overline{Y}, \overline{t})$, ρ the density of fluid, μ the dynamic viscosity, g the acceleration due to gravity, \overline{k} permeability of the porous medium parameter, β the inclination of applied magnetic field and α^* the thermal expansion coefficient. We also denote C_p as the specific heat, K the thermal conductivity and T the temperature of fluid. We further adopt $(\overline{u}, \overline{v})$ and \overline{p} as the velocity components and

pressure in the wave frame (\bar{x}, \bar{y}) . The transformations between laboratory and wave frames are

$$\bar{x} = \bar{X} - c\bar{t}, \quad \bar{y} = \bar{Y}, \quad \bar{u} = \bar{U} - c, \quad \bar{v} = \bar{V}, \quad \bar{p}(\bar{x}, \bar{y}) = \bar{P}(\bar{X}, \bar{Y}, \bar{t}). \quad (3.5)$$

The governing equations in the wave frame are given by

$$\frac{\partial \bar{u}}{\partial \bar{x}} + \frac{\partial \bar{v}}{\partial \bar{y}} = 0, \quad (3.6)$$

$$\begin{aligned} \rho \left((\bar{u} + c) \frac{\partial}{\partial \bar{x}} + \bar{v} \frac{\partial}{\partial \bar{y}} \right) (\bar{u} + c) &= -\frac{\partial \bar{p}}{\partial \bar{x}} + 2 \frac{\partial}{\partial \bar{x}} \left(\bar{\mu}(T) \frac{\partial \bar{u}}{\partial \bar{x}} \right) + \frac{\partial}{\partial \bar{y}} \left[\bar{\mu}(T) \left(\frac{\partial \bar{v}}{\partial \bar{x}} + \frac{\partial \bar{u}}{\partial \bar{y}} \right) \right] \\ -\sigma B_0^2 \cos \beta ((\bar{u} + c) \cos \beta - \bar{v} \sin \beta) &+ \rho g \alpha^* (T - T_0) \sin \alpha_1 + \rho g \sin \alpha_1 - \frac{\bar{\mu}(T)(\bar{u}+c)}{\bar{k}}, \end{aligned} \quad (3.7)$$

$$\begin{aligned} \rho \left((\bar{u} + c) \frac{\partial}{\partial \bar{x}} + \bar{v} \frac{\partial}{\partial \bar{y}} \right) (\bar{v}) &= -\frac{\partial \bar{p}}{\partial \bar{y}} + 2 \frac{\partial}{\partial \bar{y}} \left(\bar{\mu}(T) \frac{\partial \bar{v}}{\partial \bar{y}} \right) + \frac{\partial}{\partial \bar{x}} \left[\bar{\mu}(T) \left(\frac{\partial \bar{v}}{\partial \bar{x}} + \frac{\partial \bar{u}}{\partial \bar{y}} \right) \right] \\ -\sigma B_0^2 \sin \beta ((\bar{u} + c) \cos \beta - \bar{v} \sin \beta) &- \rho g \alpha^* (T - T_0) \cos \alpha_1 - \rho g \cos \alpha_1 - \frac{\bar{\mu}(T)(\bar{v})}{\bar{k}}, \end{aligned} \quad (3.8)$$

$$\begin{aligned} \rho C_p ((\bar{u} + c) T_{\bar{x}} + \bar{v} T_{\bar{y}}) &= K [T_{\bar{x}\bar{x}} + T_{\bar{y}\bar{y}}] + \bar{\mu}(T) \left[2 \left\{ \left(\frac{\partial \bar{u}}{\partial \bar{x}} \right)^2 + \left(\frac{\partial \bar{v}}{\partial \bar{y}} \right)^2 \right\} + \left(\frac{\partial \bar{v}}{\partial \bar{x}} + \frac{\partial \bar{u}}{\partial \bar{y}} \right)^2 \right] \\ &+ \sigma B_0^2 ((\bar{u} + c) \cos \beta - \bar{v} \sin \beta)^2 + \frac{\bar{\mu}(T)(\bar{u} + c)^2}{\bar{k}}, \end{aligned} \quad (3.9)$$

Defining the dimensionless quantities

$$\begin{aligned} x &= \frac{\bar{x}}{\lambda}, \quad y = \frac{\bar{y}}{d_1}, \quad u = \frac{\bar{u}}{c}, \quad v = \frac{\bar{v}}{c\delta}, \quad \delta = \frac{d_1}{\lambda}, \quad h = \frac{\bar{H}}{d_1}, \quad a = \frac{a_1}{d_1}, \quad p = \frac{d_1^2 \bar{p}}{c\lambda\mu_0}, \quad v = \frac{\mu_0}{\rho}, \\ \mu(\theta) &= \frac{\bar{\mu}(T)}{\mu_0}, \quad M^2 = \left(\frac{\sigma}{\mu_0} \right)^2 B_0^2 d_1^2, \quad Re = \frac{\rho c d_1}{\mu_0}, \quad t = \frac{c\bar{t}}{\lambda}, \quad \theta = \frac{T - T_0}{T_0}, \quad Gt = \frac{\rho g \alpha^* T_0 d_1^2}{\mu_0 c}, \\ Fr &= \frac{c^2}{g d_1}, \quad k = \frac{\bar{k}}{d_1^2}, \quad Br = \text{Pr } E, \quad E = \frac{c^2}{C_p T_0}, \quad Pr = \frac{\mu_0 C_p}{K}, \quad u = \psi_y, \quad v = -\psi_x, \end{aligned} \quad (3.10)$$

and adopting long wavelength and low Reynolds number approach, the equations in terms of stream function ψ are

$$p_x = \frac{\partial}{\partial y} \left[\mu(\theta) \frac{\partial^2 \psi}{\partial y^2} \right] - \left\{ M^2 \cos^2 \beta + \frac{\mu(\theta)}{k} \right\} \left(\frac{\partial \psi}{\partial y} + 1 \right) + G_t \theta \text{Si} n \alpha_1 + \frac{\text{Re} \text{Si} n \alpha_1}{Fr}, \quad (3.11)$$

$$p_y = 0, \quad (3.12)$$

$$\theta_{yy} + Br \mu(\theta) (\psi_{yy})^2 + Br \left[M^2 \cos^2 \beta + \frac{\mu(\theta)}{k} \right] \left(\frac{\partial \psi}{\partial y} + 1 \right)^2 = 0, \quad (3.13)$$

Note that the incompressibility condition is automatically satisfied and Eq. (3.11) witnesses that $p \neq p(y)$. From Eqs. (3.10) and (3.11) we have

$$0 = \frac{\partial^2}{\partial y^2} \left[\mu(\theta) \frac{\partial^2 \psi}{\partial y^2} \right] - \left\{ M^2 \cos^2 \beta + \frac{\mu(\theta)}{k} \right\} \left(\frac{\partial^2 \psi}{\partial y^2} \right) + G_t \frac{\partial \theta}{\partial y} \text{Si} n \alpha_1. \quad (3.14)$$

Here ν denotes the kinematic viscosity, Re the Reynolds number, Br the Brinkman number, E the Eckret number, Pr the Prandtl number, δ the wave number, Gr the Grashoff number, Fr the Froud number, k the dimensionless permeability parameter and θ the dimensionless temperature.

We consider the temperature dependent viscosity in the form

$$\mu(\theta) = e^{-\alpha\theta}$$

which gives

$$\mu(\theta) = 1 - \alpha\theta, \quad \text{for } \alpha \ll 1.$$

where α is the viscosity parameter. Note that for $\alpha = 0$ our problem reduces to the constant viscosity case.

The dimensionless volume flow rate in laboratory frame is defined by

$$Q = \int_0^{\bar{H}} \bar{U}(\bar{X}, \bar{Y}, \bar{t}) dY \quad (3.15)$$

and in wave frame we have

$$q = \int_0^h \bar{u}(x, y) dy \quad (3.16)$$

in which h is function of x alone. From Eqs. (3.14), (3.15) and (3.6) one has

$$Q = q + ch(x).$$

The time averaged flow over a period T_f is

$$\overline{Q} = \frac{1}{T} \int_0^{T_f} Q dt$$

which implies that

$$\overline{Q} = q + ca.$$

Defining η and F as the dimensionless mean flows in the laboratory and wave frames by

$$\eta = \frac{\overline{Q}}{ca}, \quad F = \frac{q}{ca} \quad (3.17)$$

one can write

$$\eta = F + 1, \quad (3.18)$$

where

$$F = \int_0^h \frac{\partial \psi}{\partial y} dy. \quad (3.19)$$

The corresponding boundary conditions for the present flow configuration are

$$\begin{aligned} \psi &= 0, \quad \psi_{yy} = 0, \quad \theta_y = 0, \quad y = 0, \\ \psi &= F, \quad \psi_y = -1, \quad \theta = 0, \quad y = h, \end{aligned} \quad (3.20)$$

with

$$h(x) = 1 + a \cos(2\pi x). \quad (3.21)$$

3.2 Solution and analysis

Numerical solutions of the derived problems are obtained. For that we have taken 0.01 as the step size for the variations of x and y . The obtained results are analyzed graphically in this section.

The graphs of pressure gradient, stream function, velocity and temperature are examined. Moreover, the numerical values of heat transfer rate at the wall are computed and analyzed through Table 3.1. Hence Figs. 3.1(a-h) are plotted to analyze the pressure gradient variation with respect to different embedded parameters. Figs. 3.2-3.8 depict the behavior of streamlines, Figs. 3.9(a-f) for velocity and Figs. 3.10(a-f) for the temperature profile.

It is seen that the pressure gradient varies and has maximum value at the wider part of the channel. Minimum value of the pressure gradient is found near the more occlude part of the channel. It is observed that value of the pressure gradient increases with an increase in the variable viscosity parameter i.e. the pressure gradient has a higher value for the variable viscosity fluid than that of the fluid with constant viscosity (see Fig. 3.1a). Presence of porous medium decreases the value of pressure gradient (see Fig. 3.1b). Pressure gradient is larger when we move from the horizontal to the vertical channel. Increase in the Hartman number and decrease in the magnetic field inclination tend to decrease the pressure gradient (Figs. 3.1d and f). An increase in Froud number decreases the pressure gradient while the Brinkman number increases its value (Figs. 3.1e and h). Corresponding value of the pressure gradient is higher in the case of resisting (or opposing) flow when compared to that of the assisting flow (Fig. 3.1g).

The volume of the fluid trapped within a streamline is usually termed as bolus. This study showed that the size of the trapped bolus decreases with an increase in the magnetic field parameter M (see Fig. 3.2). Bolus size is smaller in the case of fluid with constant viscosity (see Fig. 3.3). Size of the trapped bolus increases with an increase in the value of the porosity parameter k . It means that the bolus size gets reduced in case of flow through porous medium (Fig. 3.4). From Fig. 3.5 it is observed that the impact of channel inclination on the size of the trapped bolus is not very significant. However an increase in channel inclination enhances the bolus size by a very small amount. An increase in both magnetic field inclination and Brinkman number give rise to an increase in the size of the trapped bolus (see Figs. 3.6 and 3.7). Bolus is found to have a comparatively larger size in the case of assisting flow (+ value of g) (see Fig.

3.8).

Velocity profile is seen to follow a parabolic trajectory with maximum value near the center of the channel. Such value of the velocity increases when we move from constant viscosity fluid to the fluid with temperature dependent viscosity. It is seen from Fig. 3.9b that the velocity decreases in the case of porous medium. Increase in the Hartman number decreases the velocity near the center line whereas the case is opposite for an increase in Brinkman number (see Figs. 3.9d and f). Inclination of the channel results in the increase of the velocity for both assisting and resisting flows (see Fig. 3.9c). Fig. 3.9e revealed that the velocity has a higher value for assisting flow.

Dimensionless temperature is analyzed in the Figs. 3.10(a-f). Fig. 3.10a showed that the temperature is higher for the case of constant viscosity fluid when compared with the fluid of variable viscosity. Fig. 3.10b depicts that an increase in the value of permeability parameter decreases the value of the dimensionless temperature. Dimensionless temperature increases with an increase in the value of the Hartman number (Fig. 3.10 c). Similarly temperature is higher for the case of assisting flow (see Fig. 3.10 d). Increase in inclination of channel gives higher value of the temperature whereas the case is opposite for the inclination of magnetic field (see Figs. 3.10 e and f).

Numerical values of the heat transfer rate at the wall for different parameters are plotted in Table 3.1. It is noted that the heat transfer rate decreases by increasing the viscosity parameter α , permeability parameter k , Grashoff number G_t and channel and magnetic field inclinations (α_1 and β respectively). However it increases due to increase in Hartman number (M) and Brinkman number Br .

3.3 Key findings

Numerical solution for the peristaltic transport of the variable viscosity fluid with porous medium and heat transfer in an inclined channel is obtained and analyzed. The main points of present attempt are listed below.

- Pressure gradient has a higher value for variable viscosity fluid than constant viscosity fluid.

- There is a decrease of pressure gradient in presence of porous medium.
- Pressure gradient has higher value when channel is vertical and there is resisting flow.
- Size of the trapped bolus increases with an increase in viscosity and permeability parameters.
- Trapped bolus has a larger size for assisting flow case.
- Fluid velocity with constant viscosity is less when compared to that of variable viscosity.
- Effects of porous medium on pressure gradient and velocity are qualitatively similar.
- Unlike the velocity, the temperature of the fluid is higher for constant viscosity case.
- Temperature is higher for the case of assisting flow.
- Heat transfer rate at the wall decreases with the increase in channel and magnetic field inclinations.

The used values of the parameters here are $\alpha = 0.2, k = 1.0, \alpha_1, \beta = \pi/4, \text{Re} = 5, Fr = 2, Br = 0.5, M = 0.5, G_t = 0.5, a = 0.3$ and $\eta = 0.3$ (unless stated otherwise).

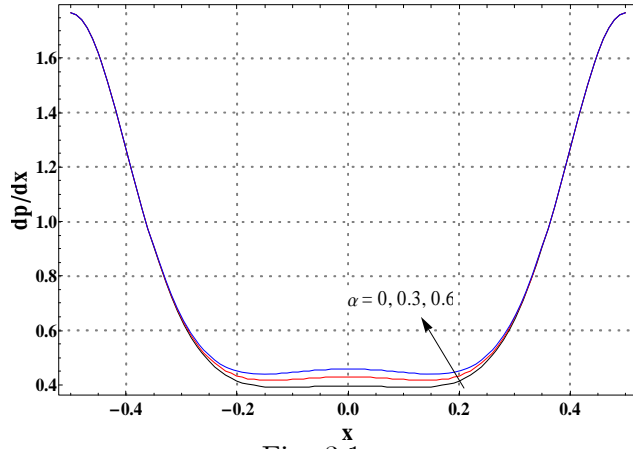


Fig. 3.1 a

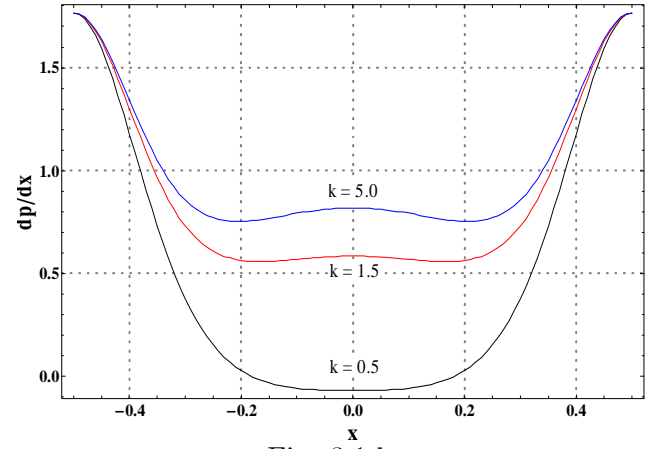


Fig. 3.1 b

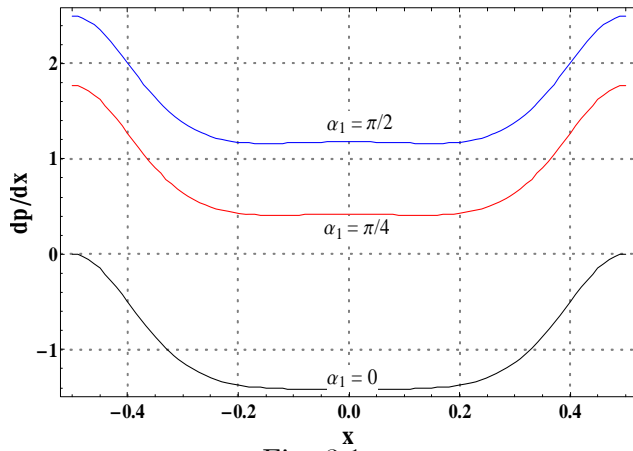


Fig. 3.1 c

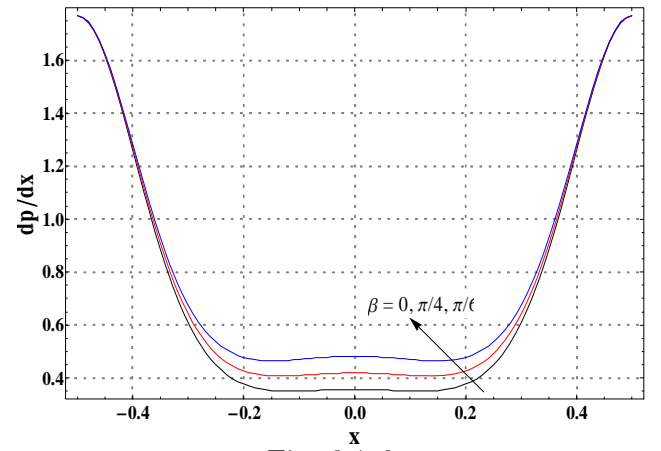


Fig. 3.1 d

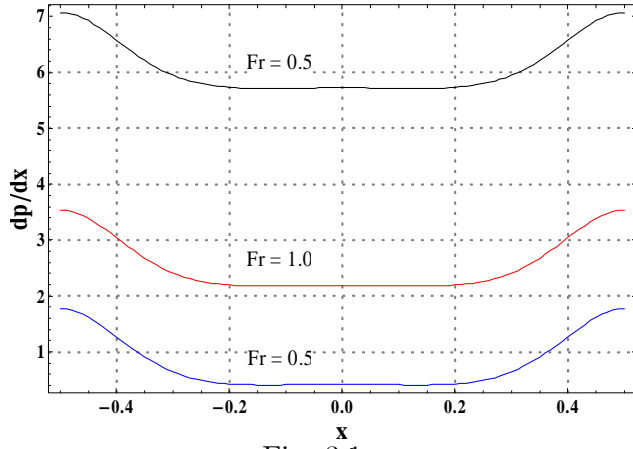


Fig. 3.1 e

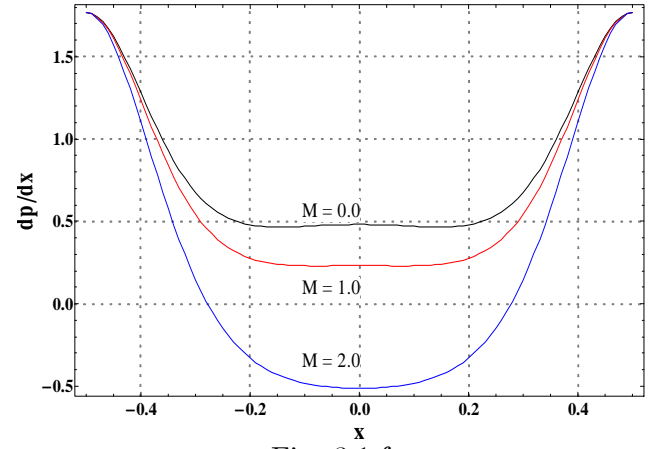


Fig. 3.1 f

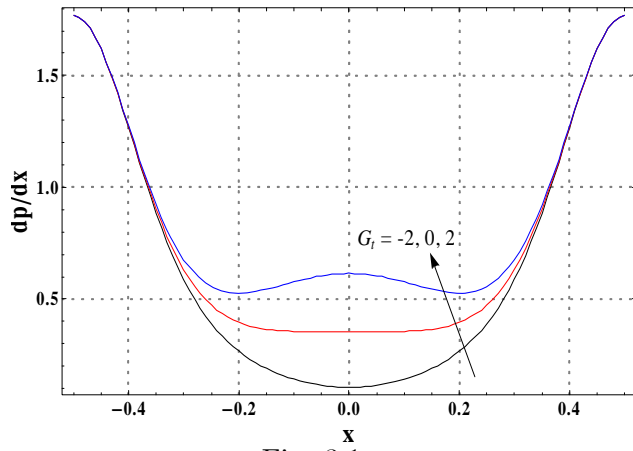


Fig. 3.1 g

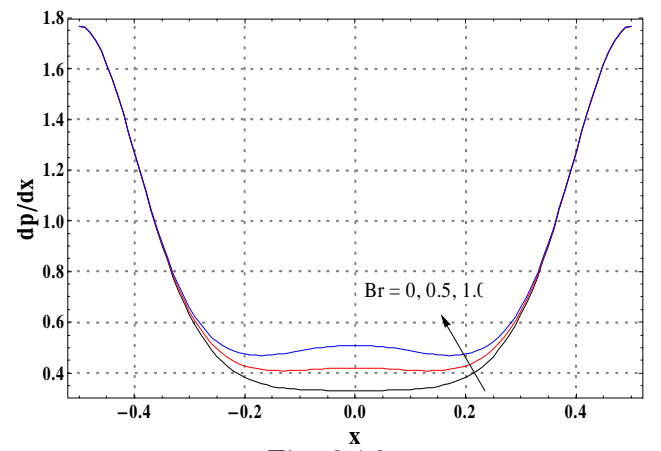


Fig. 3.1 h

Figs. 3.1 (a-h) Pressure gradient for the various parameters.

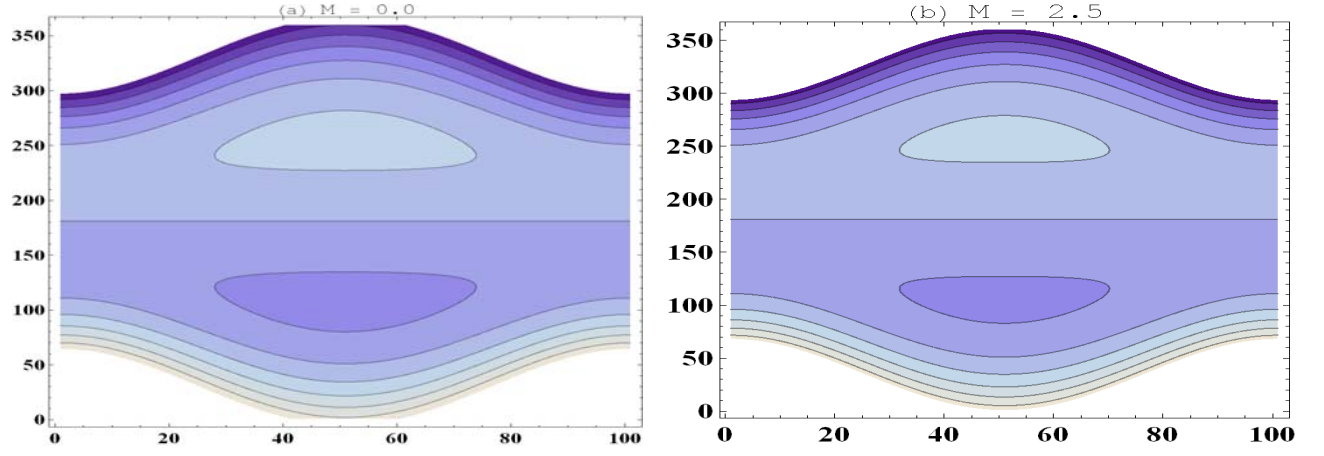


Fig. 3.2 Streamlines for variation of Hartman number.

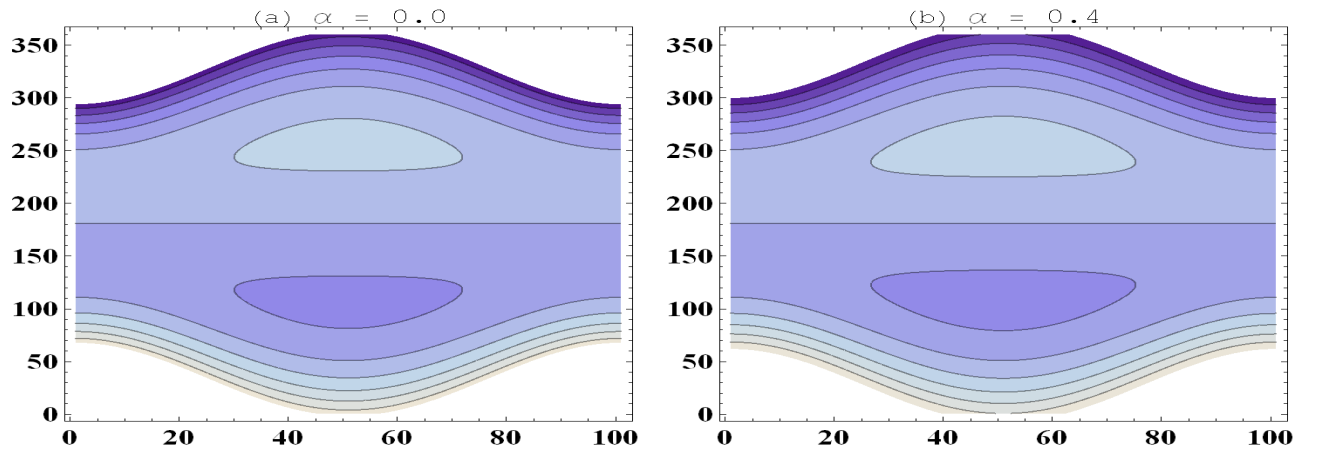


Fig. 3.3 Streamlines for variation of viscosity parameter.

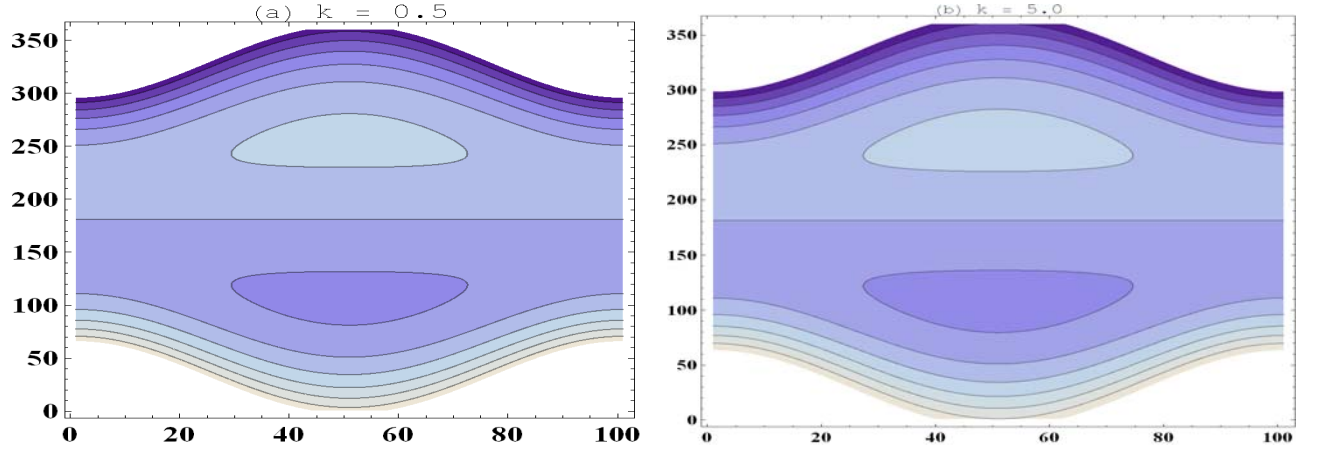


Fig. 3.4 Streamlines for variation of porosity parameter.

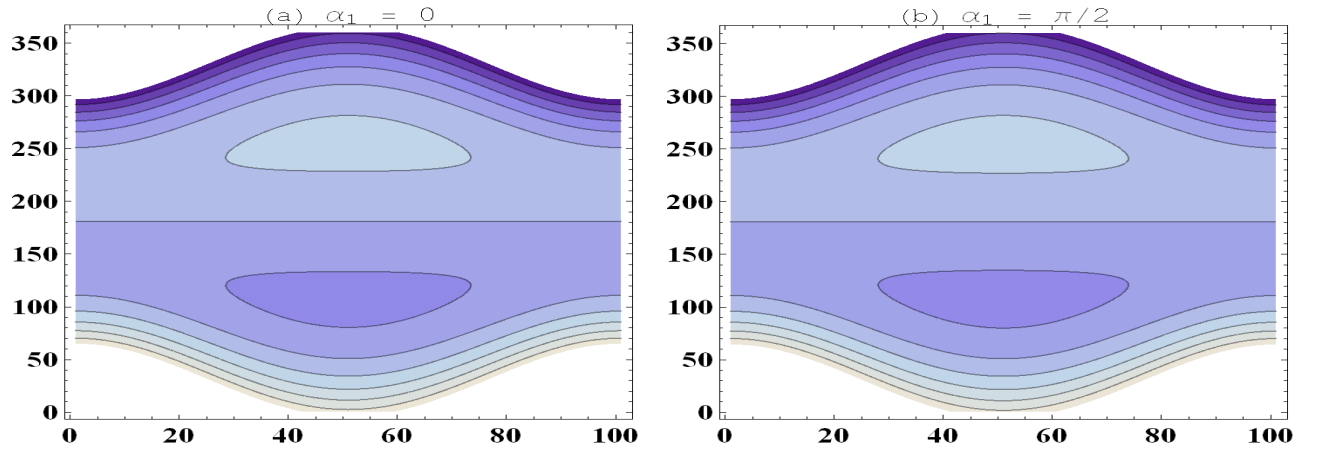


Fig. 3.5 Streamlines for variation of channel inclination.

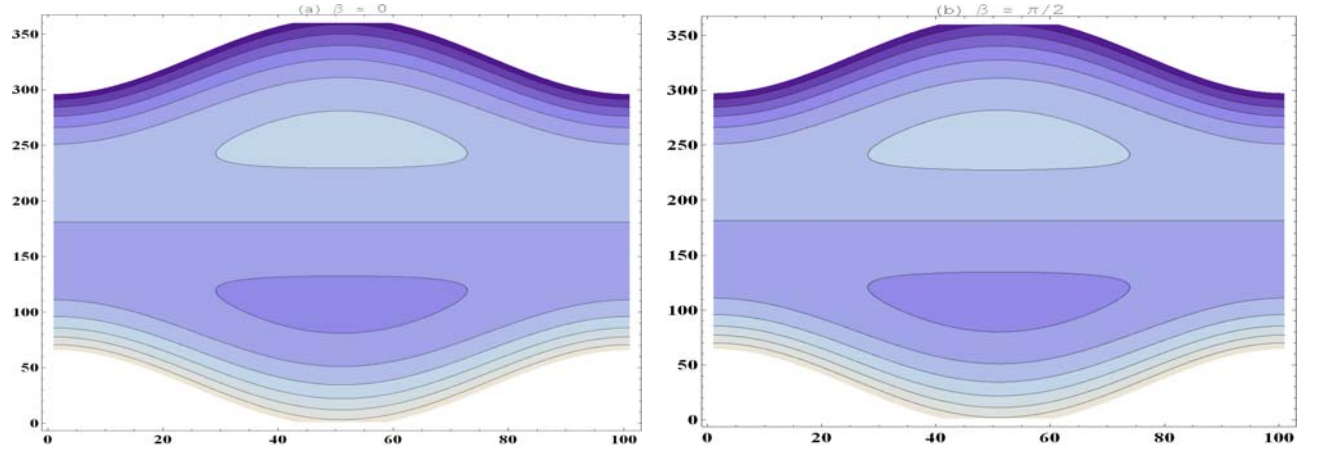


Fig. 3.6 Streamlines for different inclinations of magnetic field.

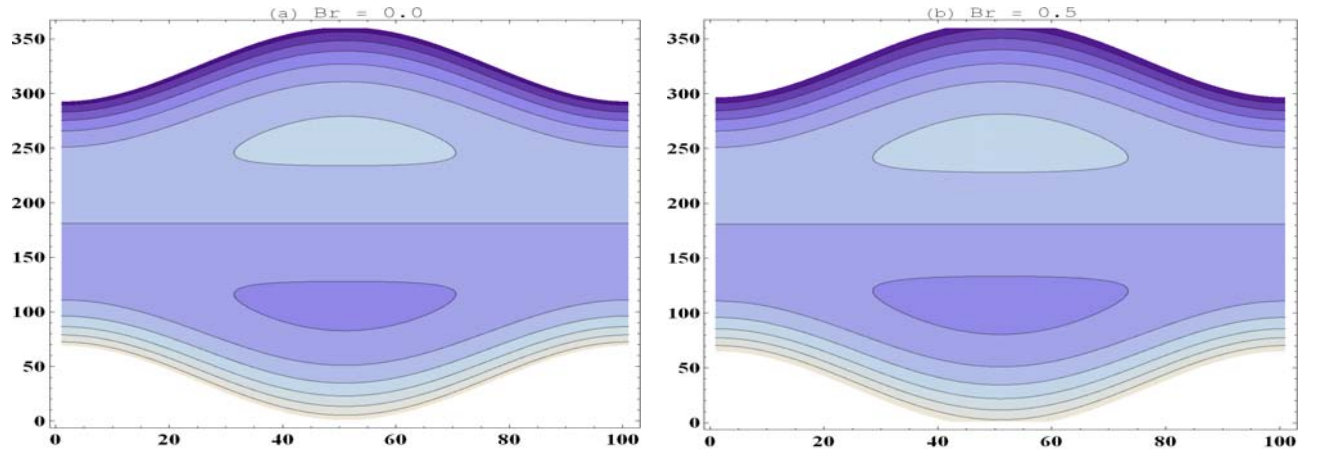


Fig. 3.7 Streamlines for different Brinkman number.

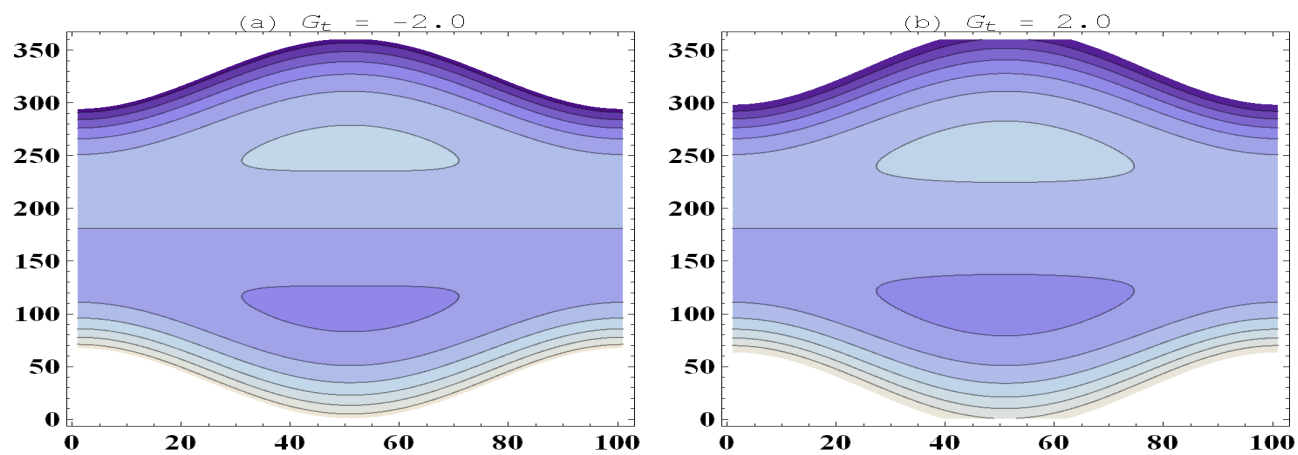


Fig. 3.8 Streamlines for different Grashoff number.

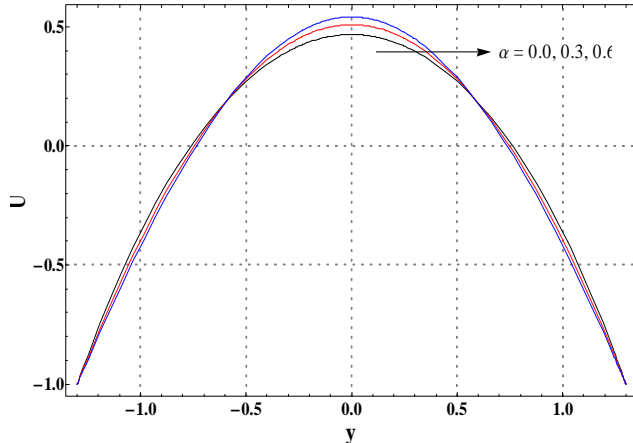


Fig. 3.9 a

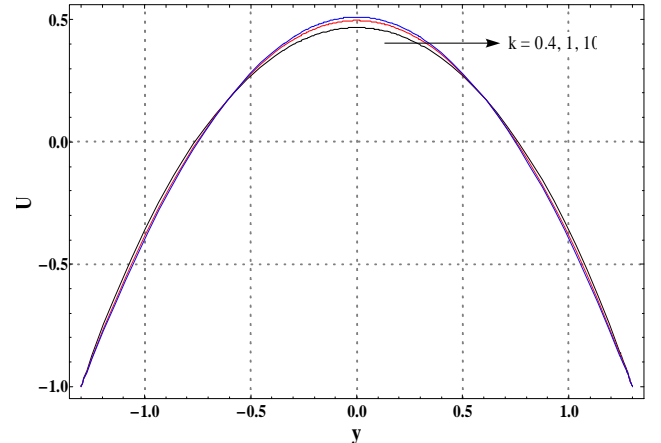


Fig. 3.9 b

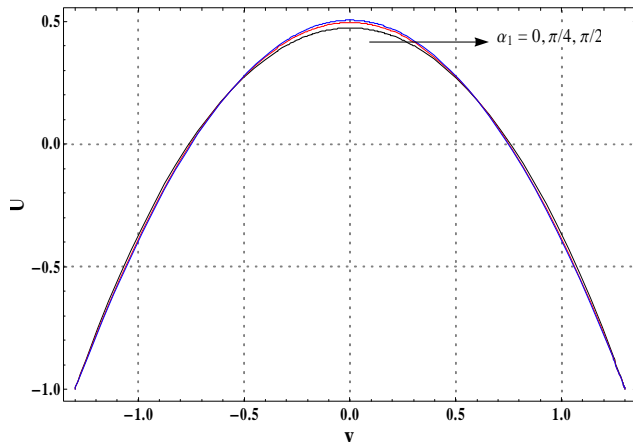


Fig. 3.9 c

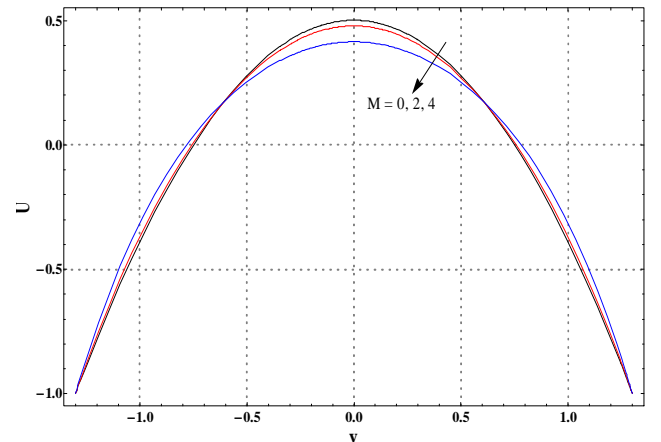


Fig. 3.9 d

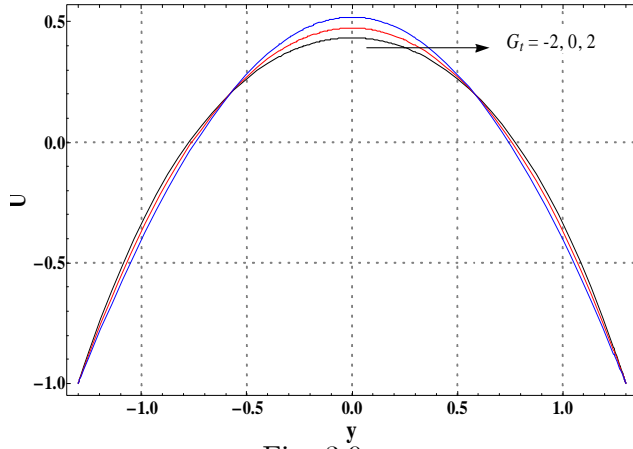


Fig. 3.9 e

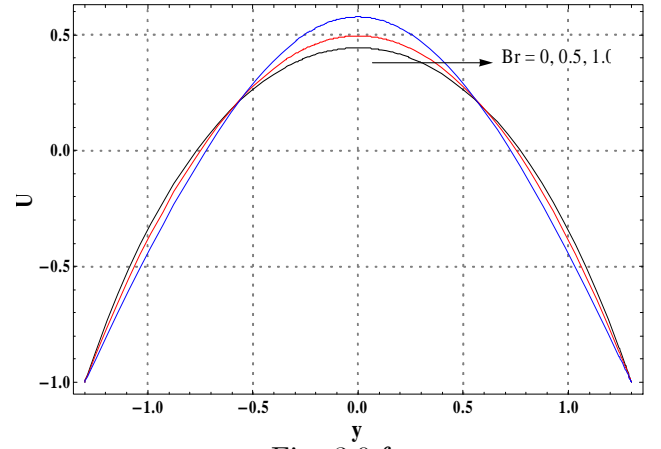


Fig. 3.9 f

Figs. 3.9 (a-f) Velocity profile for different parameters.

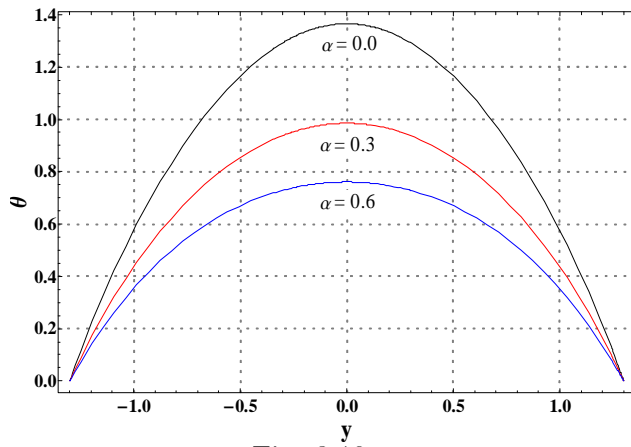


Fig. 3.10 a

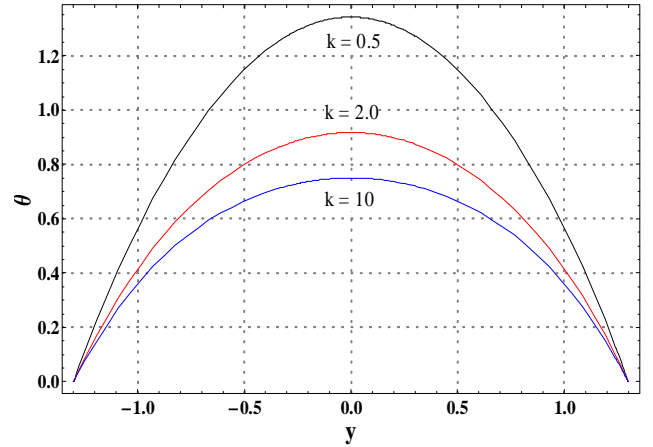


Fig. 3.10 b

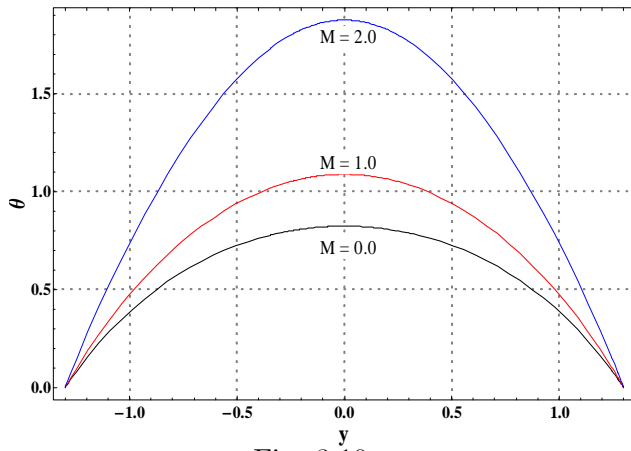


Fig. 3.10 c

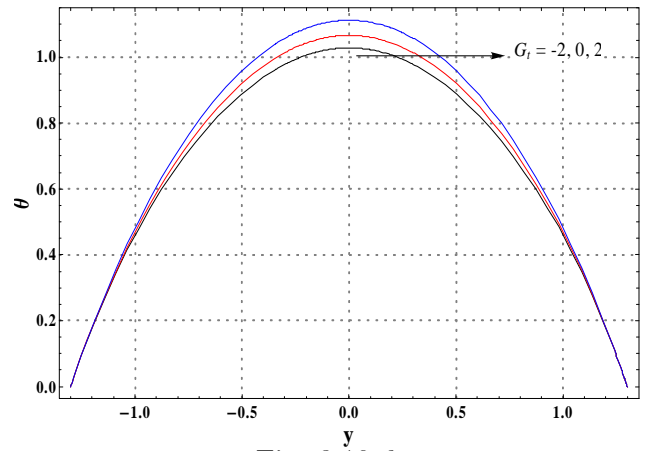


Fig. 3.10 d

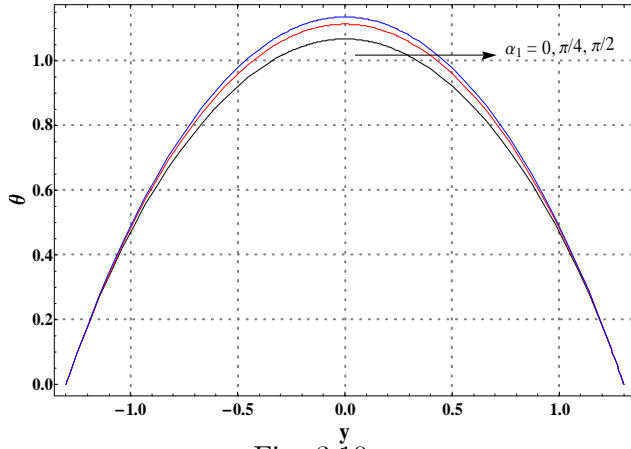


Fig. 3.10 e

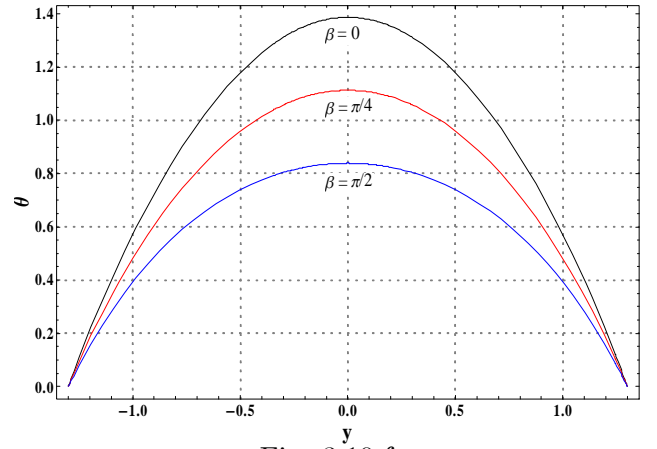


Fig. 3.10 f

Figs. 3.10 (a-f) Temperature profile for different parameters.

α	k	M	G_t	α_1	β	Br	$\theta'(h)$
0.0	1.0	1.0	2	$\pi/4$	$\pi/4$	0.5	2.32081
0.3							1.76871
0.6							1.44276
0.2	0.5						2.24094
	2.0						1.71568
	10.0						1.52373
	1.0	0.0					1.61917
		1.0					1.91839
		2.0					2.8159
		1.0	-2.0				1.95425
			0.0				1.93242
			2.0				1.91839
			1.0	0.0			1.93242
				$\pi/4$			1.92427
				$\pi/2$			1.92153
				$\pi/4$	0.0		2.22499
					$\pi/4$		1.92427
					$\pi/2$		1.62345
					$\pi/4$	0.1	0.401872
						0.2	0.795321
						0.3	1.18027

Table 3.1. Numerical values of heat transfer rate at the wall for different parameters.

Chapter 4

Peristaltic flow in an asymmetric channel with convective boundary conditions and Joule heating

This chapter concentrates on the peristaltic transport of viscous fluid in an asymmetric channel. The channel walls exhibit convective type boundary conditions. Both cases of hydrodynamic and magnetohydrodynamic (MHD) fluids are considered. Analytic solutions for stream function and temperature are constructed. Numerical integration is carried out for pressure rise per wavelength. Effects of influential flow parameters are pointed out through graphs.

4.1 Mathematical analysis

Consider the peristaltic transport of an incompressible MHD viscous fluid in an asymmetric channel of width $d_1 + d_2$. The \bar{X} -axis is taken along the length of the channel whereas the \bar{Y} -axis is taken normal to the \bar{X} -axis. The flow is due to the waves travelling on the walls of channel. A constant magnetic field B_0 is applied in the \bar{Y} - direction. The fluid is electrically conducting while the channel walls are non-conducting. The upper \bar{H}_1 and lower \bar{H}_2 walls are maintained at the temperature T_0 and T_1 respectively. The geometry of the walls is given as follows

$$\begin{aligned}\overline{H}_1(\overline{X}, \overline{t}) &= d_1 + a_1 \cos \left(\frac{2\pi}{\lambda} (\overline{X} - c\overline{t}) \right), \\ \overline{H}_2(\overline{X}, \overline{t}) &= -d_2 - b_1 \cos \left(\frac{2\pi}{\lambda} (\overline{X} - c\overline{t}) + \gamma \right),\end{aligned}\tag{4.1}$$

where a_1 and b_1 are the amplitudes of the waves travelling on the upper and lower walls, λ is the wavelength, c is the wave speed, γ is the phase difference and \overline{t} is the time. The laws of mass, momentum and energy yield

$$\frac{\partial \overline{U}}{\partial \overline{X}} + \frac{\partial \overline{V}}{\partial \overline{Y}} = 0, \tag{4.2}$$

$$\rho \left(\frac{\partial}{\partial \overline{t}} + \overline{U} \frac{\partial}{\partial \overline{X}} + \overline{V} \frac{\partial}{\partial \overline{Y}} \right) \overline{U} = -\frac{\partial \overline{P}}{\partial \overline{X}} + \mu \left[\frac{\partial^2 \overline{U}}{\partial \overline{X}^2} + \frac{\partial^2 \overline{U}}{\partial \overline{Y}^2} \right] - \sigma B_0^2 \overline{U}, \tag{4.3}$$

$$\rho \left(\frac{\partial}{\partial \overline{t}} + \overline{U} \frac{\partial}{\partial \overline{X}} + \overline{V} \frac{\partial}{\partial \overline{Y}} \right) \overline{V} = -\frac{\partial \overline{P}}{\partial \overline{Y}} + \mu \left[\frac{\partial^2 \overline{V}}{\partial \overline{X}^2} + \frac{\partial^2 \overline{V}}{\partial \overline{Y}^2} \right], \tag{4.4}$$

$$\begin{aligned}\rho C_p \left(\frac{\partial}{\partial \overline{t}} + \overline{U} \frac{\partial}{\partial \overline{X}} + \overline{V} \frac{\partial}{\partial \overline{Y}} \right) T &= K \left[\frac{\partial^2 T}{\partial \overline{X}^2} + \frac{\partial^2 T}{\partial \overline{Y}^2} \right] \\ + \mu \left[2 \left(\left(\frac{\partial \overline{U}}{\partial \overline{X}} \right)^2 + \left(\frac{\partial \overline{V}}{\partial \overline{Y}} \right)^2 \right) + \left(\frac{\partial \overline{U}}{\partial \overline{Y}} + \frac{\partial \overline{V}}{\partial \overline{X}} \right)^2 \right] &+ \sigma B_0^2 \overline{U}^2,\end{aligned}\tag{4.5}$$

where $(\overline{U}, \overline{V})$ are the velocity components in $(\overline{X}, \overline{Y})$ directions respectively, P the pressure, μ the dynamic viscosity, ρ the density of fluid, σ the electrical conductivity, K the thermal conductivity and C_p the specific heat. We have an interest to transform our problem from the fixed frame $(\overline{X}, \overline{Y})$ to the moving/wave frame $(\overline{x}, \overline{y})$. For that we define

$$\overline{x} = \overline{X} - c\overline{t}, \quad \overline{y} = \overline{Y}, \quad \overline{u} = \overline{U} - c, \quad \overline{v} = \overline{V}, \quad \overline{p}(\overline{x}, \overline{y}) = \overline{P}(\overline{X}, \overline{Y}, \overline{t}). \tag{4.6}$$

On setting

$$\begin{aligned}
x &= \frac{\bar{x}}{\lambda}, \quad y = \frac{\bar{y}}{d_1}, \quad u = \frac{\bar{u}}{c}, \quad v = \frac{\bar{v}}{c\delta}, \quad \delta = \frac{d_1}{\lambda}, \quad h_1 = \frac{\bar{H}_1}{d_1}, \\
h_2 &= \frac{\bar{H}_2}{d_1}, \quad d = \frac{d_2}{d_1}, \quad a = \frac{a_1}{d_1}, \quad b = \frac{b_1}{d_1}, \quad p = \frac{d_1^2 \bar{p}}{c\lambda\mu}, \quad v = \frac{\mu}{\rho}, \\
Re &= \frac{\rho c d_1}{\mu}, \quad t = \frac{c\bar{t}}{\lambda}, \quad M = \left(\frac{\sigma}{\mu}\right)^{1/2} B_0 d_1, \quad \theta = \frac{T - T_0}{T_1 - T_0}, \quad Br = \text{Pr } E, \\
E &= \frac{c^2}{C_p (T_1 - T_0)}, \quad Pr = \frac{\mu C_p}{K}, \quad u = \frac{\partial \psi}{\partial y}, \quad v = -\frac{\partial \psi}{\partial x}
\end{aligned} \tag{4.7}$$

dimensionless form of Eqs. (4.2 – 4.5) take the following form

$$\frac{\partial u}{\partial x} + \frac{\partial v}{\partial y} = 0, \tag{4.8}$$

$$\delta \text{Re} \left((u+1) \frac{\partial u}{\partial x} + v \frac{\partial u}{\partial y} \right) = -\frac{\partial p}{\partial x} + \left(\delta^2 \frac{\partial^2 u}{\partial x^2} + \frac{\partial^2 u}{\partial y^2} \right) - M^2(u+1), \tag{4.9}$$

$$\delta^3 \text{Re} \left((u+1) \frac{\partial v}{\partial x} + v \frac{\partial v}{\partial y} \right) = -\frac{\partial p}{\partial y} + \delta^2 \left(\delta^2 \frac{\partial^2 v}{\partial x^2} + \frac{\partial^2 v}{\partial y^2} \right), \tag{4.10}$$

$$\begin{aligned}
&\delta \text{Pr Re} \left((u+1) \frac{\partial \theta}{\partial x} + v \frac{\partial \theta}{\partial y} \right) = \delta^2 \frac{\partial^2 \theta}{\partial x^2} + \frac{\partial^2 \theta}{\partial y^2} \\
&+ Br \left[2\delta^2 \left(\left(\frac{\partial v}{\partial y} \right)^2 + \left(\frac{\partial u}{\partial x} \right)^2 \right) + \left(\delta^2 \frac{\partial v}{\partial x} + \frac{\partial u}{\partial y} \right)^2 \right] + Br M^2(u+1)^2.
\end{aligned} \tag{4.11}$$

Here v denotes the kinematic viscosity, M the Hartman number, Re the Reynolds number, Br the Brinkman number, E the Eckret number, Pr the Prandtl number, δ the wave number and θ the dimensionless temperature. Making use of the long wavelength and low Reynolds number approximation we have

$$\frac{dp}{dx} = \frac{\partial^3 \psi}{\partial y^3} - M^2 \left(\frac{\partial \psi}{\partial y} + 1 \right), \tag{4.12}$$

$$\frac{\partial p}{\partial y} = 0, \tag{4.13}$$

$$0 = \frac{\partial^2 \theta}{\partial y^2} + Br \left(\frac{\partial^2 \psi}{\partial y^2} \right)^2 + Br M^2 \left(\frac{\partial \psi}{\partial y} + 1 \right)^2, \tag{4.14}$$

where Eq. (4.12) indicates that $p \neq p(y)$.

Defining η and F as the dimensionless mean flows in laboratory and wave frames by

$$\eta = \frac{\bar{Q}}{cd_1}, \quad F = \frac{q}{cd_1}, \quad (4.15)$$

which after using $Q = q + c(d_1 + d_2)$ give

$$\eta = F + 1 + d, \quad (4.16)$$

where

$$F = \int_{h_2}^{h_1} \frac{\partial \psi}{\partial y} dy. \quad (4.17)$$

The convective boundary condition for the temperature can be expressed as follows

$$-K \frac{\partial T}{\partial Y} = l(T - T_w),$$

in which K is the thermal conductivity, l the wall heat transfer coefficient and T_w the temperature of the wall. Physically this condition states that the rate of heat transfer from the wall to the fluid (or vice versa) is proportional to the difference of their temperature. Having in mind the asymmetric nature of considered channel, we choose l_1 and l_2 the respective heat transfer coefficients of upper and lower walls. Hence the dimensionless boundary conditions are

$$\begin{aligned} \psi &= \frac{F}{2}, \quad \frac{\partial \psi}{\partial y} = -1, \quad \frac{\partial \theta}{\partial y} + Bi_1 \theta = 0, \quad \text{at } y = H_1, \\ \psi &= -\frac{F}{2}, \quad \frac{\partial \psi}{\partial y} = -1, \quad \frac{\partial \theta}{\partial y} - Bi_2(\theta - 1) = 0, \quad \text{at } y = H_2, \end{aligned} \quad (4.18)$$

$$h_1(x) = 1 + a \cos(2\pi x), \quad h_2(x) = -d - b \cos(2\pi x + \phi), \quad (4.19)$$

$$Bi_1 = \frac{l_1 d_1}{K}, \quad Bi_2 = \frac{l_2 d_1}{K}, \quad (4.20)$$

where $Bi_{1,2}$ are the Biot-numbers for the upper and lower walls. Pressure rise per wavelength is given by

$$\Delta p_\lambda = \int_0^1 \frac{dp}{dx} dx. \quad (4.21)$$

4.2 Solution expressions

The solutions of Eqs. (4.12) and (4.14) subject to the conditions (4.18) are

$$\psi = \frac{-e^{-My}}{2L_1} (L_2 - L_3), \quad (4.22)$$

$$\theta = \frac{1}{L_4} \left(\frac{-L_5}{A_1} + (1 + Bi_1 h_1) L_6 + \frac{L_7}{(A_1)} \right). \quad (4.23)$$

For $M = 0$ one has

$$\psi = -\frac{(h_1 + h_2 - 2y)(-2(h_1 - h_2)(h_1 - y)(h_2 - y) + FL_8)}{2(h_1 - h_2)^3}, \quad (4.24)$$

$$\begin{aligned} \theta = & 1 + \frac{6Br(F + h_1 - h_2)^2}{Bi_2(h_1 - h_2)^3} + \frac{3Bi_2Br(F + h_1 - h_2)^2}{4Bi_2(h_1 - h_2)^2} - \frac{C_1}{Bi_2C_2} \\ & - \frac{3Br(F + h_1 - h_2)^2(h_1 + h_2 - 2y)^4}{4(h_1 - h_2)^6} + \frac{C_3y}{C_2}. \end{aligned} \quad (4.25)$$

and L_i s, A_i s and C_i s are given as follows:

$$\begin{aligned}
C_1 &= \left(Bi_1 \left(Bi_2 (h_1 - h_2)^3 + 6Br (F + h_1 - h_2)^2 \right) + 6Bi_2 Br (F + h_1 - h_2)^2 \right) (-1 + Bi_2 h_2), \\
C_2 &= (h_1 - h_2)^3 (Bi_1 + Bi_2 + Bi_2 Bi_1 h_1 - Bi_2 Bi_1 h_2), \\
C_3 &= \left(-Bi_1 \left(Bi_2 (h_1 - h_2)^3 + 6Br (F + h_1 - h_2)^2 \right) + 6Bi_2 Br (F + h_1 - h_2)^2 \right), \\
L_1 &= \left(e^{h_1 M} (-2 + h_1 M - h_2 M) + e^{h_2 M} (2 + h_1 M - h_2 M) \right), \\
L_2 &= (F + h_1 - h_2) \left(2e^{(h_1 + h_2)M} - 2e^{2My} \right), \\
L_3 &= e^{My} (h_1 + h_2 - 2y) \left(e^{Mh_2} (-2 + FM) - e^{Mh_1} (2 + FM) \right), \\
L_4 &= Bi_1 + Bi_2 + Bi_2 Bi_1 h_1 - Bi_2 Bi_1 h_2, \\
L_5 &= Br (1 - Bi_2 + h_2) M^2 (MA_2 + A_3 - A_4 - Bi_1 (A_5 + A_6)), \\
L_6 &= Bi_2 - \frac{1}{(A_1)} \times (Br M^2 (-A_2 - A_7)) + \left(\frac{Br Bi_2 M^2}{(A_1)} \times A_8 \right) - A_9, \\
L_7 &= Br M^2 (A_{10} - A_{11} y^2), \\
L_8 &= (h_1^2 - 4h_1 h_2 + h_2^2 + 2(h_1 + h_2)y - 2y^2). \\
A_1 &= 4 \left(e^{h_1 M} (-2 + h_1 M - h_2 M) + e^{h_2 M} (2 + h_1 M - h_2 M) \right)^2, \\
A_2 &= -2e^{2h_1 M} (F + h_1 - h_2)^2 (1 + M^2) + 2e^{2h_2 M} (F + h_1 - h_2)^2 (1 + M^2) \\
&\quad - 8e^{h_1 M} (F + h_1 - h_2) \left(e^{h_1 M} (-2 + h_1 M - h_2 M) + e^{h_2 M} (2 + h_1 M - h_2 M) \right), \\
A_3 &= 8e^{h_2 M} (F + h_1 - h_2) M \left(e^{h_1 M} (-2 + h_1 M - h_2 M) + e^{h_2 M} (2 + h_1 M - h_2 M) \right) \\
&\quad - 4h_1 \left(e^{2h_2 M} (2 + h_1 M - h_2 M)^2 + e^{2h_1 M} (2 + h_1 M - h_2 M)^2 \right), \\
A_4 &= 2e^{(h_1 + h_2)M} A_{13}, \\
A_5 &= e^{2h_1 M} (F + h_1 - h_2)^2 (1 + M^2) + 2e^{2h_2 M} (F + h_1 - h_2)^2 (1 + M^2) \\
&\quad - 8e^{h_1 M} (F + h_1 - h_2) \left(e^{h_1 M} (-2 + h_1 M - h_2 M) + e^{h_2 M} (2 + h_1 M - h_2 M) \right) \\
&\quad + 8e^{h_2 M} (F + h_1 - h_2), \\
A_6 &= 2h_1^2 \left(e^{2h_2 M} (2 + h_1 M - h_2 M)^2 + e^{2h_1 M} (2 - h_1 M + h_2 M)^2 - 2e^{(h_1 + h_2)M} A_{13} \right), \\
A_7 &= 8e^{h_2 M} (F + h_1 - h_2) M \left(e^{h_1 M} (-2 + h_1 M - h_2 M) + e^{h_2 M} (2 + h_1 M - h_2 M) \right) \\
&\quad + 4h_2 A_{12}, \\
A_8 &= e^{2h_1 M} (F + h_1 - h_2)^2 (1 + M^2) + 2e^{2h_2 M} (F + h_1 - h_2)^2 (1 + M^2) + 8A_{14},
\end{aligned}$$

$$\begin{aligned}
A_9 &= 8e^{h_2 M} (F + h_1 - h_2) \left(e^{h_1 M} (-2 + h_1 M - h_2 M) + e^{h_2 M} (2 + h_1 M - h_2 M) \right) + 2h_2^2 A_{12}, \\
A_{10} &= e^{2M(h_1+h_2-y)} (F + h_1 - h_2)^2 (1 + M^2) + 2e^{2yM} (F + h_1 - h_2)^2 (1 + M^2) \\
&\quad + 8e^{M(h_1+h_2-y)} (F + h_1 - h_2) A_{14}, \\
A_{11} &= 8e^{yM} (F + h_1 - h_2) M \left(e^{h_1 M} (-2 + h_1 M - h_2 M) + e^{h_2 M} (2 + h_1 M - h_2 M) \right) + 2A_{12}, \\
A_{12} &= e^{2h_2 M} (2 + h_1 M - h_2 M)^2 + e^{2h_1 M} (2 - h_1 M + h_2 M)^2 - 2e^{(h_1+h_2)M} A_{13}, \\
A_{13} &= 4 + h_1^2 M^4 - 2h_1 h_2 M^4 + h_2^2 M^4 + 2F(h_1 - h_2) M^2 (1 + M^2) + F^2 (M^2 + M^4), \\
A_{14} &= e^{h_1 M} (F + h_1 - h_2) \left(e^{h_1 M} (-2 + h_1 M - h_2 M) + e^{h_2 M} (2 + h_1 M - h_2 M) \right).
\end{aligned}$$

4.3 Graphical analysis

This section is concerned with the discussion of streamlines, pressure gradient and pressure rise per wavelength. This objective is achieved through Figs. 4.1-4.4. Dimensionless temperature profile is observed in the Figs. 4.5-4.7 for various parameters. In addition the heat transfer rate at the upper wall is numerically tabulated. Such numerical values are presented in Table 4.1.

Figs. 4.1 (a and b) examine the streamlines plotted against rate of volume flow η when $M = 0$. It is observed that there is a lower limit of flow rate below which no trapping occurs. This shows that without sufficient volume of the fluid flowing per unit time through the channel, trapping is unlikely to occur. The "threshold" or critical value of flow rate in present problem is observed which approximately is equal to 1.6. It is noticed that when the value of flow rate is increased from the critical value then the size of the trapped bolus not only increases but also it gets elongated (see Figs. 4.1a & 1b). Figs. 4.2 showed that the size of the trapped bolus decreases for a given value of flow rate and eventually vanishes when Hartman number increases.

Fig. 4.3 plots the pressure gradient. It is seen that the pressure gradient is maximum at the center of the channel i.e. in the wider part of the channel. Moreover the corresponding value of the pressure gradient is decreased when M has higher values. Pressure rise per wavelength decreases with an increase in flow rate and for a fixed value of flow rate the pressure rise also decreases by increasing the value of M .

Figs. 4.5a and 4.5b examine the temperature profile. Fig 4.5a includes the Joule heating

effect whereas Fig. 4.5b is without such effect. It is shown that there is no significant effect of M on the temperature profile when there is no Joule heating. However the temperature in presence of Joule heating effect increases significantly for an increase in M .

Figs. 4.6 (a and b) analyze the effects of Bi_1 and Bi_2 separately on the temperature. It is found that variation of Bi_1 has significant effect near the upper wall and hardly has any effect near the lower wall. Similarly the variation of Bi_2 is significant near the lower wall. Further the temperature decreases by increasing $Bi_{1,2}$. Fig. 4.7 is for the case when both the walls have same heat transfer coefficient i.e. $Bi_1 = Bi_2 = Bi$. Here the temperature also decreases with an increase in Bi . However such decrease is initially large.

Numerical values of heat transfer rate at the upper wall is given in Table 4.1. Here $\theta'(h_1)$ is the heat transfer rate for θ given in (4.21) and $(\theta^*)'(h_1)$ is one when we neglect the Joule heating effect. It is seen that the transfer rate increases when M and Bi 's are increased. This increase in heat transfer differs a lot in the two cases when Joule heating is considered and neglected. It is seen that Bi for one wall has very little or no effect (for large value of Bi) on transfer rate at the other wall.

4.4 Concluding remarks

Effects of convective boundary conditions and Joule heating on the peristaltic transport of MHD viscous fluid are examined. The key findings of the presented analysis are mentioned below.

- There is a critical value of the flow rate below which trapping is not likely to occur.
- The applied magnetic field tends to decrease the size of trapped bolus.
- Magnetic field decreases the magnitude of pressure gradient and pressure rise.
- Temperature rises in presence of Joule heating.
- Biot number decreases the dimensionless temperature.
- Effects of Hartman and Biot numbers on the heat transfer rate at the wall are opposite.

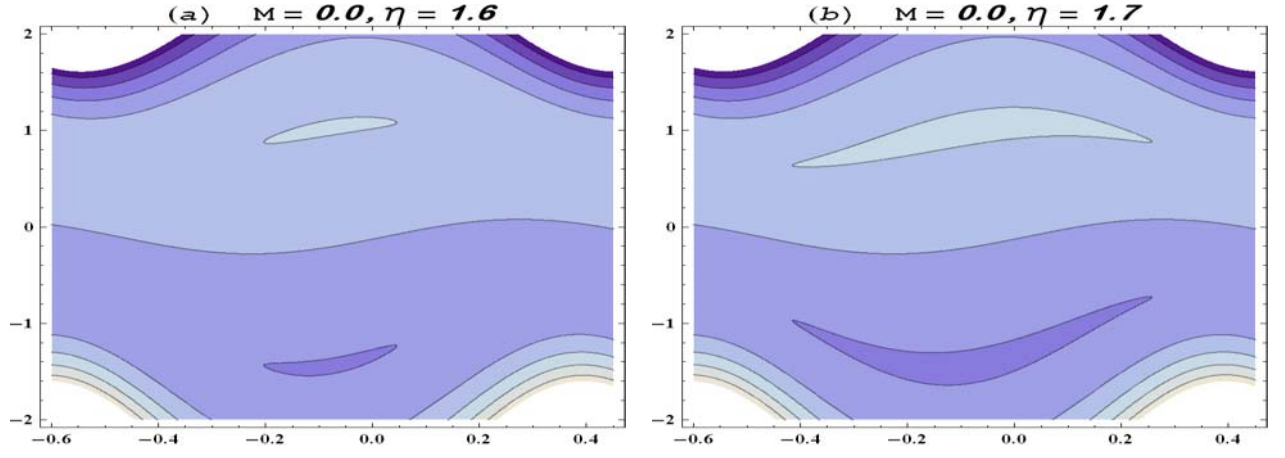


Fig. 4.1 Streamlines for $M = 0$.

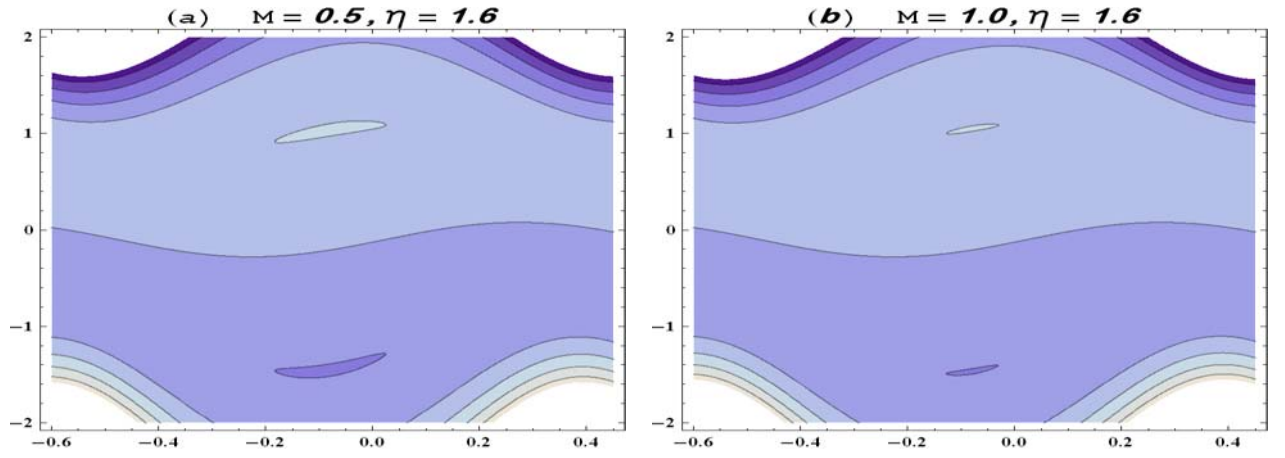


Fig. 4.2 Streamlines for $M \neq 0$.

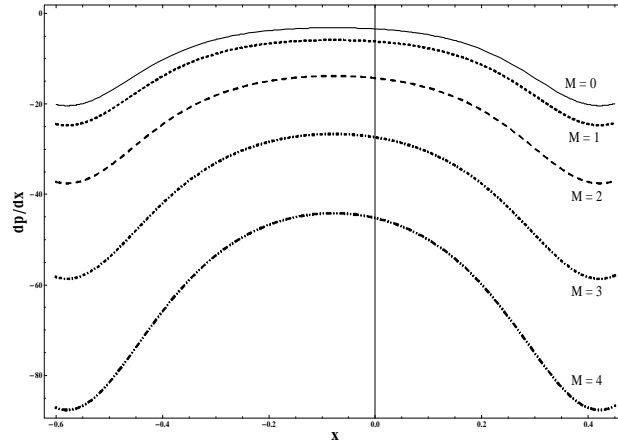


Fig. 4.3 Pressure gradient dp/dx for different values of M .

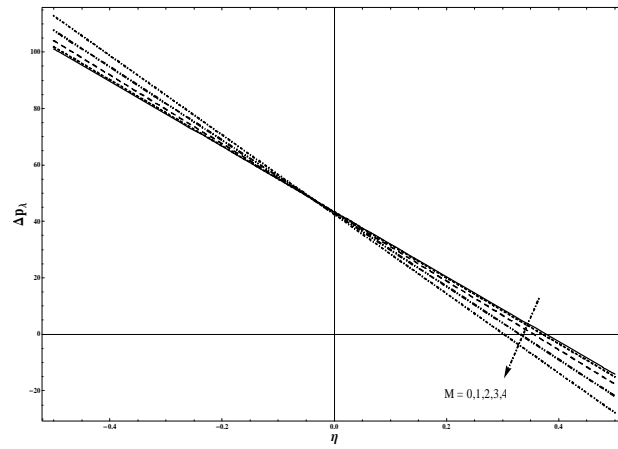


Fig. 4.4 Pressure rise Δp_λ for different values of M .

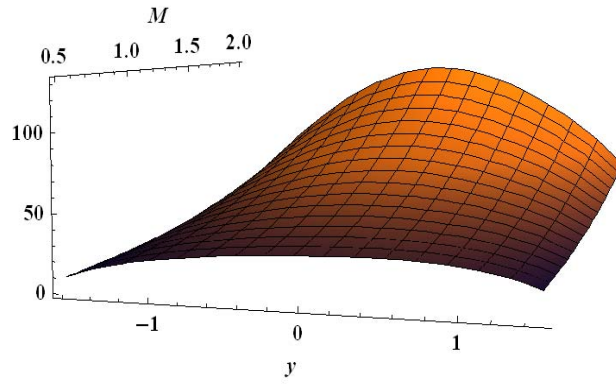


Fig. 4.5 (a)

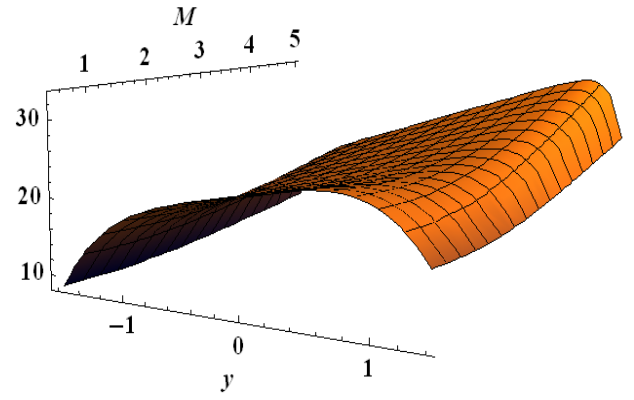


Fig. 4.5 (b)

Fig. 4.5 Dimensionless temperature with variation in M .

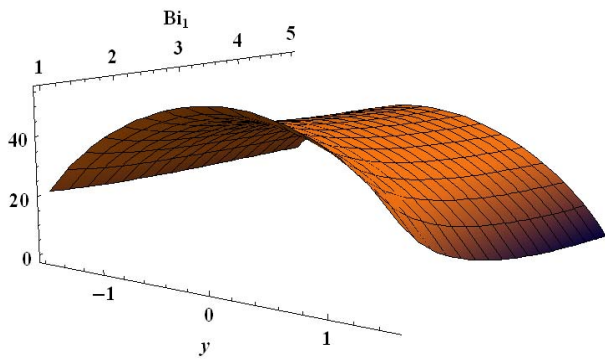


Fig. 4.6 (a)

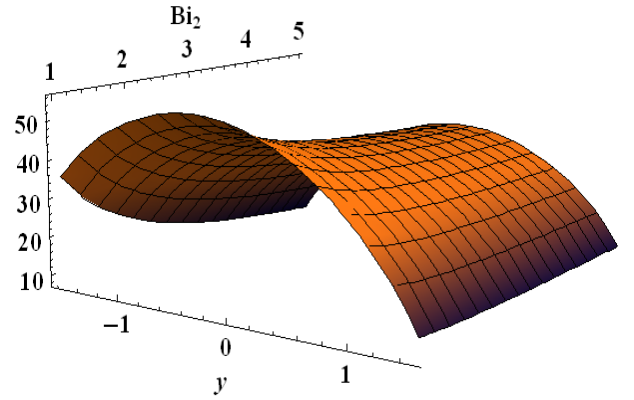


Fig. 4.6 (b)

Fig. 4.6 Dimensionless temperature with variation in $Bi_{1,2}$.

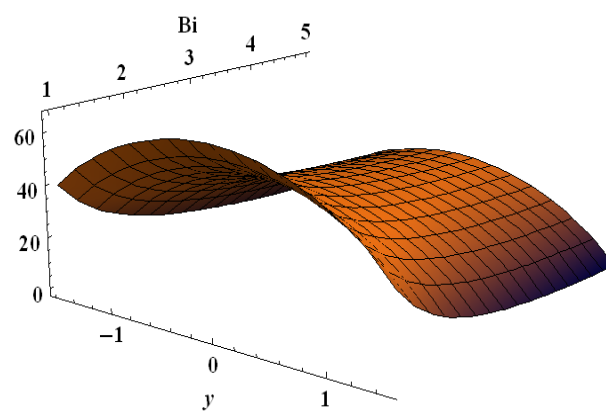


Fig. 4.7 Dimensionless temperature with $Bi_1 = Bi_2 = Bi$.

M	Bi_1	Bi_2	Br	$-\theta'(h_1)$	$-(\theta^*)'(h_1)$
0.5	1.0	2.0	2.0	12.1396	10.1291
1.0				18.1183	10.1291
1.5				27.9366	10.1291
2.0				41.4483	10.1291
			0.5	10.5343	2.70455
			1.0	20.839	5.17941
			1.5	31.1436	7.65427
			2.0	41.4483	10.1291
	0.5	0.5		46.7126	11.3298
	1.0	1.0		46.7727	11.3899
	1.5	1.5		46.8055	11.4227
	2.0	2.0		46.8262	11.4434

Table: 4.1. Effect of various parameters on heat transfer rate at the upper wall.

Chapter 5

Peristaltic motion with Soret and Dufour effects

This chapter examines the magnetohydrodynamic (MHD) peristaltic flow in a symmetric channel in the presence of Ohmic heating. Effects of Soret and Dufour are retained. Long wavelength and low Reynolds number assumptions are employed. Attention is mainly focused to analyze the flow quantities for various parameters of interest.

5.1 Mathematical analysis

We consider the flow of an incompressible MHD fluid in a channel of width $2d_1$. The \overline{X} – axis is chosen along the walls of channel and \overline{Y} – axis is selected normal to it. A uniform magnetic field \mathbf{B}_0 is applied in the Y direction and induced magnetic field is neglected. The channel walls are represented by

$$H(\overline{X}, \overline{t}) = d_1 + a_1 \cos \left(\frac{2\pi}{\lambda} (\overline{X} - c\overline{t}) \right), \quad (5.1)$$

where a_1 is the wave amplitude, λ is the wavelength, c is the wave velocity and \overline{t} is the time. The equations governing the two-dimensional flow are

$$\frac{\partial \overline{U}}{\partial \overline{X}} + \frac{\partial \overline{V}}{\partial \overline{Y}} = 0, \quad (5.2)$$

$$\rho \left(\frac{\partial}{\partial \bar{t}} + \bar{U} \frac{\partial}{\partial \bar{X}} + \bar{V} \frac{\partial}{\partial \bar{Y}} \right) \bar{U} = -\frac{\partial \bar{P}}{\partial \bar{X}} + \mu \left[\frac{\partial^2 \bar{U}}{\partial \bar{X}^2} + \frac{\partial^2 \bar{U}}{\partial \bar{Y}^2} \right] - \sigma B_0^2 \bar{U}, \quad (5.3)$$

$$\rho \left(\frac{\partial}{\partial \bar{t}} + \bar{U} \frac{\partial}{\partial \bar{X}} + \bar{V} \frac{\partial}{\partial \bar{Y}} \right) \bar{V} = -\frac{\partial \bar{P}}{\partial \bar{Y}} + \mu \left[\frac{\partial^2 \bar{V}}{\partial \bar{X}^2} + \frac{\partial^2 \bar{V}}{\partial \bar{Y}^2} \right], \quad (5.4)$$

$$\begin{aligned} \rho C_p \left(\frac{\partial}{\partial \bar{t}} + \bar{U} \frac{\partial}{\partial \bar{X}} + \bar{V} \frac{\partial}{\partial \bar{Y}} \right) \bar{T} &= K \left[\frac{\partial^2 \bar{T}}{\partial \bar{X}^2} + \frac{\partial^2 \bar{T}}{\partial \bar{Y}^2} \right] + \\ \mu \left[2 \left(\left(\frac{\partial \bar{U}}{\partial \bar{X}} \right)^2 + \left(\frac{\partial \bar{V}}{\partial \bar{Y}} \right)^2 \right) + \left(\frac{\partial \bar{U}}{\partial \bar{Y}} + \frac{\partial \bar{V}}{\partial \bar{X}} \right)^2 \right] &+ \sigma B_0^2 \bar{U}^2 + \frac{DK_T}{C_s} \left[\frac{\partial^2 \bar{C}}{\partial \bar{X}^2} + \frac{\partial^2 \bar{C}}{\partial \bar{Y}^2} \right] \end{aligned} \quad (5.5)$$

$$\left[\frac{\partial}{\partial \bar{t}} + \bar{U} \frac{\partial}{\partial \bar{X}} + \bar{V} \frac{\partial}{\partial \bar{Y}} \right] \bar{C} = D \left[\frac{\partial^2 \bar{C}}{\partial \bar{X}^2} + \frac{\partial^2 \bar{C}}{\partial \bar{Y}^2} \right] + \frac{DK_T}{T_m} \left[\frac{\partial^2 \bar{T}}{\partial \bar{X}^2} + \frac{\partial^2 \bar{T}}{\partial \bar{Y}^2} \right], \quad (5.6)$$

where (\bar{U}, \bar{V}) are velocity components in the laboratory frame (\bar{X}, \bar{Y}) , \bar{P} is pressure, \bar{C} the concentration field, \bar{T} the temperature field, D mass diffusivity, K_T thermal diffusion ratio, C_p specific heat, C_s concentration susceptibility, C_0 concentration at boundary, T_m and T_0 the fluid mean temperature and temperature at boundary respectively.

If (\bar{u}, \bar{v}) are the velocity components in the wave frame (\bar{x}, \bar{y}) then introducing

$$\bar{x} = \bar{X} - c\bar{t}, \quad \bar{y} = \bar{Y}, \quad \bar{u} = \bar{U} - c, \quad \bar{v} = \bar{V}, \quad \bar{p}(\bar{x}, \bar{y}) = \bar{P}(\bar{X}, \bar{Y}, \bar{t}) \quad (5.7)$$

equations (5.2)-(5.6) in wave frame are reduced as follows:

$$\frac{\partial \bar{u}}{\partial \bar{x}} + \frac{\partial \bar{v}}{\partial \bar{y}} = 0, \quad (5.8)$$

$$\rho \left((\bar{u} + c) \frac{\partial \bar{u}}{\partial \bar{x}} + \bar{v} \frac{\partial \bar{u}}{\partial \bar{y}} \right) = -\frac{\partial \bar{p}}{\partial \bar{x}} + \mu \left[\frac{\partial^2 \bar{u}}{\partial \bar{x}^2} + \frac{\partial^2 \bar{u}}{\partial \bar{y}^2} \right] - \sigma B_0^2 (\bar{u} + c), \quad (5.9)$$

$$\rho \left((\bar{u} + c) \frac{\partial \bar{v}}{\partial \bar{x}} + \bar{v} \frac{\partial \bar{v}}{\partial \bar{y}} \right) = -\frac{\partial \bar{p}}{\partial \bar{y}} + \mu \left[\frac{\partial^2 \bar{v}}{\partial \bar{x}^2} + \frac{\partial^2 \bar{v}}{\partial \bar{y}^2} \right], \quad (5.10)$$

$$\begin{aligned} \rho C_p \left((\bar{u} + c) \frac{\partial}{\partial \bar{x}} + \bar{v} \frac{\partial}{\partial \bar{y}} \right) \bar{T} &= K \left[\frac{\partial^2 \bar{T}}{\partial \bar{x}^2} + \frac{\partial^2 \bar{T}}{\partial \bar{y}^2} \right] + \\ \mu \left[2 \left(\left(\frac{\partial \bar{u}}{\partial \bar{x}} \right)^2 + \left(\frac{\partial \bar{v}}{\partial \bar{y}} \right)^2 \right) + \left(\frac{\partial \bar{u}}{\partial \bar{y}} + \frac{\partial \bar{v}}{\partial \bar{x}} \right)^2 \right] &+ \sigma B_0^2 (\bar{u} + c)^2 + \frac{DK_T}{C_s} \left[\frac{\partial^2 \bar{C}}{\partial \bar{x}^2} + \frac{\partial^2 \bar{C}}{\partial \bar{y}^2} \right] \end{aligned} \quad (5.11)$$

$$\left[(\bar{u} + c) \frac{\partial}{\partial \bar{x}} + \bar{v} \frac{\partial}{\partial \bar{y}} \right] \bar{C} = D \left[\frac{\partial^2 \bar{C}}{\partial \bar{x}^2} + \frac{\partial^2 \bar{C}}{\partial \bar{y}^2} \right] + \frac{DK_T}{T_m} \left[\frac{\partial^2 \bar{T}}{\partial \bar{x}^2} + \frac{\partial^2 \bar{T}}{\partial \bar{y}^2} \right]. \quad (5.12)$$

Defining

$$\begin{aligned}
x &= \frac{\bar{x}}{\lambda}, \quad y = \frac{\bar{y}}{d_1}, \quad u = \frac{\bar{u}}{c}, \quad v = \frac{\bar{v}}{c\delta}, \quad \delta = \frac{d_1}{\lambda}, \quad h = \frac{H}{d_1}, \quad a = \frac{a_1}{d_1}, \quad p = \frac{d_1^2 \bar{p}}{c\lambda\mu}, \\
\theta &= \frac{T - T_0}{T_0}, \quad \phi = \frac{C - C_0}{C_0}, \quad M = \left(\frac{\sigma}{\mu}\right)^{1/2} B_0 d_1, \quad v = \frac{\mu}{\rho}, \quad Re = \frac{\rho c d_1}{\mu}, \\
t &= \frac{c\bar{t}}{\lambda}, \quad Br = Pr E, \quad Du = \frac{DC_0 K_T}{C_s C_p \mu T_0}, \quad Sr = \frac{\rho D K_T T_0}{\mu T_m C_0}, \\
Sc &= \frac{\mu}{\rho D}, \quad E = \frac{c^2}{C_p T_0}, \quad Pr = \frac{\mu C_p}{K}, \quad u = \frac{\partial \psi}{\partial y} \text{ and } v = -\frac{\partial \psi}{\partial x},
\end{aligned} \tag{5.13}$$

the equations (5.8) – (5.12) in dimensionless form are stated as follows:

$$\frac{\partial u}{\partial x} + \frac{\partial v}{\partial y} = 0, \tag{5.14}$$

$$\delta Re \left((u+1) \frac{\partial u}{\partial x} + v \frac{\partial u}{\partial y} \right) = -\frac{\partial p}{\partial x} + \left(\delta^2 \frac{\partial^2 u}{\partial x^2} + \frac{\partial^2 u}{\partial y^2} \right) - M^2(u+1), \tag{5.15}$$

$$\delta^3 Re \left((u+1) \frac{\partial v}{\partial x} + v \frac{\partial v}{\partial y} \right) = -\frac{\partial p}{\partial y} + \delta^2 \left(\delta^2 \frac{\partial^2 v}{\partial x^2} + \frac{\partial^2 v}{\partial y^2} \right), \tag{5.16}$$

$$\begin{aligned}
\delta Pr Re \left((u+1) \frac{\partial \theta}{\partial x} + v \frac{\partial \theta}{\partial y} \right) &= \delta^2 \frac{\partial^2 \theta}{\partial x^2} + \frac{\partial^2 \theta}{\partial y^2} + Br \left[2\delta^2 \left(\left(\frac{\partial v}{\partial y} \right)^2 + \left(\frac{\partial u}{\partial x} \right)^2 \right) + \left(\delta^2 \frac{\partial v}{\partial x} + \frac{\partial u}{\partial y} \right)^2 \right] \\
&+ Br M^2(u+1)^2 + Du Pr \left(\delta^2 \frac{\partial^2 \phi}{\partial x^2} + \frac{\partial^2 \phi}{\partial y^2} \right).
\end{aligned} \tag{5.17}$$

$$\delta \left((u+1) \frac{\partial \phi}{\partial x} + v \frac{\partial \phi}{\partial y} \right) = \frac{1}{Sc} \left(\delta^2 \frac{\partial^2 \phi}{\partial x^2} + \frac{\partial^2 \phi}{\partial y^2} \right) + Sr \left(\delta^2 \frac{\partial^2 \theta}{\partial x^2} + \frac{\partial^2 \theta}{\partial y^2} \right). \tag{5.18}$$

Making use of the long wavelength and low Reynolds number approximations we obtain

$$\frac{dp}{dx} = \frac{\partial^3 \psi}{\partial y^3} - M^2 \left(\frac{\partial \psi}{\partial y} + 1 \right), \tag{5.19}$$

$$\frac{\partial^4 \psi}{\partial y^4} - M^2 \frac{\partial \psi^2}{\partial y^2} = 0, \tag{5.20}$$

$$\frac{\partial p}{\partial y} = 0, \tag{5.21}$$

$$0 = \frac{\partial^2 \theta}{\partial y^2} + Br \left(\frac{\partial^2 \psi}{\partial y^2} \right)^2 + Br M^2 \left(\frac{\partial \psi}{\partial y} + 1 \right)^2 + Pr Du \frac{\partial^2 \phi}{\partial y^2}, \quad (5.22)$$

$$0 = \frac{1}{Sc} \frac{\partial^2 \phi}{\partial y^2} + Sr \frac{\partial^2 \theta}{\partial y^2}, \quad (5.23)$$

in which $p \neq p(y)$, ν denotes the kinematic viscosity, M the Hartman number, Re the Reynolds number, Br the Brinkman number, Du the Dufour number, Sr the Soret number, Sc the Schmidt number, E the Eckert number, Pr the Prandtl number, δ the wave number and the dimensionless temperature and concentration are θ and ϕ respectively. The boundary conditions are

$$\begin{aligned} \psi &= 0, & \frac{\partial^2 \psi}{\partial y^2} &= 0, & \frac{\partial \theta}{\partial y} &= 0, & \frac{\partial \phi}{\partial y} &= 0, & \text{at } y &= 0, \\ \psi &= F, & \frac{\partial \psi}{\partial y} &= -1, & \theta &= 0, & \phi &= 0, & \text{at } y &= h, \end{aligned} \quad (5.24)$$

$$h(x) = 1 + a \cos(2\pi x), \quad F = \int_0^h \frac{\partial \psi}{\partial y} dy. \quad (5.25)$$

Pressure rise per wavelength Δp_λ at this stage is

$$\Delta p_\lambda = \int_0^1 \frac{\partial p}{\partial x} dx. \quad (5.26)$$

Heat transfer coefficient Z for this problem is defined as

$$Z = h_x \theta_y.$$

5.2 Solutions expressions

Solving the above equations subject to the corresponding boundary conditions one finds that

$$\psi = \frac{F M y \cosh(hM) + y \sinh(hM) - (F + h) \sinh(My)}{hM \cosh(hM) - \sinh(hM)}, \quad (5.27)$$

$$\frac{dp}{dx} = - \frac{(F + h) M^3 \cosh(hM)}{hM \cosh(hM) - \sinh(hM)}, \quad (5.28)$$

$$\theta = \frac{BrM^2 (2A_1 - A_2 \cosh(hM) + A_3 + A_4)}{8(-1 + Pr ScSrDu) (-hM \cosh(hM) + \sinh(hM))^2}, \quad (5.29)$$

$$\phi = \frac{BrM^2 ScSr (B_1 + B_2 \cosh(2hM) - B_3 + B_4)}{8(-1 + Pr ScSrDu) (-hM \cosh(hM) + \sinh(hM))^2}, \quad (5.30)$$

where

$$\begin{aligned} A_1 &= h(4 + h + h^3 M^4) - (1 + h^2 M^4) y^2 + F^2 M^2 (1 + M^2) (h - y) (h + y) + 2F \\ &\quad (2 + hM^2 (1 + M^2) (h - y) (h + y)), A_2 = F^2 (1 + M^2) + 2F (4 + h + hM^2) - 2y^2 \\ &\quad + h(8 + h(3 + M^2 (1 + 2h^2 - 2y^2))), A_3 = (F + h)^2 (1 + M^2) \cosh[2My] + 4hM \\ &\quad (2F + h(2 + h) - y^2) \sinh[2hM] - 16h(F + h) M \cosh[hM] (M(h - y) + \sinh[My]), \\ A_4 &= 16(F + h) \sinh[hM] (M(h - y) + \sinh[My]) \\ B_1 &= -8F - 2h(4 + h) - 2Fh^2 (F + 2h) M^2 - 2h^2 (F + h)^2 M^4 \\ &\quad + 2(1 + F(F + 2h) M^2 + (F + h)^2 M^4) y^2, B_2 = F^2 (1 + M^2) + \\ &\quad 2F(4 + h + hM^2) - 2y^2 + h(8 + h(3 + M^2 (1 + 2h^2 - 2y^2))), \\ B_3 &= (F + h)^2 (1 + M^2) \cosh[2My] - 4hM (2F + h(2 + h) - y^2) \sinh[2hM], \\ B_4 &= 16h(F + h) M \cosh[hM] (M(h - y) + \sinh[My]) - 16(F + h) \\ &\quad \sinh[hM] (M(h - y) + \sinh[My]). \end{aligned}$$

5.3 Discussion

Here Figs. 5.1(a-e) are drawn for the temperature, Figs. 5.2(a-e) for concentration and Figs. 5.3(a-e) for the heat transfer coefficient. Tables 5.1 and 5.2 describe the temperature and concentration gradients. It is observed that with an increase in M the temperature increases. An increase in temperature becomes more apparent with an increase in M (see Fig. 5.1a). This fact agrees well to the expected results of Ohmic heating i.e. the temperature increases with an increase in the magnetic field strength. This fact is quite opposite to the observed results of behavior of M on temperature in the previous attempts by several other authors who considered the magnetic field but ignored the effects of Ohmic heating which in turn gives the lesser accurate prediction about the behavior of temperature for different values of M . From Figs. 5.1(b-d), the temperature increases with an increase in Schmidt, Dufour and Soret numbers but contrary to the previous case this increase is not much. Fig. 5.1(e) shows that there is rapid increase in temperature with an increase in the Brinkman number. From Figs.

5.2(a-e), we can clearly see that there is decrease in the concentration with an increase in M , Sr , Sc and Br . This decrease is more in case of Hartman number M and Brinkman number Br when compared with the other parameters. The result that concentration decreases effectively with an increase in M is of considerable importance. This means that we can use the heating effect of applied magnetic field to develop small thermal gradients which in turn can be used to control the concentration of any particular substance in the fluid. This result has wide range of applications especially for cure of several diseases, for instance clearing several type of blockages in many arteries that exhibit peristaltic mechanism. The thermal gradients can be used more efficiently in place of radiations with lesser side effects. These thermal gradients can also be used for the transport of several minerals and medicine within the human body on the desired location.

Heat transfer coefficient has its own physical significance in problems related to heat transfer. It is always helpful to examine the behavior of heat transfer coefficient (Z in this case) for a given problem. Keeping this in mind the Figs. 5.3(a-e) are explicitly plotted to examine how Z develops throughout the flow field. In all the Figs. 5.3(a-e), Z has oscillatory behavior which is due to peristalsis. In all these Figs. the absolute value of heat transfer coefficient is positive. Fig. 5.3(a) shows a rapid fluctuation in Z for changing values of M . From Figs. 5.3(b-d), it is quite obvious that the Du , Sc and Sr effect the heat transfer coefficient but this effect is relatively smaller when compared with the effects of other parameters like Br , M and d . Since Soret and Dufour effects have gained reasonable interest in convective heat and mass transfer. One cannot neglect such effects when there is appreciable density difference in the flow regime. The concentration gradient in fact yields the thermal energy flux (referred as Dufour effect) whereas the temperature gradients contribute to the mass fluxes (referred as Soret effect). One can neglect Soret and Dufour effects in heat and mass transfer mechanism when such effects are small in comparison to the effects by Fourier's or Fick's laws. Motivated by this fact we computed the temperature and concentration gradients at $y = h$ in the Tables 5.1 and 5.2. It is noticed from Table 1 that magnitude of temperature gradient increases when M , Du and Br are increased. However the situation is reverse when there is an increase in a . Table 5.2 depicts that concentration gradient is an increasing function of M , Du , Br and Sr . Further the concentration gradient is decreasing function of a .

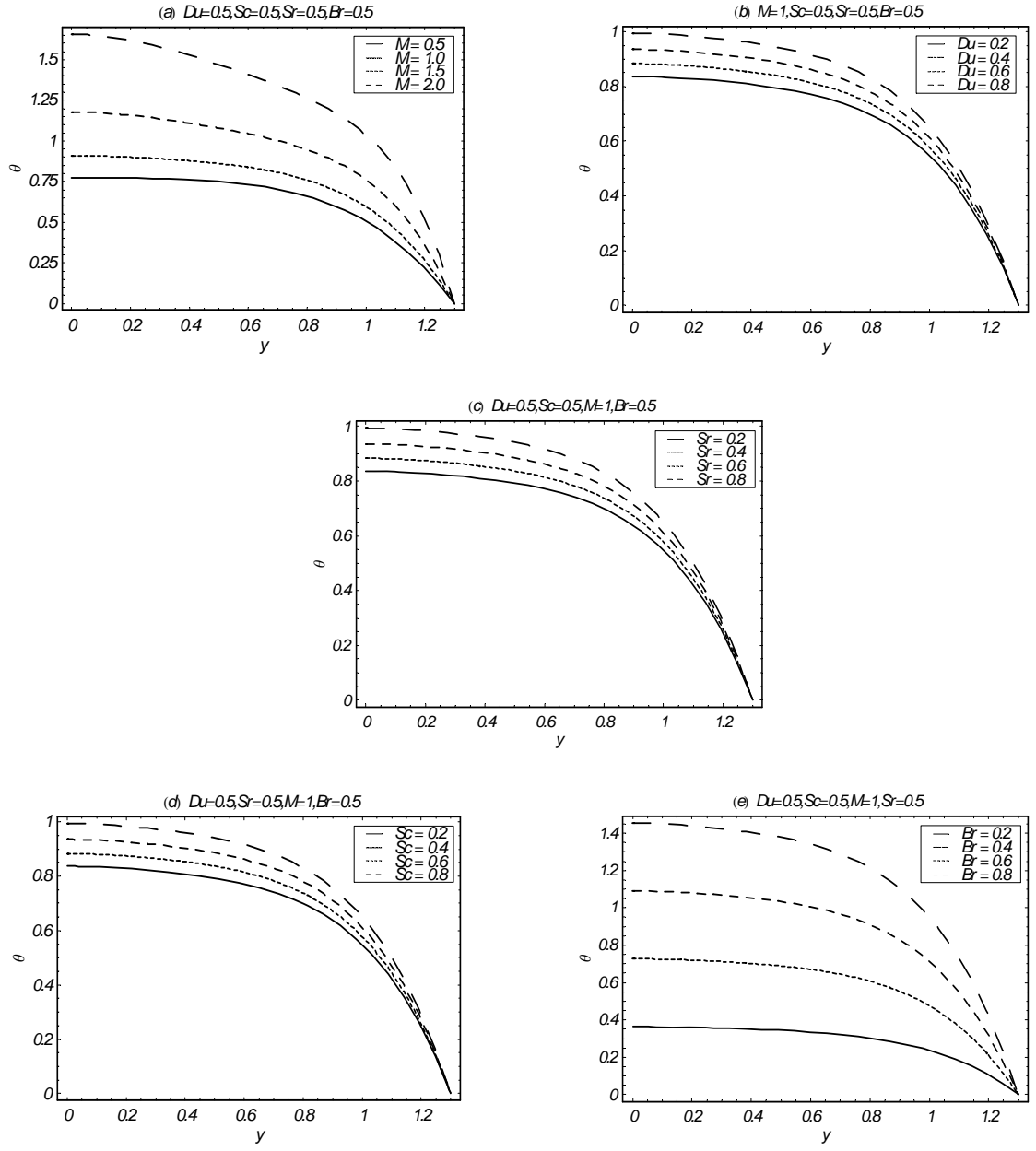


Fig. 5.1(a-e) Variation of temperature when $a = 0.3$, $\eta = 1.4$, and $x = 0$.

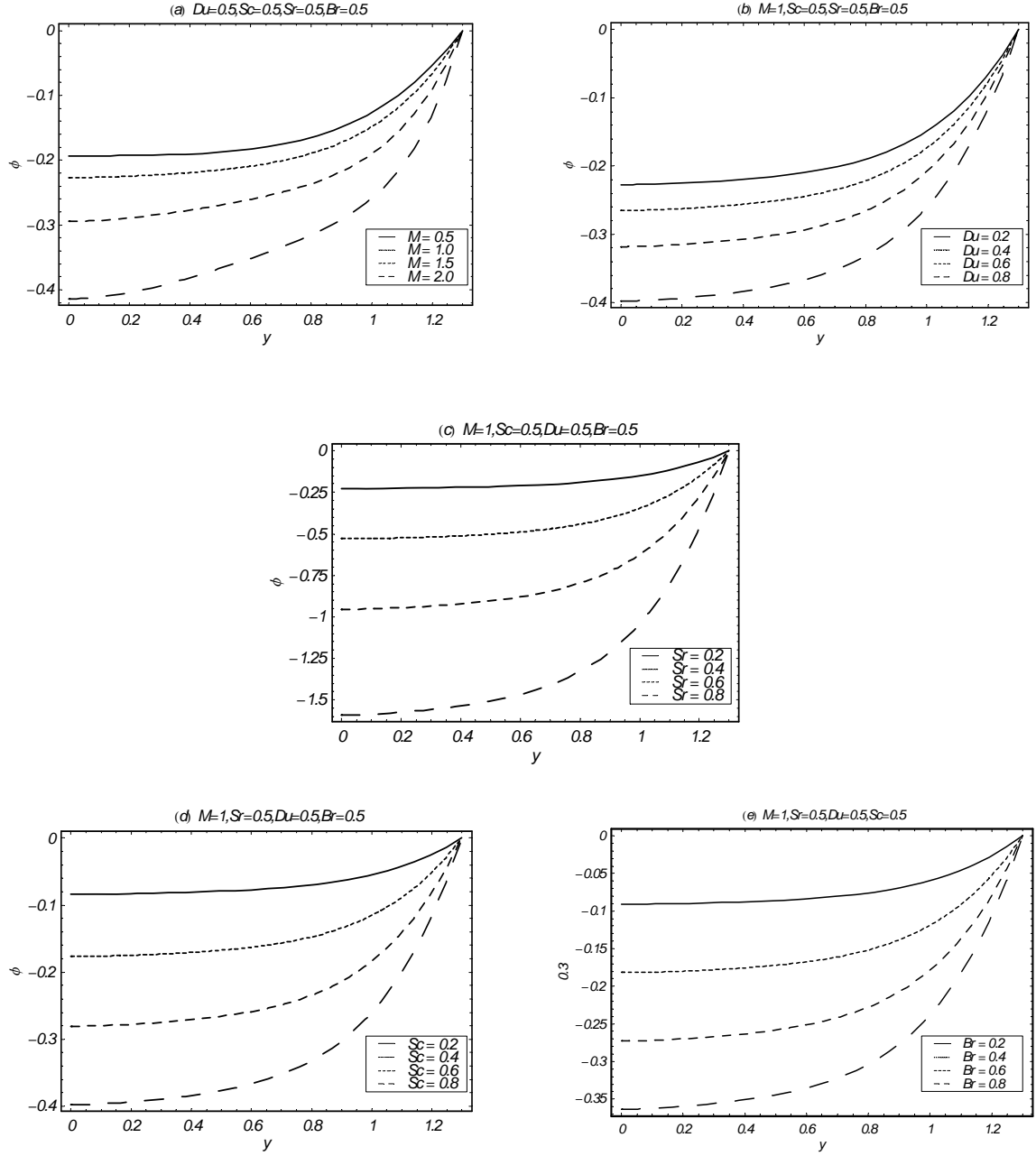


Fig. 5.2(a-e) Variation of concentration when $a = 0.3$, $\eta = 1.4$, and $x = 0$.

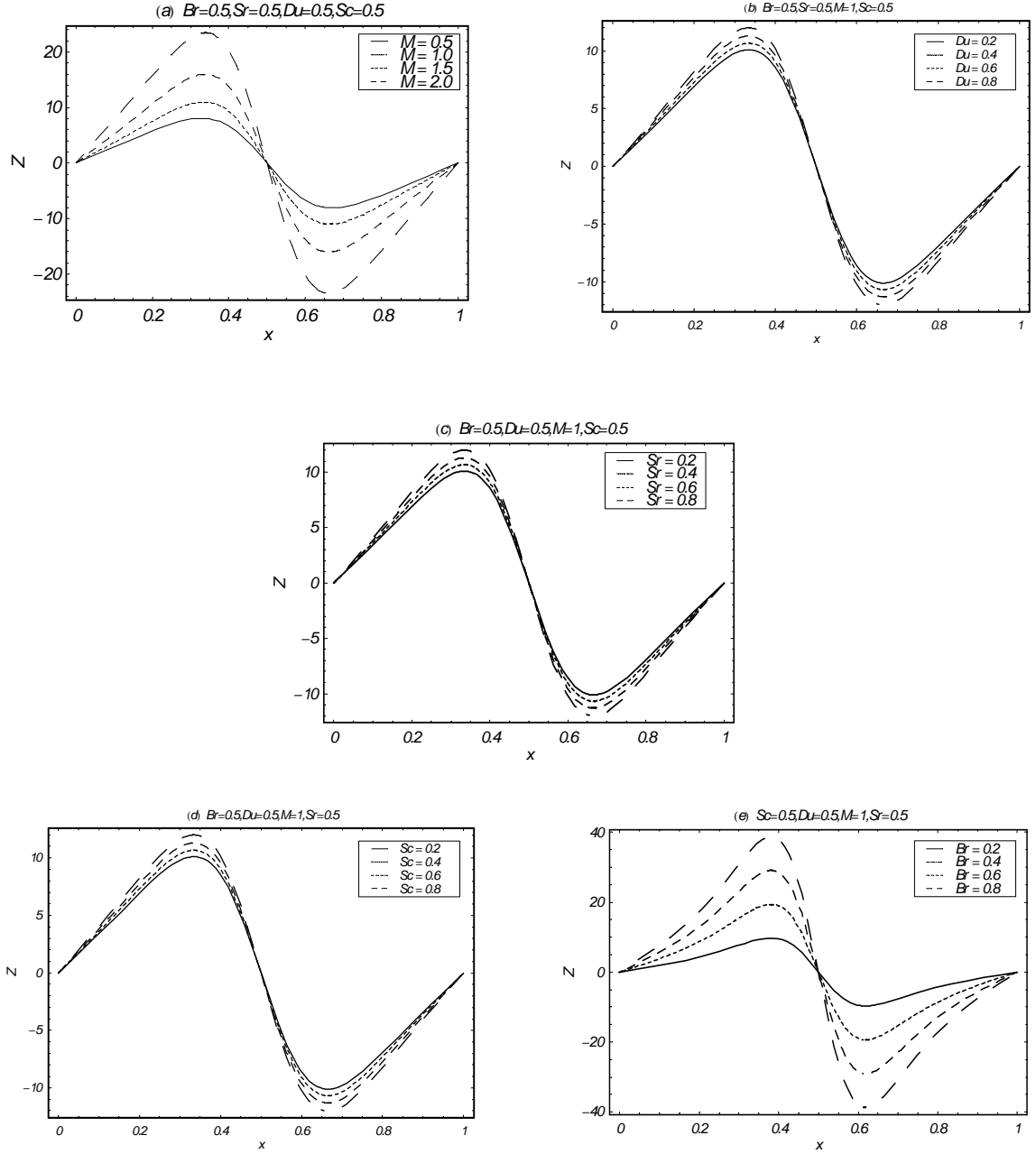


Fig. 5.3(a-e) Variation of Z when $a = 0.3$, $\eta = 1.4$, and $x = 0$.

M	Du	Br	a	$\theta'(h)$
0.5	1.0	0.5	0.3	-2.8569
1.0				-3.6054
1.5				-5.0997
2.0				-7.7157
	0.0			-2.7040
	0.5			-3.0903
	1.0			-3.6054
	1.5			-4.3265
		0.0		0.0
		0.5		-3.0903
		1.0		-6.1807
		1.5		-9.2711
			0.2	-3.3563
			0.4	-2.5868
			0.6	-2.11325
			0.8	-1.81531

Table 5.1: Variation of $\frac{\partial \theta}{\partial y}_{y=h}$ via different parameters.

M	Du	Br	a	Sr	$\phi'(h)$
0.5	1.0	0.5	0.3	0.5	0.71424
1.0					0.90136
1.5					1.2749
2.0					1.9289
	0.0				0.6760
	0.5				0.7725
	1.0				0.9013
	1.5				1.0816
		0.0			0.0
		0.5			0.7725
		1.0			1.5452
		1.5			2.3178
			0.2		0.8390
			0.4		0.6467
			0.6		0.5283
			0.8		0.4538
				0.2	0.2787
				0.4	0.5753
				0.6	0.8914
				0.8	1.2291

Table 5.2: Variation of $\frac{\partial \phi}{\partial y}_{y=h}$ via different parameters.

Chapter 6

Soret and Dufour effects on peristaltic transport of MHD fluid with variable viscosity

This chapter looks at the Soret and Dufour effects on the magnetohydrodynamic (MHD) peristaltic flow of variable viscosity fluid in a symmetric channel. Modeling is presented in the presence of Ohmic heating. Mathematical analysis is carried out through large wavelength and small Reynolds number. Results for the stream function, temperature and concentration are developed. The variations of sundry parameters on the flow quantities of interest are sketched and examined.

6.1 Mathematical analysis

Let us investigate the magnetohydrodynamic flow of an incompressible viscous fluid in a channel with width $2d_1$. The \bar{X} -axis is chosen along the walls of channel and \bar{Y} -axis is taken normal to the \bar{X} -axis. A constant magnetic field of strength \mathbf{B}_0 is exerted in the \bar{Y} -direction. Induced magnetic field is not accounted. Sinusoidal wave propagates along the channel walls with constant wave speed c represented by

$$H(\bar{X}, \bar{t}) = d_1 + a_1 \cos \left(\frac{2\pi}{\lambda} (\bar{X} - c\bar{t}) \right). \quad (6.1)$$

If (\bar{U}, \bar{V}) and (\bar{u}, \bar{v}) are the velocity components in the laboratory (\bar{X}, \bar{Y}) and wave (\bar{x}, \bar{y}) frames then transformations between laboratory and wave frames are

$$\bar{x} = \bar{X} - c\bar{t}, \quad \bar{y} = \bar{Y}, \quad \bar{u} = \bar{U} - c, \quad \bar{v} = \bar{V}, \quad \bar{p}(\bar{x}, \bar{y}) = \bar{P}(\bar{X}, \bar{Y}, \bar{t}). \quad (6.2)$$

In above expressions a_1 is the wave amplitude, λ is the wavelength, \bar{t} is the time and \bar{P} and \bar{p} are the pressures in the laboratory and wave frames respectively. Introducing the variables in the forms

$$\begin{aligned} x &= \frac{\bar{x}}{\lambda}, \quad y = \frac{\bar{y}}{d_1}, \quad u = \frac{\bar{u}}{c}, \quad v = \frac{\bar{v}}{c\delta}, \quad \delta = \frac{d_1}{\lambda}, \quad h = \frac{H}{a}, \quad a = \frac{a_1}{d_1}, \quad p = \frac{d_1^2 \bar{p}}{c\lambda\mu_0}, \\ \theta &= \frac{T - T_0}{T_0}, \quad \phi = \frac{C - C_0}{C_0}, \quad M = \left(\frac{\sigma}{\mu_0} \right)^{1/2} B_0 d_1, \quad \nu = \frac{\mu_0}{\rho}, \quad Re = \frac{\rho c d_1}{\mu_0}, \\ t &= \frac{c\bar{t}}{\lambda}, \quad u = \frac{\partial\psi}{\partial y}, \quad v = -\frac{\partial\psi}{\partial x}, \quad Br = Pr E, \quad Du = \frac{DC_0 K_T}{C_s C_p \mu_0 T_0}, \quad Sr = \frac{\rho D K_T T_0}{\mu_0 T_m C_0}, \\ Sc &= \frac{\mu_0}{\rho D}, \quad E = \frac{c^2}{C_p T_0}, \quad Pr = \frac{\mu C_p}{K}, \quad \text{and } \mu(y) = \frac{\bar{\mu}(\bar{y})}{\mu_0}. \end{aligned} \quad (6.3)$$

the governing equations after adopting long wavelength and low Reynolds number approximation become

$$\frac{dp}{dx} = \frac{\partial}{\partial y} \left(\mu(y) \frac{\partial^2 \psi}{\partial y^2} \right) - M^2 \left(\frac{\partial \psi}{\partial y} + 1 \right), \quad (6.4)$$

$$\frac{\partial^2}{\partial y^2} \left(\mu(y) \frac{\partial^2 \psi}{\partial y^2} \right) - M^2 \frac{\partial \psi^2}{\partial y^2} = 0, \quad (6.5)$$

$$0 = \frac{\partial^2 \theta}{\partial y^2} + Br \mu(y) \left(\frac{\partial^2 \psi}{\partial y^2} \right)^2 + Br M^2 \left(\frac{\partial \psi}{\partial y} + 1 \right)^2 + Pr Du \frac{\partial^2 \phi}{\partial y^2}, \quad (6.6)$$

$$0 = \frac{1}{Sc} \frac{\partial^2 \phi}{\partial y^2} + Sr \frac{\partial^2 \theta}{\partial y^2}, \quad (6.7)$$

where p is the pressure, \bar{C} the concentration field, \bar{T} the temperature field, D mass diffusivity, K_T the thermal diffusion ratio, C_p the specific heat, C_s the concentration susceptibility, $\mu(y)$ the variable viscosity, T_m the fluid mean temperature, ν the kinematic viscosity, M the Hartman number, Re the Reynolds number, Br the Brinkman number, Du the Dufour parameter, Sr the Soret parameter, Sc the Schmidt number, E the Eckert number, Pr the Prandtl number, δ the

wave number, ψ the stream function, θ the dimensionless temperature and ϕ the concentration.

The boundary conditions are

$$\begin{aligned}\psi &= 0, & \frac{\partial^2 \psi}{\partial y^2} &= 0, & \frac{\partial \theta}{\partial y} &= 0, & \frac{\partial \phi}{\partial y} &= 0, & \text{at } y &= 0, \\ \psi &= F, & \frac{\partial \psi}{\partial y} &= -1, & \theta &= 0, & \phi &= 0, & \text{at } y &= h,\end{aligned}\tag{6.8}$$

$$h(x)=1+a\cos(2\pi x), \quad F=\int_0^h \frac{\partial \psi}{\partial y} dy,\tag{6.9}$$

Pressure rise per wavelength Δp_λ is

$$\Delta p_\lambda = \int_0^1 \frac{dp}{dx} dx.\tag{6.10}$$

The dimensionless expression of space dependent viscosity is

$$\mu(y) = e^{-\alpha y} = 1 - \alpha y \quad \alpha \ll 1,$$

where " α " is the viscosity parameter.

We look for solutions in the series form represented below

$$\begin{aligned}\psi &= \psi_0 + \alpha \psi_1 + \dots \\ F &= F_0 + \alpha F_1 + \dots \\ p &= p_0 + \alpha p_1 + \dots\end{aligned}$$

Employing the procedure of perturbation method and retaining the results up to order $o(\alpha)$ we have

$$\psi = A_1 + \frac{(F+h)\alpha A_2}{8(-hM \cosh(hM) + \sinh(hM))^2},\tag{6.11}$$

$$\begin{aligned}\theta &= -\frac{BrM^2 B_1}{8(-1 + \text{Pr } ScSrDu)(hM \cosh(hM) - \sinh(hM))^2} \\ &\quad - \frac{BrM\alpha[B_2 + B_3 + B_4 - B_5 + B_6 - B_7 + B_8]}{32(-1 + \text{Pr } ScSrDu)(hM \cosh(hM) - \sinh(hM))^3},\end{aligned}\tag{6.12}$$

$$\phi = -\frac{BrM^2ScSr[C_1-C_2+C_3]}{8(-1+PrScSrDu)(hM \cosh(hM)-\sinh(hM))^2} + \frac{BrMScSr\alpha[C_4+C_5+2(C_6+C_7+\frac{1}{4}M(C_8+C_9-C_{10})-C_{11}-C_{12}+C_{13})]}{64(-1+PrScSrDu)(hM \cosh(hM)-\sinh(hM))^3}. \quad (6.13)$$

Heat transfer coefficient is defined as follows:

$$Z = h_x\theta_y.$$

The involved $A_i(i = 1, 2)$, $B_j(j = 1 - 8)$ and $C_k(k = 1 - 13)$ are

$$\begin{aligned}
A_1 &= \frac{FMy \cosh(hM) + y \sinh(hM) - (F+h) \sinh(My)}{hM \cosh(hM) - \sinh(hM)}, A_2 = yA_3 + (hMy \cosh(hM) + (h^3M^2 - y) \\
&\sinh(hM))^2 \sinh(My), A_3 = -1 + 2h^2M^2 + \cosh(2hM) + 2My \cosh(My) (-hM \\
&\cosh(hM) + \sinh(hM)) - 2hM \sinh(2hM), B_1 = -8F - 2h(4+h) - 2F + h^2(F+2h) \\
&M^2 - 2h^2(F+h)^2M^4 + 2(1+F(F+2h)M^2 + (F+h)^2M^4)y^2 + (F^2(1+M^2) \\
&+ 2F(4+h+hM^2) - 2y^2 + h(8+h(3+M^2(1+2h^2-2y^2)))) \cosh(2hM) - (F+h)^2 \\
&(1+M^2) \cosh(2My) - 4hM(2F+h(2+h)-y^2) \sinh(2hM) + 16h(F+h)M \\
&\cosh(hM)(M(h-y) + \sinh(My)) - 16(F+h) \sinh(hM)(M(h-y) + \sinh(My)), \\
B_2 &= -8h^3(F+h)(h-y) \sinh(2hM)M^4 - \frac{1}{2}(F+h)B_9 \cosh(hM) - 16h^4(F+h) \\
&M^4 \cosh(hM)^3 + 8h^3(F+h)M^4(h-y) \cosh(2hM), B_3 = \frac{1}{2}(F+h)(3(F+h) + 3 \\
&(F+h-8h^2)M^2 + 8h^4M^4) \cosh(3hM) + 16h^2(F+h)M^4y^2 \cosh(hM)^2 \cosh(My) \\
&- 2h(F+h)^2M^2(1+M^2)y \cosh(hM) \cosh(2My), B_4 = (F+h)MB_{10} \sinh(hM), \\
B_5 &= 64F1h^2M^3 \cosh(hM)^2 \sinh(hM) + 2h^3(F+h)^2M^3(1+M^2) \cosh(2My) \\
&\sinh(hM) + 2(F+h)^2M(1+M^2)y \cosh(2My) \sinh(hM) + 16(F+h)M^2y^2 \cosh(My) \\
&\sinh(hM)^2 - 8h^4(F+h)M^5(h-y) \sinh(2hM), B_6 = hMB_{11} \cosh(hM) \sinh(2hM), \\
B_7 &= hM(-4F + F^2 - 4h + 2Fh + h^2 + (F+h)^2(1+h^2)M^2 + h^2(F+h)^2M^4) \\
&\sinh(3hM) - 16h^2(F+h)M^3y \cosh(hM)^2 \sinh(My) + 16h^3(F+h)M^3 \sinh(hM)^2 \\
&\sinh(My) - 16(F+h)My \sinh(hM)^2 \sinh(My) - 8h^4(F+h)M^4 \sinh(2hM) \sinh(My), \\
B_8 &= 16h(F+h)M^2y \sinh(2hM) \sinh(My) + (F+h)^2(1+M^2)(-3+2M^2y^2) \\
&\sinh(hM) \sinh(2My) - h(F+h)M \cosh(hM)B_{12}, B_9 = F(1+M^2)(3+4hM^2(-3h \\
&+ 2h^3M^2 + 2y - 2M^2y^3)) + h(3+M^2(3+4h(h(-3+M^2(-3+2h(1+h+hM^2)))) \\
&+ 2(-3+y) + 2M^2y - 2M^2(1+M^2)y^3))), B_{10} = -3h(4+F+h) + h(F(-3+5h^2) \\
&+ h(-3+h(16+5h)))M^2 + h^3(F+h)(5+4h^2)M^4 + 4h^5(F+h)M^6 + 4(F+h) \\
&(1+M^2)y - 4h^3(F+h)M^4(1+M^2)y^2 - 4(F+h)M^2(1+M^2)y^3, B_{11} = -3(F+h)^2 \\
&+ (-3F^2 - 6Fh + 32f1h + (-3+2F(8+F))h^2 + 4(4+F)h^3 + 2h^4)M^2 + 2h^2(F+h)^2 \\
&M^4, B_{12} = 16M^2y^2 \sinh(M(h-y)) + (F+h)(1+M^2)(-3+2M^2y^2) \sinh(2My) + 16 \\
&M^2y^2 \sinh(M(h+y)), C_1 = 2C_{14} - 16h(F+h)M^2(h-y) \cosh(hM) - (F^2(1+M^2) \\
&+ 2F(4+h+hM^2) - 2y^2 + h(8+h(3+M^2(1+2h^2-2y^2)))) \cosh(2hM), C_2 = 8F \\
&\cosh(M(h-y)) - 8h \cosh(M(h-y)) + F^2 \cosh(2My) + 2Fh \cosh(2My) + h^2 \\
&\cosh(2My) + F^2M^2 \cosh(2My) + 2FhM^2 \cosh(2My) + h^2M^2 \cosh(2My) + 8(F+h)
\end{aligned}$$

$$\begin{aligned}
& \cosh(M(h+y)) + 16FhM \sinh(hM) + 16h^2M \sinh(hM) - 16FM y \sinh(hM) - 16hMy \\
& \sinh(hM), C_3 = 8FhM \sinh(2hM) + 8h^2M \sinh(2hM) + 4h^3M \sinh(2hM) - 4hMy^2 \\
& \sinh(2hM) + 8FhM \sinh(M(h-y)) + 8h^2M \sinh(M(h-y)) - 8h(F+h)M \\
& \sinh(M(h+y)), C_4 = (3(F+h)^2 + (3F^2 + 6F(1-4h)h + h(64f1 + 3(1-8h)h)) \\
& M^2) \cosh(3hM), C_5 = 2M \cosh(hM)^2 C_{15}, C_6 = -8h^3(F+h)M^4(h-y) + 2(F+h)^2 \\
& M(1+M^2)(h^3M^2+y) \cosh(My), C_7 = 2My \sinh(hM) + 16(F+h)M^2y^2 \cosh(My) \\
& \sinh(hM)^2, C_8 = 64F1hM \cosh(hM) + 32h^3(F+h)M^3(h-y) \cosh(2hM) - 64F1h \\
& M \cosh(3hM), C_9 = C_{16} \sinh(hM), C_{10} = 32h^4(F+h)M^4(h-y) \sinh(2hM) + (-h \\
& (F+h)(-8+5F+5h+(5F+(5-16h)h)M^2) + 8F1(4+F+h+(F+h-4h^2)M^2)) \\
& \sinh(3hM), C_{11} = 4MF1(4-4h^2M^2) + 4M(F+h)(-3y+h^2M^2(3h+y)) + 4M(F1 \\
& (4-4h^2M^2) + 4M(F+h)(y+h^2M^2(-h+y))) \cosh(2hM) + 4M2h(F+h)M(h^3M^2 \\
& -2y) \sinh(2hM) \sinh(My) + 4M(F+h)^2(1+M^2)(-3+2M^2y^2) \sinh(hM) \sinh(2My), \\
& C_{12} = \cosh(hM)(F+h)(F(1+M^2)(3+4hM^2(-3h+2h^3M^2+2y-2M^2y^3)) \\
& + \cosh(hM)h(3+M^2(3+4h^2(-3+M^2(-3+2h(4+h+hM^2)) + 2 \cosh(hM)(-3+y) \\
& + 2M^2y-2M^2(1+M^2)y^3))), C_{13} = 64F1hM^2 \cosh(2hM) + 4h(F+h)^2M^2(1+M^2) \\
& y \cosh(2My) + 2hM(-32F1hM^2 \sinh(2hM) + (F+h)C_{18}), C_{14} = h(4+h+h^3M^4) \\
& - (1+h^2M^4)y^2 + F^2M^2(1+M^2)(h-y)(h+y) + 2F(2+hM^2(1+M^2)(h-y)(h+y)), \\
& C_{15} = 16h^2(F+h)M^3y^2 \cosh(My) - (h(F+h)(-8+5F+5h+(5F+(5-16h)h)M^2) \\
& + 8F1(4+F+h+(F+h+4h^2)M^2)) \sinh(hM) - 8((4f1(-1+h^2M^2) + (F+h)(y+h^2 \\
& M^2(-h+y)))) \sinh(My), C_{16} = 8F1(4+F+h+(F+h-4h^2)M^2) + (F+h)C_{17}, \\
& C_{17} = h(-56+F(1+M^2)(-13+24h^2M^2+16h^4M^4) + h(-13+M^2(-13+8h(10+h \\
& (1+M^2)(3+2h^2M^2)))) + 16(F+h)(1+M^2)y - 16h^3(F+h)M^4(1+M^2)y^2 - 16 \\
& (F+h)M^2(1+M^2)y^3, C_{18} = 16M^2y^2 \sinh(M(h-y)) + (F+h)(1+M^2)(-3+2M^2y^2) \\
& \sinh(2My) + 16M^2y^2 \sinh(M(h+y)).
\end{aligned}$$

6.2 Discussion

This section describes the impacts of pertinent parameters on the temperature and concentration. We recall that theme of this study is to point out the influences of Soret and Dufour. Therefore, the results of various parameters associated with velocity are not included. In order to achieve the desired objective, we present the plots in such a way that the left panels are for

constant viscosity (i.e. for $\alpha = 0$) and the right ones are for variable viscosity ($\alpha = 0.4$). It is observed in all the graphs related to temperature that the rise in temperature for variable viscosity fluid is relatively slower when compared with fluid having constant viscosity. Here Figs. 6.1-6.5 are drawn for temperature whereas the Figs. 6.6-6.10 show variation of concentration. Temperature increases with an increase in M (Fig. 6.1). Further an increase in temperature is abrupt in view of Ohmic heating. The variations of Du , Sr , Sc and Br on the temperature are displayed in the Figs. 6.2-6.5. These Figs. indicate that there is an increase in temperature by increasing Du , Sr , Sc and Br . It is also found that an increase in temperature is more for Br when compared with the other parameters.

Figs. 6.6-6.10 are presented to examine the behavior of embedded parameters on the concentration. Increase in concentration is observed when M and Du are increased (see Figs. 6.6 & 6.7). Concentration also increases when Sr , Sc and Br are increased (Figs. 6.8-6.10).

Behavior of heat transfer coefficient Z for various parameters is shown in the Figs. 6.11-6.15. As expected Z shows an oscillatory behavior which is because of peristalsis. It is also noted that there is no variation in Z for amplitude ratio (d) between 0 and 0.3. It is observed from Fig. 6.11 that Z increases when M is increased. The absolute values of Z in variable viscosity fluid are more than the constant viscosity fluid. Figs 6.12-6.15 show that Z increases with the increase in Du , Sr , Sc and Br . Effects of Du , Sr , Sc and Br on Z are opposite to that of M .

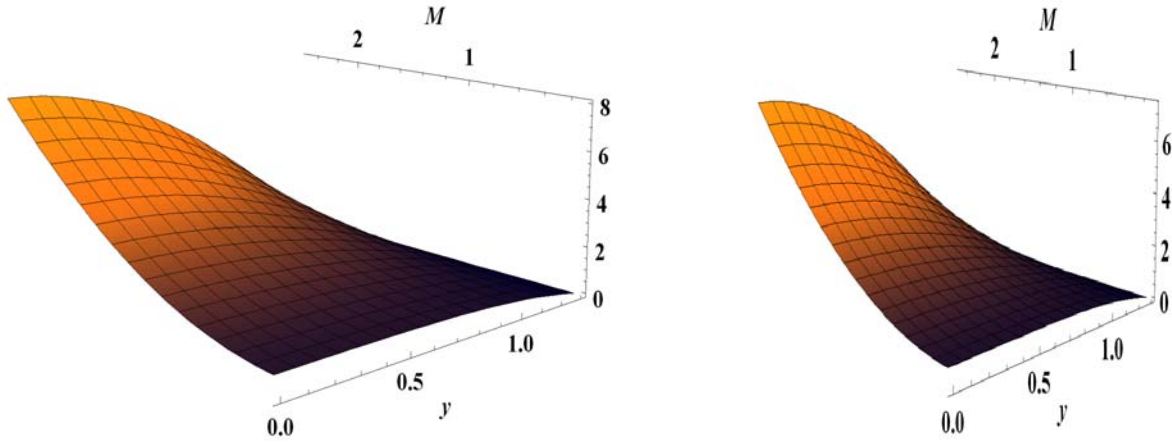


Fig. 6.1 Effect of M on θ when $Du = 0.5$, $Sr = 0.5$, $Sc = 0.5$, $a = 0.3$, $\eta = 1.4$, $Br = 0.5$ and $x = 0$.

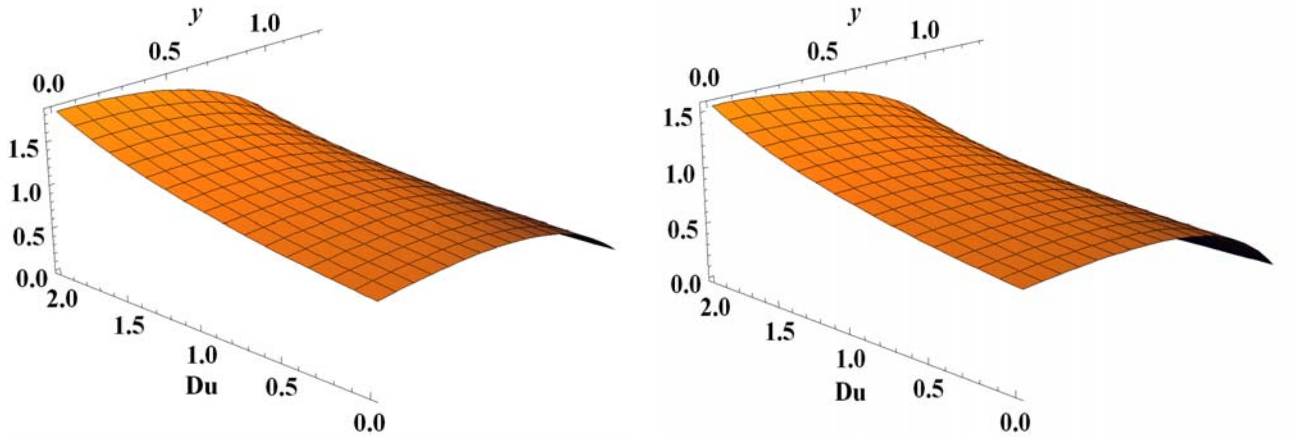


Fig. 6.2 Effect of Du on θ when $M = 0.5$, $Sr = 0.5$, $Sc = 0.5$, $a = 0.3$, $\eta = 1.4$, $Br = 0.5$ and $x = 0$.

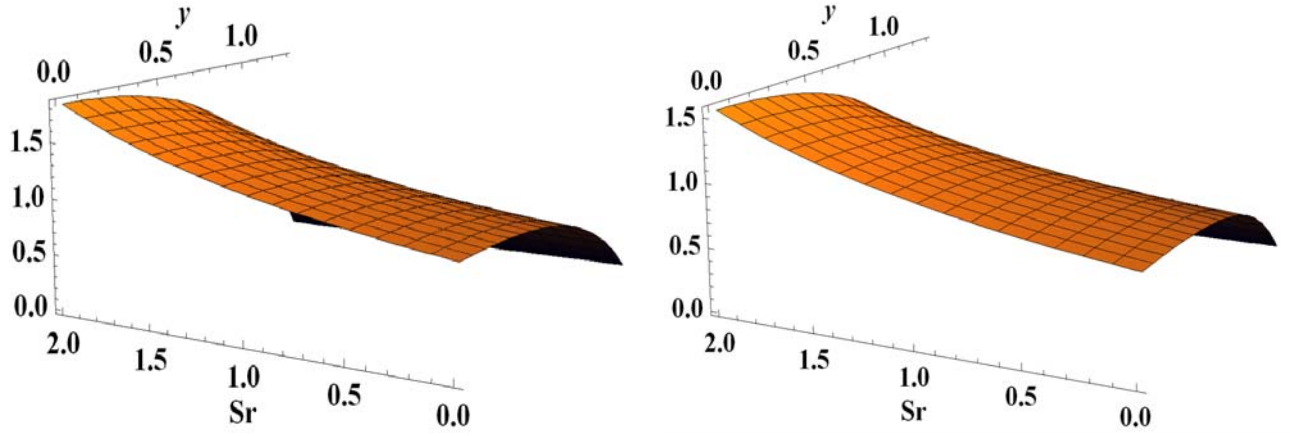


Fig. 6.3 Effect of Sr on θ when $Du = 0.5$, $M = 0.5$, $Sc = 0.5$, $a = 0.3$, $\eta = 1.4$, $Br = 0.5$ and $x = 0$.

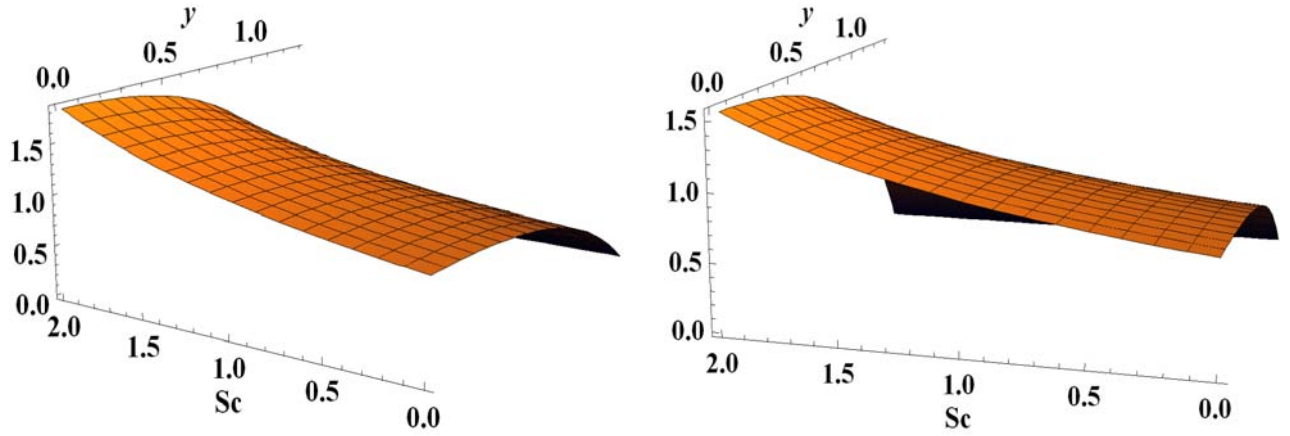


Fig. 6.4 Effect of Sc on θ when $Du = 0.5$, $Sr = 0.5$, $M = 0.5$, $a = 0.3$, $\eta = 1.4$, $Br = 0.5$ and $x = 0$.

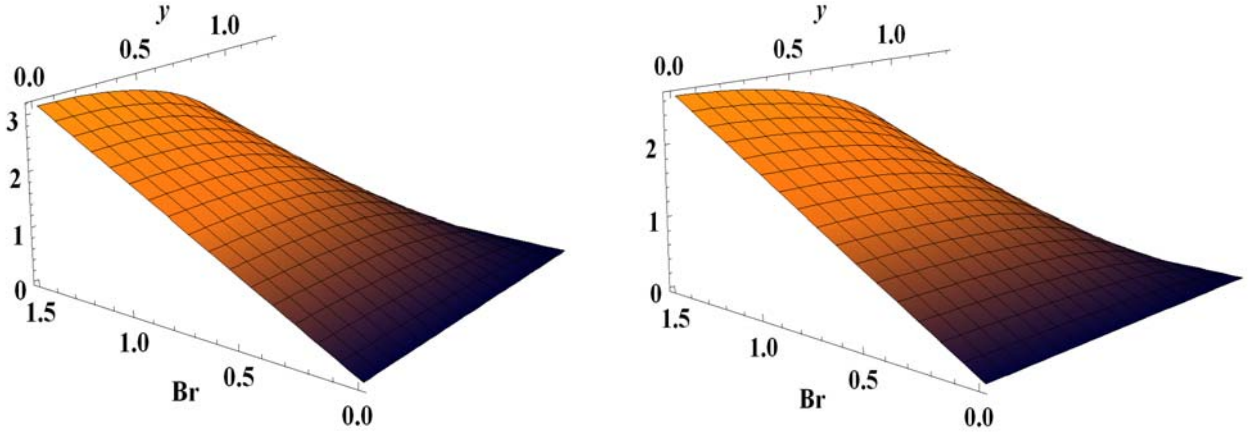


Fig. 6.5 Effect of Br on θ when $Du = 0.5$, $Sr = 0.5$, $M = 0.5$, $a = 0.3$, $\eta = 1.4$, $Sc = 0.5$ and $x = 0$.

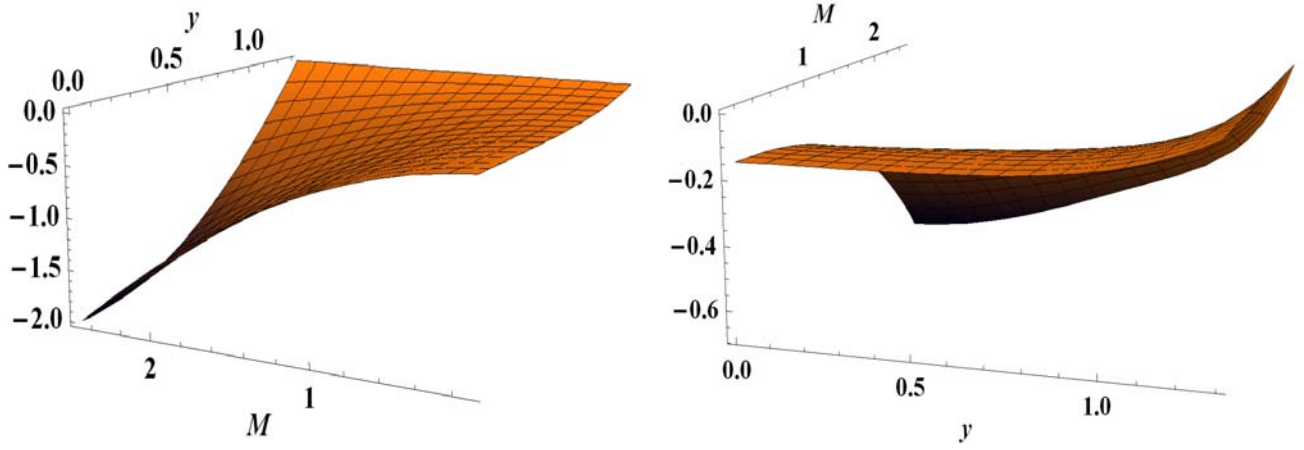


Fig. 6.6 Effect of M on ϕ when $Du = 0.5$, $Sr = 0.5$, $Sc = 0.5$, $d = 0.3$, $\eta = 1.4$, $Br = 0.5$ and $x = 0$.

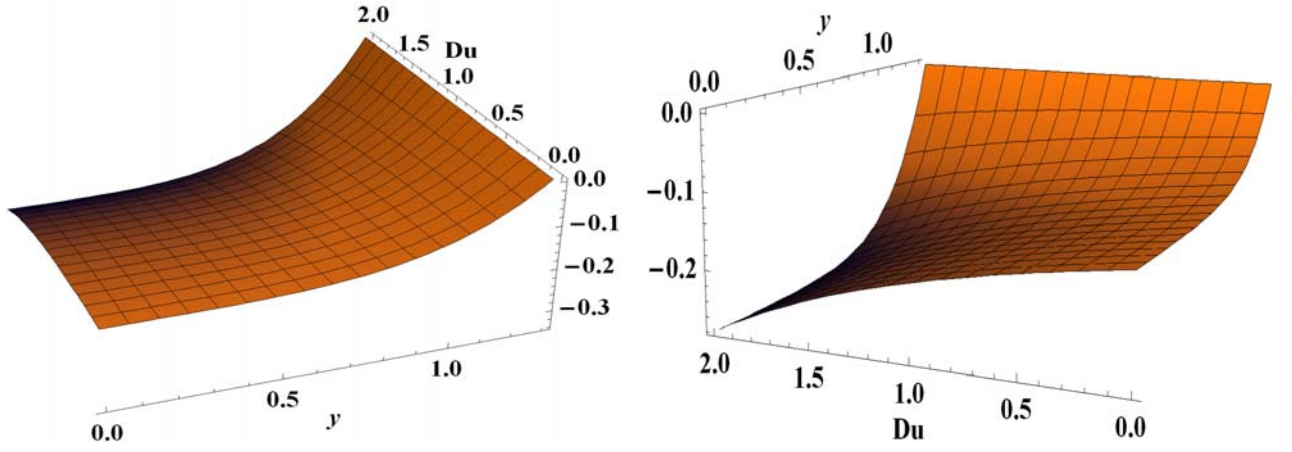


Fig. 6.7 Effect of Du on ϕ when $M = 0.5$, $Sr = 0.5$, $Sc = 0.5$, $a = 0.3$, $\eta = 1.4$, $Br = 0.5$ and $x = 0$.

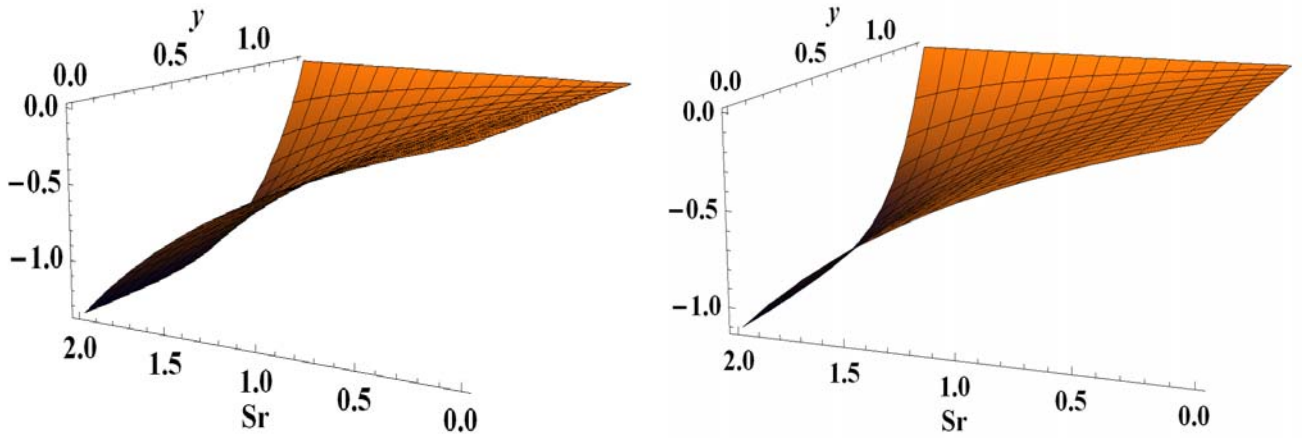


Fig. 6.8 Effect of Sr on ϕ when $Du = 0.5$, $M = 0.5$, $Sc = 0.5$, $a = 0.3$, $\eta = 1.4$, $Br = 0.5$ and $x = 0$.

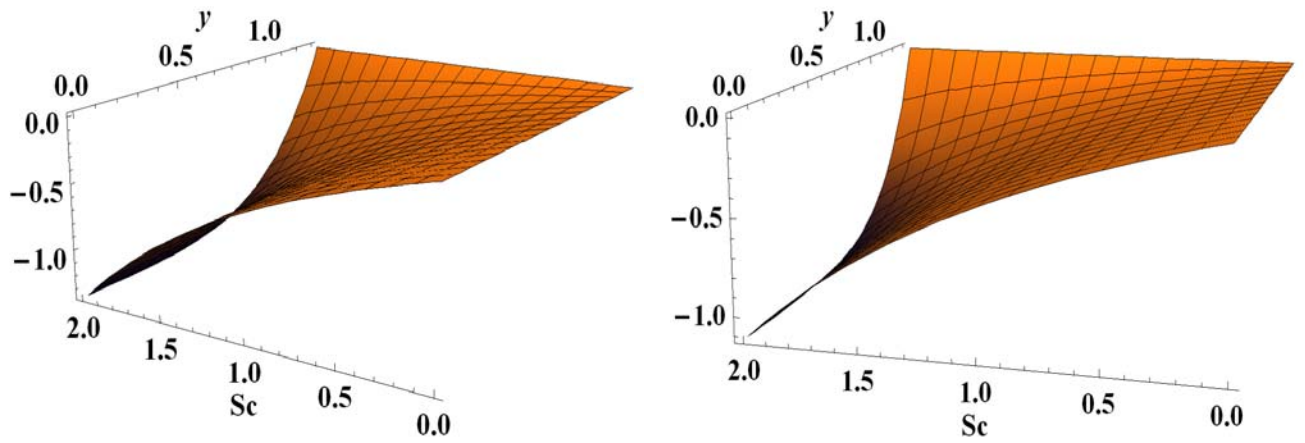


Fig. 6.9 Effect of Sc on ϕ when $Du = 0.5$, $Sr = 0.5$, $M = 0.5$, $a = 0.3$, $\eta = 1.4$, $Br = 0.5$ and $x = 0$.

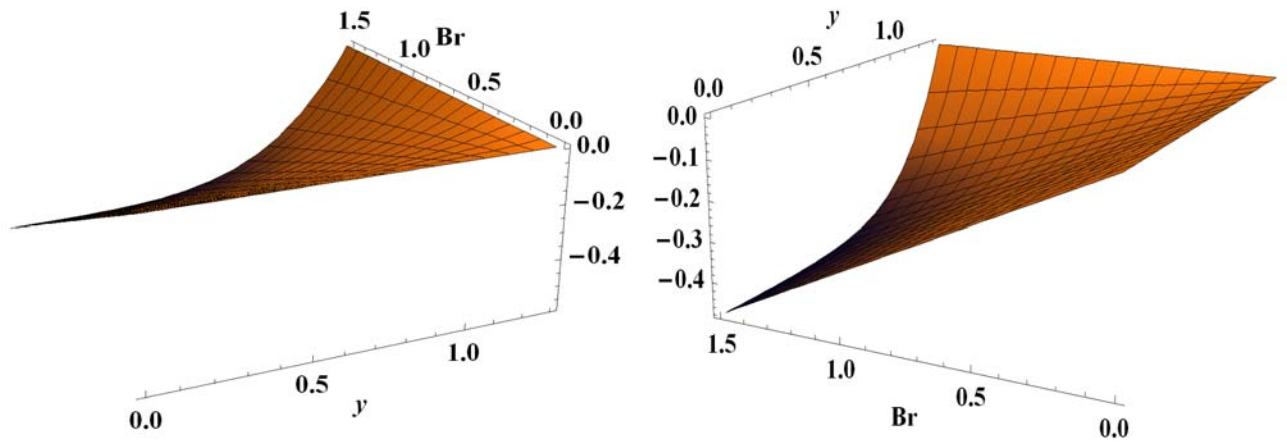


Fig. 6.10 Effect of Br on ϕ when $Du = 0.5$, $Sr = 0.5$, $M = 0.5$, $a = 0.3$, $\eta = 1.4$, $Sc = 0.5$ and $x = 0$.

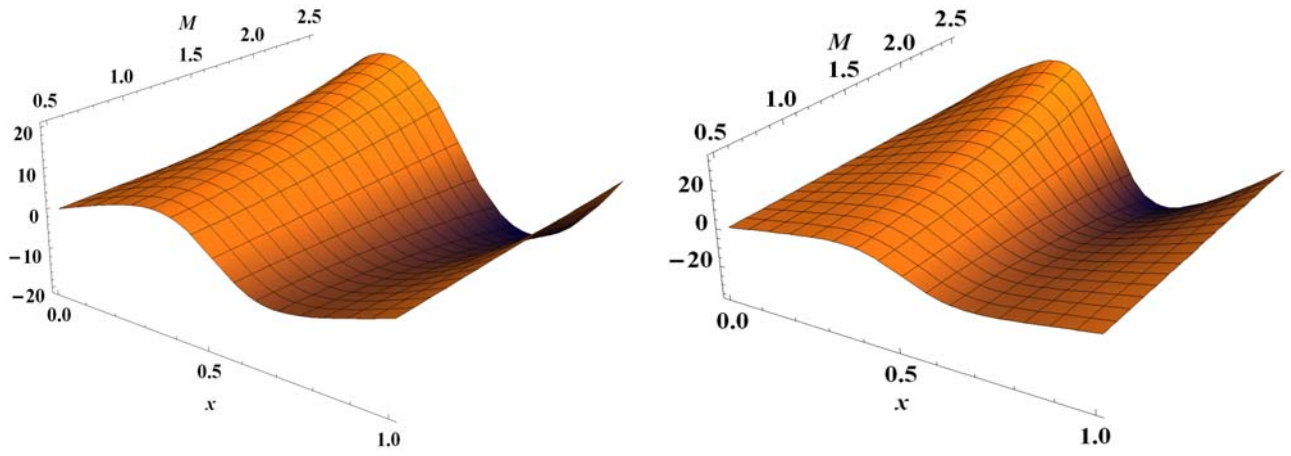


Fig. 6.11 Effect of M on Z when $Du = 0.5$, $Sr = 0.5$, $M = 0.5$, $a = 0.3$, $\eta = 1.4$ and $Br = 0.5$ and $x = 0$.

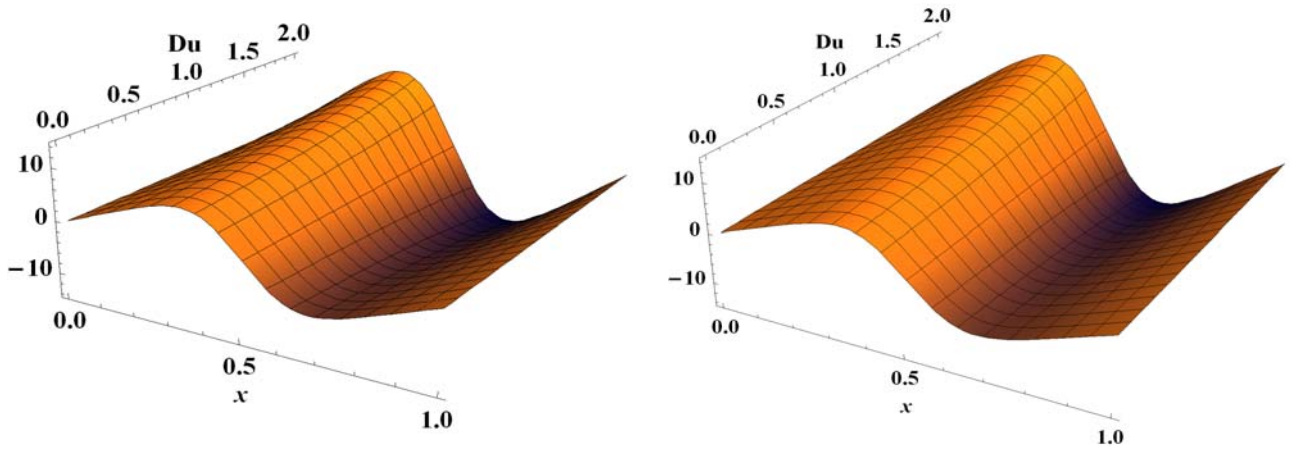


Fig. 6.12 Effect of Du on Z when $Sc = 0.5$, $Sr = 0.5$, $M = 0.5$, $a = 0.3$, $\eta = 1.4$ and $Br = 0.5$.

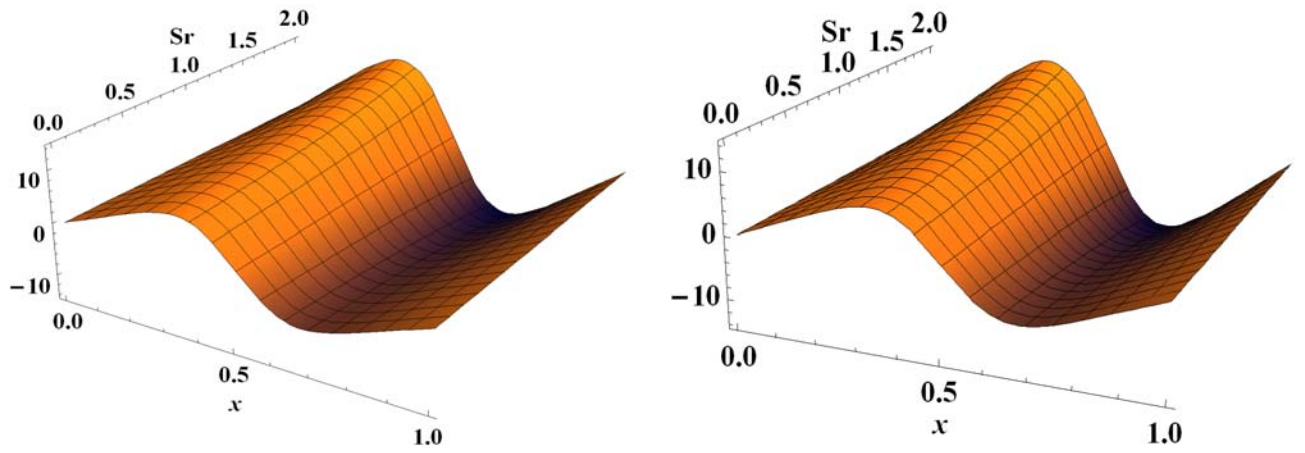


Fig. 6.13 Effect of Sr on Z when $Sc = 0.5$, $Du = 0.5$, $M = 0.5$, $a = 0.3$, $\eta = 1.4$ and $Br = 0.5$.

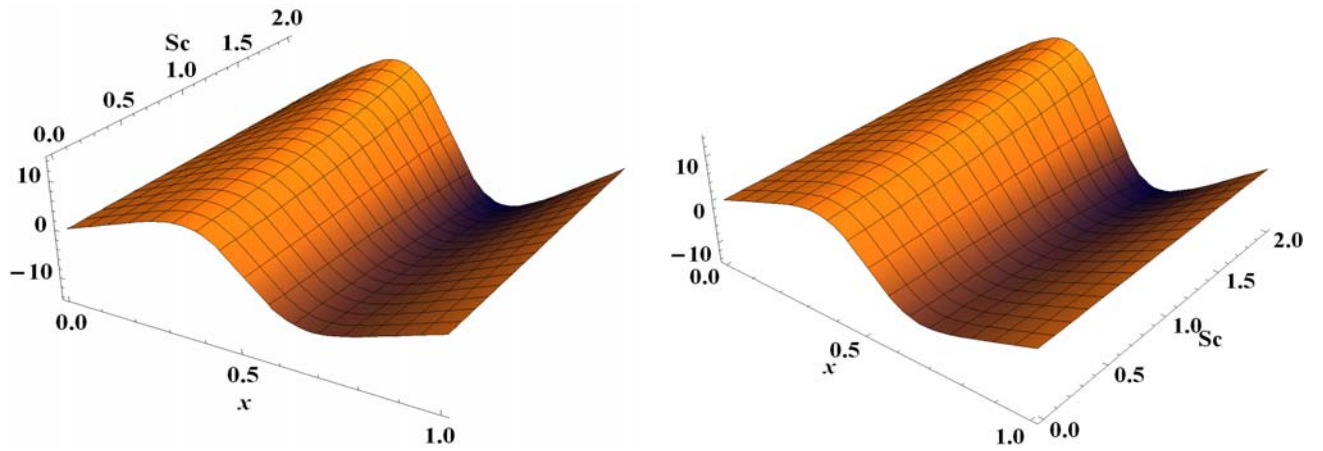


Fig. 6.14 Effect of Sc on Z when $Du = 0.5$, $Sr = 0.5$, $M = 0.5$, $a = 0.3$, $\eta = 1.4$ and $Br = 0.5$.

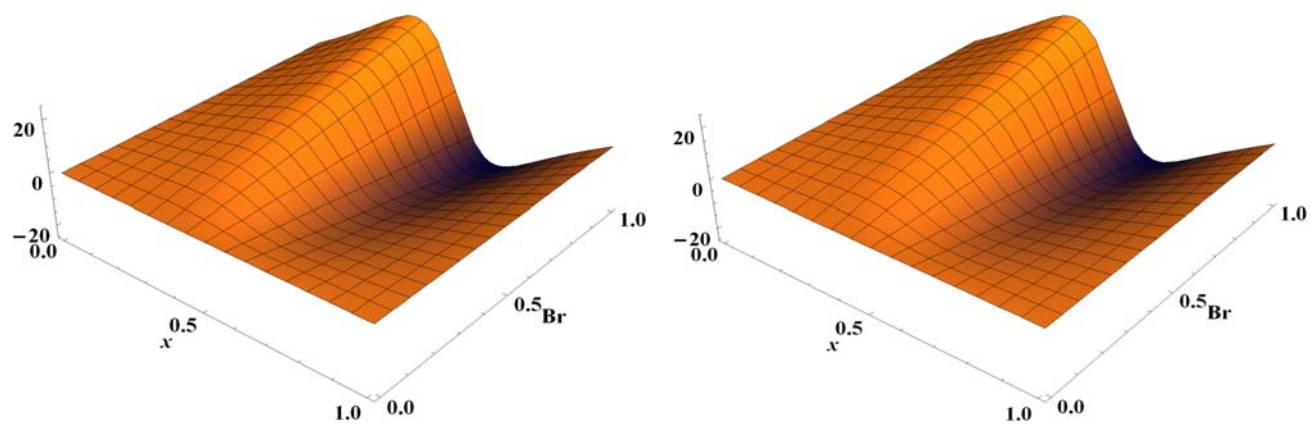


Fig. 6.15 Effect of Br on Z when $Sc = 0.5$, $Sr = 0.5$, $M = 0.5$, $a = 0.3$, $\eta = 1.4$ and $Du = 0.5$.

Chapter 7

Soret and Dufour effects on peristaltic flow in an asymmetric channel

This chapter studies the combined effects of heat and mass transfer on the peristaltic flow of magnetohydrodynamic (MHD) fluid in an asymmetric channel. Asymmetry in channel is induced because of the wave amplitude and phases. Analysis has been performed in the presence of slip conditions. Attention has been given to the Soret and Dufour effects. The obtained results are plotted and discussed.

7.1 Mathematical analysis

We consider MHD flow of incompressible fluid in an asymmetric channel. The \overline{X} -axis is selected along the channel walls and \overline{Y} -axis perpendicular to the \overline{X} -axis. The flow is due to the sinusoidal wave trains travelling on the walls of the channel with speed c . The geometry of the waves is given below

$$H_1(\overline{X}, \overline{t}) = d_1 + a_1 \cos \left(\frac{2\pi}{\lambda} (\overline{X} - c\overline{t}) \right), \quad (7.1)$$

$$H_2(\overline{X}, \overline{t}) = -d_2 - b_1 \cos \left(\frac{2\pi}{\lambda} (\overline{X} - c\overline{t}) + \gamma \right), \quad (7.2)$$

in which a_1 and b_1 are the amplitudes of the waves travelling on the upper and lower walls respectively, γ is the phase difference of two waves and $d_1 + d_2$ is the width of the channel. The phase difference γ ranges $0 \leq \gamma \leq \pi$. Here $\gamma = 0$ corresponds to the symmetric channel with waves out of phase and for $\gamma = \pi$ the waves are in phase. Moreover d_1 , d_2 , a_1 , b_1 and γ satisfy the condition

$$a_1^2 + b_1^2 + 2a_1b_1 \cos(\gamma) \leq (d_1 + d_2)^2.$$

A uniform magnetic field \mathbf{B}_0 is applied in the transverse direction to the flow. Effects of induced magnetic field are not considered by choosing low magnetic Reynolds number. However, Joule heating and Soret and Dufour effects are taken into account. The equations of mass, momentum, energy and concentration in the laboratory frame (\bar{X}, \bar{Y}) are

$$\frac{\partial \bar{U}}{\partial \bar{X}} + \frac{\partial \bar{V}}{\partial \bar{Y}} = 0, \quad (7.3)$$

$$\rho \left(\frac{\partial}{\partial \bar{t}} + \bar{U} \frac{\partial}{\partial \bar{X}} + \bar{V} \frac{\partial}{\partial \bar{Y}} \right) \bar{U} = -\frac{\partial \bar{P}}{\partial \bar{X}} + \frac{\partial}{\partial \bar{X}} \left(2\mu \frac{\partial \bar{U}}{\partial \bar{X}} \right) + \frac{\partial}{\partial \bar{Y}} \left[\mu \left(\frac{\partial \bar{V}}{\partial \bar{X}} + \frac{\partial \bar{U}}{\partial \bar{Y}} \right) \right] - \sigma B_0^2 \bar{U}, \quad (7.4)$$

$$\rho \left(\frac{\partial}{\partial \bar{t}} + \bar{U} \frac{\partial}{\partial \bar{X}} + \bar{V} \frac{\partial}{\partial \bar{Y}} \right) \bar{V} = -\frac{\partial \bar{P}}{\partial \bar{Y}} + \frac{\partial}{\partial \bar{X}} \left[\mu \left(\frac{\partial \bar{V}}{\partial \bar{X}} + \frac{\partial \bar{U}}{\partial \bar{Y}} \right) \right] + \frac{\partial}{\partial \bar{Y}} \left(2\mu \frac{\partial \bar{V}}{\partial \bar{Y}} \right), \quad (7.5)$$

$$\begin{aligned} \rho C_p \left(\frac{\partial}{\partial \bar{t}} + \bar{U} \frac{\partial}{\partial \bar{X}} + \bar{V} \frac{\partial}{\partial \bar{Y}} \right) T &= K \left[\frac{\partial^2 T}{\partial \bar{X}^2} + \frac{\partial^2 T}{\partial \bar{Y}^2} \right] \\ + \mu \left[2 \left\{ \left(\frac{\partial \bar{U}}{\partial \bar{X}} \right)^2 + \left(\frac{\partial \bar{V}}{\partial \bar{Y}} \right)^2 \right\} + \left(\frac{\partial \bar{U}}{\partial \bar{Y}} + \frac{\partial \bar{V}}{\partial \bar{X}} \right)^2 \right] &+ \sigma B_0^2 \bar{U}^2 + \frac{DK_T}{C_s} \left[\frac{\partial^2 C}{\partial \bar{X}^2} + \frac{\partial^2 C}{\partial \bar{Y}^2} \right], \end{aligned} \quad (7.6)$$

$$\left[\frac{\partial}{\partial \bar{t}} + \bar{U} \frac{\partial}{\partial \bar{X}} + \bar{V} \frac{\partial}{\partial \bar{Y}} \right] C = D \left[\frac{\partial^2 C}{\partial \bar{X}^2} + \frac{\partial^2 C}{\partial \bar{Y}^2} \right] + \frac{DK_T}{T_m} \left[\frac{\partial^2 T}{\partial \bar{X}^2} + \frac{\partial^2 T}{\partial \bar{Y}^2} \right], \quad (7.7)$$

where \bar{U} , \bar{V} are the velocity components in the \bar{X} and \bar{Y} directions respectively, \bar{P} the pressure, T the temperature, C the concentration, ρ the density of fluid, μ the dynamic viscosity, C_p the specific heat, K thermal conductivity, T_m fluid mean temperature, D the mass diffusivity, C_s the concentration susceptibility and K_T the thermal diffusion ratio. Using the following transformations in order to transform our problem in to wave frame (\bar{x}, \bar{y})

$$\bar{x} = \bar{X} - c\bar{t}, \quad \bar{y} = \bar{Y}, \quad \bar{u} = \bar{U} - c, \quad \bar{v} = \bar{V}, \quad \bar{p}(\bar{x}, \bar{y}) = \bar{P}(\bar{X}, \bar{Y}, \bar{t}). \quad (7.8)$$

We define the following dimensionless quantities

$$\begin{aligned}
x &= \frac{\bar{x}}{\lambda}, \quad y = \frac{\bar{y}}{d_1}, \quad u = \frac{\bar{u}}{c}, \quad v = \frac{\bar{v}}{c\delta}, \quad \delta = \frac{d_1}{\lambda}, \quad h_1 = \frac{H_1}{d_1}, \quad h_2 = \frac{H_2}{d_1}, \quad d = \frac{d_2}{d_1}, \quad p = \frac{d_1^2 \bar{p}}{c\lambda\mu}, \\
\theta &= \frac{T - T_0}{T_1 - T_0}, \quad \phi = \frac{C - C_0}{C_1 - C_0}, \quad M = \left(\frac{\sigma}{\mu}\right)^{1/2} B_0 d_1, \quad \mathbf{v} = \frac{\mu}{\rho}, \quad Re = \frac{\rho c d_1}{\mu}, \quad a = \frac{a_1}{d_1}, \quad b = \frac{b_1}{d_1}, \\
t &= \frac{c\bar{t}}{\lambda}, \quad Br = Pr E, \quad Du = \frac{D(C_1 - C_0)K_T}{C_s C_p \mu (T_1 - T_0)}, \quad Sr = \frac{\rho D K_T (T_1 - T_0)}{\mu T_m (C_1 - C_0)}, \\
Sc &= \frac{\mu}{\rho D}, \quad E = \frac{c^2}{C_p (T_1 - T_0)}, \quad Pr = \frac{\mu C_p}{K}, \quad u = \frac{\partial \psi}{\partial y} \text{ and } v = -\frac{\partial \psi}{\partial x},
\end{aligned} \tag{7.9}$$

in which δ is the wave number, θ the non-dimensional temperature, ϕ the dimensionless concentration, M the Hartman number, Re the Reynolds number, Br the Brinkman number, T_0 and C_0 the temperature and concentration at upper wall, T_1 and C_1 the temperature and concentration at lower wall, Pr the Prandtl number, E the Eckert number, Sr the Soret number and Sc the Schmidt number. We find that p does not depend upon y i.e. $\partial p / \partial y = 0$ and x -component of momentum equation reads to

$$\frac{dp}{dx} = \frac{\partial^3 \psi}{\partial y^3} - M^2 \left(\frac{\partial \psi}{\partial y} + 1 \right), \tag{7.10}$$

where (u, v) are the velocity components in the wave frame, p the pressure in wave frame and ψ the stream function.

Now the compatibility, energy and concentration equations are given by

$$\frac{\partial^4 \psi}{\partial y^4} - M^2 \frac{\partial \psi^2}{\partial y^2} = 0, \tag{7.11}$$

$$0 = \frac{\partial^2 \theta}{\partial y^2} + Br \left(\frac{\partial^2 \psi}{\partial y^2} \right)^2 + Br M^2 \left(\frac{\partial \psi}{\partial y} + 1 \right)^2 + Pr Du \frac{\partial^2 \phi}{\partial y^2}, \tag{7.12}$$

$$0 = \frac{1}{Sc} \frac{\partial^2 \phi}{\partial y^2} + Sr \frac{\partial^2 \theta}{\partial y^2}. \tag{7.13}$$

The non-dimensional boundary conditions in terms of slip are

$$\begin{aligned}\psi &= \frac{F}{2}, \quad \frac{\partial\psi}{\partial y} + \beta_1 \frac{\partial^2\psi}{\partial y^2} = -1, \quad \theta + \beta_2 \frac{\partial\theta}{\partial y} = 0, \quad \phi + \beta_3 \frac{\partial\Phi}{\partial y} = 0, \quad \text{at } y = h_1, \\ \psi &= -\frac{F}{2}, \quad \frac{\partial\psi}{\partial y} - \beta_1 \frac{\partial^2\psi}{\partial y^2} = -1, \quad \theta - \beta_2 \frac{\partial\theta}{\partial y} = 1, \quad \phi - \beta_3 \frac{\partial\Phi}{\partial y} = 1, \quad \text{at } y = h_2,\end{aligned}\quad (7.14)$$

in which β_1 , β_2 and β_3 are the dimensionless velocity, temperature and concentration slip parameters respectively. These are defined as

$$\beta_1 = \frac{\mu\beta_1^*}{d_1}, \beta_2 = \frac{\beta_2^*}{d_1}, \beta_3 = \frac{\beta_3^*}{d_1},$$

where β_1^* , β_2^* and β_3^* are the dimensional velocity, temperature and concentration slip parameters respectively.

Now the dimensionless expressions of wave shapes are

$$h_1(x) = 1 + a \cos(2\pi x), \quad h_2(x) = -d - b \cos(2\pi x + \gamma). \quad (7.15)$$

Flow rate and pressure rise per wavelength Δp_λ are defined as follows:

$$F = \int_{h_2}^{h_1} \frac{\partial\psi}{\partial y} dy, \quad (7.16)$$

$$\Delta p_\lambda = \int_0^1 \frac{\partial p}{\partial x} dx. \quad (7.17)$$

Heat transfer coefficient Z_1 at the upper wall is defined by

$$Z_1 = h_{1x} \theta_y.$$

The solution of the involved problems through **Mathematica** are analyzed in the next section.

7.2 Discussion

This section is especially prepared to examine the effects of pertinent parameters. Here we arrange the variations of such parameters in the Figs. 7.1-7.4. These Figs. depict the plots of

stream lines, temperature, concentration and heat transfer coefficient at the upper wall. Figs. 7.1(a-d) illustrate the streamlines for an increase in velocity slip parameter β_1 . The volume of fluid trapped within a streamline is termed as bolus. It is observed that the trapped bolus gets elongated and its size increases when the slip parameter increases.

Figs. 7.2(a-i) exhibit the temperature variation. It is seen that the temperature increases due to increase in M , β_2 , Du , Sr , Sc , Pr and γ . However it is found that the temperature decreases when d and β_1 are increased. Increase in θ is rapid and much in cases of M and Pr (see Figs. 7.2a and 7.2f) but slower and small for β_2 , Du , Sr and Sc (see Figs. 7.2b, 2c, 2d and 2e).

Figs. 7.3(a-h) demonstrate how concentration field develops when certain parameters of interest are varied. Key observations from these Figs. are that concentration decreases with the increase in M , β_3 , Du , Sr , Sc and Pr whereas it increases by increasing β_1 and γ . Here decrease in ϕ is much for M , β_3 , Sr , Sc , Pr and small for Du . Moreover the concentration remains invariant for thermal slip parameter β_2 .

Figs. 7.4(a-e) are plotted to see the behavior of heat transfer coefficient Z_1 at the upper wall. Because of peristalsis it is found that, Z_1 has an oscillatory behavior. Moreover Z_1 has maximum value near the upper wall. It increases with the increase in M and γ . Further Z_1 decreases with increase in d and β_1 . An interesting and noteworthy fact is that the thermal slip parameter β_2 has no meaningful variation on Z_1 .

7.3 Main points

Simultaneous effects of heat and mass transfer on the peristaltic transport of viscous fluid in an asymmetric channel with slip effects are analyzed. Their main observations are summarized as follows:

- The trapped bolus gets elongated as the value of viscosity parameter is increased.
- Effects of Hartman number M , Dufour number Du and temperature slip parameter β_2 on the temperature are opposite to that of velocity slip parameter β_1 .
- Increase in temperature subject to an increase in Hartman number M is rapid when

compared to that of other parameters.

- Increase in applied magnetic field results in decrease of concentration.
- Thermal slip parameter has no effect on the fluid concentration.
- Absolute value of the heat transfer coefficient increases with increase in the Hartman number M .

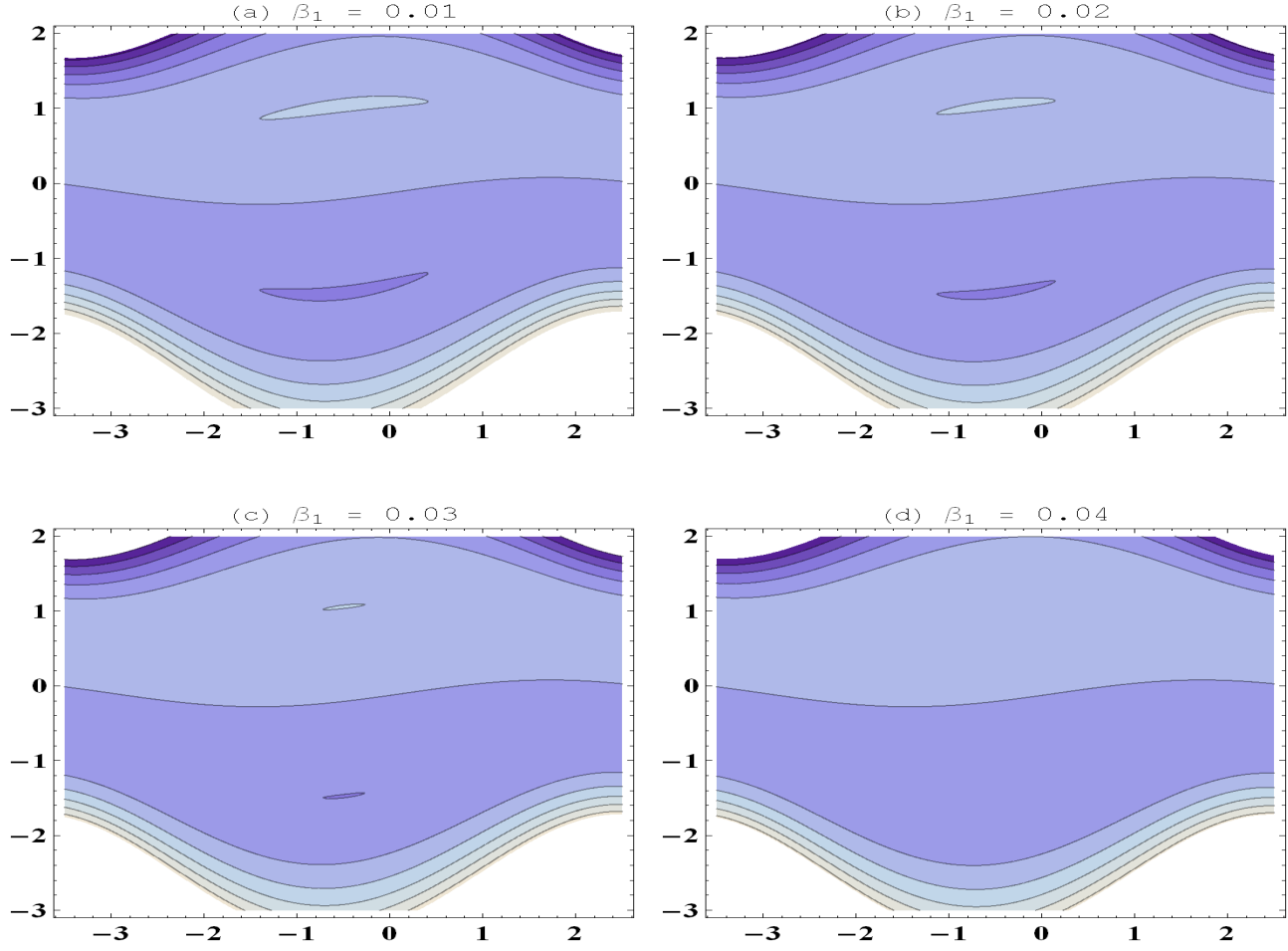


Fig. 7.1. Effect of velocity slip parameter β_1 on stream lines.

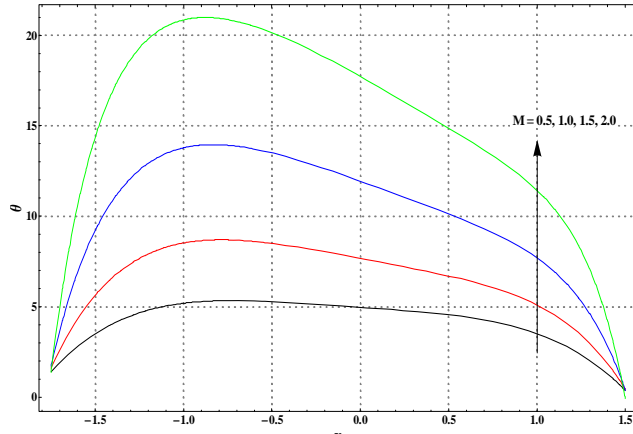


Fig. 7.2 a

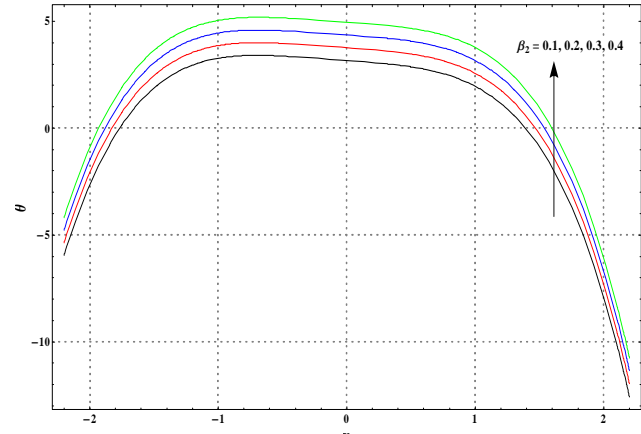


Fig. 7.2 b

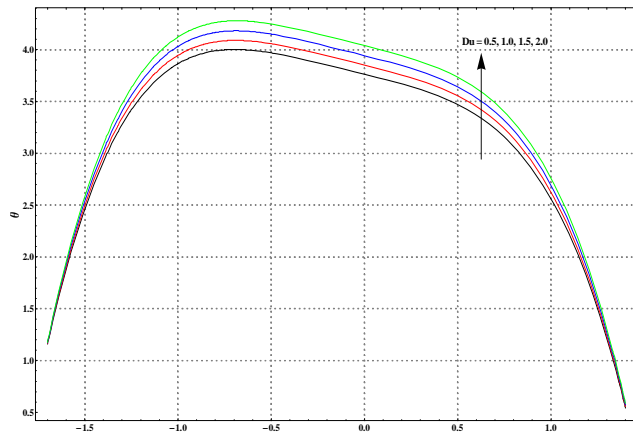


Fig. 7.2 c

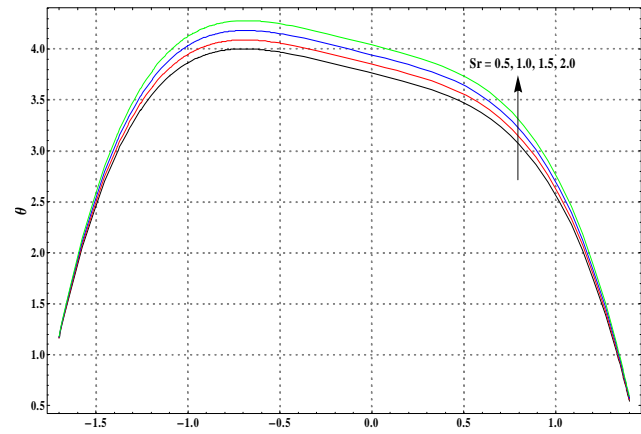


Fig. 7.2 d

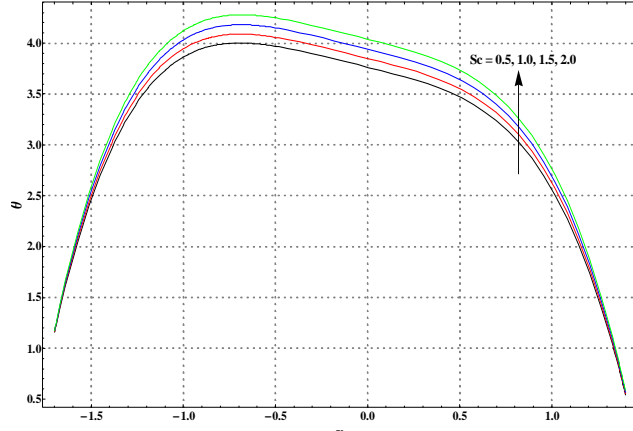


Fig. 7.2 e

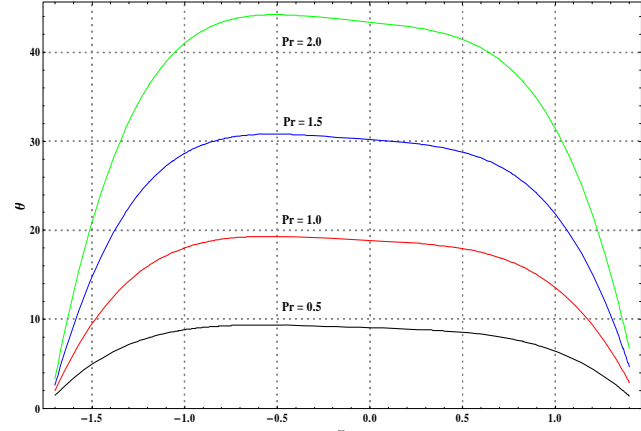


Fig. 7.2 f

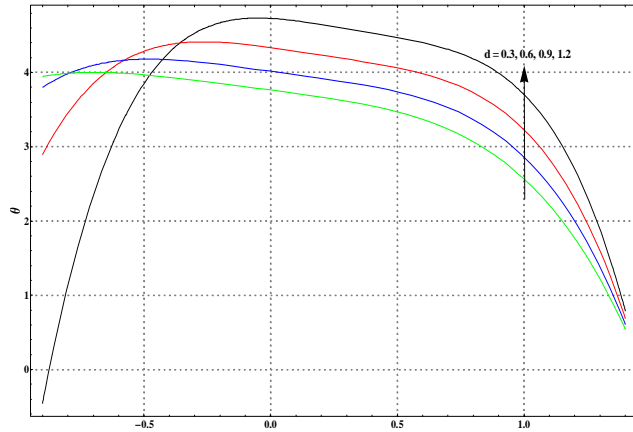


Fig. 7.2 g

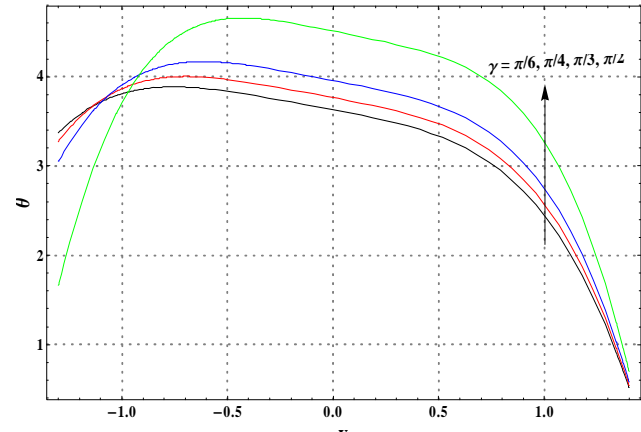


Fig. 7.2 h

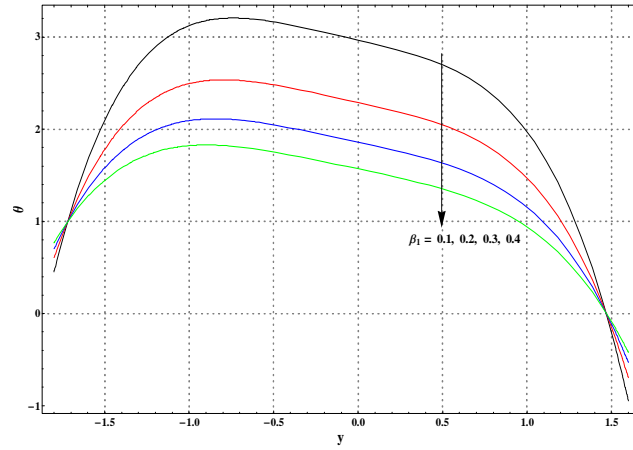


Fig. 7.2 i

Figs. 7.2(a-i). Effects of various parameters on temperature θ .

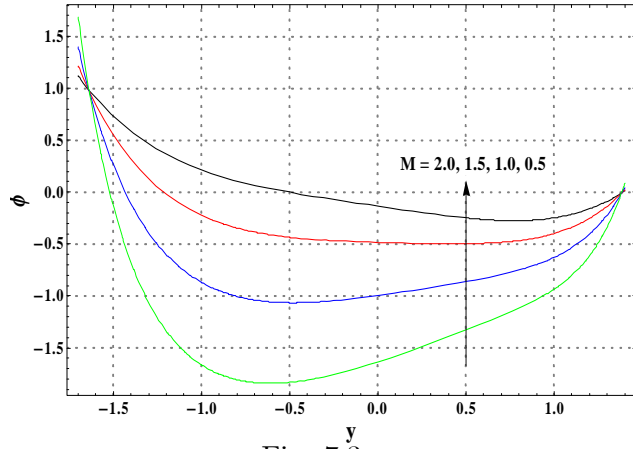


Fig. 7.3 a

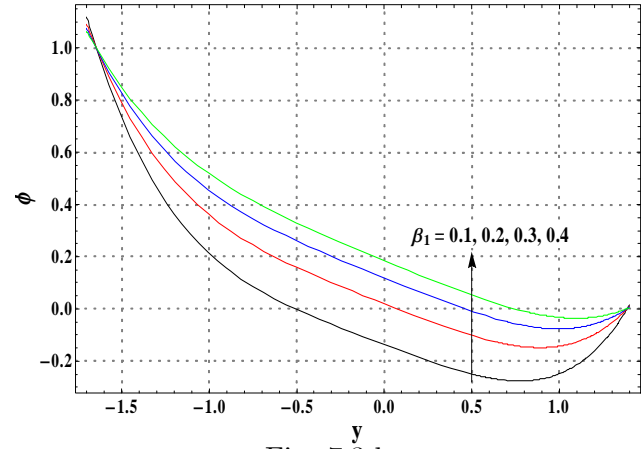


Fig. 7.3 b

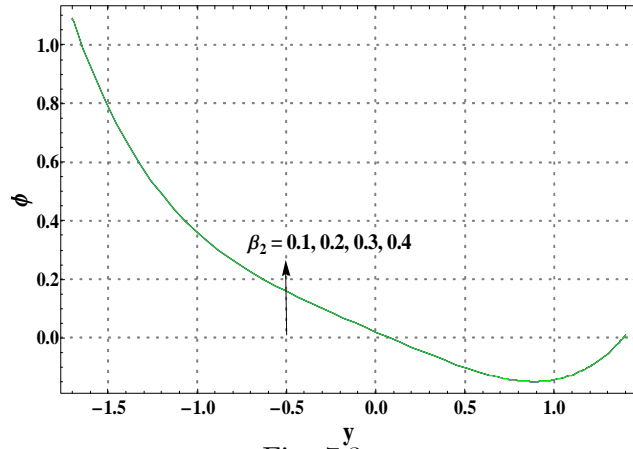


Fig. 7.3 c

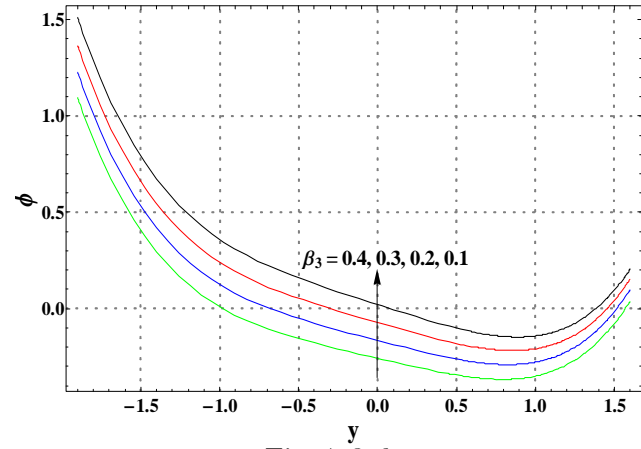
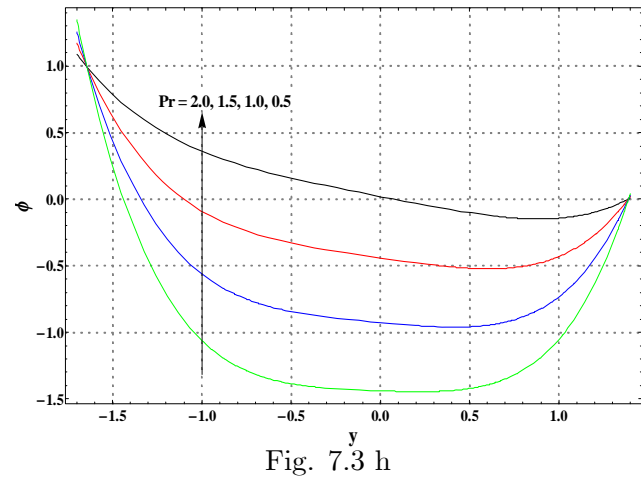
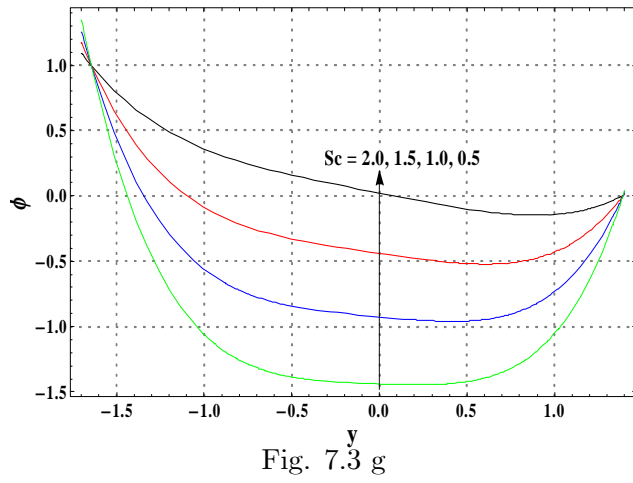
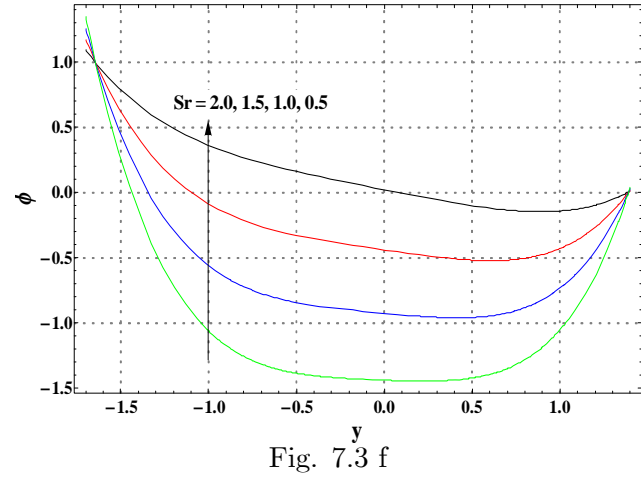
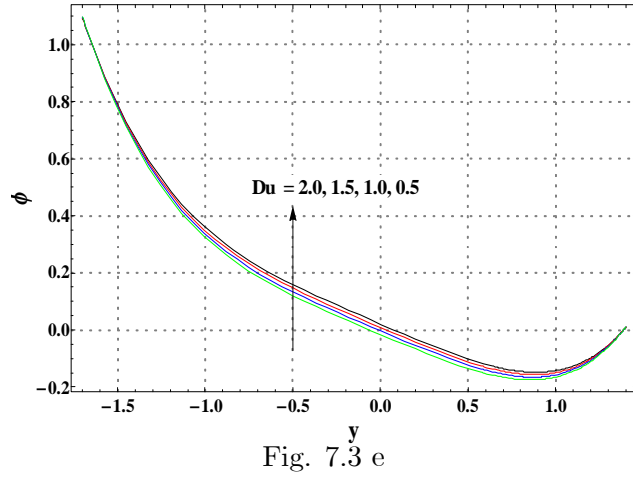


Fig. 7.3 d



Figs. 7.3(a-h). Effects of various parameters on concentration.

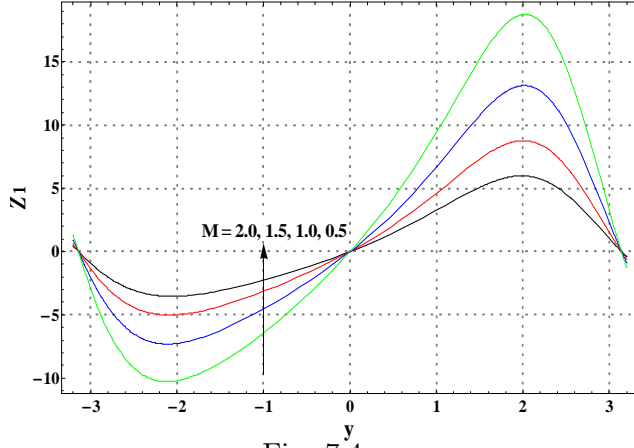


Fig. 7.4 a

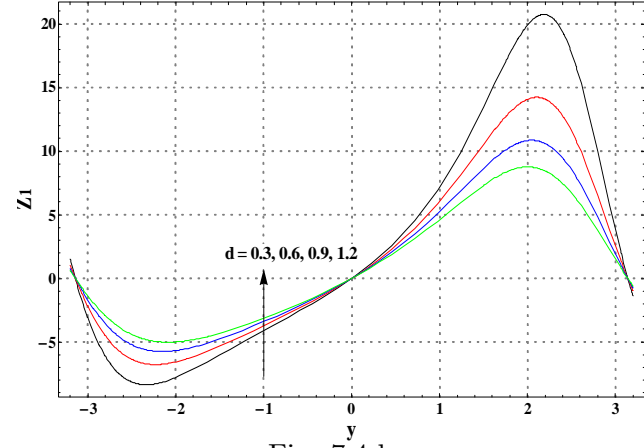


Fig. 7.4 b

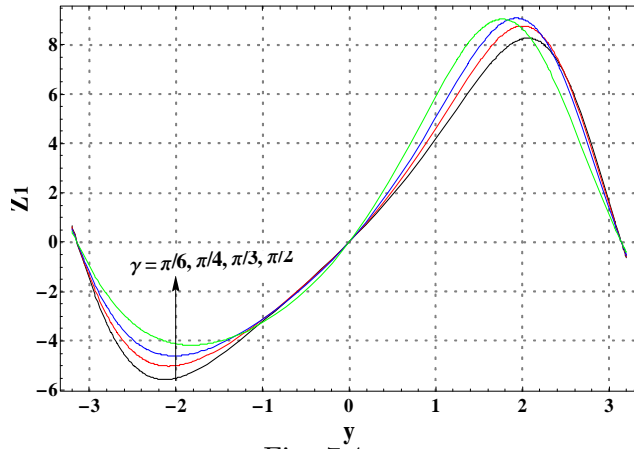


Fig. 7.4 c

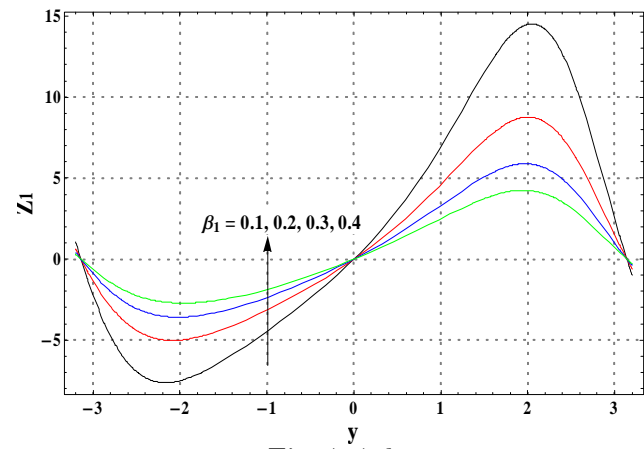


Fig. 7.4 d

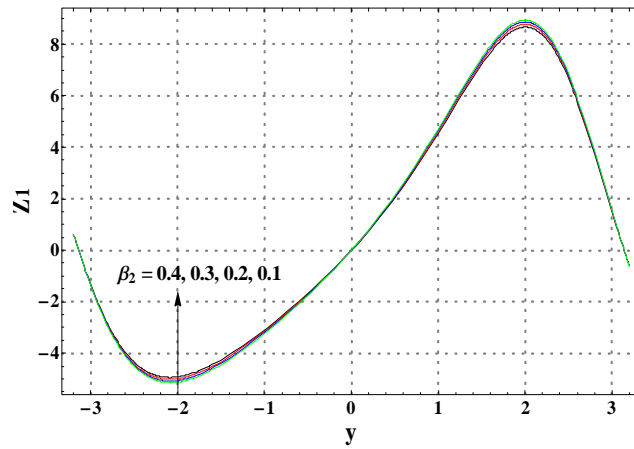


Fig. 7.4 e

Figs. 7.4(a-e). Behavior of Z_1 for different parameters.

Chapter 8

Peristaltic transport in a vertical channel subject to Soret and Dufour effects

This chapter looks at the simultaneous effects of heat and mass transfer in peristaltic transport of viscous fluid. Mathematical modelling is provided in the presence of Joule heating and Soret and Dufour effects. Perturbation solution is prepared for small Brinkman number. Flow quantities of interest are plotted and analyzed.

8.1 Mathematical formulation

Here our aim is to develop a model for the peristaltic transport of viscous fluid in a vertical channel. An incompressible fluid is considered in a vertical channel. Magnetohydrodynamic (MHD) character of fluid is accounted. The flow is generated by sinusoidal waves having constant speed c . The channel width is taken as $2d_1$. An incompressible and magnetohydrodynamic (MHD) fluid fills the region in the channel. The fluid is conducting through uniform applied magnetic field \mathbf{B}_0 . Induced magnetic field is not taken into account. Electric field is absent.

Geometry of flow problem is given below

The wall shape is taken as

$$H(\bar{X}, \bar{t}) = d_1 + a_1 \cos \left(\frac{2\pi}{\lambda} (\bar{X} - c\bar{t}) \right), \quad (8.1)$$

where a_1 is the wave amplitude, λ the wavelength and \bar{t} the time. The velocity field in two-dimensional flow is given by

$$V = [\bar{U}(\bar{X}, \bar{Y}, \bar{t}), \bar{V}(\bar{X}, \bar{Y}, \bar{t}), 0].$$

Conservation laws of mass, momentum and energy in the present flow consideration are reduced in the following expressions

$$\frac{\partial \bar{U}}{\partial \bar{X}} + \frac{\partial \bar{V}}{\partial \bar{Y}} = 0, \quad (8.2)$$

$$\begin{aligned} \rho \left(\frac{\partial}{\partial \bar{t}} + \bar{U} \frac{\partial}{\partial \bar{X}} + \bar{V} \frac{\partial}{\partial \bar{Y}} \right) \bar{U} &= -\frac{\partial \bar{P}}{\partial \bar{X}} + \mu \left[\frac{\partial^2 \bar{U}}{\partial \bar{X}^2} + \frac{\partial^2 \bar{U}}{\partial \bar{Y}^2} \right] - \sigma B_0^2 \bar{U} + \rho g \alpha^* (T - T_0) \\ &\quad + \rho g \alpha^{**} (C - C_0), \end{aligned} \quad (8.3)$$

$$\rho \left(\frac{\partial}{\partial \bar{t}} + \bar{U} \frac{\partial}{\partial \bar{X}} + \bar{V} \frac{\partial}{\partial \bar{Y}} \right) \bar{V} = -\frac{\partial \bar{P}}{\partial \bar{Y}} + \mu \left[\frac{\partial^2 \bar{V}}{\partial \bar{X}^2} + \frac{\partial^2 \bar{V}}{\partial \bar{Y}^2} \right], \quad (8.4)$$

$$\rho C_p \left(\frac{\partial}{\partial \bar{t}} + \bar{U} \frac{\partial}{\partial \bar{X}} + \bar{V} \frac{\partial}{\partial \bar{Y}} \right) T = K \left[\frac{\partial^2 T}{\partial \bar{X}^2} + \frac{\partial^2 T}{\partial \bar{Y}^2} \right] + \mu \left[2 \left(\left(\frac{\partial \bar{U}}{\partial \bar{X}} \right)^2 + \left(\frac{\partial \bar{V}}{\partial \bar{Y}} \right)^2 \right) + \left(\frac{\partial \bar{U}}{\partial \bar{Y}} + \frac{\partial \bar{V}}{\partial \bar{X}} \right)^2 \right] + \sigma B_0^2 \bar{U}^2 + \frac{DK_T}{C_s} \left[\frac{\partial^2 C}{\partial \bar{X}^2} + \frac{\partial^2 C}{\partial \bar{Y}^2} \right] + \Phi^* \quad (8.5)$$

$$\left[\frac{\partial}{\partial \bar{t}} + \bar{U} \frac{\partial}{\partial \bar{X}} + \bar{V} \frac{\partial}{\partial \bar{Y}} \right] C = D \left[\frac{\partial^2 C}{\partial \bar{X}^2} + \frac{\partial^2 C}{\partial \bar{Y}^2} \right] + \frac{DK_T}{T_m} \left[\frac{\partial^2 T}{\partial \bar{X}^2} + \frac{\partial^2 T}{\partial \bar{Y}^2} \right]. \quad (8.6)$$

In above expressions (\bar{U}, \bar{V}) are the velocity components in the laboratory frame (\bar{X}, \bar{Y}) , \bar{P} the pressure, g the acceleration due to gravity, α^* the coefficient of thermal expansion, α^{**} the coefficient of expansion due to concentration, K the thermal conductivity, C the concentration field, T the temperature field, D the mass diffusivity, K_T the thermal diffusion ratio, Φ^* the constant heat addition/absorption, C_p the specific heat, C_s the concentration susceptibility, C_0 the concentration at boundary, T_m and T_0 the fluid mean temperature and temperature at the boundary respectively.

If (\bar{u}, \bar{v}) are the velocity components in the wave frame (\bar{x}, \bar{y}) then using the transformations

$$\bar{x} = \bar{X} - c\bar{t}, \quad \bar{y} = \bar{Y}, \quad \bar{u} = \bar{U} - c, \quad \bar{v} = \bar{V}, \quad \bar{p}(\bar{x}, \bar{y}) = \bar{P}(\bar{X}, \bar{Y}, \bar{t}) \quad (8.7)$$

and taking

$$\begin{aligned} x &= \frac{\bar{x}}{\lambda}, \quad y = \frac{\bar{y}}{d_1}, \quad u = \frac{\bar{u}}{c}, \quad v = \frac{\bar{v}}{c\delta}, \quad \delta = \frac{d_1}{\lambda}, \quad h = \frac{H}{d_1}, \quad a = \frac{a_1}{d_1}, \quad p = \frac{d_1^2 \bar{p}}{c\lambda\mu}, \\ \theta &= \frac{T - T_0}{T_0}, \quad \phi = \frac{C - C_0}{C_0}, \quad M^2 = \left(\frac{\sigma}{\mu} \right) B_0^2 d_1^2, \quad \nu = \frac{\mu}{\rho}, \quad Re = \frac{\rho c d_1}{\mu}, \\ t &= \frac{c\bar{t}}{\lambda}, \quad Br = Pr E, \quad Du = \frac{DC_0 K_T}{C_s C_p \mu T_0}, \quad Sr = \frac{\rho D K_T T_0}{\mu T_m C_0}, \quad Sc = \frac{\mu}{\rho D}, \\ E &= \frac{c^2}{C_p T_0}, \quad Pr = \frac{\mu C_p}{K}, \quad G_t = \frac{\rho g \alpha^* T_0 d_1^2}{\mu c}, \quad G_c = \frac{\rho g \alpha^{**} C_0 d_1^2}{\mu c}, \\ \Phi &= \frac{a^2 \Phi^*}{k(T - T_0)}, \quad u = \frac{\partial \psi}{\partial y}, \quad v = -\frac{\partial \psi}{\partial x}, \end{aligned} \quad (8.8)$$

incompressibility condition (8.2) is clearly satisfied while Eqs. (8.3)-(8.6) through standard definition of stream function ψ can be written as

$$\frac{dp}{dx} = \frac{\partial^3 \psi}{\partial y^3} - M^2 \left(\frac{\partial \psi}{\partial y} + 1 \right) + G_t \theta + G_c \phi, \quad (8.9)$$

$$\frac{\partial^4 \psi}{\partial y^4} - M^2 \frac{\partial \psi^2}{\partial y^2} + G_t \frac{\partial \theta}{\partial y} + G_c \frac{\partial \phi}{\partial y} = 0, \quad (8.10)$$

$$\frac{\partial p}{\partial y} = 0, \quad (8.11)$$

$$0 = \frac{\partial^2 \theta}{\partial y^2} + Br \left(\frac{\partial^2 \psi}{\partial y^2} \right)^2 + Br M^2 \left(\frac{\partial \psi}{\partial y} + 1 \right)^2 + Pr Du \frac{\partial^2 \phi}{\partial y^2} + \Phi, \quad (8.12)$$

$$0 = \frac{1}{Sc} \frac{\partial^2 \phi}{\partial y^2} + Sr \frac{\partial^2 \theta}{\partial y^2}. \quad (8.13)$$

From Eq (8.11) $p \neq p(y)$. Here ν denotes the kinematic viscosity, M the Hartman number, Re the Reynolds number, G_t the local temperature Grashoff number, G_c the local concentration Grashoff number, Φ the dimensionless heat source/sink parameter, Br the Brinkman number, Du the Dufour number, Sr the Soret number, Sc the Schmidt number, E the Eckret number, Pr the Prandtl number, δ the wave number and the dimensionless temperature and concentration are denoted by θ and ϕ respectively. The boundary conditions are prescribed in the following forms

$$\begin{aligned} \psi &= 0, & \frac{\partial^2 \psi}{\partial y^2} &= 0, & \frac{\partial \theta}{\partial y} &= 0, & \frac{\partial \phi}{\partial y} &= 0, & \text{at } y &= 0, \\ \psi &= F, & \frac{\partial \psi}{\partial y} &= -1, & \theta &= 0, & \phi &= 0, & \text{at } y &= h, \end{aligned} \quad (8.14)$$

$$h(x) = 1 + a \cos(2\pi x), \quad F = \int_0^h \frac{\partial \psi}{\partial y} dy, \quad (8.15)$$

where h is the dimensionless form of the wall shape. The dimensionless mean flow rates in laboratory (η) and wave (F) frames are related by

$$\eta = F + 1.$$

Pressure rise per wavelength Δp_λ can be put into the following relation

$$\Delta p_\lambda = \int_0^1 \frac{dp}{dx} dx. \quad (8.16)$$

8.2 Series expressions

We are interested to develop the series solutions of the resulting problems. For that we expand the stream function in terms of small Brinkman number and write

$$\psi = \psi_0 + Br\psi_1 + \dots$$

Similarly the other physical quantities like θ , ϕ , F and P are also expanded. It is worth mentioning to point out that the condition $Br \ll 1$ is not an unrealistic condition. For example, the most common Newtonian fluid i.e. water, at 25°C ($298\text{ Kelvin} \approx \text{room temperature}$) has dynamic viscosity $\mu = 0.89\text{ cP}$ (centi poise) and thermal conductivity 0.58 W/mK (watt per meter Kelvin). If we consider the characteristic speed 1m/s (meter per second) and wall temperature to be 310 Kelvin ($\approx \text{equal to body temperature}$), then the Brinkman number comes out to be $1.2787 \times 10^{-4} \ll 1$. This provides us a confidence regarding the selection of Brinkman number Br as a small quantity. Resulting zeroth and first order systems are given by

$$\frac{dp_0}{dx} = \frac{\partial^3 \psi_0}{\partial y^3} - M^2 \left(\frac{\partial \psi_0}{\partial y} + 1 \right) + G_t \theta_0 + G_c \phi_0,$$

$$0 = \frac{\partial^2 \theta_0}{\partial y^2} + \text{Pr} Du \frac{\partial^2 \phi_0}{\partial y^2} + \Phi,$$

$$0 = \frac{1}{Sc} \frac{\partial^2 \phi_0}{\partial y^2} + Sr \frac{\partial^2 \theta_0}{\partial y^2},$$

$$\psi_0 = 0, \quad \frac{\partial^2 \psi_0}{\partial y^2} = 0, \quad \frac{\partial \theta_0}{\partial y} = 0, \quad \frac{\partial \phi_0}{\partial y} = 0, \quad \text{at } y = 0,$$

$$\psi_0 = F_0, \quad \frac{\partial \psi_0}{\partial y} = -1, \quad \theta_0 = 0, \quad \phi_0 = 0, \quad \text{at } y = h.$$

First order system

$$\frac{dp_1}{dx} = \frac{\partial^3 \psi_1}{\partial y^3} - M^2 \frac{\partial \psi_1}{\partial y} + G_t \theta_1 + G_c \phi_1,$$

$$0 = \frac{\partial^2 \theta_1}{\partial y^2} + \text{Pr} Du \frac{\partial^2 \phi_1}{\partial y^2} + \left(\frac{\partial^2 \psi_0}{\partial y^2} \right)^2 + M^2 \left(\frac{\partial \psi_0}{\partial y} + 1 \right)^2,$$

$$0 = \frac{1}{Sc} \frac{\partial^2 \phi_1}{\partial y^2} + Sr \frac{\partial^2 \theta_1}{\partial y^2},$$

$$\begin{aligned} \psi_1 &= 0, & \frac{\partial^2 \psi_1}{\partial y^2} &= 0, & \frac{\partial \theta_1}{\partial y} &= 0, & \frac{\partial \phi_1}{\partial y} &= 0, & \text{at } y &= 0, \\ \psi_1 &= F_1, & \frac{\partial \psi_1}{\partial y} &= 0, & \theta_1 &= 0, & \phi_1 &= 0, & \text{at } y &= h. \end{aligned}$$

The solutions of above systems yield the following expressions

$$\begin{aligned} \psi &= \frac{e^{-My} e^{M(h+2y)}}{6L_2} \left(-6(-1+A) A_1(y) + 2e^{hM} L_{1y} (6A_3) \right) \beta \\ &+ Br \left[-\frac{e^{5Mh+(y)}}{L_{11}} A_4(y) + L_{12} \right], \end{aligned}$$

$$\theta = \frac{(-h^2 + y^2) \beta}{2(-1+A)} - \frac{Br L_7}{360 L_6^2},$$

$$\phi = \frac{L_8}{360(-1+A)^3} + \frac{Br L_{10}}{L_9^2}.$$

Where

$$\begin{aligned}
L_1 &= (3(-1+A)(F+h)M^2A_2(y))e^{M(h+2y)}, \\
L_2 &= (-1+A)M^2\left(1+hM+e^{2hM}(-1+hM)\right), \\
L_3 &= 16e^{-2My+3M(h+y)}h(-1+h^2M^2)(G_t-G_cScSr)\Phi^2, \\
L_4 &= A_6(y)+A_7(y)(-1+A)(F+h)+A_8(y)+A_9(y), \\
L_5 &= (-1+A)^3M^{10}\left(1+hM+e^{2hM}(-1+hM)\right), \\
L_6 &= (-1+A)^3\left(1+hM+e^{2hM}(-1+hM)\right), \\
L_7 &= 720(-1+A)^2e^{M(h-y)F^2M^2}B_1(y)+B_2(y)+B_3(y)+B_4(y)+B_5(y), \\
L_8 &= ScSr\left(180(-1+A)^2(h-y)(h+y)\Phi\right), \\
L_9 &= \left(360(-1+A)^3\right)\left(1+hM+e^{2hM}(-1+hM)\right), \\
L_{10} &= C_1(y)+C_2(y)+C_3(y)+C_4(y)+C_5(y), \\
L_{11} &= \left(1+hM+e^{2hM}(-1+hM)\right), \\
L_{12} &= A_5(y)+\frac{L_3}{L_5^5}\left\{e^{M(h+2y)}L_4\right\}+A_{10}(y),
\end{aligned}$$

$A = PrScSrDu$, and A_i s, B_i s and C_i s are given below

$$\begin{aligned}
A_1 &= \frac{FM y \cosh(hM) + y \sinh(hM) - (F+h) \sinh(My)}{(hM \cosh(hM) - \sinh(hM))^2}, \\
A_2 &= A_1(y^2 A_3 + G_c(hM y \cosh(hM) + (h^3 M^2 - y)) \cosh(hM))^2 \cosh(My), \\
&+ \sinh(hM) - 2hM \sinh(2hM), \\
A_3 &= (F+h)^2 (1+h^2) M^2 + h^2 (F+h)^2 M^4 + G_t(2(F+h)^2 M (1+M^2) y \\
&\cosh(2My) \sinh(hM) + 16(F+h) M^2 y^2 \cosh(My)), \\
A_4 &= (F+h-8h^2) M^2 + 8h^4 M^4 \cosh(3hM) + 16h^2 (F+h) M^4 y^2 \cosh(hM)^2 \cosh(My) \\
&G_t(\sinh(My) - 16(F+h) My \sinh(hM)^2 \sinh(My)), \\
A_5 &= 2F(4+h+hM^2) - 2y^2 + G_c(h(8+h(3+M^2(1+2h^2-2y^2)))) \cosh(2hM), \\
A_6 &= 2y^2(h+y)(2F(4+h+hM^2) - G_t 2y^2 + h(8+h(3+M^2(1+2h^2-2y^2)))), \\
A_7 &= (y+2h^3) M^2 \cosh(2My) + 2FhM^2 \cosh(2My) + h^2 M^2 \cosh(2My) + 8(F+h), \\
A_8 &= e^{0y+2h} G_t(16(F+h) \sinh(hM) (M(h-y) + \sinh(My))), \\
A_9 &= 16M^2 y^2 \sinh(M(h-y)) + (F+h) (1+M^2) (-3+2M^2 y^2) \sinh(2My) + 16G_c \\
&+ M^2 y^2 \sinh(M(h+y)), \\
A_{10} &= (1+M^2) y - 4h^3 (F+h) M^4 (1+M^2) y^2 - 4(F+h) M^2 (1+M^2) y^3, \\
B_1 &= A_1(-8F^2 - 2h(4+h+3y) - 2Fy + h^2(F+2h) M^2 - 2h^2(F+h)^2 M^4) \\
&+ 2(1+F(F+2h) M^2 + (F+h)^2 M^4) y^2 + (F^2(1+M^2) + 2F(4+h+hM^2) \\
&- 2y^2 + h(8+h(3+M^2(1+2h^2-2y^2)))) \cosh(2hM) - (F+h)^2 (1+M^2) \cosh(2My). \\
B_2 &= 16h(F+h) M G_c y^3 (h+M^2 y) \cosh(hM) (M(h-y) + \sinh(My)) - 16(F+h) \\
&h \sinh(hM) (M(h-y) + y \sinh(My)), \\
B_3 &= \frac{1}{2} (F+h) B_9 \cosh(hM) - 16h^4 (F+h) A_3 + 8h^3 (F+h) M^4 (h-y) \cosh(2hM), \\
B_4 &= 128F1h^3 M^4 \cosh(hM)^2 \sinh(hM) + 2h^3 (F+h)^2 M^3 (1+M^2) \cosh(2My) + 8h^3 \\
&(F+h) M^4 (h-y) A_5, \\
B_5 &= h^4 M y (-4Fy + F^2 - 4h + 2y^2 Fh + h^2 + (F+h)^2 (1+h^2) M^2 + h^2 (F+h)^2 M^4), \\
C_1 &= 16h(F+h) M^2 (h-y) \cosh(hM) y G_c - (F^2(1+M^2) + 2F(4+h+hM^2) \\
&- 2y^2 + h(8+h(3+M^2(1+2h^2-2y^2)))) \cosh(2hM), \\
C_2 &= F^2 M^2 \cosh(2My) + 2FhM^2 \cosh(2My) + h^2 M^2 \cosh(2My) + 8(F+h) F^2 \\
&\cosh(2My) + 2Fh \cosh(2My), \\
C_3 &= 32y^2 (F+h) M^3 y^2 \cosh(My) B_2 - (h(F+h) (-8+5F+5h+(5F+(5-16h)h) M^2)), \\
C_4 &= 8F(4+F+h+(F+h+4h^2) M^2) \sinh(hM) - 8((4y(-1+h^2 M^2) + (F+h)), \\
C_5 &= h(-64+Fy(1+M^2) A_6 (-13+24h^2 M^2 + 16h^4 M^4) + h B_3 (-13+M^2(-13+8h(10+h)))).
\end{aligned}$$

8.3 Graphical results and analysis

This section emphasizes the impact of embedding flow parameters in the solution expressions. Here plots are prepared in the two and three dimensions. Arrangement of the graphs is made in such a way that Figs. 8.1 (a-d) show the pressure gradient, Figs. 8.2 (a-d) the pressure rise per wavelength, Figs. 8.3 (a-d) the 3-D plots for velocity profile, Figs. 8.4-8.9 the stream lines and Figs. 8.10 and 8.11 the 3D plots for temperature and concentration fields respectively.

Figs. 8.1 (a-d) reveal that pressure gradient decreases by increasing M and Sr . However, the pressure gradient increases with an increase in Φ and Du . It is further noticed that the change in dp/dx is larger in the cases of Φ and M when compared with Du and Sr .

Pressure rise per wavelength via mean flow rate η is displayed in the Figs. 8.2 (a-d). These Figs. show that the pressure rise decreases when flow rate increases. For a given constant value of the mean flow rate, the pressure rise increases with an increase in Φ and G_t but it decreases with increase in G_c (see Figs. 8.2 a,c and d). Behavior of pressure rise for M is however different. The pressure rise increases for negative value of mean flow rate when M increases. However, the behavior is opposite for positive values of mean flow rate (Fig. 8.2b).

We displayed the 3D plots for velocity, temperature and concentration. Here it is observed from Fig. 8.3 that the velocity decreases when M is increased. Such decrease largely depends upon the values of M . Physically the decrease in velocity is due to the reason that the Lorentz force has a role of retarding force. Consequently it increases the friction resistance which opposes the motion of fluid.

Figs. 8.3 (b-d) depict that the velocity is increasing function of Φ and G_t . However reverse situation is observed for G_c i.e. the velocity decreases when G_c increases.

Trapping is considered interesting feature of the peristaltic transport. The volume of fluid that gets trapped in a stream line during peristaltic motion is known as bolus. Figs. 8.4-8.9 depict that the size of trapped bolus decreases when M , G_c and Sr are larger. It is also found that the results are opposite for the cases of G_t , Φ and Du .

The variations of temperature and concentration fields can be seen through Figs. 8.10 and 8.11. These Figs show that the temperature increases when M , G_t , Φ and Du are increased. Clearly the rise in temperature with an increase in M and Du is more than Φ and G_t . Effects of G_c on the temperature are not significant.

Figs. 8.11 plot the influences of M , Φ , Du , G_t and G_c on the concentration field. Here concentration field decreases when there is an increase in M , Φ and Du . Further, the variations of concentration field for G_t and G_c are insignificant. It is also concluded that temperature increases and concentration decreases when M increases.

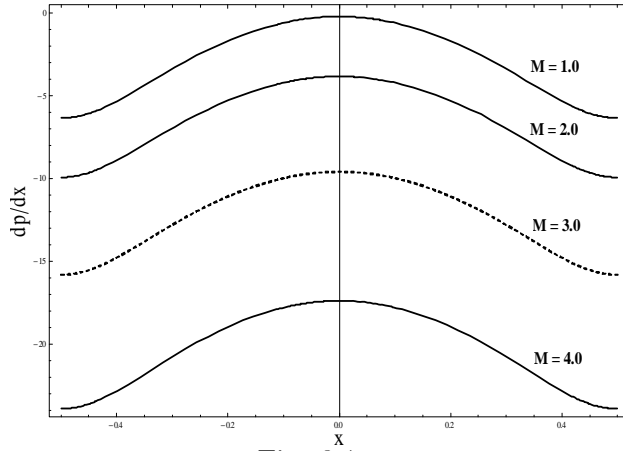


Fig. 8.1 a

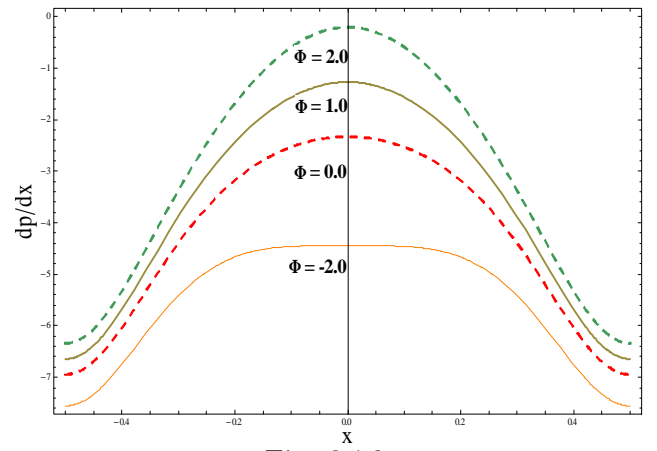


Fig. 8.1 b

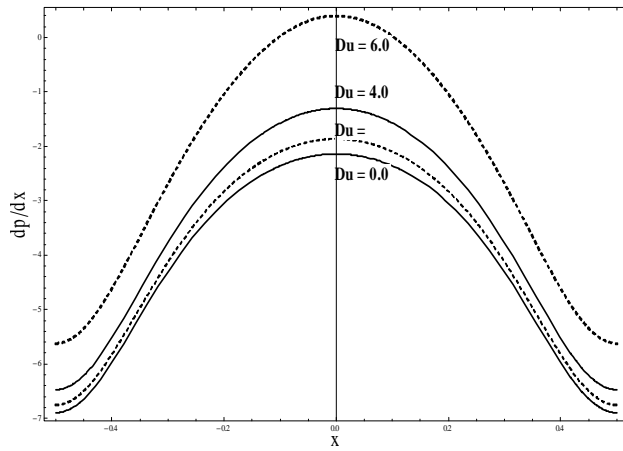


Fig. 8.1 c

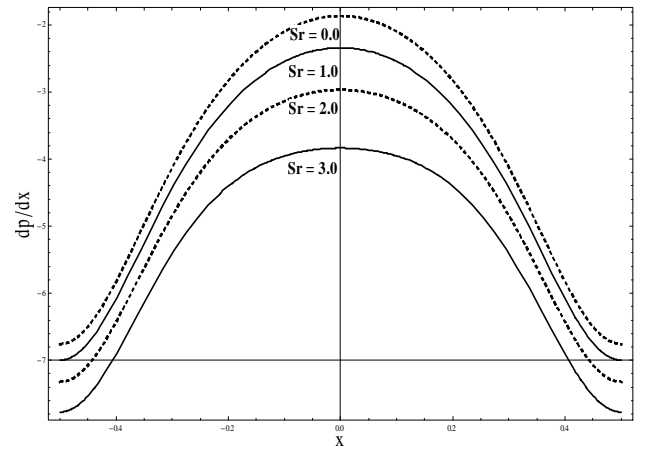


Fig. 8.1 d

Figs. 8.1 (a-d) Behavior of pressure gradient for variations in M , Φ , Du and Sr .

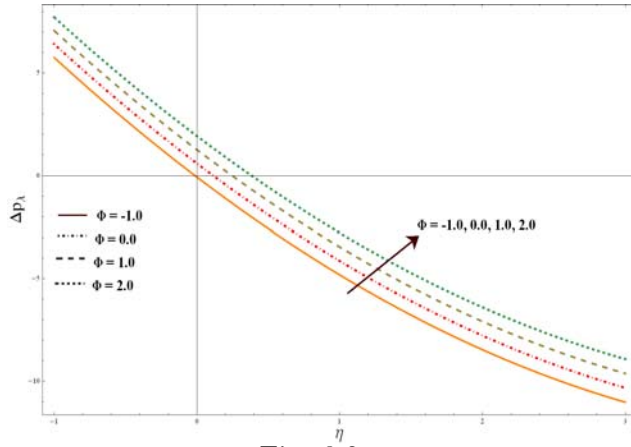


Fig. 8.2 a

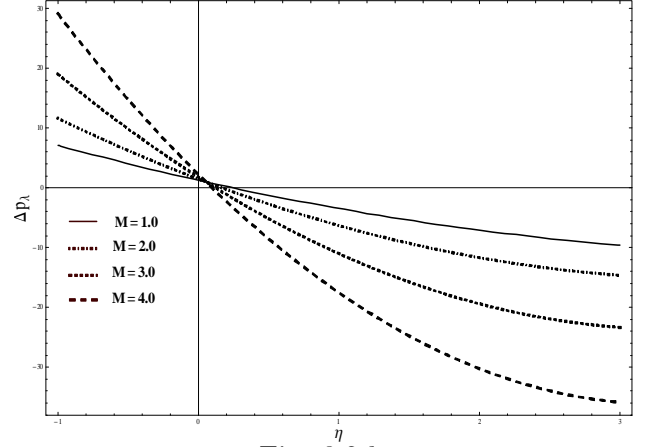


Fig. 8.2 b

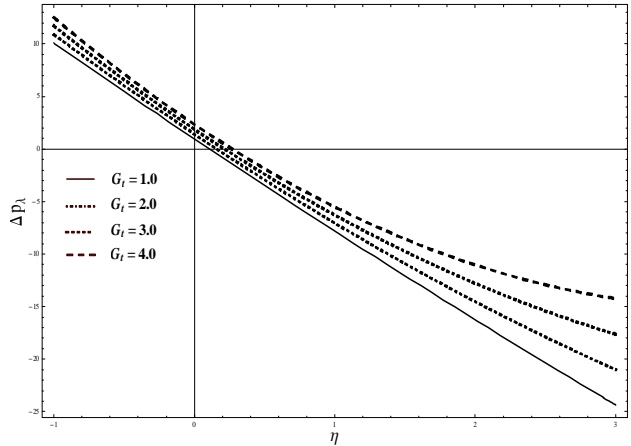


Fig. 8.2 c

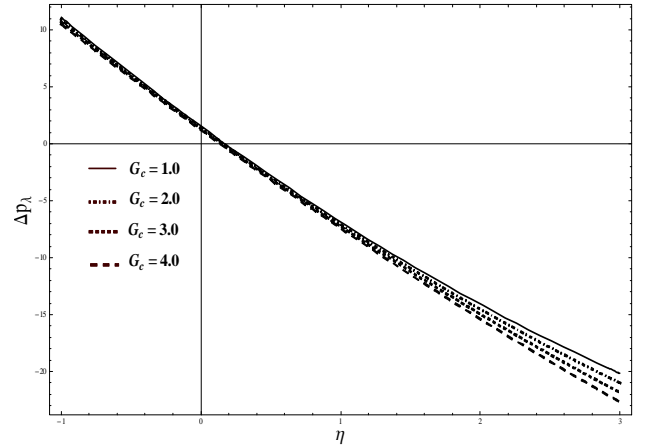


Fig. 8.2 d

Fig. 8.2 (a-d) Pressure rise per wavelength.

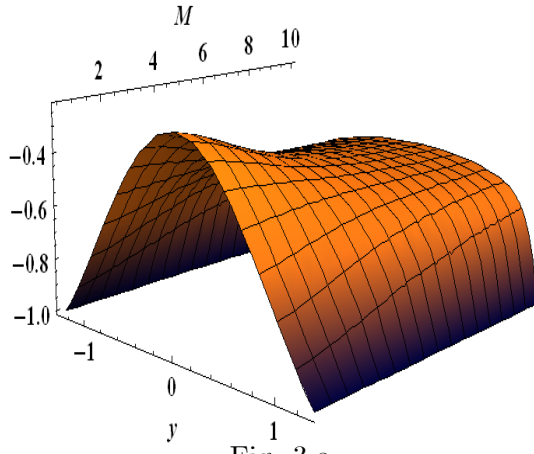


Fig. 3 a

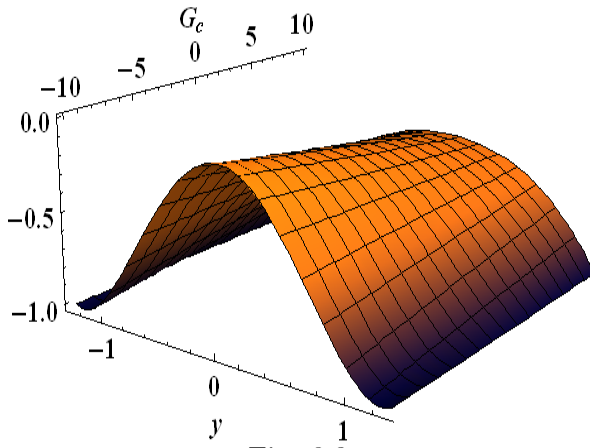
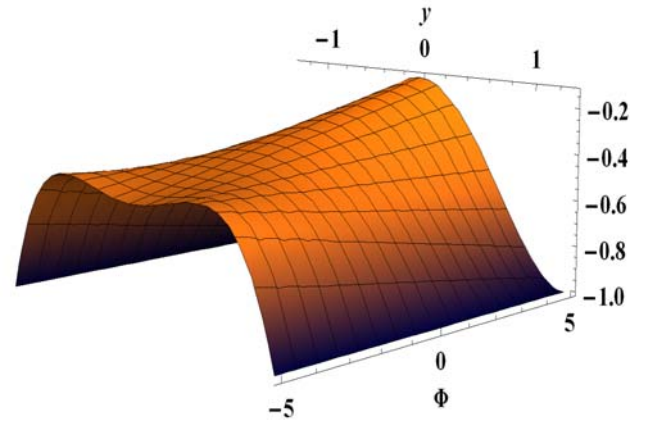


Fig. 8.3 c

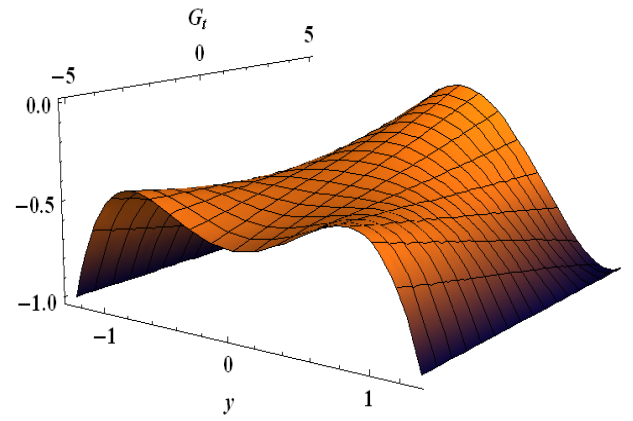


Fig. 8.3 d

Fig. 8.3(a-d) Velocity profile with variations of M , Φ , G_c and G_t .

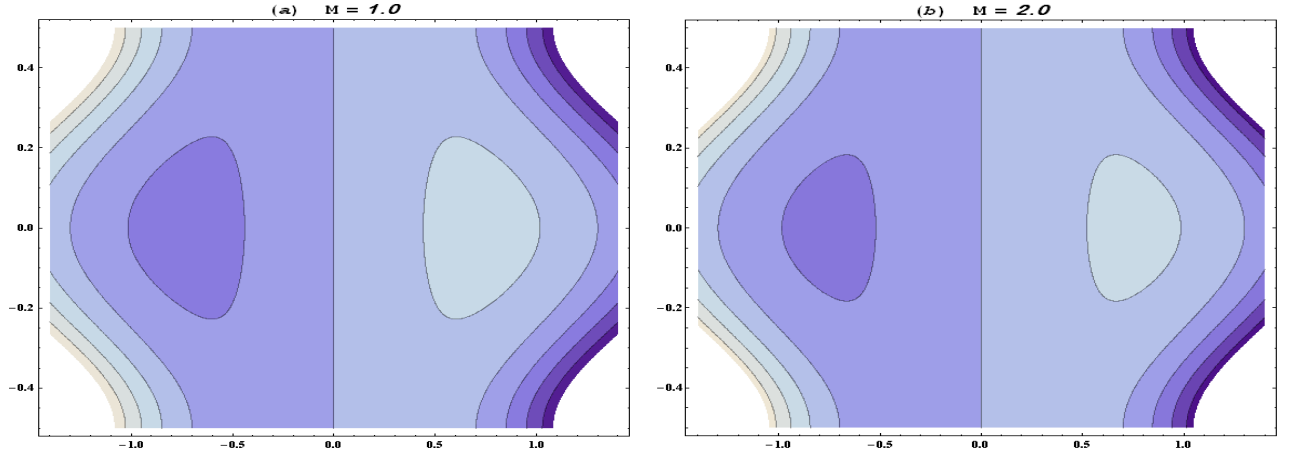


Fig. 8.4 Effect of Hartman number (M) on stream lines when $\Phi = 1$, $Sr = 0.5$, $Sc = 0.5$, $Br = 0.25$, $G_c = 2$ and $G_t = 1$.

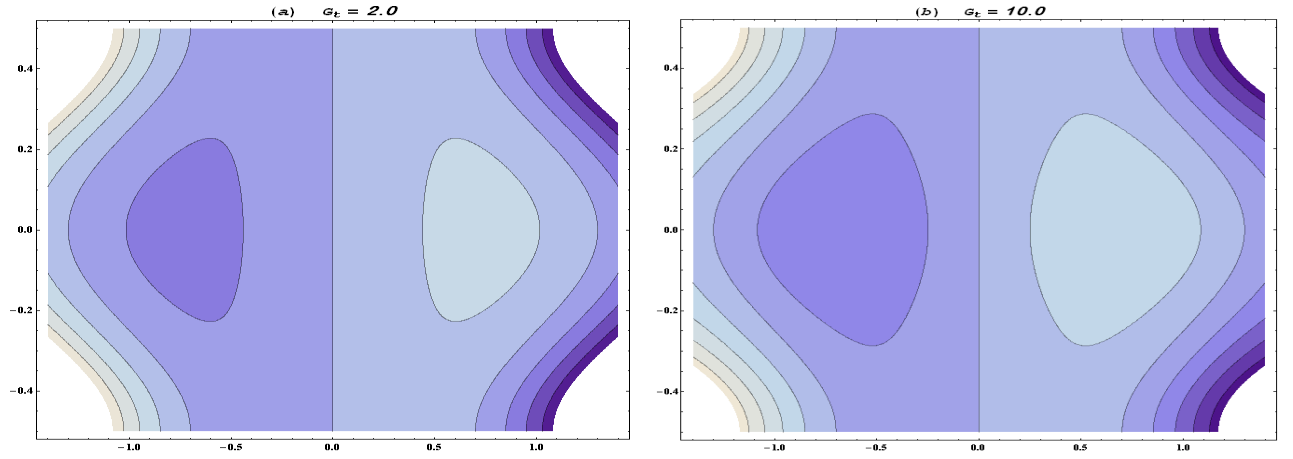


Fig. 8.5 Effect of G_t on stream lines for $\Phi = 1$, $Sr = 0.5$, $Sc = 0.5$, $Br = 0.25$, $G_c = 2$ and $M = 1$.

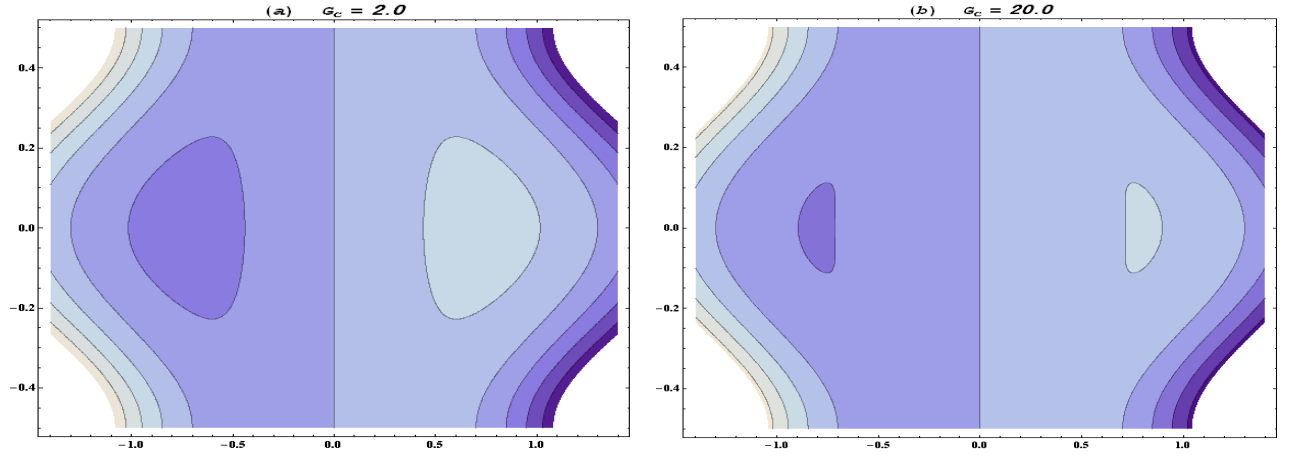


Fig. 8.6 Effect of G_c on stream lines when $\Phi = 1$, $Sr = 0.5$, $Sc = 0.5$, $Br = 0.25$, $G_t = 2$ and $M = 1$.

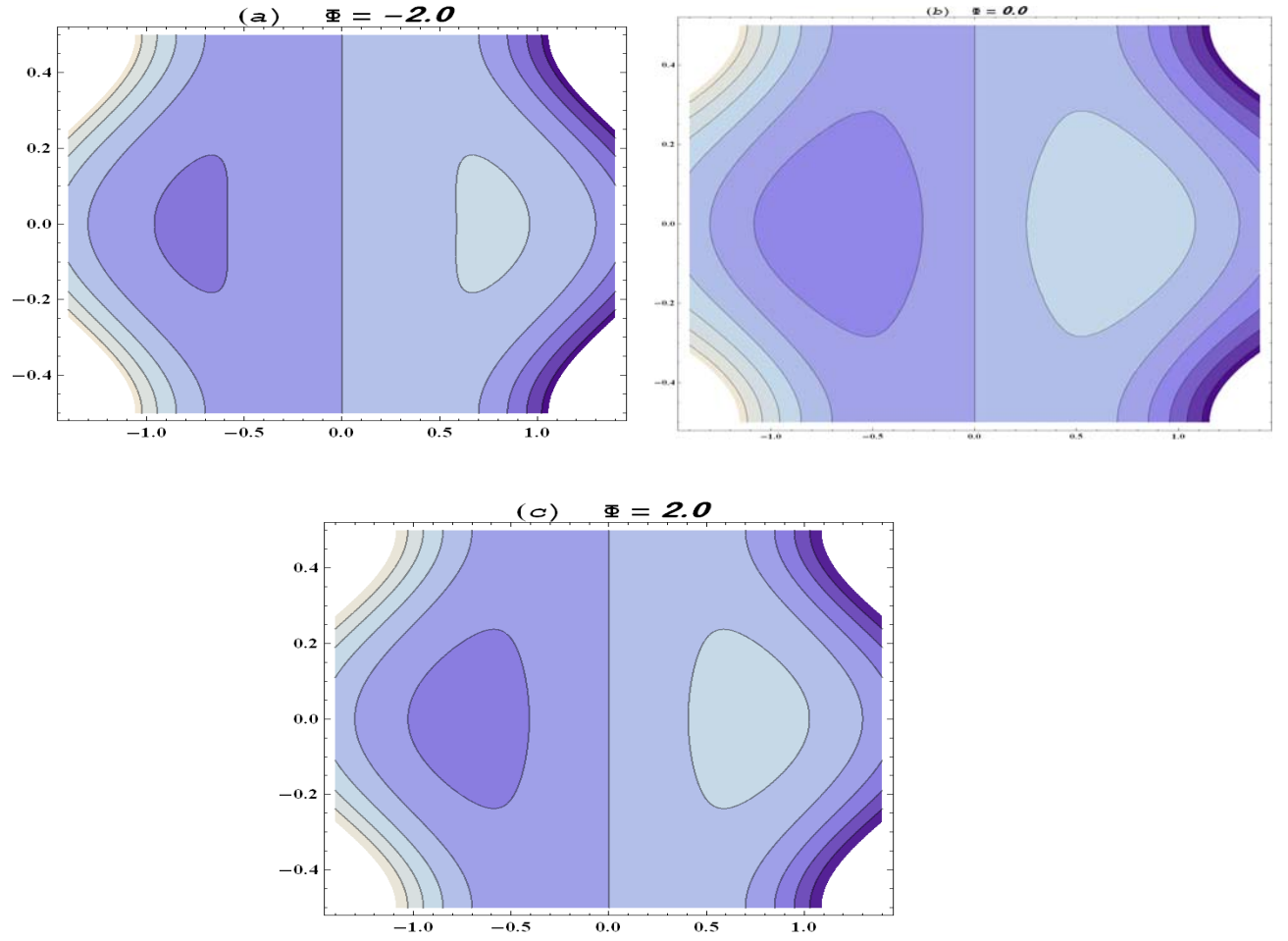


Fig. 8.7 Effect of Φ on stream lines when $G_c = 2$, $Sr = 0.5$, $Sc = 0.5$, $Br = 0.25$, $G_t = 2$ and $M = 1$.

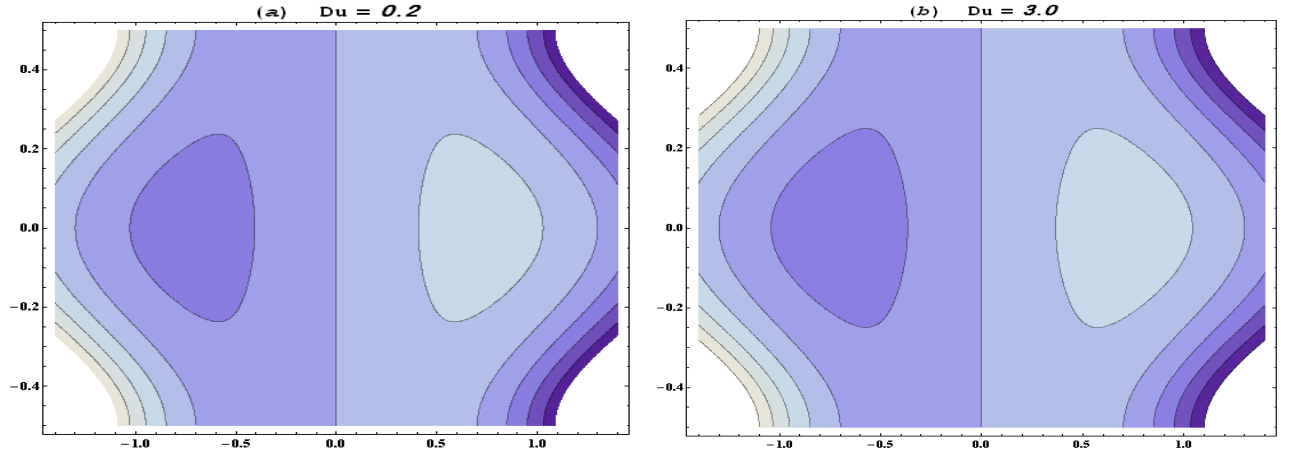


Fig. 8.8 Effect of Du on stream lines for $\Phi = 1$, $G_c = 2$, $Sr = 0.5$, $Sc = 0.5$, $Br = 0.25$, $G_t = 2$ and $M = 1$.

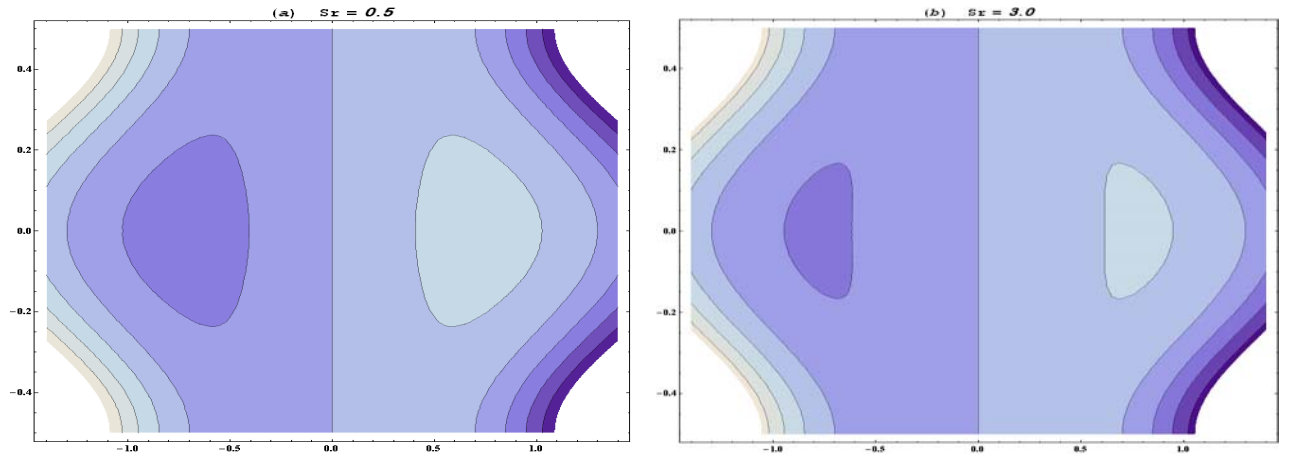


Fig. 8.9 Effect of Sr on stream lines when $\Phi = 1$, $G_c = 2$, $Du = 0.5$, $Sc = 0.5$, $Br = 0.25$, $G_t = 2$ and $M = 1$.

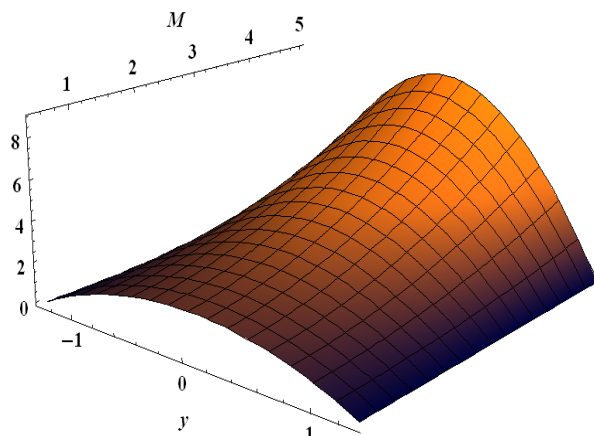


Fig. 8.10 a

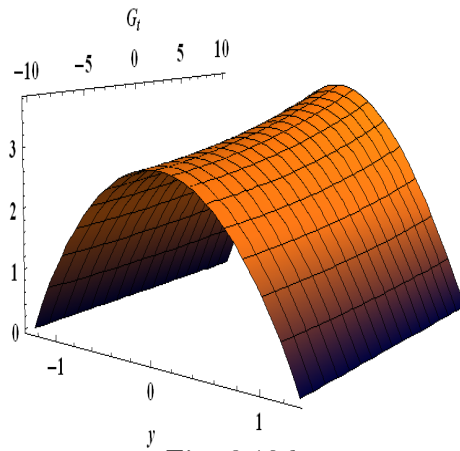


Fig. 8.10 b

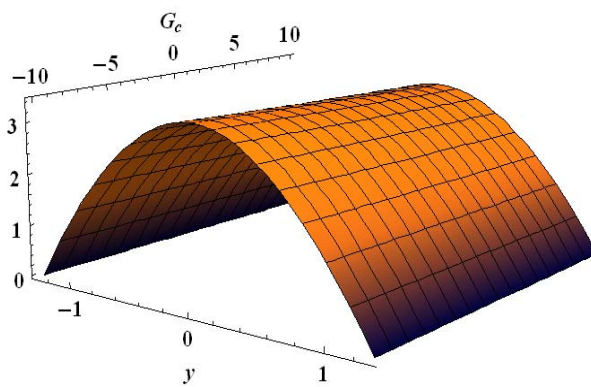


Fig. 8.10 c

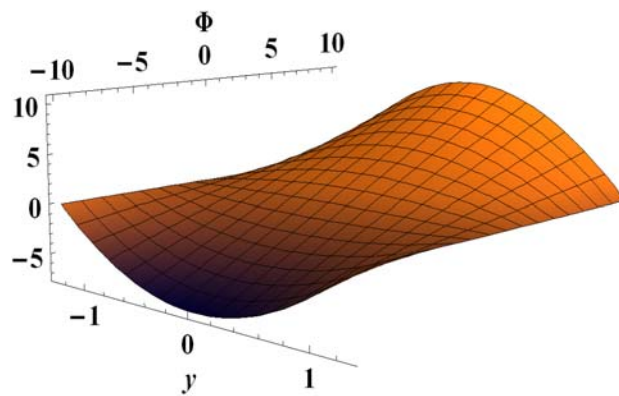


Fig. 8.10 d

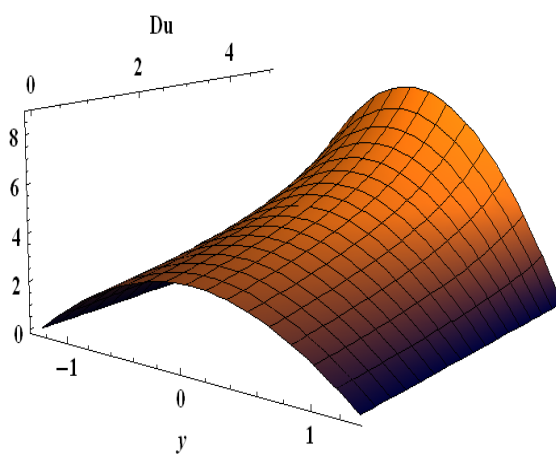


Fig. 8.10 e

Figs. 8.10 (a-e) Variations of M , G_t , G_c , Φ and Du on temperature.

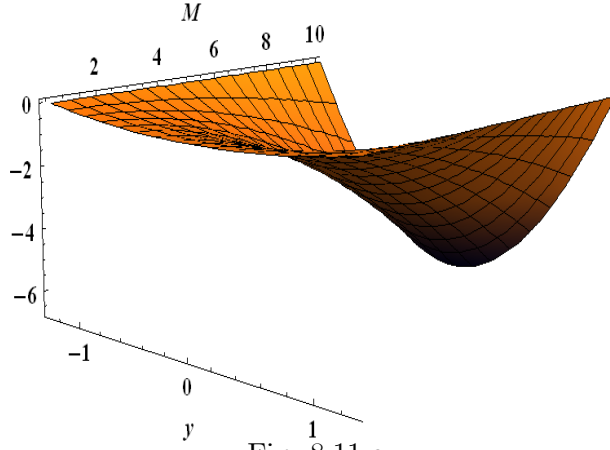


Fig. 8.11 a

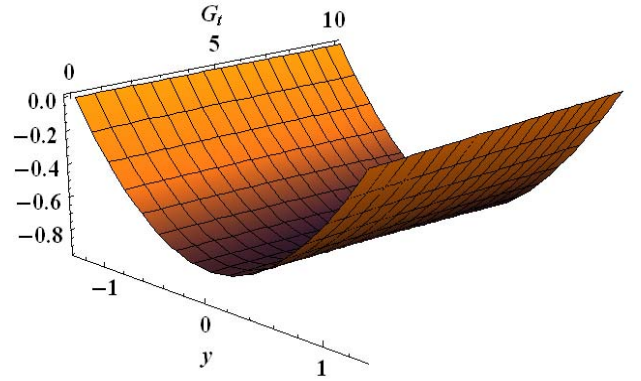


Fig. 8.11 b

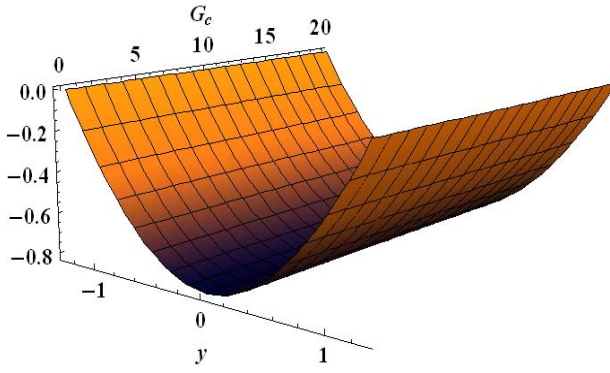


Fig. 8.11 c

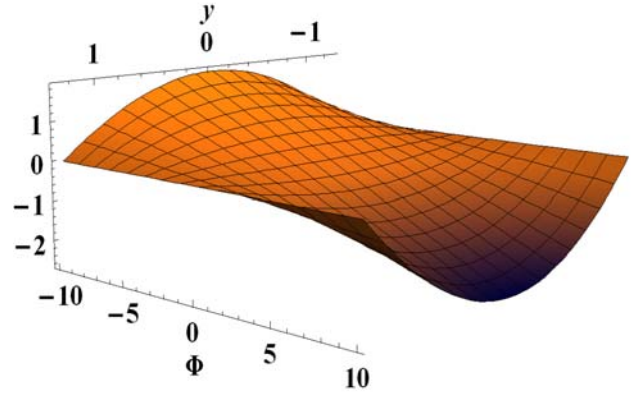


Fig. 8.11 d

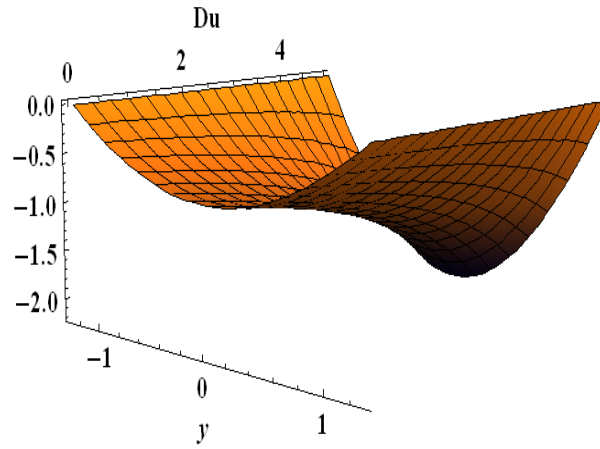


Fig. 8.11 e

Figs. 8.11 (a-e) Diagrams analyzing the development of concentration field when M , G_t , G_c , Φ , and Du are varied.

Chapter 9

Mixed convective heat and mass transfer for peristaltic transport in an asymmetric channel with Soret and Dufour effects

The aim of present chapter is to address the simultaneous effects of heat and mass transfer in the mixed convection peristaltic flow of viscous fluid in an asymmetric channel. The channel walls exhibit the convective boundary conditions. In addition the effects due to Soret and Dufour are taken in to consideration. Resulting problems are solved for the series solutions. Numerical values of heat and mass transfer rates are displayed and studied.

9.1 Mathematical analysis

We consider an asymmetric channel of width $d_1 + d_2$ with flexible walls. An incompressible viscous fluid is considered. Cartesian coordinate system is adopted such that the \overline{X} -axis is along the length of the channel and the \overline{Y} -axis is normal to the \overline{X} -axis. The flow is generated due to peristaltic waves propagating on the channel walls with speed c . Moreover, the channel walls possess the characteristics of convective type boundary condition. We intend to study

the flow in the presence of Soret and Dufour effects. The channel walls are described by the following expressions

$$\overline{H}_1(\overline{X}, \overline{t}) = d_1 + \xi_1, \quad \text{left wall and } \overline{H}_2(\overline{X}, \overline{t}) = -(d_2 + \xi_2), \quad \text{right wall}$$

where ξ_1 and ξ_2 are the disturbances produced due to propagation of peristaltic waves at the left and right walls respectively. The values of ξ_1 and ξ_2 can be written in the forms

$$\begin{aligned} \xi_1 &= a_1 \cos \left(\frac{2\pi}{\lambda} (\overline{X} - c\overline{t}) \right), \\ \xi_2 &= b_1 \cos \left(\frac{2\pi}{\lambda} (\overline{X} - c\overline{t}) + \gamma \right). \end{aligned}$$

in which \overline{t} is time, γ is the phase difference and a_1, b_1 are the amplitudes of the waves travelling on the left and right walls with speed c respectively. Temperature and concentration at the walls are assumed to be T_i and C_i ($i = 0$ for left wall and $i = 1$ for right one) respectively. Velocity field for this problem is $\overline{V} = [U(\overline{X}, \overline{Y}, \overline{t}), V(\overline{X}, \overline{Y}, \overline{t}), 0]$.

Fundamental equations governing the flow of an incompressible viscous fluid are

$$\overline{\nabla} \cdot \overline{V} = 0, \tag{9.1}$$

$$\rho \frac{d\overline{V}}{dt} = -\overline{\nabla} \overline{P} + \mu (\overline{\nabla}^2 \overline{V}) + \rho g \alpha^* (T - T_0) + \rho g \alpha^{**} (C - C_0), \tag{9.2}$$

in which ρ is the density of fluid, \overline{P} is the pressure, μ is the dynamic viscosity, g is the acceleration due to gravity and α^* and α^{**} are the thermal and concentration expansion coefficients respectively. The energy and concentration equations can be expressed as

$$\begin{aligned} C_p \frac{dT}{dt} &= \frac{K}{\rho} [T_{\overline{X}\overline{X}} + T_{\overline{Y}\overline{Y}}] + \\ v [2 (\overline{U}_{\overline{X}}^2 + \overline{V}_{\overline{Y}}^2) + (\overline{U}_{\overline{Y}} + \overline{V}_{\overline{X}})^2] &+ \frac{DK_T}{\rho C_s} [C_{\overline{X}\overline{X}} + C_{\overline{Y}\overline{Y}}], \end{aligned} \tag{9.3}$$

$$\frac{dC}{dt} = D [C_{\overline{X}\overline{X}} + C_{\overline{Y}\overline{Y}}] + \frac{DK_T}{T_m} [T_{\overline{X}\overline{X}} + T_{\overline{Y}\overline{Y}}]. \tag{9.4}$$

Here C_p is the specific heat, K is the thermal conductivity, D is the mass diffusivity, K_T is the thermal diffusion ratio, C_s is the concentration susceptibility, T_m is the mean temperature, T

and C are respectively the temperature and concentration of the fluid.

We consider (\bar{u}, \bar{v}) and \bar{p} as the velocity components and pressure in the wave frame (\bar{x}, \bar{y}) .

The transformations between laboratory and wave frames are

$$\bar{x} = \bar{X} - c\bar{t}, \quad \bar{y} = \bar{Y}, \quad \bar{u} = \bar{U} - c, \quad \bar{v} = \bar{V}, \quad \bar{p}(\bar{x}, \bar{y}) = \bar{P}(\bar{X}, \bar{Y}, \bar{t}). \quad (9.5)$$

where (\bar{U}, \bar{V}) and \bar{P} are the velocity components and pressure in the laboratory frame. The fundamental equations in wave frame are reduced as follows:

$$\frac{\partial \bar{u}}{\partial \bar{x}} + \frac{\partial \bar{v}}{\partial \bar{y}} = 0, \quad (9.6)$$

$$\begin{aligned} \rho \left((\bar{u} + c) \frac{\partial}{\partial \bar{x}} + \bar{v} \frac{\partial}{\partial \bar{y}} \right) (\bar{u} + c) &= -\frac{\partial \bar{p}}{\partial \bar{x}} + \mu \left[\frac{\partial^2 \bar{u}}{\partial \bar{x}^2} + \frac{\partial^2 \bar{u}}{\partial \bar{y}^2} \right] + \rho g \alpha^* (T - T_0) \\ &\quad + \rho g \alpha^{**} (C - C_0), \end{aligned} \quad (9.7)$$

$$\rho \left((\bar{u} + c) \frac{\partial}{\partial \bar{x}} + \bar{v} \frac{\partial}{\partial \bar{y}} \right) \bar{v} = -\frac{\partial \bar{p}}{\partial \bar{y}} + \mu \left[\frac{\partial^2 \bar{v}}{\partial \bar{x}^2} + \frac{\partial^2 \bar{v}}{\partial \bar{y}^2} \right], \quad (9.8)$$

$$\begin{aligned} C_p ((\bar{u} + c) T_{\bar{x}} + \bar{v} T_{\bar{y}}) &= \frac{K}{\rho} [T_{\bar{x}\bar{x}} + T_{\bar{y}\bar{y}}] + \\ v \left[2 \left((\bar{u} + c) \frac{\partial}{\partial \bar{x}} + \bar{v} \frac{\partial}{\partial \bar{y}} \right)^2 \right] &+ \frac{DK_T}{\rho C_s} [C_{\bar{x}\bar{x}} + C_{\bar{y}\bar{y}}], \end{aligned} \quad (9.9)$$

$$(\bar{u} + c) C_{\bar{x}} + \bar{v} C_{\bar{y}} = D [C_{\bar{x}\bar{x}} + C_{\bar{y}\bar{y}}] + \frac{DK_T}{T_m} [T_{\bar{x}\bar{x}} + T_{\bar{y}\bar{y}}]. \quad (9.10)$$

Letting

$$\begin{aligned}
x &= \frac{\bar{x}}{\lambda}, \quad y = \frac{\bar{y}}{d_1}, \quad u = \frac{\bar{u}}{c}, \quad v = \frac{\bar{v}}{c\delta}, \quad \delta = \frac{d_1}{\lambda}, \quad h_1 = \frac{\bar{H}_1}{d_1}, \\
h_2 &= \frac{\bar{H}_2}{d_1}, \quad d = \frac{d_2}{d_1}, \quad a = \frac{a_1}{d_1}, \quad b = \frac{b_1}{d_1}, \quad p = \frac{d_1^2 \bar{p}}{c\lambda\mu}, \quad v = \frac{\mu}{\rho}, \\
Re &= \frac{\rho c d_1}{\mu}, \quad \theta = \frac{T - T_0}{T_1 - T_0}, \quad \phi = \frac{C - C_0}{C_1 - C_0}, \quad Du = \frac{D(C_1 - C_0)K_T}{C_s C_p \mu (T_1 - T_0)}, \\
Br &= Pr E, \quad E = \frac{c^2}{C_p (T_1 - T_0)}, \quad Sr = \frac{\rho D K_T (T_1 - T_0)}{\mu T_m (C_1 - C_0)}, \quad t = \frac{c\bar{t}}{\lambda}, \\
Sc &= \frac{\mu}{\rho D}, \quad G_t = \frac{\rho g \alpha^* (T_1 - T_0) d_1^2}{\mu c}, \quad G_c = \frac{\rho g \alpha^{**} (C_1 - C_0) d_1^2}{\mu c}, \\
Pr &= \frac{\mu C_p}{K}, \quad u = \psi_y, \quad v = -\psi_x,
\end{aligned} \tag{9.11}$$

and adopting long wavelength and low Reynolds number approach we have in terms of stream function ψ the following equations

$$p_x = \psi_{yyy} + G_t \theta + G_c \phi, \tag{9.12}$$

$$p_y = 0, \tag{9.13}$$

$$\theta_{yy} + Br (\psi_{yy})^2 + Pr Du (\phi_{yy}) = 0, \tag{9.14}$$

$$\frac{1}{Sc} \phi_{yy} + Sr \theta_{yy} = 0. \tag{9.15}$$

Here v denotes the kinematic viscosity, Re the Reynolds number, Br is the Brinkman number, E is the Eckret number, Pr is the Prandtl number, δ is the wave number, G_t is the temperature Grashoff number, G_c is the concentration Grashoff number, ϕ is dimensionless concentration, θ is the dimensionless temperature and incompressibility condition is automatically satisfied.

Defining η and F as the dimensionless mean flows in laboratory and wave frames we have

$$\eta = F + 1 + d \tag{9.16}$$

where

$$F = \int_{h_2}^{h_1} \frac{\partial \psi}{\partial y} dy. \tag{9.17}$$

The convective boundary conditions for the temperature and concentration are given by

$$-K \frac{\partial T}{\partial Y} = l(T - T_w),$$

$$-D \frac{\partial C}{\partial Y} = k(C - C_w).$$

The dimensionless boundary conditions for our problem can be imposed as follows:

$$\begin{aligned} \psi &= \frac{F}{2}, \quad \psi_y = -1, \quad \theta_y + Bi(\theta) = 0, \quad \phi_y + Mi(\phi) = 0, \quad y = h_1, \\ \psi &= -\frac{F}{2}, \quad \psi_y = -1, \quad \theta_y - Bi(\theta - 1) = 0, \quad \phi_y - Mi(\phi - 1) = 0, \quad y = h_2, \end{aligned} \quad (9.18)$$

where

$$h_1(x) = 1 + a \cos(2\pi x), \quad h_2(x) = -d - b \cos(2\pi x + \gamma), \quad (9.19)$$

$$Bi = \frac{ld_1}{K}, \quad Mi = \frac{kd_1}{D}. \quad (9.20)$$

In above expressions l and k are dimensionless transfer coefficients, Bi is heat transfer Biot-number and Mi is mass transfer Biot-number.

9.2 Solution of the problem

The problems consisting of Eqs. (9.12)-(9.15) have been solved for both the perturbation and numerical solutions. Perturbation solution is obtained for small Brinkman number. Numerical solution is presented using Mathematica. For perturbation solutions we have the following zeroth and first order systems:

$$\psi_{0yyy} + G_t \theta_{0y} + G_c \phi_{0y} = 0, \quad (9.21)$$

$$\theta_{0yy} + \text{Pr} Du(\phi_{0yy}) = 0, \quad (9.22)$$

$$\phi_{0yy} + ScSr\theta_{0yy} = 0, \quad (9.23)$$

$$\begin{aligned}
\psi_0 &= \frac{F_0}{2}, \quad \psi_{0y} = -1, \quad \theta_{0y} + Bi(\theta_0) = 0, \quad \phi_{0y} + Mi(\phi_0) = 0, \quad y = h_1, \\
\psi_0 &= -\frac{F_0}{2}, \quad \psi_{0y} = -1, \quad \theta_{0y} - Bi(\theta_0 - 1) = 0, \quad \phi_{0y} - Mi(\phi_0 - 1) = 0, \quad y = h_2,
\end{aligned} \tag{9.24}$$

and

$$\psi_{1yyy} + G_t \theta_{1y} + G_c \phi_{1y} = 0, \tag{9.25}$$

$$\theta_{1yy} + (\psi_{0yy})^2 + \text{Pr} Du(\phi_{1yy}) = 0, \tag{9.26}$$

$$\phi_{1yy} + ScSr(\theta_{1yy}) = 0, \tag{9.27}$$

$$\begin{aligned}
\psi_1 &= \frac{F_1}{2}, \quad \psi_{1y} = 0, \quad \theta_{1y} + Bi(\theta_1) = 0, \quad \phi_{1y} + Mi(\phi_1) = 0, \quad y = h_1, \\
\psi_1 &= -\frac{F_1}{2}, \quad \psi_{1y} = 0, \quad \theta_{1y} - Bi(\theta_1) = 0, \quad \phi_{1y} - Mi(\phi_1) = 0, \quad y = h_2.
\end{aligned} \tag{9.28}$$

The perturbation solutions of above problem are given

$$\begin{aligned}
\psi &= -\frac{F(h_1 + h_2 - 2y)(h_1^2 - 4h_1h_2 + h_2^2 + 2(h_1 + h_2)y - 2y^2)}{2(h_1 - h_2)^3} \\
&\quad + \frac{L_0(y)}{24(2 + Bi(h_1 - h_2))(h_1 - h_2)^2(2 + h_1M - h_2M)} \\
&\quad + \frac{BrL_1(y)}{241920(h_1 - h_2)^6},
\end{aligned} \tag{9.29}$$

$$\theta = \frac{1 + Bi h_1 - Bi y}{2 + Bi h_1 - Bh_2} + \frac{Br}{1440(-1 + A)} L_2(y), \tag{9.30}$$

$$\phi = \frac{1 + Mi h_1 - Mi y}{2 + Mi h_1 - Mi h_2} + \frac{BrScSr}{1440(-1 + A)} [L_3(y)], \tag{9.31}$$

where L_i s are given below

$$\begin{aligned}
L_1 = & \frac{FMy \cosh(h_1) + y \sinh(h_2) - (F+h) \sinh(y)}{(h \cosh(h_1) - \sinh(h_2))^2} + (F+h_1)^2 G_t^2 (1+h_1^2) Mi^2 \\
& + h^2 (F+h_1)^2 Mi^4 + G_t (2(F+h_2)^2 Mi (1+M^2) y \cosh(2y) \sinh(h_2) \\
& + 16(F+h_2) Mi^2 y^2 \cosh(y)) + 62G_c Bi (F+h_1 - 8h_1^2) Mi^2 + 8h_2^4 Bi^4 \\
& \cosh(3h_2 Mi) + 16Bi h^2 (F+h_2) M^4 y^2 \cosh(h_2 Mi)^2 \cosh(y) G_t (\sinh(y) \\
& - 16Mi (F+h_1) Bi y \sinh(h_2)^2 \sinh(y)) - 2F (4+h_2 + h_2 Bi^2) - 2y^2 \\
& + 2y^3 G_c (h_2 (8 + Bi Mi h_1 (3 + M^2 (1 + 2h_1^2 - 2y^2)))) \cosh(2h_2), \\
L_2 = & 2y^2 Bi G_t (h_1 + h_2 + y^2) (2F (4 + h_1 + 8h Mi^2) - G_t 2y^2 + h_2 (8 + h_1 (3 \\
& + Bi^2 (1 + 2h_1^2 - 2y^2)))) + Mi^2 Bi^3 G_c (y + h_1 + 2h_2^3) G_c^2 \cosh(2y) \\
& + 2Fh Bi^2 \cosh(2y) + h^2 Bi^2 \cosh(2y) + 8(F+h_2) + e^{(y+2h_2+h_1)} G_t (16(F \\
& + h_2 + 4h_1) \sinh(hM) (M(h-y) + \sinh(My))) + (F+h_2 + 4h_1) (1 + Bi^2) \\
& (-3 + 2Mi^2 y^2) \sinh(2My) + 16G_c + (h_1 + 4h_2)^2 y^2 \sinh((h_2 + y)), \\
L_3 = & (1 + Mi^2) y - 4h_2^3 (F+h_1) Mi^4 (1 + Bi^2) y^2 - 4(F+h_2) Bi^2 (1 + Mi^2) y^3 \\
& (h_1 - h_2) (-8F^2 - 2h_2 (4 + h_1 + 3y) - 2Fy + h_2^2 (F + 2h_1) Mi^2 - 2h_1^2 (F + h_2)^2 \\
& Bi Mi^4) + 2(1 + F(F + 2h_1) Mi^2 + (F + h_2 + 4h_1)^2 Mi^4) y^2 + (F^2 (1 + h_1^2)).
\end{aligned}$$

9.3 Graphical analysis

In order to provide a comparative study of the results by the two methods, we have plotted graphs for both solutions. Left panel depicts the perturbation solution whereas right panel for the numerical solution. Graphical analysis is carried out for the dimensionless temperature, concentration and velocity fields. Numerical values for the rates of heat and mass transfer at the left wall are given in the Tables 9.1 and 9.2 respectively.

The values of different parameters in all the graphs are taken as follows:

$$\begin{aligned}
\eta &= 1, \gamma = \pi/4, a = 0.5, b = 0.7, d = 0.8, x = 0, G_t = 1, G_c = 2, Bi = 0.5, \\
Mi &= 0.5, Du = 1, Br = 0.25, Sc = 0.5, Sr = 0.7.
\end{aligned}$$

The graphs of temperature profile showed that the temperature decreases with an increase in the values of Bi and it increases by increasing Mi. The decrease in the temperature with increase in the heat transfer Biot-number is very rapid for $Bi \leq 1$. It is noted that for $Bi \geq 1$

corresponding decrease in temperature becomes very slow (see Fig. 9.1). This fact is totally opposite to the case of increase in Mi in which temperature not only increases by increasing Mi but also such increase is constant and very slow (Fig. 9.2).

Fig. 9.3 showed that the temperature increases when G_t is increased. Increase in the temperature is smaller for small values of G_t but this increase becomes much for higher values of G_t . However this increase in temperature is observed throughout the channel. Unlike the case of G_t , small increase in temperature is observed when G_c increases but this increase is not uniform throughout the channel. Near the right wall the temperature tends to decrease very slowly by increasing G_c (see Fig. 9.4).

Figs. 9.5-9.7 are plotted to analyze the concentration profile in detail. It is found that the concentration increases when Mi is increased. This increase is large for $Mi \leq 1$ and very slow for large values of Mi (see Fig. 9.5). It is noticed from Figs. 9.6 and 9.7 that the concentration generally decreases with an increase in G_t and G_c . This decrease is much and constant for G_t and G_c respectively. However concentration profile showed different behavior near the right wall. The concentration here increases which is quite different for its behavior at all other parts of the channel. Figs. 9.8 and 9.9 depict that the value of velocity increases by increasing G_t but it remains constant with variation in G_c . The velocity in both cases is increased for increasing G_t and G_c in the region where "y" is negative and decreased for positive y.

Tables 9.1 and 9.2 are plotted for the numerical values of rates of heat and mass transfer. It is seen that solution up to first order perturbation gives an agreement with the numerical results up to second decimal place. Table 9.1 shows that heat transfer rate is increasing function of Biot-number. However the Grashoff numbers and mass transfer Biot number reduce the heat transfer rate (see Table 9.1). Table 9.2 illustrates that the mass transfer rate at the wall tends to decrease when Bi , Mi , G_c and G_t are increased.

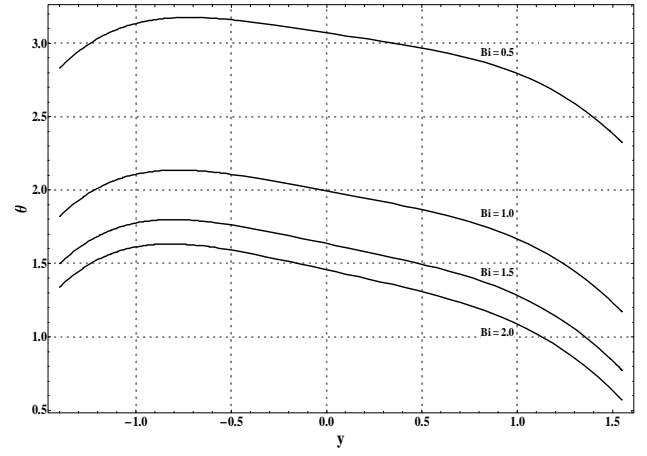
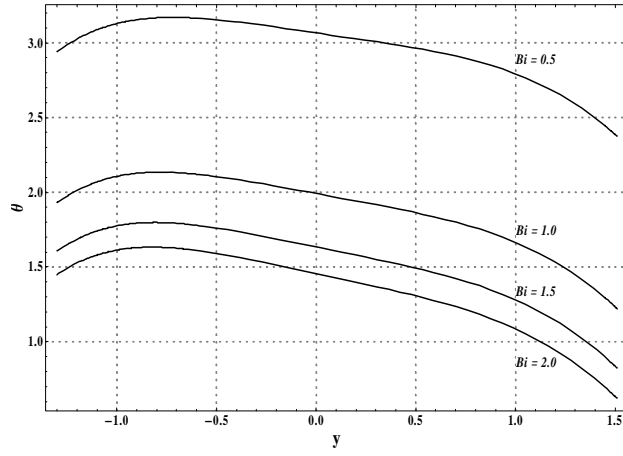


Fig. 9.1 Effect of Bi on the temperature profile.

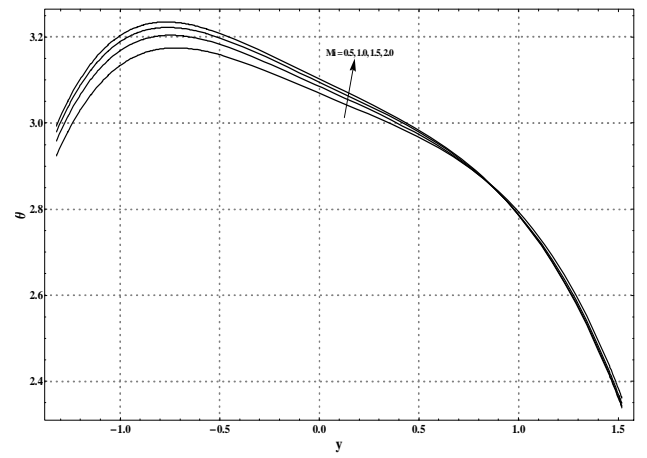
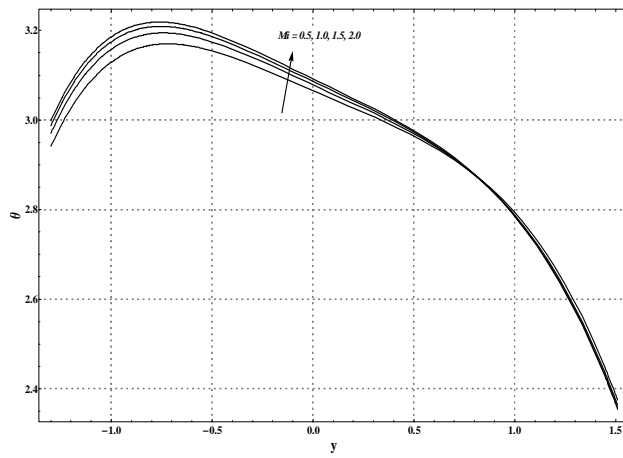


Fig. 9.2 Effect of Mi on the temperature profile.

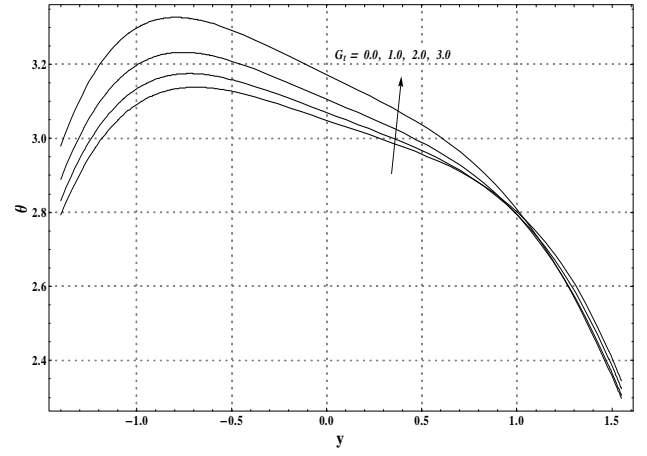
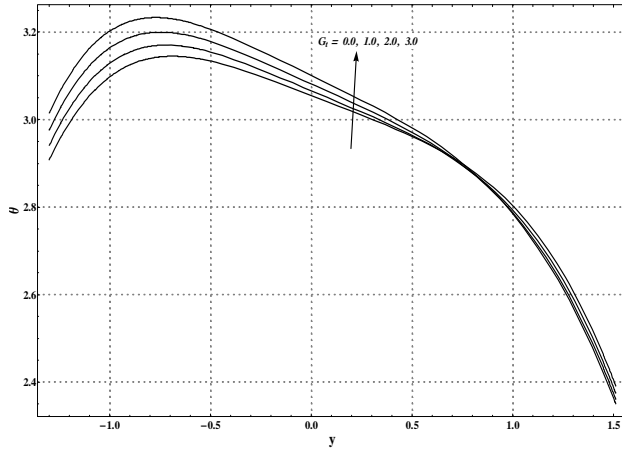


Fig. 9.3 Effect of G_t on the temperature profile.

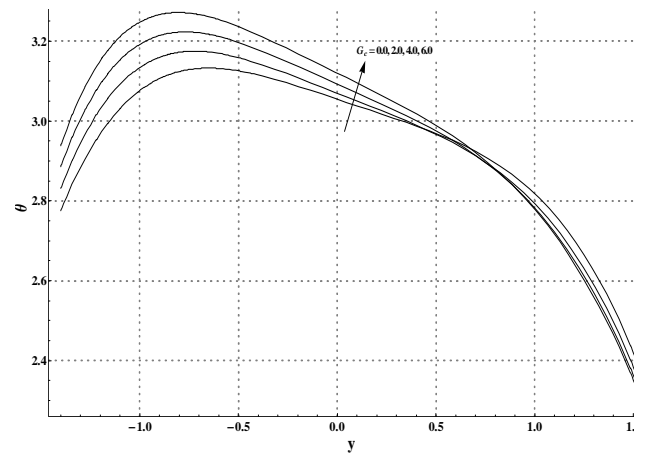
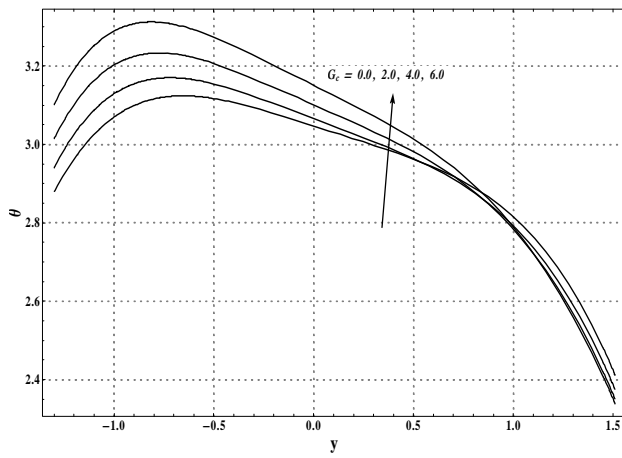


Fig. 9.4 Effect of G_c on the temperature profile.

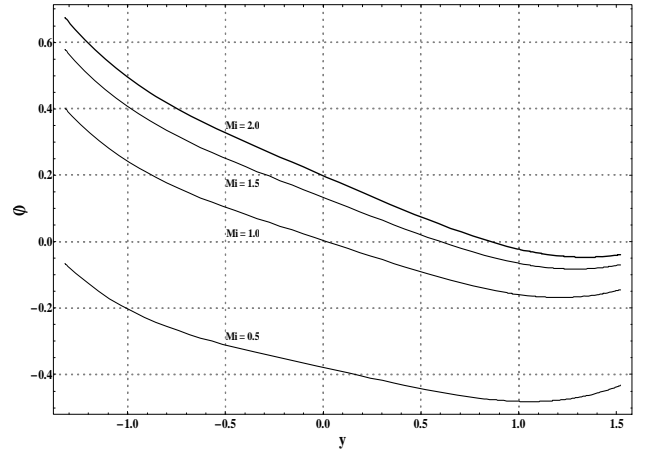
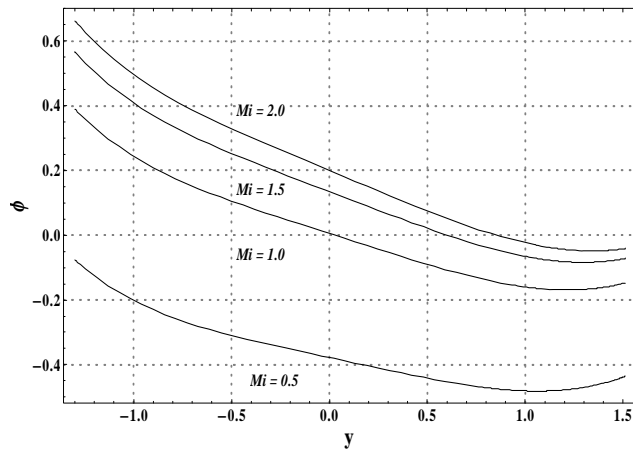


Fig. 9.5 Effect of Mi on the concentration profile.

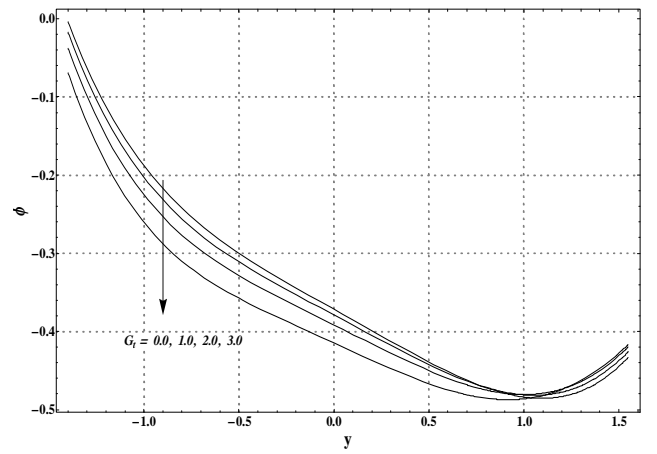
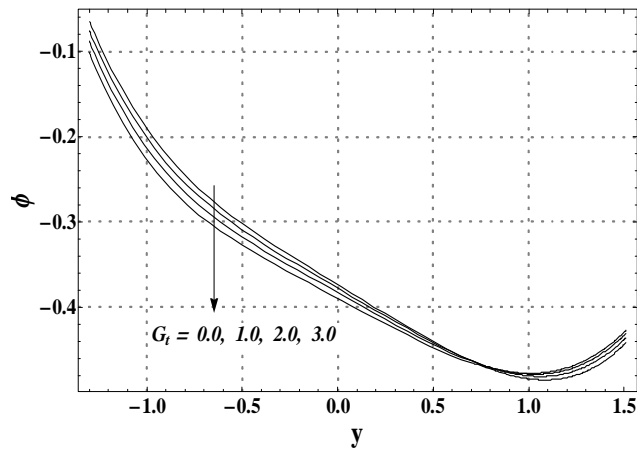


Fig. 9.6 Effect of G_t on the concentration profile.

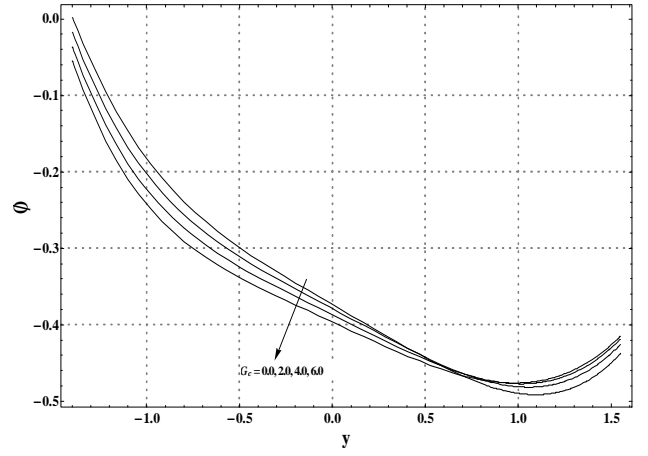
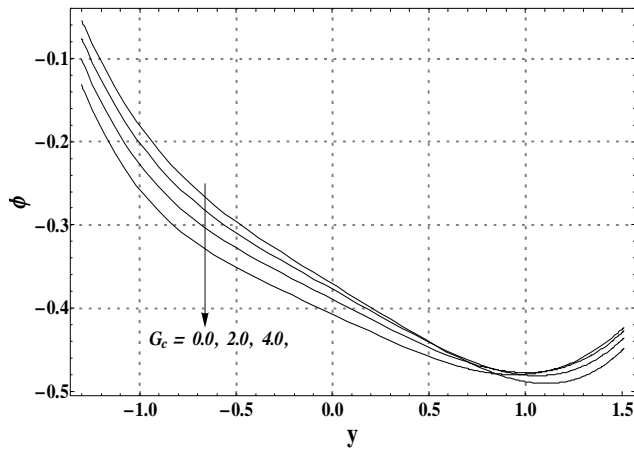


Fig. 9.7 Effect of G_c on the concentration profile.

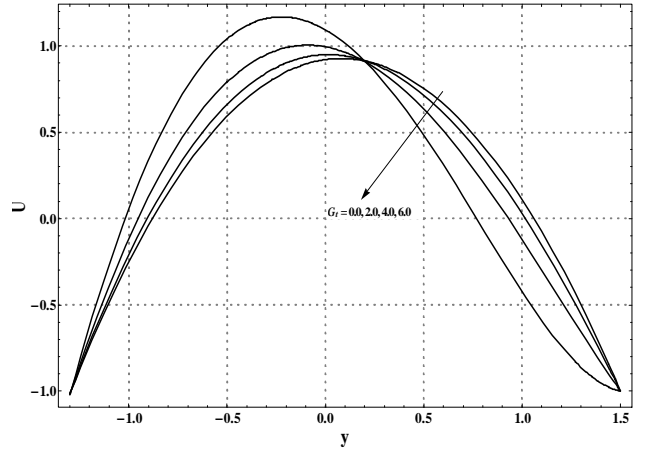
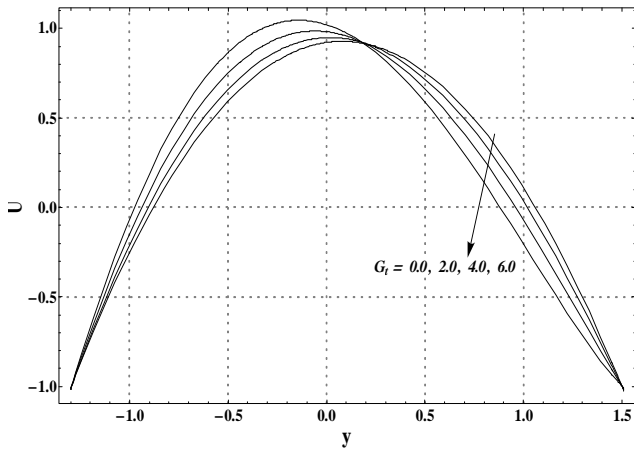


Fig. 9.8 Effect of G_t on the velocity profile.

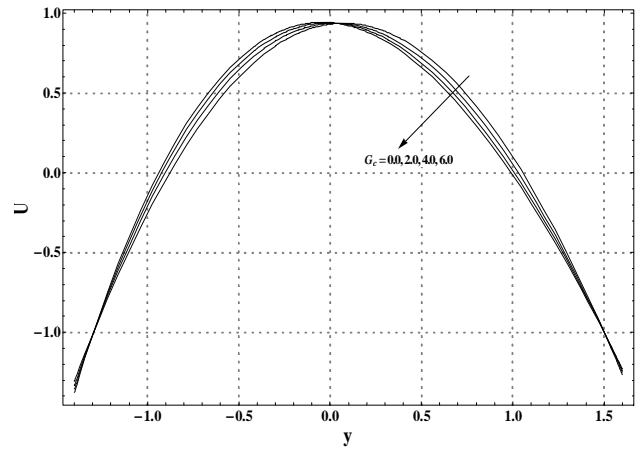
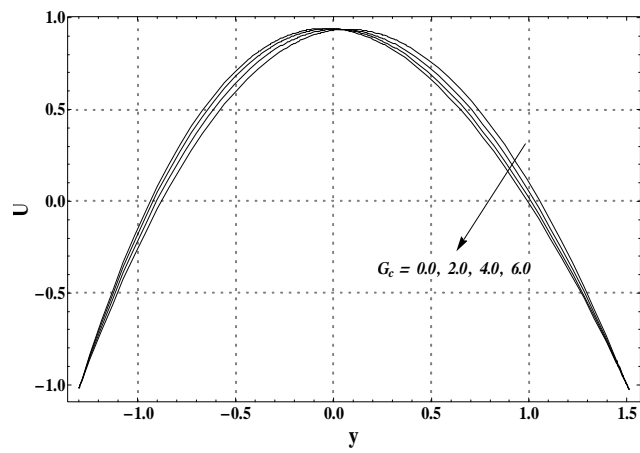


Fig. 9.9 Effect of G_c on the Velocity profile.

Bi	G_t	G_c	Mi	$-\theta'(h_1)$	$-(\theta')^*(h_1)$
0.5	1.0	2.0	0.5	1.1935	1.1927
1.0				1.2343	1.2343
1.5				1.2550	1.2560
2.0				1.2674	1.2693
	0.0			1.2988	1.3018
	1.0			1.2674	1.2693
	2.0			1.2411	1.2402
	3.0			1.2197	1.2176
		0.0		1.2439	1.2349
		1.0		1.2310	1.2254
		2.0		1.2197	1.2176
		3.0		1.2100	1.2110
			0.5	1.2100	1.2110
			1.0	1.1999	1.2006
			1.5	1.1955	1.1967
			2.0	1.1930	1.1951

Table 9.1. Numerical values of heat transfer rate at h_1 .

Bi	G_t	G_c	Mi	$\phi'(h_1)$	$(\phi')^*(h_1)$
0.5	1.0	2.0	0.5	0.2190	0.2187
1.0				0.2179	0.2179
1.5				0.2174	0.2176
2.0				0.2171	0.2173
	0.0			0.2219	0.2225
	1.0			0.2171	0.2173
	2.0			0.2139	0.2141
	3.0			0.2125	0.2139
		0.0		0.2142	0.2146
		1.0		0.2131	0.2141
		2.0		0.2125	0.2139
		3.0		0.2125	0.2140
			0.5	0.2125	0.2140
			1.0	0.1346	0.1360
			1.5	0.0903	0.0914
			2.0	0.0618	0.0625

Table 9.2. Numerical values of mass transfer rate at h_1 .

Chapter 10

Variable viscosity effects on the peristaltic motion of a third-order fluid

The effect of variable viscosity on the peristaltic motion of MHD non-Newtonian fluid in a channel is studied. Constitutive relations of third order fluid are employed in the development of flow. Mathematical analysis is presented when no-slip condition is no longer valid. The series solutions for stream function, longitudinal velocity and pressure gradient are first derived and then discussed in detail. The pressure rise and frictional forces are monitored through numerical integration. Physical interpretation is also made.

10.1 Governing problem

We consider an incompressible magnetohydrodynamic (MHD) third order fluid with variable viscosity in a uniform channel of width $2d_1$. A uniform magnetic field \mathbf{B}_0 is applied in the y -direction. The induced magnetic and electric fields are not considered. Wave shapes are written as

$$H(\overline{X}, \bar{t}) = d_1 + a_1 \cos \left[\frac{2\pi}{\lambda} (\overline{X} - c\bar{t}) \right], \quad (10.1)$$

where c is the velocity of propagation of the wave, a_1 is the wave amplitude, λ is the wavelength, \bar{t} is the time, \bar{X} is the direction of wave propagation and \bar{Y} is transverse to \bar{X} .

The constitutive equations for the third order fluid are given through Eqs. (1.17-1.19). Hence we directly write the following governing equations for two dimensional flow of MHD third order fluid as

$$\frac{\partial \bar{U}}{\partial \bar{X}} + \frac{\partial \bar{V}}{\partial \bar{Y}} = 0, \quad (10.2)$$

$$\rho \left(\frac{\partial}{\partial \bar{t}} + \bar{U} \frac{\partial}{\partial \bar{X}} + \bar{V} \frac{\partial}{\partial \bar{Y}} \right) \bar{U} = -\frac{\partial \bar{P}}{\partial \bar{X}} + \frac{\partial \bar{S}_{\bar{X}\bar{X}}}{\partial \bar{X}} + \frac{\partial \bar{S}_{\bar{X}\bar{Y}}}{\partial \bar{Y}} - \sigma B_0^2 \bar{U}, \quad (10.3)$$

$$\rho \left(\frac{\partial}{\partial \bar{t}} + \bar{U} \frac{\partial}{\partial \bar{X}} + \bar{V} \frac{\partial}{\partial \bar{Y}} \right) \bar{V} = -\frac{\partial \bar{P}}{\partial \bar{Y}} + \frac{\partial \bar{S}_{\bar{X}\bar{Y}}}{\partial \bar{X}} + \frac{\partial \bar{S}_{\bar{Y}\bar{Y}}}{\partial \bar{Y}}, \quad (10.4)$$

$$\begin{aligned} \bar{S}_{\bar{X}\bar{X}} = & \mu(2\bar{U}_{\bar{X}}) + \alpha_1(2\bar{U}_{\bar{X}\bar{t}} + 2\bar{U}\bar{U}_{\bar{X}\bar{X}} + 2\bar{V}\bar{U}_{\bar{X}\bar{Y}} + 4\bar{U}_{\bar{X}}^2 + 2\bar{V}_{\bar{X}}\bar{U}_{\bar{Y}} + 2\bar{V}_{\bar{X}}^2) + \alpha_2 \\ & (4\bar{U}_{\bar{X}}^2 + \bar{U}_{\bar{Y}}^2 + \bar{V}_{\bar{X}}^2 + 2\bar{U}_{\bar{Y}}\bar{V}_{\bar{X}}) + \beta_1(2\bar{U}_{\bar{X}\bar{t}} + 2\bar{U}_{\bar{t}}\bar{U}_{\bar{X}\bar{X}} + 4\bar{U}\bar{U}_{\bar{X}\bar{X}\bar{t}} + 2\bar{V}_{\bar{t}} \\ & \bar{U}_{\bar{X}\bar{Y}} + 4\bar{V}\bar{U}_{\bar{X}\bar{Y}\bar{t}} + 12\bar{U}_{\bar{X}}\bar{U}_{\bar{X}\bar{t}} + 4\bar{V}_{\bar{X}}\bar{U}_{\bar{Y}\bar{t}} + 14\bar{U}\bar{U}_{\bar{X}}\bar{U}_{\bar{X}\bar{X}} + 10\bar{V}\bar{U}_{\bar{X}}\bar{U}_{\bar{X}\bar{Y}} - \\ & 6\bar{V}\bar{V}_{\bar{X}}\bar{U}_{\bar{X}\bar{X}} + 6\bar{U}\bar{V}_{\bar{X}}\bar{V}_{\bar{X}\bar{X}} + 6\bar{V}_{\bar{X}}\bar{V}_{\bar{X}\bar{t}} + 6\bar{U}\bar{V}_{\bar{X}}\bar{U}_{\bar{X}\bar{Y}} + 4\bar{V}\bar{V}_{\bar{X}}\bar{U}_{\bar{Y}\bar{Y}} + 8\bar{U}_{\bar{X}}^3 \\ & + 8\bar{U}_{\bar{X}}\bar{V}_{\bar{X}}\bar{U}_{\bar{Y}} + 2\bar{U}_{\bar{Y}}\bar{V}_{\bar{X}\bar{t}} + 2\bar{U}^2\bar{U}_{\bar{X}\bar{X}\bar{X}} + 4\bar{U}\bar{V}\bar{U}_{\bar{X}\bar{X}\bar{Y}} + 2\bar{U}\bar{U}_{\bar{Y}}\bar{V}_{\bar{X}\bar{X}} + 2 \\ & \bar{V}^2\bar{U}_{\bar{X}\bar{Y}\bar{Y}}) + \beta_2(8\bar{U}_{\bar{X}}\bar{U}_{\bar{X}\bar{t}} + 8\bar{U}\bar{U}_{\bar{X}}\bar{U}_{\bar{X}\bar{X}} + 8\bar{V}\bar{U}_{\bar{X}}\bar{U}_{\bar{X}\bar{Y}} + 16\bar{U}_{\bar{X}}^3 + 8\bar{U}_{\bar{X}} \\ & \bar{V}_{\bar{X}}\bar{U}_{\bar{Y}} + 4\bar{U}_{\bar{X}}\bar{V}_{\bar{X}}^2 + 2\bar{U}_{\bar{Y}}\bar{U}_{\bar{Y}\bar{t}} + 2\bar{U}_{\bar{Y}}\bar{V}_{\bar{X}\bar{t}} + 2\bar{U}\bar{U}_{\bar{Y}}\bar{V}_{\bar{X}\bar{X}} - 2\bar{V}\bar{U}_{\bar{Y}}\bar{U}_{\bar{X}\bar{X}} + \\ & 2\bar{U}\bar{U}_{\bar{Y}}\bar{U}_{\bar{X}\bar{Y}} + 2\bar{V}\bar{U}_{\bar{Y}}\bar{U}_{\bar{Y}\bar{Y}} + 4\bar{U}_{\bar{X}}\bar{U}_{\bar{Y}}^2 + 2\bar{V}_{\bar{X}}\bar{U}_{\bar{Y}\bar{t}} + 2\bar{V}_{\bar{X}}\bar{V}_{\bar{X}\bar{t}} + 2\bar{U}\bar{V}_{\bar{X}}\bar{V}_{\bar{X}\bar{X}} \\ & - 2\bar{V}\bar{V}_{\bar{X}}\bar{U}_{\bar{X}\bar{X}} + 2\bar{U}\bar{V}_{\bar{X}}\bar{U}_{\bar{X}\bar{Y}} + 2\bar{V}\bar{V}_{\bar{X}}\bar{U}_{\bar{Y}\bar{Y}}) + \beta_3(16\bar{U}_{\bar{X}}^3 + 4\bar{U}_{\bar{X}}\bar{U}_{\bar{Y}}^2 + \\ & 4\bar{U}_{\bar{X}}\bar{V}_{\bar{X}}^2 + 8\bar{U}_{\bar{X}}\bar{U}_{\bar{Y}}\bar{V}_{\bar{X}}), \end{aligned}$$

$$\begin{aligned}
\bar{S}_{\bar{X}\bar{Y}} = & \mu(\bar{U}_{\bar{Y}} + \bar{V}_{\bar{X}}) + \alpha_1(\bar{U}_{\bar{Y}\bar{t}} + \bar{U}\bar{U}_{\bar{X}\bar{Y}} + \bar{V}\bar{U}_{\bar{Y}\bar{Y}} + \bar{V}_{\bar{X}\bar{t}} + \bar{U}\bar{V}_{\bar{X}\bar{X}} - \bar{V}\bar{U}_{\bar{X}\bar{X}} + 2\bar{U}_{\bar{X}}\bar{U}_{\bar{Y}} - 2\bar{V}_{\bar{X}}\bar{U}_{\bar{X}}) \\
& + \beta_1(\bar{U}_{\bar{Y}\bar{t}} + \bar{U}_{\bar{t}}\bar{U}_{\bar{X}\bar{Y}} + \bar{V}_{\bar{t}}\bar{U}_{\bar{Y}\bar{Y}} + \bar{V}_{\bar{X}\bar{t}} + \bar{U}_{\bar{t}}\bar{V}_{\bar{X}\bar{X}} + \bar{V}_{\bar{t}}\bar{U}_{\bar{X}\bar{X}} + 2\bar{U}\bar{V}_{\bar{X}\bar{X}\bar{t}} + 4\bar{U}_{\bar{Y}}\bar{U}_{\bar{X}\bar{t}} + \\
& 2\bar{U}_{\bar{X}}\bar{U}_{\bar{Y}\bar{t}} - 2\bar{U}_{\bar{X}}\bar{V}_{\bar{X}\bar{t}} - 4\bar{V}_{\bar{X}}\bar{U}_{\bar{X}\bar{t}} + \bar{U}^2\bar{U}_{\bar{X}\bar{X}\bar{Y}} + \bar{U}\bar{V}_{\bar{X}}\bar{U}_{\bar{Y}\bar{Y}} - \bar{U}\bar{U}_{\bar{X}}\bar{V}_{\bar{X}\bar{X}} + \bar{U}^2\bar{V}_{\bar{X}\bar{X}\bar{X}} \\
& - 5\bar{U}\bar{V}_{\bar{X}}\bar{U}_{\bar{X}\bar{X}} + 4\bar{U}\bar{U}_{\bar{Y}}\bar{U}_{\bar{X}\bar{X}} + \bar{V}\bar{U}_{\bar{X}}\bar{U}_{\bar{Y}\bar{Y}} + \bar{V}^2\bar{U}_{\bar{Y}\bar{Y}\bar{Y}} + \bar{V}\bar{U}_{\bar{Y}}\bar{V}_{\bar{X}\bar{X}} + 3\bar{V}\bar{U}_{\bar{X}}\bar{U}_{\bar{X}\bar{X}} \\
& - \bar{V}^2\bar{U}_{\bar{X}\bar{X}\bar{Y}} - 4\bar{V}\bar{V}_{\bar{X}}\bar{U}_{\bar{X}\bar{Y}} + 2\bar{U}\bar{V}\bar{U}_{\bar{X}\bar{Y}\bar{Y}} + 2\bar{U}\bar{V}\bar{U}_{\bar{X}\bar{X}\bar{X}} + 2\bar{V}\bar{U}_{\bar{Y}\bar{Y}\bar{t}} + 2\bar{U}\bar{U}_{\bar{X}\bar{Y}\bar{t}} + 3\bar{U}\bar{U}_{\bar{X}}\bar{U}_{\bar{X}\bar{Y}} \\
& + 5\bar{V}\bar{U}_{\bar{Y}}\bar{U}_{\bar{X}\bar{Y}} - 2\bar{V}\bar{U}_{\bar{X}\bar{X}\bar{t}} + 4\bar{U}_{\bar{X}}^2\bar{U}_{\bar{Y}} + 4\bar{V}_{\bar{X}}\bar{U}_{\bar{X}}^2 + 4\bar{U}_{\bar{Y}}\bar{V}_{\bar{X}}^2 + 4\bar{V}_{\bar{X}}\bar{U}_{\bar{X}}^2) \\
& + \beta_2(8\bar{U}_{\bar{X}}^2\bar{U}_{\bar{Y}} + 6\bar{U}_{\bar{Y}}^2\bar{V}_{\bar{X}} + 2\bar{U}_{\bar{Y}}^3 + 8\bar{V}_{\bar{X}}\bar{U}_{\bar{X}}^2 + 6\bar{U}_{\bar{Y}}\bar{V}_{\bar{X}}^2 + 2\bar{V}_{\bar{X}}^3) \\
& \beta_3(8\bar{U}_{\bar{X}}^2\bar{U}_{\bar{Y}} + 8\bar{U}_{\bar{X}}^2\bar{V}_{\bar{X}} + 2\bar{U}_{\bar{Y}}^3 + 6\bar{U}_{\bar{Y}}\bar{V}_{\bar{X}}^2 + 6\bar{U}_{\bar{Y}}^2\bar{V}_{\bar{X}} + 2\bar{V}_{\bar{X}}^3),
\end{aligned}$$

$$\begin{aligned}
\bar{S}_{\bar{Y}\bar{Y}} = & \mu(-2\bar{U}_{\bar{X}}) + \alpha_1(-2\bar{U}_{\bar{X}\bar{t}} - 2\bar{U}\bar{U}_{\bar{X}\bar{X}} - 2\bar{V}\bar{U}_{\bar{X}\bar{Y}} + 4\bar{U}_{\bar{X}}^2 + 2\bar{V}_{\bar{X}}\bar{U}_{\bar{Y}} + 2\bar{U}_{\bar{Y}}^2) \\
& + \alpha_2(4\bar{U}_{\bar{X}}^2 + \bar{U}_{\bar{Y}}^2 + \bar{V}_{\bar{X}}^2 + 2\bar{U}_{\bar{Y}}\bar{V}_{\bar{X}}) \\
& + \beta_1(-2\bar{U}_{\bar{X}\bar{t}} - 2\bar{U}_{\bar{t}}\bar{U}_{\bar{X}\bar{X}} - 4\bar{U}\bar{U}_{\bar{X}\bar{X}\bar{t}} - 2\bar{V}_{\bar{t}}\bar{U}_{\bar{X}\bar{Y}} - 4\bar{V}\bar{U}_{\bar{X}\bar{Y}\bar{t}} \\
& + 12\bar{U}_{\bar{X}}\bar{U}_{\bar{X}\bar{t}} + 2\bar{V}_{\bar{X}}\bar{U}_{\bar{Y}\bar{t}} + 4\bar{U}_{\bar{Y}}\bar{V}_{\bar{X}\bar{t}} + 6\bar{U}_{\bar{Y}}\bar{U}_{\bar{Y}\bar{t}} + 10\bar{U}\bar{U}_{\bar{X}}\bar{U}_{\bar{X}\bar{X}} - 2\bar{U}^2\bar{U}_{\bar{X}\bar{X}\bar{X}} \\
& - 4\bar{U}\bar{V}\bar{U}_{\bar{X}\bar{X}\bar{Y}} + 4\bar{U}\bar{U}_{\bar{Y}}\bar{V}_{\bar{X}\bar{X}} + 6\bar{U}\bar{U}_{\bar{Y}}\bar{U}_{\bar{X}\bar{Y}} - 6\bar{V}\bar{U}_{\bar{Y}}\bar{U}_{\bar{X}\bar{X}} + 14\bar{V}\bar{U}_{\bar{X}}\bar{U}_{\bar{X}\bar{Y}} - 2\bar{V}^2\bar{U}_{\bar{X}\bar{Y}\bar{Y}} \\
& + 2\bar{V}\bar{V}_{\bar{X}}\bar{U}_{\bar{Y}\bar{Y}} + 6\bar{V}\bar{U}_{\bar{Y}}\bar{U}_{\bar{Y}\bar{Y}} - 8\bar{U}_{\bar{X}}\bar{V}_{\bar{X}}\bar{U}_{\bar{Y}} - 8\bar{U}_{\bar{X}}^3) \\
& + \beta_2(2\bar{U}_{\bar{Y}}\bar{U}_{\bar{Y}\bar{t}} + 2\bar{U}_{\bar{Y}}\bar{V}_{\bar{X}\bar{t}} + 2\bar{U}\bar{U}_{\bar{Y}}\bar{V}_{\bar{X}\bar{X}} - 2\bar{V}\bar{U}_{\bar{Y}}\bar{U}_{\bar{X}\bar{X}} + 2\bar{U}\bar{U}_{\bar{Y}}\bar{U}_{\bar{X}\bar{Y}} + 2\bar{V}\bar{U}_{\bar{Y}}\bar{U}_{\bar{Y}\bar{Y}} \\
& - 4\bar{U}_{\bar{Y}}^2\bar{U}_{\bar{X}} - 8\bar{U}_{\bar{X}}\bar{V}_{\bar{X}}\bar{U}_{\bar{Y}} + 2\bar{V}_{\bar{X}}\bar{U}_{\bar{Y}\bar{t}} + 2\bar{V}_{\bar{X}}\bar{V}_{\bar{X}\bar{t}} + 2\bar{U}\bar{V}_{\bar{X}}\bar{V}_{\bar{X}\bar{X}} - 2\bar{V}\bar{V}_{\bar{X}}\bar{U}_{\bar{X}\bar{X}} + \\
& 2\bar{U}\bar{V}_{\bar{X}}\bar{U}_{\bar{X}\bar{Y}} + 2\bar{V}\bar{V}_{\bar{X}}\bar{U}_{\bar{Y}\bar{Y}} - 4\bar{V}_{\bar{X}}^2\bar{U}_{\bar{X}} + 8\bar{U}_{\bar{X}}\bar{U}_{\bar{X}\bar{t}} + 8\bar{U}\bar{U}_{\bar{X}}\bar{U}_{\bar{X}\bar{X}} + 8\bar{V}\bar{U}_{\bar{X}}\bar{U}_{\bar{X}\bar{Y}} - 16\bar{U}_{\bar{X}}^3 \\
& + \beta_3(-16\bar{U}_{\bar{X}}^3 - 4\bar{U}_{\bar{X}}\bar{U}_{\bar{Y}}^2 - 4\bar{U}_{\bar{X}}\bar{V}_{\bar{X}}^2 - 8\bar{U}_{\bar{X}}\bar{U}_{\bar{Y}}\bar{V}_{\bar{X}}),
\end{aligned}$$

where (\bar{U}, \bar{V}) and \bar{P} are the velocity components and pressure in the fixed frame (\bar{X}, \bar{Y}) and the subscripts denote the partial derivatives

If (\bar{u}, \bar{v}) and \bar{p} indicate the velocity components and pressure in the wave frame then defining

$$\bar{x} = \bar{X} - c\bar{t}, \quad \bar{y} = \bar{Y}, \quad \bar{u} = \bar{U} - c, \quad \bar{v} = \bar{V}, \quad \bar{p}(\bar{x}, \bar{y}) = \bar{P}(\bar{X}, \bar{Y}, \bar{t}) \quad (10.5)$$

and using

$$\begin{aligned}
x &= \frac{\bar{x}}{\lambda}, \quad y = \frac{\bar{y}}{d_1}, \quad u = \frac{\bar{u}}{c}, \quad v = \frac{\bar{v}}{c\delta}, \quad \delta = \frac{d_1}{\lambda}, \quad h = \frac{H}{d_1}, \quad d = \frac{a_1}{d_1}, \quad p = \frac{a^2 \bar{p}}{c\lambda\mu_0}, \\
S &= \frac{d_1}{\mu_0 c} \bar{S}(\bar{x}), \quad \mu(y) = \frac{\bar{\mu}(\bar{y})}{\mu_0}, \quad M = \left(\frac{\sigma}{\mu_0} \right)^{1/2} B_0 d_1, \quad v_0 = \frac{\mu_0}{\rho}, \quad Re = \frac{\rho c d_1}{\mu_0}, \\
t &= \frac{c\bar{t}}{\lambda}, \quad u = \frac{\partial \psi}{\partial y}, \quad v = -\frac{\partial \psi}{\partial x}, \quad \gamma_2 = \frac{\beta_2 c^2}{\mu_0 d_1^2}, \quad \gamma_3 = \frac{\beta_3 c^2}{\mu_0 d_1^2},
\end{aligned} \tag{10.6}$$

we obtain under the long wavelength and low Reynolds number approximation the following expressions

$$-\frac{\partial p}{\partial x} + \frac{\partial}{\partial y} \left[\mu(y) \frac{\partial^2 \psi}{\partial y^2} + 2\Gamma \left(\frac{\partial^2 \psi}{\partial y^2} \right)^3 \right] - M^2 \left(\frac{\partial \psi}{\partial y} + 1 \right) = 0, \tag{10.7}$$

$$0 = -\frac{\partial p}{\partial y}, \tag{10.8}$$

in which $\Gamma(= \gamma_2 + \gamma_3)$ is the Deborah number, ψ is the stream function, v_0 is the constant kinematic viscosity, M is the Hartman number, Re is the Reynolds number, ρ is the fluid density, σ is the electrical conductivity, $\bar{\mu}(\bar{y})$ is the viscosity function, δ is the wave number, μ_0 is the constant viscosity and continuity equation is automatically satisfied. Further Eq. (10.8) indicates that $p \neq p(y)$. From Eqs. (10.7) and (10.8) we have

$$\frac{\partial^2}{\partial y^2} \left(\mu(y) \frac{\partial^2 \psi}{\partial y^2} + 2\Gamma \left(\frac{\partial^2 \psi}{\partial y^2} \right)^3 \right) - M^2 \frac{\partial^2 \psi}{\partial y^2} = 0. \tag{10.9}$$

The subjected boundary conditions in dimensionless form become

$$\begin{aligned}
\psi &= 0, \quad \frac{\partial^2 \psi}{\partial y^2} = 0, \quad \text{at } y = 0, \\
\psi &= F, \quad \frac{\partial \psi}{\partial y} + \beta_1 S_{xy} = -1, \quad \text{at } y = h,
\end{aligned} \tag{10.10}$$

$$h(x) = 1 + a \cos(2\pi x), \quad F = \int_0^1 \frac{\partial \psi}{\partial y} dy. \tag{10.11}$$

In above equations $\mu(y) = e^{-\alpha y}$ or $\mu(y) = 1 - \alpha y$ for $(\alpha \ll 1)$, α is the viscosity parameter, β_1

is the non-dimensional velocity slip parameter and

$$S_{xy} = \mu(y) \frac{\partial^2 \psi}{\partial y^2} + 2\Gamma \left(\frac{\partial^2 \psi}{\partial y^2} \right)^3. \quad (10.12)$$

Pressure rise per wavelength Δp_λ and frictional force F_λ (at the wall) are defined by the following expression

$$\Delta p_\lambda = \int_0^1 \frac{dp}{dx} dx. \quad (10.13)$$

$$F_\lambda = \int_0^1 h \left(-\frac{dp}{dx} \right) dx. \quad (10.14)$$

In the next section the problem consisting of Eqs. (10.9) and (10.10) will be solved for small Deborah number Γ and small viscosity parameter α .

10.2 Series expressions

Letting

$$\psi = \psi_0 + \Gamma \psi_1 + \dots$$

$$F = F_0 + \Gamma F_1 + \dots$$

$$p = p_0 + \Gamma p_1 + \dots$$

and

$$\psi_0 = \psi_{00} + \alpha \psi_{01} + \dots$$

$$\psi_1 = \psi_{10} + \alpha \psi_{11} + \dots$$

$$F_0 = F_{00} + \alpha F_{01} + \dots$$

$$F_1 = F_{10} + \alpha F_{11} + \dots$$

$$p_0 = p_{00} + \alpha p_{01} + \dots$$

$$p_1 = p_{10} + \alpha p_{11} + \dots$$

we arrive at the following systems:

System for ψ_{00}

$$-\frac{\partial p_{00}}{\partial x} + \frac{\partial^3 \psi_{00}}{\partial y^3} - M^2 \left(\frac{\partial \psi_{00}}{\partial y} + 1 \right) = 0, \quad (10.15)$$

$$\frac{\partial^4 \psi_{00}}{\partial y^4} - M^2 \frac{\partial^2 \psi_{00}}{\partial y^2} = 0,$$

$$\psi_{00} = 0 = \frac{\partial^2 \psi_{00}}{\partial y^2} \quad \text{at } y = 0,$$

$$\psi_{00} = F_{00} \quad \frac{\partial \psi_{00}}{\partial y} + \beta_1 \frac{\partial^2 \psi_{00}}{\partial y^2} = -1 \quad \text{at } y = h.$$

System for ψ_{01}

$$-\frac{\partial p_{01}}{\partial x} + \frac{\partial^3 \psi_{01}}{\partial y^3} - M^2 \frac{\partial \psi_{01}}{\partial y} = \frac{\partial}{\partial y} \left(y \frac{\partial^2 \psi_{00}}{\partial y^2} \right), \quad (10.16)$$

$$\frac{\partial^4 \psi_{01}}{\partial y^4} - M^2 \frac{\partial^2 \psi_{01}}{\partial y^2} = \frac{\partial^2}{\partial y^2} \left(y \frac{\partial^2 \psi_{00}}{\partial y^2} \right),$$

$$\psi_{01} = 0 = \frac{\partial^2 \psi_{01}}{\partial y^2}, \quad \text{at } y = 0,$$

$$\psi_{00} = F_{01}, \quad \frac{\partial \psi_{01}}{\partial y} + \beta_1 \frac{\partial^2 \psi_{01}}{\partial y^2} = \beta y \frac{\partial^2 \psi_{00}}{\partial y^2} \quad \text{at } y = h.$$

System for ψ_{10}

$$-\frac{\partial p_{10}}{\partial x} + \frac{\partial^3 \psi_{10}}{\partial y^3} - M^2 \frac{\partial \psi_{10}}{\partial y} + 6 \left(\frac{\partial^2 \psi_{00}}{\partial y^2} \right)^2 \frac{\partial^3 \psi_{00}}{\partial y^3} = 0, \quad (10.17)$$

$$\frac{\partial^4 \psi_{10}}{\partial y^4} - M^2 \frac{\partial^2 \psi_{10}}{\partial y^2} + 6 \frac{\partial}{\partial y} \left(\left(\frac{\partial^2 \psi_{00}}{\partial y^2} \right)^2 \frac{\partial^3 \psi_{00}}{\partial y^3} \right) = 0,$$

$$\psi_{10} = 0 = \frac{\partial^2 \psi_{10}}{\partial y^2}, \quad \text{at } y = 0,$$

$$\psi_{10} = F_{10}, \quad \frac{\partial \psi_{10}}{\partial y} + \beta_1 \frac{\partial^2 \psi_{10}}{\partial y^2} + 2\beta_1 \left(\frac{\partial^2 \psi_{00}}{\partial y^2} \right)^3 = 0 \quad \text{at } y = h.$$

The solutions of above systems finally give

$$\psi = \frac{FM y \cosh[hM] + y(1 + FM^2\beta_1) \sinh[hM] - (F + h) \sinh[My]}{hM \cosh[hM] + (-1 + hM\beta_1^2) M\beta_1 \sinh[hM]} + \alpha m_1 + \Gamma m_2, \quad (10.18)$$

$$u = \frac{1}{32(hM \cosh[hM] + (-1 + hM\beta_1^2) M\beta_1 \sinh[hM])^4} \times \quad (10.19)$$

$$\left[\begin{array}{c} 72(F + h)^3 M^6 y \Gamma \cosh[My] (hM \cosh[hM] + (-1 + hM^2\beta_1) \sinh[hM]) \\ + 6u_1 - u_2 + u_3 + u_4 - u_5 + \frac{1}{M}u_6 \end{array} \right],$$

$$\frac{dp}{dx} = -\frac{(F + h) M^3 (\cosh[hM] + M\beta_1 \sinh[hM])}{hM \cosh[hM] + (-1 + hM\beta_1^2) M\beta_1 \sinh[hM]} + \alpha n_1 + \Gamma n_2, \quad (10.20)$$

with

$$\begin{aligned}
m_1 &= \frac{(F+h)(m_3+2\sinh[hM](m_4)+2hM\cosh[hM](m_5))}{8M(hM\cosh[hM]+(-1+hM\beta_1^2)M\beta_1\sinh[hM])^2}, \\
m_2 &= \frac{(e^{-3My}e^{-3My}(F+h)^3M^4)m_9}{32(hM\cosh[hM]+(-1+hM\beta_1^2)M\beta_1\sinh[hM])^4}, \\
m_3 &= -4My(h+\beta_1+hM^2\beta_1)+2My(2\beta_1+h(-1+2M^2\beta_1))\cosh[2hM] \\
&\quad +M(-2h^2+y^2+h(-4+M^2((-4+h)h-y^2))\beta_1)\sinh[My], \\
m_4 &= 3y(-1+hM^2\beta_1)\cosh[My]+M(-2h^2+y^2+h(-4+M^2((-4+h)h-y^2))\beta_1)\sinh[My], \\
m_5 &= 3y\cosh[My]+M(-y^2+h(h+\beta_1))\sinh[My], \\
m_6 &= -3hM\cosh[3hM]+12M(y+hM(h+2\beta_1-My\beta_1))\sinh[hM] \\
&\quad + (1-9hM^2\beta_1)\sinh[3hM], \\
m_7 &= 3hM\cosh[3hM]-12M(-y+hM(h+2\beta_1+My\beta_1))\sinh[hM] \\
&\quad + (-1+9hM^2\beta_1)\sinh[3hM], \\
m_8 &= 12My(h+\beta_1)-16My\beta_1\cosh[2hM]+4My\beta_1\cosh[4hM] \\
&\quad -8y\sinh[2hM]+y\sinh[4hM]+h\cosh[hM](12M(-y\cosh[MY] \\
&\quad +hM\beta_1\sinh[My]+\sinh[3My]))+\sinh[3My], \\
m_9 &= (1-hM^2\beta_1)\sinh[hM]+e^{6My}(m_6)+e^{2My}(m_7)+2e^{3My}M(m_8).
\end{aligned}$$

$$\begin{aligned}
u_1 &= u_7 + u_8, \\
u_2 &= 6(F + h)^3 M^6 y \Gamma(u_9), \\
u_3 &= 2(F + h)^3 M^5 (1 + 3My) \Gamma(u_{10}), \\
u_4 &= 2(F + h)^3 M^5 \Gamma(u_{11}) \sinh[My], \\
u_5 &= 6(F + h)^3 M^5 \Gamma(\sinh[3hM] + 3hM(u_{12})) \sinh[My], \\
u_6 &= 4(F + h) \alpha(hM \cosh[hM] + (-1 + hM^2 \beta) \sinh[hM])^2 (u_{13} + 2\sinh[hM](u_{14})), \\
u_7 &= (F + h)^3 M^5 y \Gamma \cosh[3My] (hM \cosh[hM] + (-1 + hM^2 \beta_1) \sinh[hM]) \\
&\quad + 32(hM \cosh[hM] + (-1 + hM^2 \beta_1) \sinh[hM])^3 ((- (F + h) M \cosh[My] \\
&\quad + \sinh[hM] + FM(Cosh[hM] + M\beta_1 \sinh[hM]))), \\
u_8 &= 2(F + h)^3 M^5 \Gamma \cosh[My] (12hM(-1 - 3My + hM^2 \beta_1) \cosh[hM] \\
&\quad - 3hM \cosh[3hM]) + 12(1 + M(3y + hM(h + \beta_1 - 3My\beta_1))) \sinh[hM] \\
&\quad + (1 - 9hM^2 \beta_1) \sinh[3hM], \\
u_9 &= 12M(h + \beta_1) + 4M\beta(-4\cosh[2hM] + \cosh[4hM]) - 8\sinh[2hM] + \sinh[4hM], \\
u_{10} &= 12M(h + \beta_1) + 4M\beta_1(-4\cosh[2hM] + \cosh[4hM]) - 8\sinh[2hM] \\
&\quad + \sinh[4hM], u_{11} = \sinh[3hM] + M(4hM(-y + 3hM\beta_1) \cosh[hM] - 3h \cosh[3hM] \\
&\quad + 4(y + hM(3h + 6\beta_1 - My\beta_1)) \sinh[hM] - 9hM\beta_1 \sinh[3hM]), \\
u_{12} &= ((- \cosh[3hM] + M(4hM\beta_1 \cosh[hM] + 4(h + 2\beta_1) \sinh[hM] - 3\beta_1 \sinh[3hM]))), \\
u_{13} &= -4M(h + \beta_1 + h\beta_1 M^2) + 2M(2\beta_1 + h(-1 + 2M^2 \beta_1)) \cosh[2hM] \\
&\quad + 3\sinh[2hM] - 4hM^2 \beta_1 \sinh[2hM] + 2hM \cosh[hM] ((3 + M^2(-y^2 + h(h + \beta_1))) \\
&\quad \cosh[My] + My \sinh[My]), \\
u_{14} &= (-3 + M^2(-2h^2 + y^2 + h(-1 + M^2((-4 + h)h - y^2))\beta_1)) \cosh[My] \\
&\quad + My(-1 + hM^2 \beta_1) \sinh[My]. \\
\\
n_1 &= \frac{(F+h)Mn_3}{8(hM \cosh[hM] + (-1 + hM^2 \beta_1) \sinh[hM])^2}, \\
n_2 &= \frac{(F+h)^3 M^7 n_4}{16(hM \cosh[hM] + (-1 + hM^2 \beta_1) M\beta_1 \sinh[hM])^4}, \\
n_3 &= 4M(h + \beta_1 + hM^2 \beta_1) + 2M(h - 2(1 + hM^2) \beta_1) \cosh[2hM] + (-3 + 4hM^2 \beta_1) \\
&\quad \sinh[2hM], \\
n_4 &= 12M(h + \beta_1) + 4M\beta_1(-4 \cosh[2hM] + \cosh[4hM]) - 8 \sinh[2hM] + \sinh[4hM].
\end{aligned}$$

10.3 Results and discussion

In this section the main objective is to study the influence of various parameters of interest on the flow quantities. In particular the variations of Hartman number (M), Deborah number (Γ), amplitude ratio (a), slip parameter (β_1) and viscosity parameter (α) on the longitudinal velocity, pressure gradient, pressure rise (Δp_λ) and frictional force (F_λ) per wavelength have been examined.

Figs.10.1-10.3 show the effects of M , β_1 and Γ on the longitudinal velocity u . The plots show that velocity at the center of the channel and near the walls has opposite behavior. Further the velocity at the center of the channel decreases with an increase in M and β_1 but it increases by increasing Γ .

The variation of pressure gradient for certain values of M , β_1 and Γ are depicted in the Figs 10.4-10.6 It is anticipated that the absolute value of pressure gradient increases with an increase in M and β_1 but it decreases when Γ is increased.

The pressure rise and frictional force per wavelength have been computed numerically. The pressure rise verses flow rate has been plotted in the Figs 10.7-10.11. It is noticed from Fig. 10.7 that the pressure rise decreases with an increase in β_1 . It is found that magnitude of pressure rise per wavelength increases by increasing M (see Fig. 10.8). Fig. 10.9 depicts an important phenomenon that is the graph for pressure rise for $\Gamma = 0$ is linear whereas in the case of non zero Γ it is non linear. Fig 10.11 shows that the pressure rise increases with an increase in the amplitude ratio a . The free pumping flux increases by increasing α (see Fig.10.10).

Figs. 10.12-10.16 monitor the features of frictional force (F_λ). It is clear that there exists a critical value of η below which F_λ resists the flow and above which it assists the flow. This critical value of η decreases by increasing β_1 and M (see Figs. 10.12 and 10.13). Contrary to this the critical value of η increases with an increase in a and α (see Figs 10.14 and 10.15). It is revealed from Fig. 16 that the effect of Γ on frictional force is quiet opposite to that of pressure rise.

Another important fact of interest here is a comparison between the viscous and non-Newtonian fluids (see Figs. 10.3, 10.6, 10.9 and 10.14). In all these Figs. the case of viscous fluid is given by putting $\Gamma = 0$. Fig. 10.3 shows that velocity at the center of the channel in non-Newtonian fluid is larger when compared with a viscous fluid. Fig. 10.6 shows that the

non-Newtonian fluid exhibits larger pressure gradient than the viscous fluid.

Figs. 10.17-10.20 examine the trapping phenomenon. It is observed that the size of the trapped bolus decreases with an increase in β_1 and M . The size of trapped bolus also increases by increasing the viscosity parameter α (see Figs. 10.17 and 10.18). It is noted that by increasing the Deborah number Γ , the size of the bolus decreases whereas it increases by increasing a .

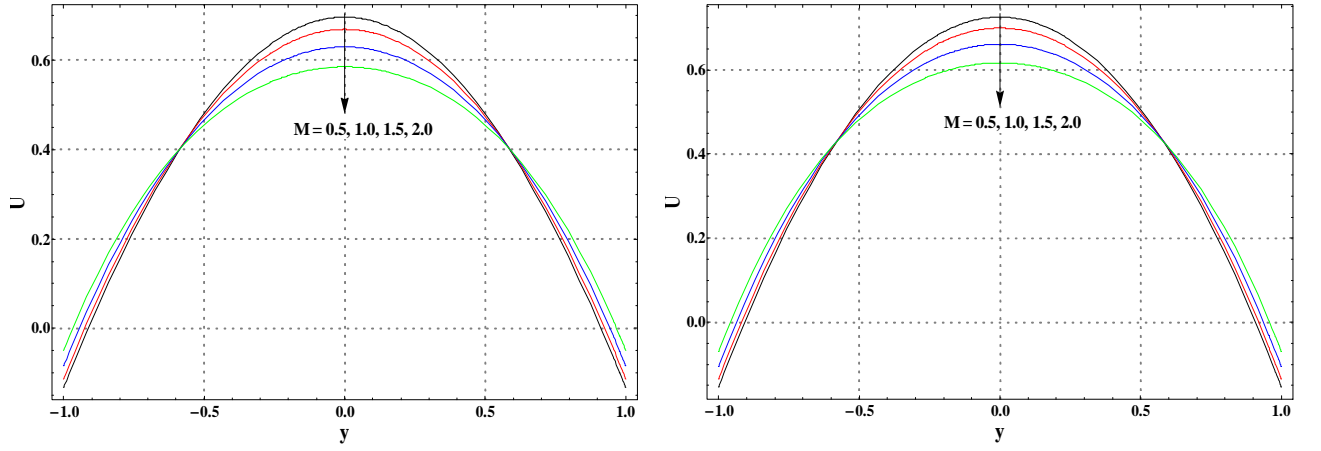


Fig. 10.1. Effect of M on velocity u when $\beta_1 = 0.2, \Gamma = 0.04, x = 1, \eta = 1.3$ and $a = 0.3$. Left panel is for $\alpha = 0$ and right panel is for $\alpha = 0.4$.

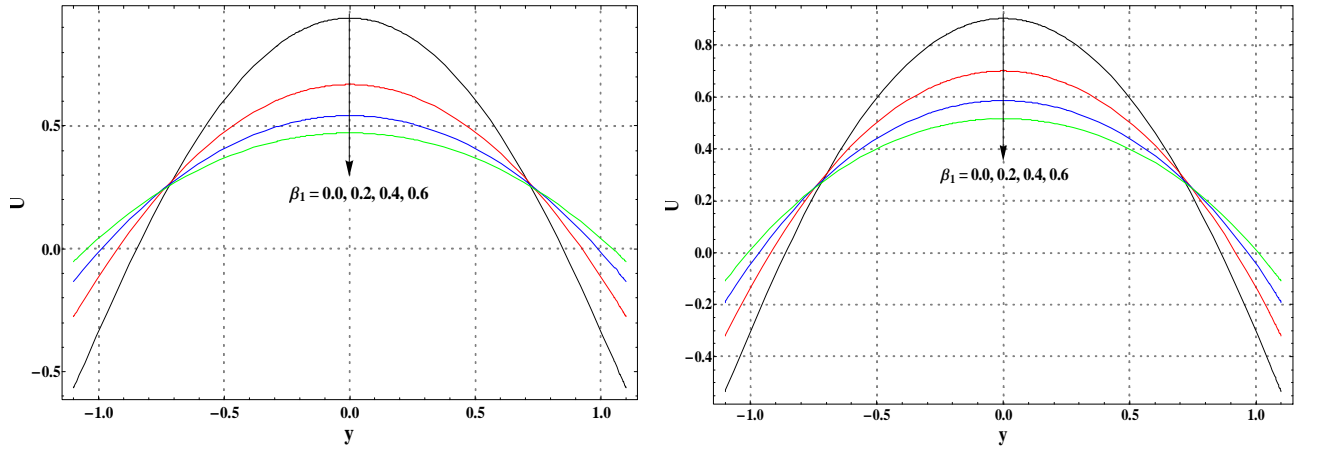


Fig. 10.2. Effect of β_1 on velocity u when $M = 1, \Gamma = 0.04, x = 1, \eta = 1.3$ and $a = 0.3$. Left panel is for $\alpha = 0$ and right panel is for $\alpha = 0.4$.

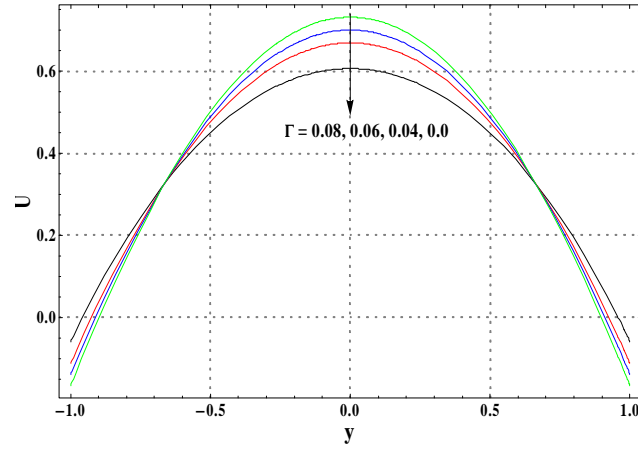


Fig. 10.3. Effect of Γ on velocity u when $M = 1$, $\beta_1 = 0.04$, $x = 1$, $\eta = 1.3$ and $a = 0.3$.

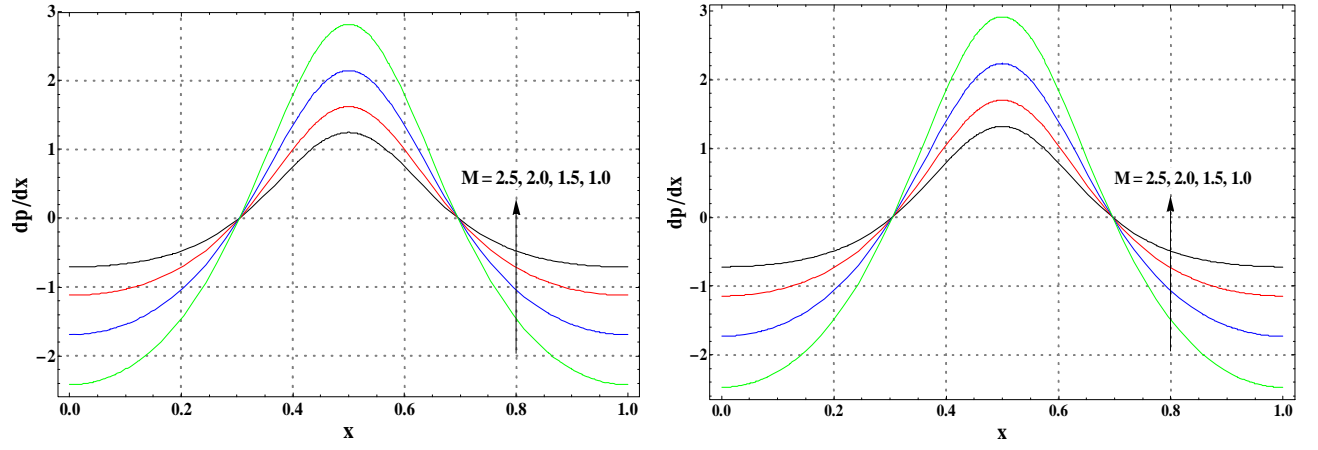


Fig. 10.4. Effect of M on pressure gradient when $\beta_1 = 0.2$, $\Gamma = 0.001$, $\eta = 0.1$ and $a = 0.3$.

Left panel is for $\alpha = 0$ and right panel is for $\alpha = 0.4$.

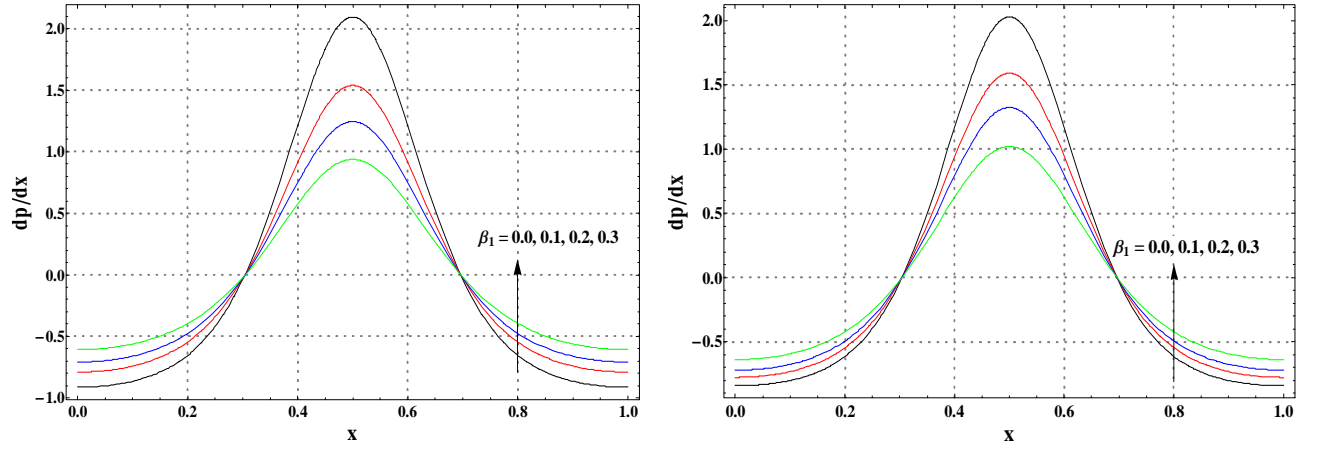


Fig. 10.5. Effect of β_1 on pressure gradient when $M = 1$, $\Gamma = 0.001$, $\eta = 0.1$ and $a = 0.3$. Left panel is for $\alpha = 0$ and right panel is for $\alpha = 0.4$.

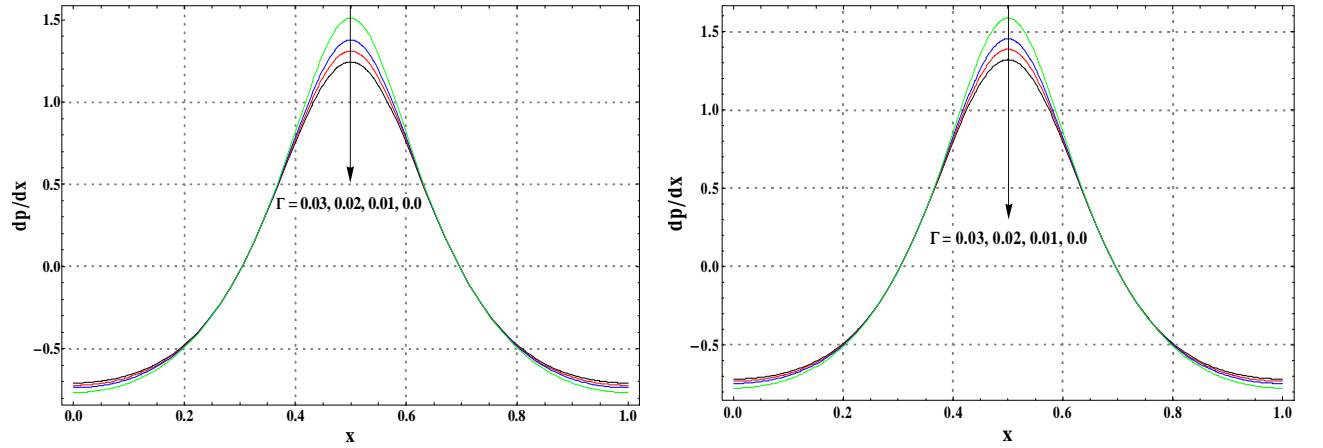


Fig. 10.6. Effect of Γ on pressure gradient when $M = 1$, $\beta_1 = 0.2$, $\eta = 0.1$ and $a = 0.3$. Left panel is for $\alpha = 0$ and right panel is for $\alpha = 0.4$.

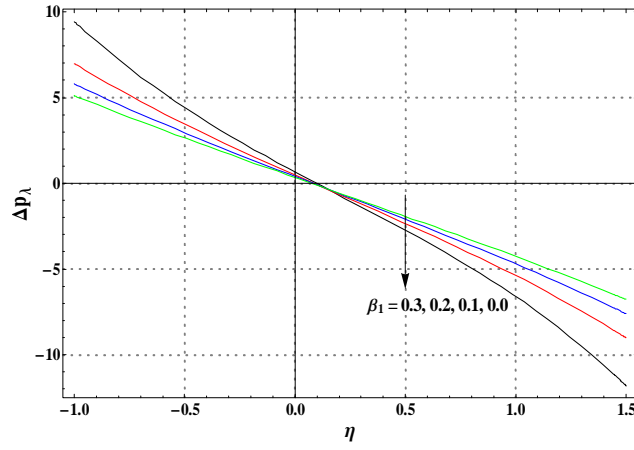


Fig. 10.7. Variation of β_1 on Δp_λ when $\Gamma = 0.01$, $M = 1.5$, $a = 0.3$ and $\alpha = 0.2$.

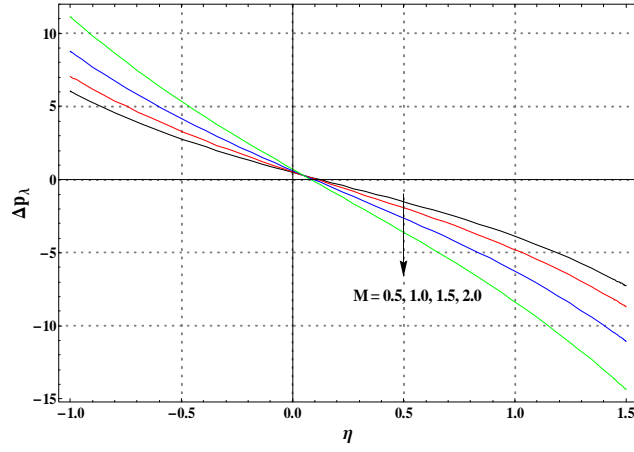


Fig. 10.8. Variation of M on Δp_λ when $\Gamma = 0.01$, $\beta_1 = 0.02$, $a = 0.3$ and $\alpha = 0.2$.

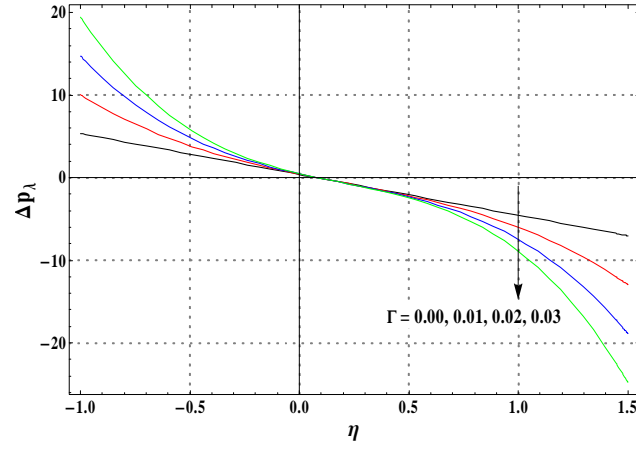


Fig. 10.9. Variation of Γ on Δp_λ when $\beta_1 = 0.02$, $M = 1.5$, $a = 0.3$ and $\alpha = 0.2$.

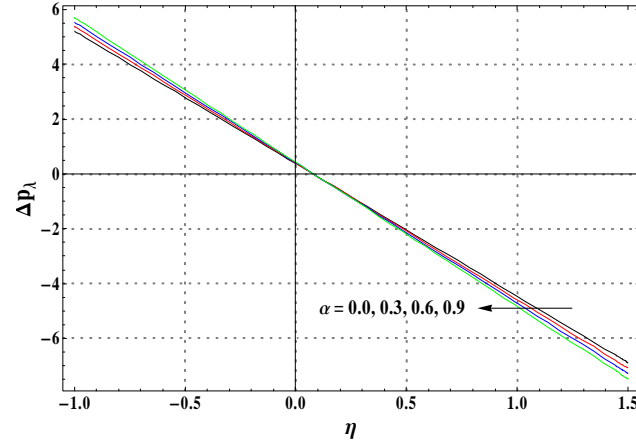


Fig. 10.10. Variation of α on Δp_λ when $\beta_1 = 0.02$, $M = 1.5$, $a = 0.3$ and $\Gamma = 0.01$.

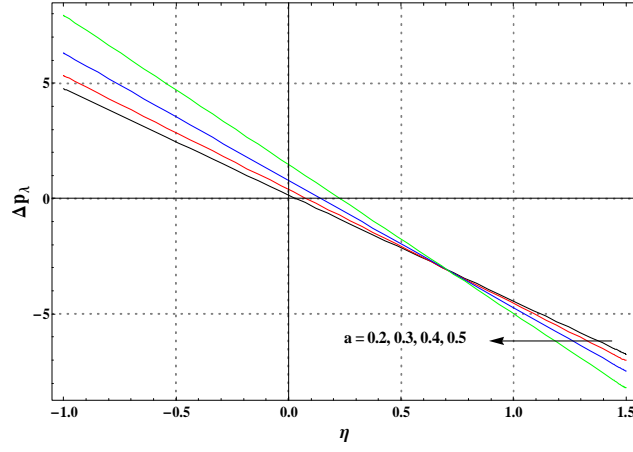


Fig. 10.11. Variation of a on Δp_λ when $\beta_1 = 0.02$, $M = 1.5$, $\alpha = 0.2$ and $\Gamma = 0.01$.

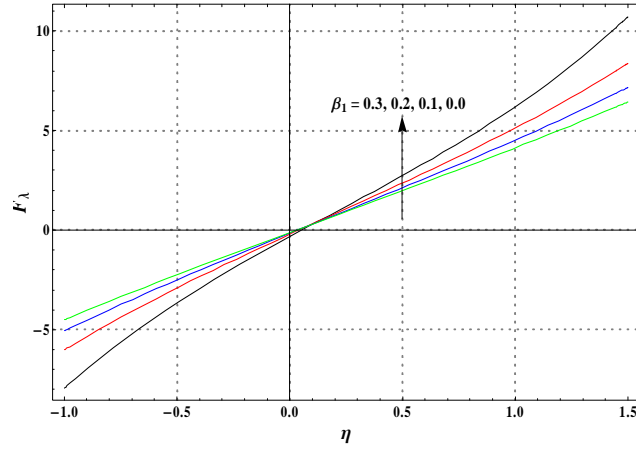


Fig. 10.12. Variation of β_1 on F_λ when $a = 0.3$, $M = 1.5$, $\alpha = 0.2$ and $\Gamma = 0.01$.

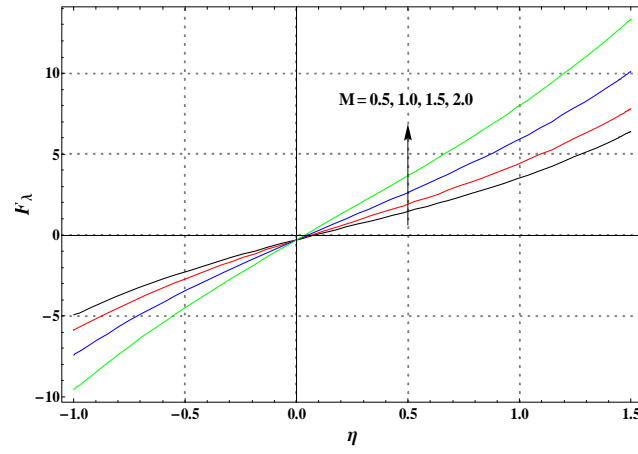


Fig. 10.13 Variation of M on F_λ when $a = 0.3$, $\beta_1 = 0.02$, $\alpha = 0.2$ and $\Gamma = 0.01$.

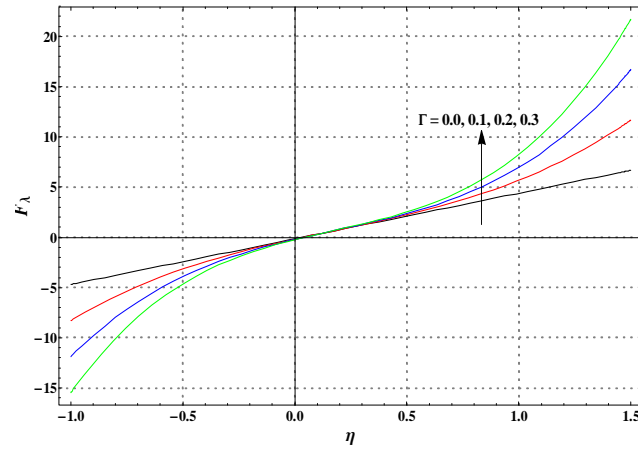


Fig. 10.14. Variation of Γ on F_λ when $a = 0.3$, $M = 1.5$, $\alpha = 0.2$ and $\beta_1 = 0.02$.

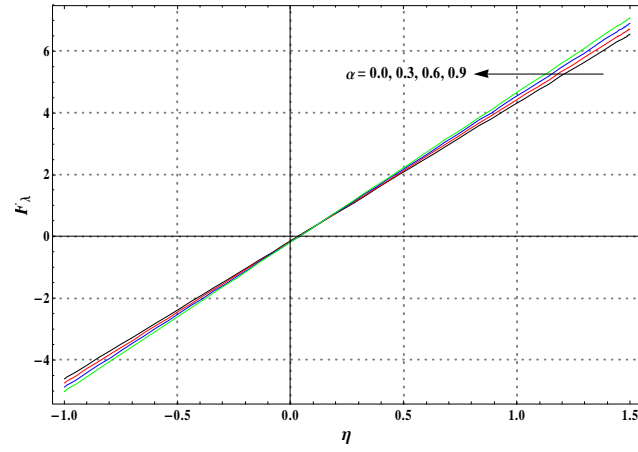


Fig. 10.15. Variation of α on F_λ when $a = 0.3$, $M = 1.5$, $\Gamma = 0.01$ and $\beta_1 = 0.02$.

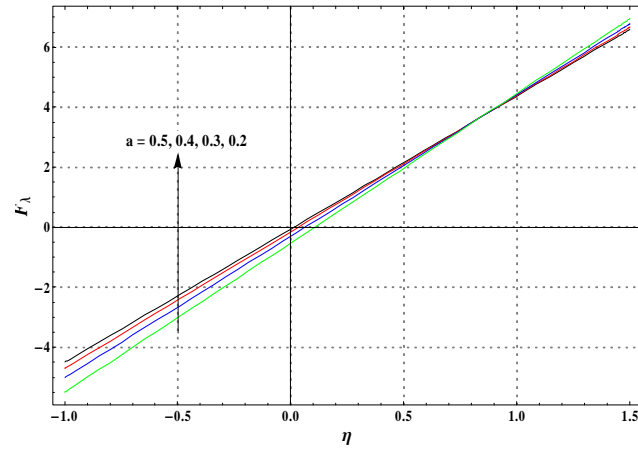


Fig. 10.16. Variation of a on F_λ when $\alpha = 0.2$, $M = 1.5$, $\Gamma = 0.01$ and $\beta_1 = 0.02$.

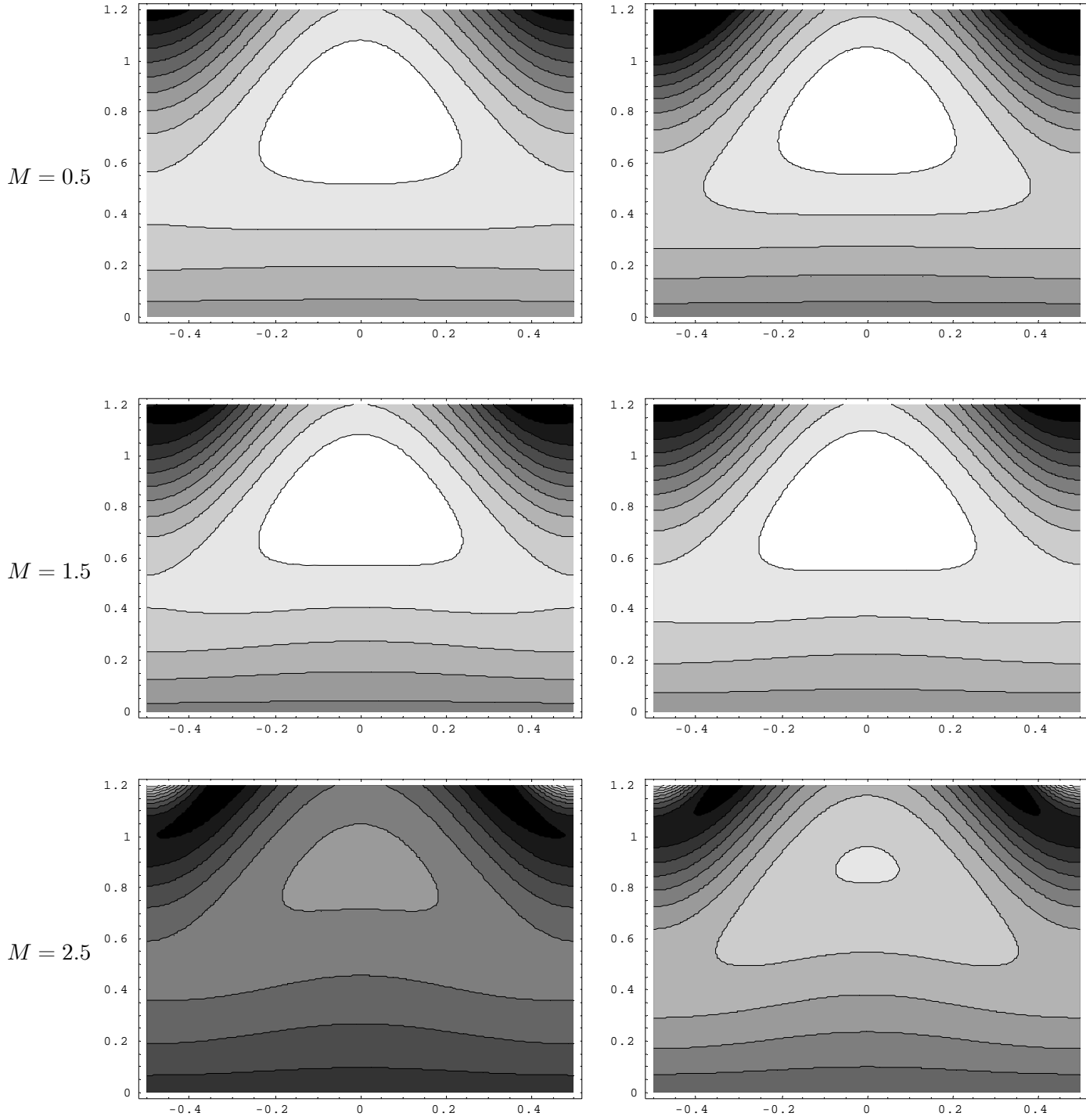


Fig. 10.17. Effect of M on stream lines when $\Gamma = 0.04, \phi = 0.3, \eta = 1.1$, and $\beta = 0.2$ Left panels are for $\alpha = 0$, and right panels are for $\alpha = 0.4$.

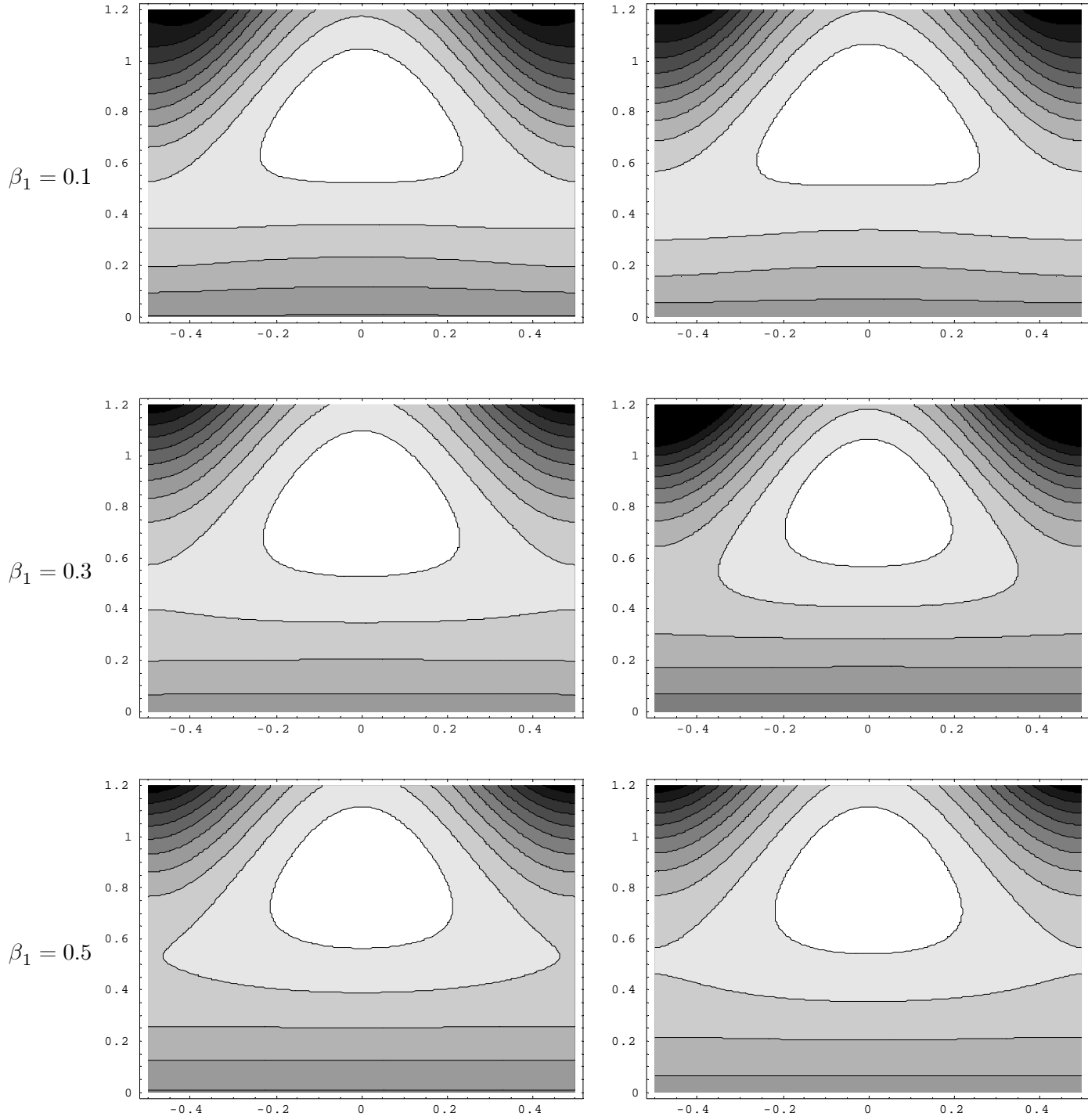


Fig. 10.18. Effect of β_1 on stream lines when $\Gamma = 0.04, a = 0.3, \eta = 1.1$ and $M = 0.5$. Left panels are for $\alpha = 0$ and right panels are for $\alpha = 0.4$.

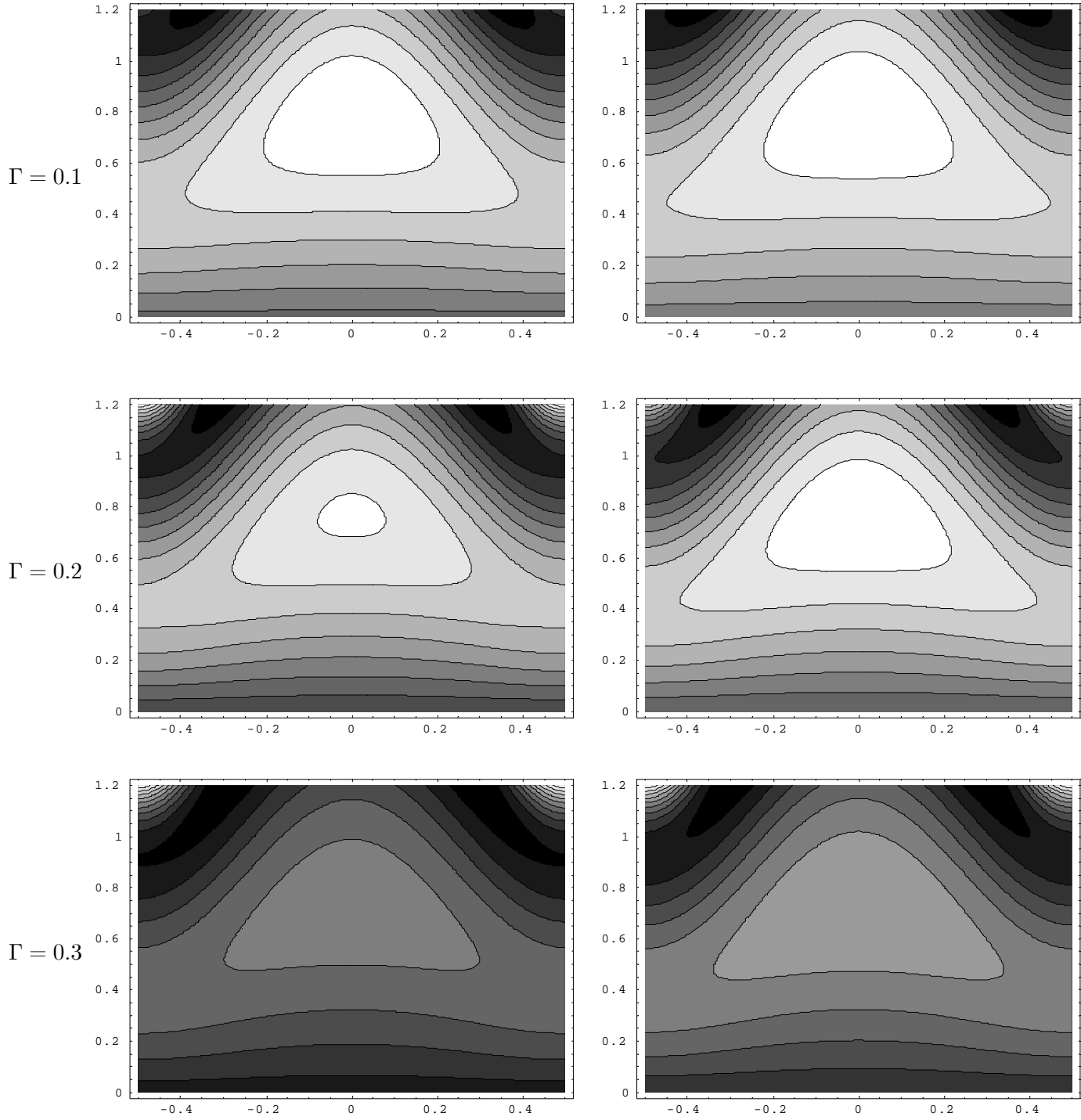


Fig. 10.19. Effect of Γ on stream lines when $\beta_1 = 0.2, a = 0.3, \eta = 1.1$ and $M = 0.5$. Left panels are for $\alpha = 0$ and right panels are for $\alpha = 0.4$.

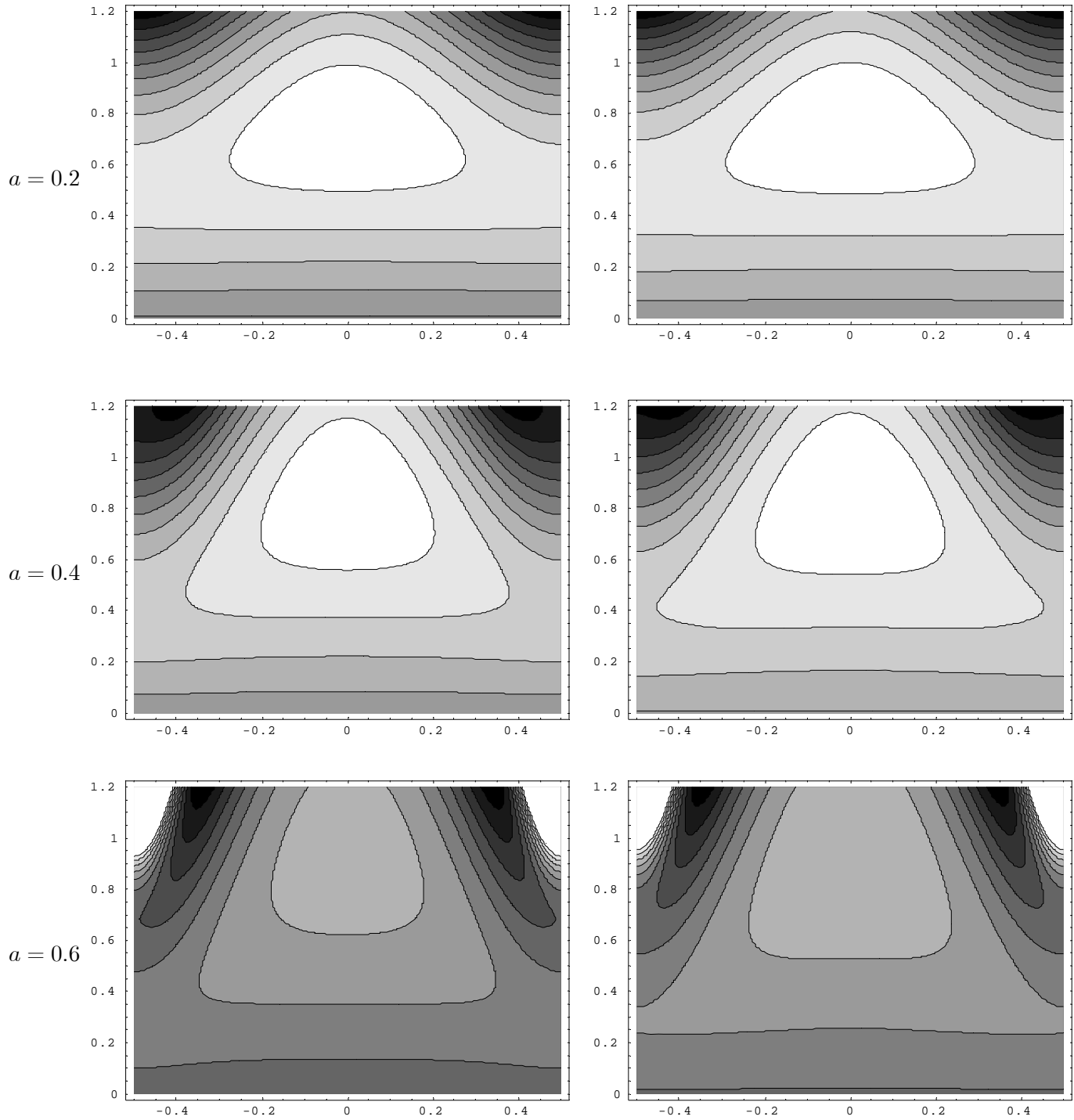


Fig. 10.20. Effect of a on stream lines when $\beta_1 = 0.2, x = 1, \Gamma = 0.04, \eta = 1.1$ and $M = 0.5$.

Left panels are for $\alpha = 0$ and right panels are for $\alpha = 0.4$.

Chapter 11

Heat transfer analysis for peristaltic mechanism in variable viscosity fluid

This chapter extends the analysis of previous chapter in the presence of heat transfer. Thermal slip is also considered. Viscous dissipation is present. Perturbation solution is constructed and a comparative study between the cases of constant and variable viscosities is presented and analyzed.

11.1 Statement of the problem

Here we study an incompressible magnetohydrodynamic (MHD) third order fluid with variable viscosity in a uniform channel of width $2d_1$. The \overline{X} – *axis* is selected along the centerline of the channel whereas \overline{Y} is perpendicular to the \overline{X} – *axis*. The fluid is electrically conducting under an applied magnetic field \mathbf{B}_0 in the \overline{Y} – direction. The electric and induced magnetic field effects are neglected. Sinusoidal waves propagating on the channel induce the flow. Such waves are described by the following equations

$$H(\overline{X}, \bar{t}) = d_1 + a_1 \cos \left(\frac{2\pi}{\lambda} (\overline{X} - c\bar{t}) \right). \quad (11.1)$$

In above expression c is the speed of propagation of the wave, a_1 the wave amplitude, λ the wavelength and \bar{t} the time. Further the channel walls have a constant temperature T_0 . The

governing equations are

$$\frac{\partial \bar{U}}{\partial \bar{X}} + \frac{\partial \bar{V}}{\partial \bar{Y}} = 0, \quad (11.2)$$

$$\rho \left(\frac{\partial}{\partial \bar{t}} + \bar{U} \frac{\partial}{\partial \bar{X}} + \bar{V} \frac{\partial}{\partial \bar{Y}} \right) \bar{U} = -\frac{\partial \bar{P}}{\partial \bar{X}} + \frac{\partial \bar{S}_{\bar{X}\bar{X}}}{\partial \bar{X}} + \frac{\partial \bar{S}_{\bar{X}\bar{Y}}}{\partial \bar{Y}} - \sigma B_0^2 \bar{U}, \quad (11.3)$$

$$\rho \left(\frac{\partial}{\partial \bar{t}} + \bar{U} \frac{\partial}{\partial \bar{X}} + \bar{V} \frac{\partial}{\partial \bar{Y}} \right) \bar{V} = -\frac{\partial \bar{P}}{\partial \bar{Y}} + \frac{\partial \bar{S}_{\bar{X}\bar{Y}}}{\partial \bar{X}} + \frac{\partial \bar{S}_{\bar{Y}\bar{Y}}}{\partial \bar{Y}}, \quad (11.4)$$

$$\rho \zeta \left(\frac{\partial}{\partial \bar{t}} + \bar{U} \frac{\partial}{\partial \bar{X}} + \bar{V} \frac{\partial}{\partial \bar{Y}} \right) T = k \nabla^2 T + \bar{\Phi}, \quad (11.5)$$

where $\bar{\Phi}$ is the dimensional viscous dissipation term. In light of the following dimensionless quantities

$$\begin{aligned} x &= \frac{\bar{x}}{\lambda}, \quad y = \frac{\bar{y}}{d_1}, \quad u = \frac{\bar{u}}{c}, \quad v = \frac{\bar{v}}{c\delta}, \quad \delta = \frac{d_1}{\lambda}, \quad h = \frac{H}{a}, \quad a = \frac{a_1}{d_1}, \quad p = \frac{d_1^2 \bar{p}}{c\lambda\mu_0}, \\ S &= \frac{d_1}{\mu_0 c} \bar{S}(\bar{x}), \quad \mu(y) = \frac{\bar{\mu}(\bar{y})}{\mu_0}, \quad M = \left(\frac{\sigma}{\mu_0} \right)^{1/2} B_0 d_1, \quad v_0 = \frac{\mu_0}{\rho}, \quad Re = \frac{\rho c d_1}{\mu_0}, \\ t &= \frac{c \bar{t}}{\lambda}, \quad u = \frac{\partial \psi}{\partial y}, \quad v = -\frac{\partial \psi}{\partial x}, \quad \gamma_2 = \frac{\beta_2 c^2}{\mu_0 d_1^2}, \quad \gamma_3 = \frac{\beta_3 c^2}{\mu_0 d_1^2}, \quad \theta = \frac{T - T_0}{T_0}, \\ Pr &= \frac{\mu_0 C_p}{K}, \quad E = \frac{c^2}{C_p T_0}, \quad \bar{\zeta} = \frac{\mu_0 c^2}{a^2} \zeta \end{aligned} \quad (11.6)$$

equations (11.2)-(11.5) give

$$\delta R_e \left[\left(\frac{\partial \psi}{\partial y} \frac{\partial}{\partial x} - \frac{\partial \psi}{\partial x} \frac{\partial}{\partial y} \right) \frac{\partial \psi}{\partial y} \right] = -\frac{\partial p}{\partial x} + \delta \frac{\partial S_{xx}}{\partial x} + \frac{\partial S_{xy}}{\partial y} - M^2 \left(\frac{\partial \psi}{\partial y} + 1 \right), \quad (11.7)$$

$$-\delta^3 R_e \left[\left(\frac{\partial \psi}{\partial y} \frac{\partial}{\partial x} - \frac{\partial \psi}{\partial x} \frac{\partial}{\partial y} \right) \frac{\partial \psi}{\partial x} \right] = -\frac{\partial p}{\partial y} + \delta^2 \frac{\partial S_{xy}}{\partial x} + \delta \frac{\partial S_{yy}}{\partial y}, \quad (11.8)$$

$$\delta R_e \left[\left(\frac{\partial \psi}{\partial y} \frac{\partial \theta}{\partial x} - \frac{\partial \psi}{\partial x} \frac{\partial \theta}{\partial y} \right) \right] = E \Phi + \frac{1}{Pr} \left(\delta^2 \frac{\partial^2 \theta}{\partial x^2} + \frac{\partial^2 \theta}{\partial y^2} \right), \quad (11.9)$$

where C_p is the specific heat, K the thermal conductivity, $\Gamma(= \gamma_2 + \gamma_3)$ the Deborah number, ψ the stream function, v_0 the constant kinematic viscosity, M the Hartman number, Re the Reynolds number, ρ the fluid density, σ the electrical conductivity, $\bar{\mu}(\bar{y})$ the viscosity function, δ the wave number, μ_0 the constant viscosity, $Br(= Pr E)$ the Brinkman number, Φ the dimensionless viscous dissipation term, Pr the Prandtl number and E the Eckert number. The

governing problems subject to long wavelength and low Reynolds number are

$$-\frac{\partial p}{\partial x} + \frac{\partial}{\partial y} S_{xy} - M^2 \left(\frac{\partial \psi}{\partial y} + 1 \right) = 0, \quad 0 = -\frac{\partial p}{\partial y}, \quad (11.10)$$

$$\frac{\partial^2 \theta}{\partial y^2} = -Br\zeta, \quad (11.11)$$

$$S_{xy} = \mu(y) \frac{\partial^2 \psi}{\partial y^2} + 2\Gamma \left(\frac{\partial^2 \psi}{\partial y^2} \right)^3, \quad \zeta = \mu(y) \left(\frac{\partial^2 \Psi}{\partial y^2} \right)^2 + 2\Gamma \left(\frac{\partial^2 \Psi}{\partial y^2} \right)^4, \quad (11.12)$$

$$\begin{aligned} \psi &= 0, & \frac{\partial^2 \psi}{\partial y^2} &= 0, & \frac{\partial \theta}{\partial y} &= 0 & \text{at } y = 0, \\ \psi &= F, & \frac{\partial \psi}{\partial y} + \beta_1 S_{xy} &= -1, & \theta - \beta_2 \frac{\partial \theta}{\partial y} &= 0 & \text{at } y = h, \end{aligned} \quad (11.13)$$

$$h(x) = 1 + \phi \cos(2\pi x), \quad F = \int_0^1 \frac{\partial \psi}{\partial y} dy, \quad (11.14)$$

where β_2 is the dimensionless thermal slip parameter, $\mu(y) = e^{-\alpha y}$ or $\mu(y) = 1 - \alpha y$ for $(\alpha \ll 1)$; α the viscosity parameter, β_1 the dimensionless velocity slip parameter, ψ the stream function, θ the temperature and F the dimensionless flow rate in wave frame. Further Eq. (11.10) indicates that $p \neq p(y)$ and finally we write

$$\frac{\partial^2}{\partial y^2} \left(\mu(y) \frac{\partial^2 \psi}{\partial y^2} + 2\Gamma \left(\frac{\partial^2 \psi}{\partial y^2} \right)^3 \right) - M^2 \frac{\partial^2 \psi}{\partial y^2} = 0. \quad (11.15)$$

Pressure rise per wavelength Δp_λ and frictional force F_λ (at the wall) are

$$\Delta p_\lambda = \int_0^1 \frac{dp}{dx} dx, \quad F_\lambda = \int_0^1 h \left(-\frac{dp}{dx} \right) dx. \quad (11.16)$$

11.2 Solution expressions

The solutions for small Γ and α are

$$\psi = \frac{FM y \cosh[hM] + y(1 + FM^2 \beta_1) \sinh[hM] - (F + h) \sinh[My]}{hM \cosh[hM] + (-1 + hM \beta_1^2) M \beta_1 \sinh[hM]} + \alpha m_1 + \Gamma m_2, \quad (11.17)$$

$$\frac{dp}{dx} = -\frac{(F+h)M^3(\cosh[hM] + M\beta_1 \sinh[hM])}{hM \cosh[hM] + (-1 + hM\beta_1^2)M\beta_1 \sinh[hM]} + \alpha n_1 + \Gamma n_2, \quad (11.18)$$

$$\begin{aligned} \theta = & \frac{Br(F+h)^2 M^2 (-Cosh[2hM] + Cosh[2My] + 2M(M(h^2 - y^2 - 2h\gamma) + \beta_2 Sinh[2hM]))}{8(hMCosh[hM] + (-1 + hM^2\beta_1)Sinh[hM])^2} \\ & + \frac{Br(F+h)^2 M\alpha}{192(hMCosh[hM] + (-1 + hM^2\beta_1)Sinh[hM])^3} \times \\ & (q_1 + M(q_2 - q_3 - q_4 + q_5)) \\ & + \frac{Br(F+h)^4 M^6 \Gamma}{512(hMCosh[hM] + (-1 + hM^2\beta_1)Sinh[hM])^5} \times \\ & (L_1 + 4(L_2 + M(L_3 + L_4 + L_5 + L_6))) \end{aligned} \quad (11.19)$$

where the involved m_i ($i = 1 - 8$), n_j ($j = 1, 2$), q_l ($l = 1 - 6$) and L_k ($k = 1 - 8$) are given as follows:

$$\begin{aligned} m_1 &= \frac{(F+h)(m_3+2\sinh[hM](m_4)+2hM\cosh[hM](m_5))}{8M(hM\cosh[hM]+(-1+hM\beta^2)M\beta\sinh[hM])^2}, \\ m_2 &= \frac{e^{-3My}e^{-3My}(F+h)^3M^4(((1-hM^2\beta)\sinh[hM]+e^{6My}(m_6)+e^{2My}(m_7)+2e^{3My}M(m_8)))}{32(hM\cosh[hM]+(-1+hM\beta^2)M\beta\sinh[hM])^4}, \\ m_3 &= -4My(h+\beta+hM^2\beta)+2My(2\beta+h(-1+2M^2\beta))\cosh[2hM] \\ &+y(3-4hM^2\beta)\sinh[2hM], \quad m_4 = 3y(-1+hM^2\beta)\cosh[My]+M(-2h^2 \\ &+y^2+h(-4+M^2((-4+h)h-y^2))\beta)\sinh[My], \\ m_4 &= 3y(-1+hM^2\beta)\cosh[My]+M(-2h^2+y^2+h(-4+M^2((-4+h)h-y^2))\beta) \\ &\sinh[My], \\ m_5 &= 3y\cosh[My]+M(-y^2+h(h+\beta))\sinh[My], \\ m_6 &= -3hM\cosh[3hM]+12M(y+hM(h+2\beta-My\beta))\sinh[hM] \\ &+(1-9hM^2\beta)\sinh[3hM], \\ m_7 &= 3hM\cosh[3hM]-12M(-y+hM(h+2\beta+My\beta))\sinh[hM] \\ &+(-1+9hM^2\beta)\sinh[3hM], \\ m_8 &= 12My(h+\beta)-16My\beta\cosh[2hM]+4My\beta\cosh[4hM]-8y\sinh[2hM] \\ &+y\sinh[4hM]+h\cosh[hM](12M(-y\cosh[MY]+hM\beta\sinh[My]+\sinh[3My]) \\ &+\sinh[3My]). \end{aligned}$$

$$\begin{aligned}
n_1 &= \frac{(F+h)Mn_3}{8(hM \cosh[hM] + (-1+hM^2\beta) \sinh[hM])^2}, \\
n_2 &= \frac{(F+h)^3 M^7 n_4}{16(hM \cosh[hM] + (-1+hM\beta^2) M\beta \sinh[hM])^4}, \\
n_3 &= 4M(h + \beta + hM^2\beta) + 2M(h - 2(1 + hM^2)\beta) \cosh[2hM] + (-3 + 4hM^2\beta) \sinh[2hM], \\
n_4 &= 12M(h + \beta) + 4M\beta(-4 \cosh[2hM] + \cosh[4hM]) - 8 \sinh[2hM] + \sinh[4hM].
\end{aligned}$$

$$\begin{aligned}
q_1 &= (3 + hM^2(-3\beta + 4M^2(2y^3 + h(h(-2h - 3\beta + 6M^2(h - y)(h + y)\beta) - 3(-1 + 4h^2M^2)\beta\gamma)))) \cosh[hM] - 3(1 + hM^2(-\beta + 4h(1 + \gamma M^2\beta))) \cosh[3hM] + 6 \sinh[hM] \sinh[2My], \\
q_2 &= 3M(2(h - y)y + h(1 + 2M^2(h^2 + y^2))\beta) \cosh[M(h - 2y)] + 3M(2y(h + y) + h(q_6)\beta) \cosh[M(h + 2y)], \\
q_3 &= 3h \sinh[hM] + 20h^3M^2 \sinh[hM] + 24h^5M^4 \sinh[hM] - 24h^3M^4y^2 \sinh[hM] \\
&\quad - 8M^2y^3 \sinh[hM], \\
q_4 &= 32h^4M^4\beta \sinh[hM] + 24h^2M^4y^2\beta \sinh[hM] + 8hM^4y^3\beta \sinh[hM] - 36h^2M^2\gamma \sinh[hM] \\
&\quad - 48h^4M^4\gamma \sinh[hM] + 96h^3M^4\beta\gamma \sinh[hM] + 9h \sinh[3hM] + 12h^2M^2\gamma \sinh[3hM] \\
&\quad + 3h \sinh[M(h - 2y)] + 6h^3M^2 \sinh[M(h - 2y)] - 6y \sinh[M(h - 2y)], \\
q_5 &= 6hM^2y^2 \sinh[M(h - 2y)] - 6h^2M^2\beta \sinh[M(h - 2y)] + 6hM^2y\beta \sinh[M(h - 2y)] \\
&\quad + 3(-2y + h(-1 + 2M^2(h - y)(h + y - \beta))) \sinh[M(h + 2y)], \\
q_6 &= -1 + 2M^2(h - y)(h + y).
\end{aligned}$$

$$\begin{aligned}
L_1 &= 16M \left(-6\gamma + h \left(5 + 2M^2 (L_7) \right) \right) \text{Cosh}[hM] + 3M (36\gamma + h (L_8)) \text{Cosh}[3hM] + 16\text{Sinh}[hM] \\
&\quad - 25\text{Sinh}[3hM] + \text{Sinh}[5hM] - 5\text{Sinh}[M(h - 4y)], \\
L_2 &= 5\text{Sinh}[M(h - 2y)] + \text{Sinh}[M(3h - 2y)] + 5\text{Sinh}[M(h + 2y)] + \text{Sinh}[M(3h + 2y)] \\
&\quad - 5\text{Sinh}[M(h + 4y)], \\
L_3 &= (7h - 4 (3 + 13hM^2\beta) \gamma) \text{Cosh}[5hM] + 5h\text{Cosh}[M(h - 4y)] - 20h\text{Cosh}[M(h - 2y)] \\
&\quad - 48y\text{Cosh}[M(h - 2y)] + 48h^2M^2\beta\text{Cosh}[M(h - 2y)], \\
L_4 &= 48hM^2y\beta\text{Cosh}[M(h - 2y)] - 12h\text{Cosh}[M(3h - 2y)] - 20h\text{Cosh}[M(h + 2y)] \\
&\quad + 48y\text{Cosh}[M(h + 2y)] + 48h^2M^2\beta\text{Cosh}[M(h + 2y)] - 48hM^2y\beta\text{Cosh}[M(h + 2y)] \\
&\quad - 12h\text{Cosh}[M(3h + 2y)] + 5h\text{Cosh}[M(h + 4y)] + 288h^2M\text{Sinh}[hM], \\
L_5 &= 192h^4M^3\text{Sinh}[hM] - 192My^2\text{Sinh}[hM] - 192h^2M^3y^2\text{Sinh}[hM] + 112hM\beta\text{Sinh}[hM] \\
&\quad + 192h^3M^3\beta\text{Sinh}[hM] - 192hM^3y^2\beta\text{Sinh}[hM] - 544hM\gamma\text{Sinh}[hM] - 384h^3M^3\gamma\text{Sinh}[hM] \\
&\quad - 192h^2M^3\beta\gamma\text{Sinh}[hM] + 16h^2MM\text{Sinh}[3hM] - 16My^2\text{Sinh}[3hM] - 71hM\beta\text{Sinh}[3hM] \\
&\quad - 144h^3M^3\beta\text{Sinh}[3hM] + 144hM^3y^2\beta\text{Sinh}[3hM] - 4hM\gamma\text{Sinh}[3hM], \\
L_6 &= 288h^2M^3\beta\gamma\text{Sinh}[3hM] + 31hM\beta\text{Sinh}[5hM] - 4hM\gamma\text{Sinh}[5hM] + 5hM\beta \\
&\quad \text{Sinh}[M(h - 4y)] + 48h^2M\text{Sinh}[M(h - 2y)] + 48hMy\text{Sinh}[M(h - 2y)] + 76h \\
&\quad M\beta\text{Sinh}[M(h - 2y)] - 36hM\beta\text{Sinh}[M(3h - 2y)] + 48h^2M\text{Sinh}[M(h + 2y)] \\
&\quad - 48hMy\text{Sinh}[M(h + 2y)] + 76hM\beta\text{Sinh}[M(h + 2y)] - 36hM\beta\text{Sinh}[M(3h + 2y)] \\
&\quad + 5hM\beta\text{Sinh}[M(h + 4y)], \\
L_7 &= 6y^2 + 3h \left(-2h + (-1 + 2M^2(h - y)(h + y)) \beta \right) - (\beta + 6h (-1 + 2hM^2\beta)) \gamma, \\
L_8 &= -11 + 4M^2 (-4h^2 + 4y^2 + 8h\gamma + 7\beta\gamma).
\end{aligned}$$

The heat transfer coefficient is

$$Z = h_x\theta_y. \quad (11.20)$$

11.3 Graphical analysis and key points

This section provides a comparative study of temperature for the effects of various parameters in the constant ($\alpha = 0$ left panels) and variable ($\alpha = 0.2$ right panels) fluid viscosities in the presence of heat transfer.

It is observed in Figs. 11.1 (a-d) that θ decreases when M and β_1 are increased. Further temperature in variable viscosity fluid is less when compared with constant viscosity fluid. From

Figs. 11.2 (a-d), an increase in θ is observed when Br increases whereas θ decreases when β_2 increases. Although the plots for heat transfer coefficient Z are not included to save space for variation of M and Γ . It is also seen that impact of M on Z is quite opposite to that of β_1 . Z is an increasing function of M . Figs. 11.3 (a-d) show that Z decreases when β_1 increases whereas it increases by increasing Br .

The main points of present chapter can be summarized as follows.

- i) Temperature in constant viscosity fluid is greater than variable viscosity situation.
- ii) Temperature is decreasing function of thermal slip parameter β_2 .
- iii) The qualitative effects of Br and β_1 on the temperature are opposite.
- iv) Behavior of β_1 on the heat transfer coefficient is opposite to that of Br .

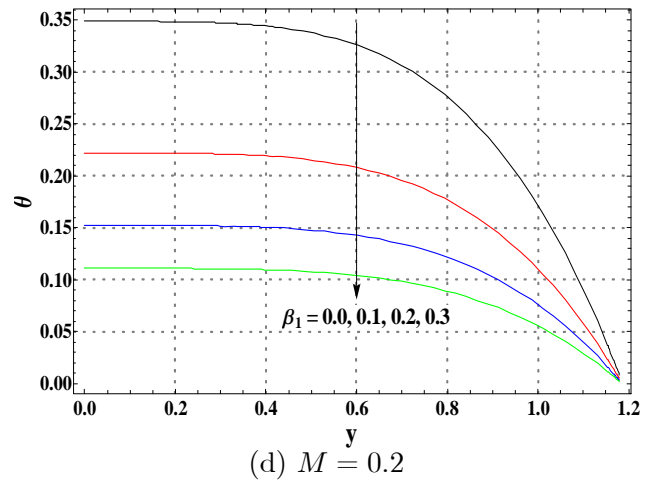
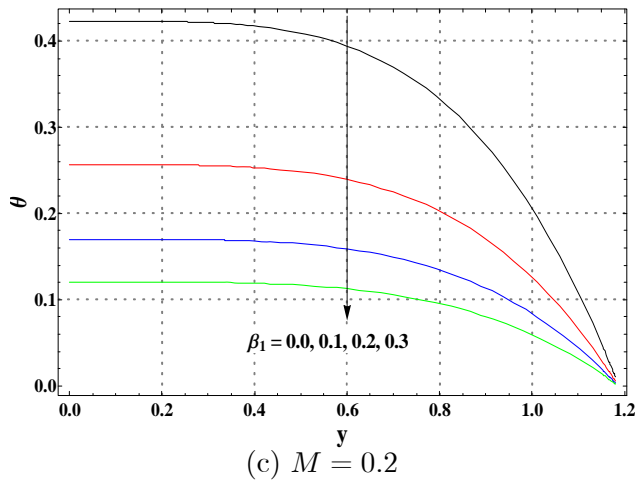
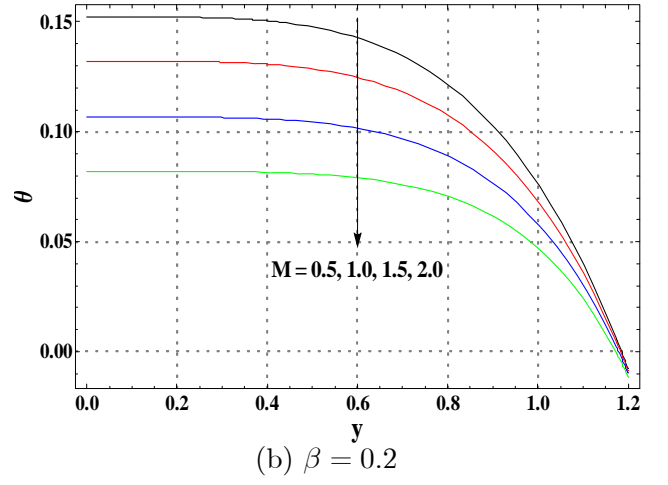
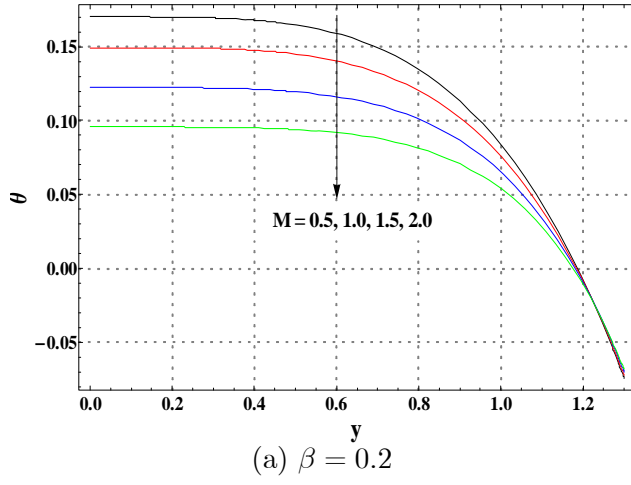


Fig. 11.1 (a-d): Variation of η for $\Gamma = 0.04$, $\phi = 0.3$, $\eta = 1.1$, $\gamma = 0.1$ and $\text{Br} = 0.5$.

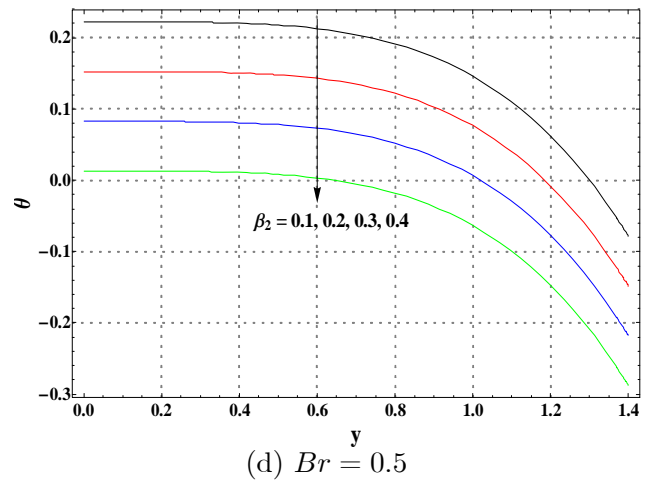
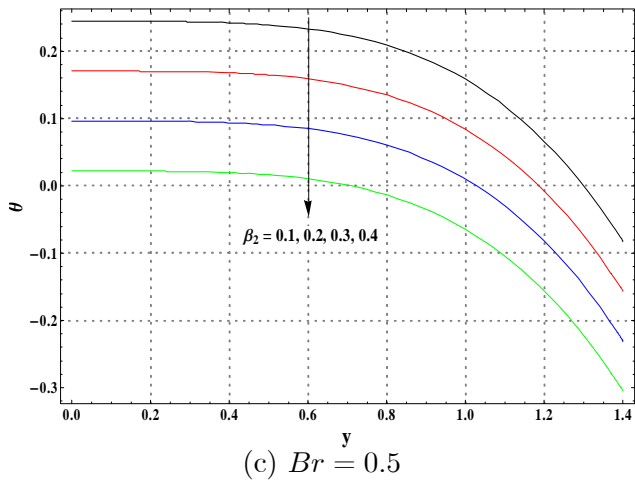
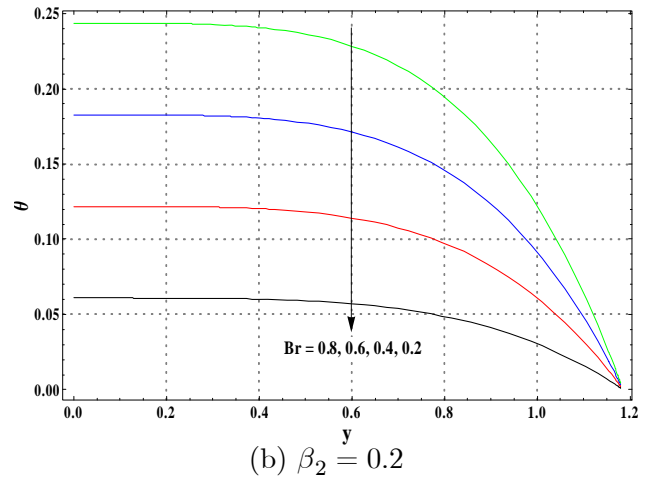
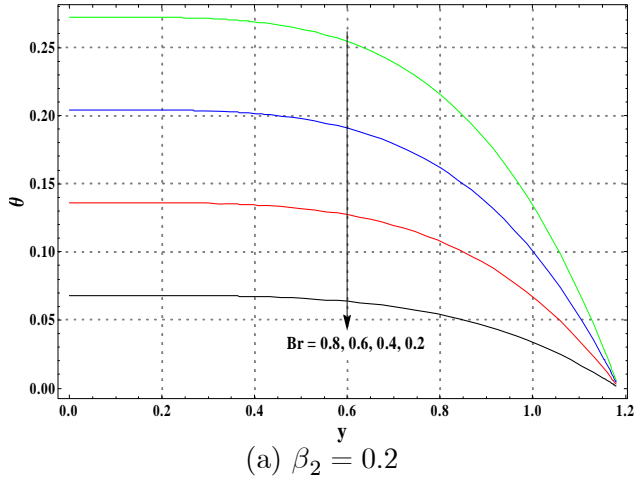


Fig. 11.2 (a-d): Variation of η for $M = 1$, $\Gamma = 0.04$, $\phi = 0.3$, $\eta = 1.1$, and $\beta = 0.2$.

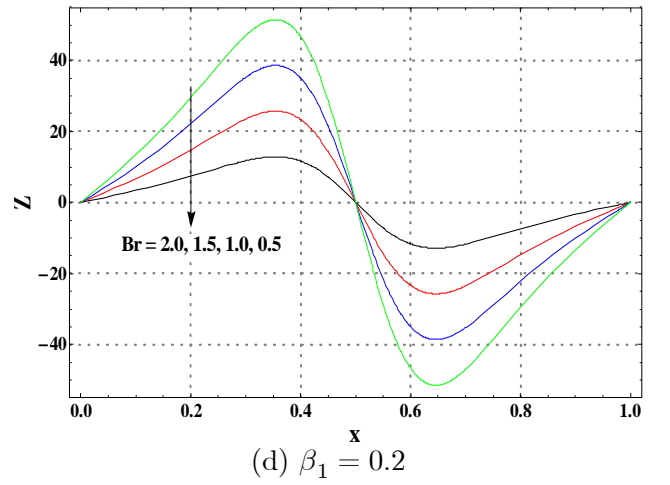
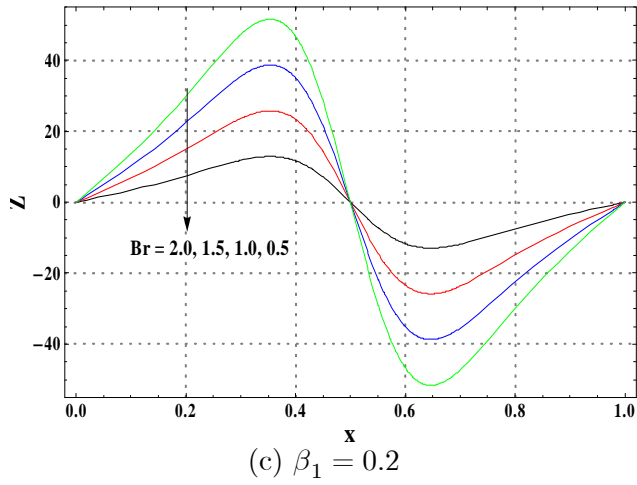
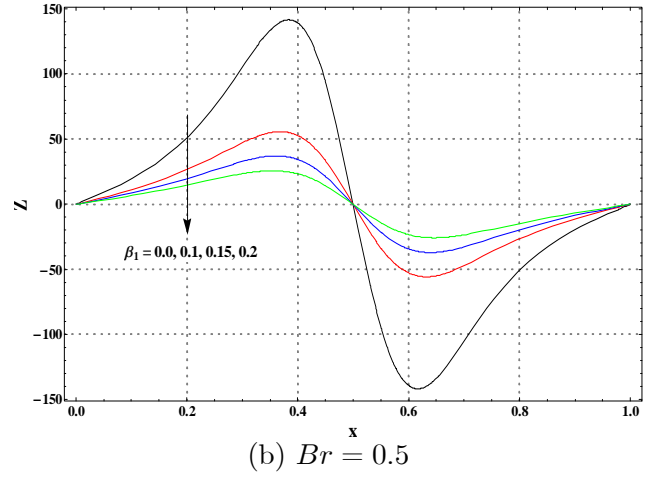
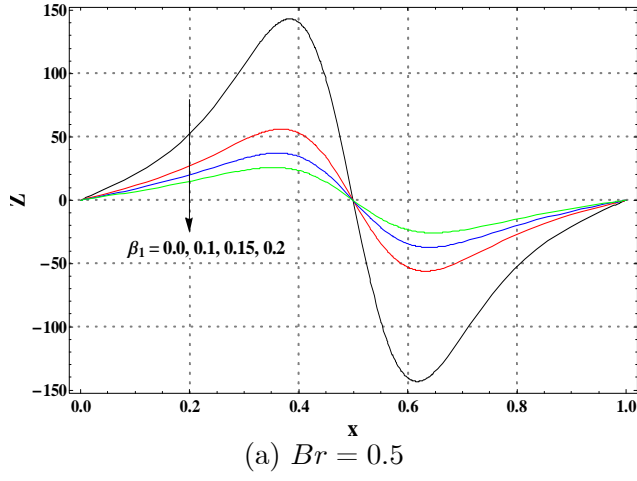


Fig. 11.3 (a-d): Variation of Z when $\Gamma = 0.04$, $\phi = 0.3$, $\eta = 1.1$, and $M = 1$.

Chapter 12

Soret and Dufour effects on peristaltic transport of a third order fluid

Soret and Dufour effects on peristaltic transport of third order fluid in a symmetric channel have been reported in this chapter. Joule heating effect is also taken in to account. The governing nonlinear problem is solved using perturbation approach. Graphical results are reported and discussed for various parameters of interest entering into the problem

12.1 Mathematical formulation

We consider the magnetohydrodynamic (MHD) flow of third order fluid in a channel of width $2d_1$. The \overline{X} -axis is chosen along the walls of channel and \overline{Y} -axis is taken normal to the \overline{X} -axis. A constant magnetic field of strength \mathbf{B}_0 is applied in the \overline{Y} -direction. Induced magnetic field is not accounted. Sinusoidal wave propagating on channel walls with constant wave speed c is represented by

$$H(\overline{X}, \overline{t}) = d_1 + a_1 \cos \left(\frac{2\pi}{\lambda} (\overline{X} - c\overline{t}) \right), \quad (12.1)$$

where a_1 is the wave amplitude, λ is the wavelength and \bar{t} is the time . The continuity, momentum, energy and concentration equations of the problem may be written as follows:

$$\frac{\partial \bar{U}}{\partial \bar{X}} + \frac{\partial \bar{V}}{\partial \bar{Y}} = 0, \quad (12.2)$$

$$\rho \left(\frac{\partial}{\partial \bar{t}} + \bar{U} \frac{\partial}{\partial \bar{X}} + \bar{V} \frac{\partial}{\partial \bar{Y}} \right) \bar{U} = -\frac{\partial \bar{P}}{\partial \bar{X}} + \frac{\partial \bar{S}_{\bar{X}\bar{X}}}{\partial \bar{X}} + \frac{\partial \bar{S}_{\bar{X}\bar{Y}}}{\partial \bar{Y}} - \sigma B_0^2 \bar{U}, \quad (12.3)$$

$$\rho \left(\frac{\partial}{\partial \bar{t}} + \bar{U} \frac{\partial}{\partial \bar{X}} + \bar{V} \frac{\partial}{\partial \bar{Y}} \right) \bar{V} = -\frac{\partial \bar{P}}{\partial \bar{Y}} + \frac{\partial \bar{S}_{\bar{X}\bar{Y}}}{\partial \bar{X}} + \frac{\partial \bar{S}_{\bar{Y}\bar{Y}}}{\partial \bar{Y}}, \quad (12.4)$$

$$C_p \left(\frac{\partial}{\partial \bar{t}} + \bar{U} \frac{\partial}{\partial \bar{X}} + \bar{V} \frac{\partial}{\partial \bar{Y}} \right) T = \frac{K}{\rho} \left(\frac{\partial^2 T}{\partial \bar{X}^2} + \frac{\partial^2 T}{\partial \bar{Y}^2} \right) + v\bar{\zeta} + \frac{\sigma B_0^2 \bar{U}^2}{\rho} + \frac{DK_T}{\rho C_s} \left(\frac{\partial^2 C}{\partial \bar{X}^2} + \frac{\partial^2 C}{\partial \bar{Y}^2} \right), \quad (12.5)$$

$$\left(\frac{\partial}{\partial \bar{t}} + \bar{U} \frac{\partial}{\partial \bar{X}} + \bar{V} \frac{\partial}{\partial \bar{Y}} \right) C = D \left(\frac{\partial^2 C}{\partial \bar{X}^2} + \frac{\partial^2 C}{\partial \bar{Y}^2} \right) + \frac{DK_T}{T_m} \left(\frac{\partial^2 T}{\partial \bar{X}^2} + \frac{\partial^2 T}{\partial \bar{Y}^2} \right). \quad (12.6)$$

In the above equations, \bar{U} and \bar{V} are the velocity components along \bar{X} and \bar{Y} directions respectively in fixed (laboratory frame), ρ is the density, \bar{P} is the pressure, v is the kinematic viscosity, σ is the electrical conductivity, K is the thermal conductivity, B_0 is the applied magnetic field, T is the temperature field, C_p is the specific heat, $v\bar{\zeta}$ is the viscous dissipation, D is mass diffusivity, K_T is the thermal diffusion ratio, C_s is the concentration susceptibility, C is the concentration field and T_m is the mean temperature.

Extra stress tensor $\bar{\mathbf{S}}$ in third order fluid is

$$\bar{\mathbf{S}} = \left(\mu + \beta_3 \text{tr} \bar{\mathbf{A}}_1^2 \right) \mathbf{A}_1 + \alpha_1 \bar{\mathbf{A}}_2 + \alpha_2 \bar{\mathbf{A}}_1^2 + \beta_1 \bar{\mathbf{A}}_3 + \beta_2 \left(\bar{\mathbf{A}}_1 \bar{\mathbf{A}}_2 + \bar{\mathbf{A}}_2 \bar{\mathbf{A}}_1 \right),$$

in which μ , α_i ($i = 1, 2$) and β_i ($i = 1, 2, 3$) are the material constants. The Rivlin-Ericksen tensors can be represented as follows

$$\begin{aligned} \bar{\mathbf{A}}_1 &= \bar{\mathbf{L}} + \bar{\mathbf{L}}^t, \\ \bar{\mathbf{A}}_{n+1} &= \frac{d\bar{\mathbf{A}}_n}{dt} + \bar{\mathbf{A}}_n \bar{\mathbf{L}} + \bar{\mathbf{L}}^t \bar{\mathbf{A}}_n \end{aligned} \quad n = 1, 2,$$

where $\bar{\mathbf{L}} = \text{grad } \bar{\mathbf{V}}$ and t indicates the matrix transpose.

If (\bar{U}, \bar{V}) and (\bar{u}, \bar{v}) are the velocity components in the laboratory (\bar{X}, \bar{Y}) and wave (\bar{x}, \bar{y}) frames respectively then defining

$$\bar{x} = \bar{X} - c\bar{t}, \quad \bar{y} = \bar{Y}, \quad \bar{u} = \bar{U} - c, \quad \bar{v} = \bar{V}, \quad \bar{p}(\bar{x}, \bar{y}) = \bar{P}(\bar{X}, \bar{Y}, \bar{t}), \quad (12.7)$$

and introducing the following dimensionless variables

$$\begin{aligned} x &= \frac{\bar{x}}{\lambda}, \quad y = \frac{\bar{y}}{d_1}, \quad u = \frac{\bar{u}}{c}, \quad v = \frac{\bar{v}}{c\delta}, \quad \delta = \frac{d_1}{\lambda}, \quad h = \frac{H}{d_1}, \quad a = \frac{a_1}{d_1}, \quad p = \frac{a^2 \bar{p}}{c\lambda\mu}, \\ \theta &= \frac{T - T_0}{T_0}, \quad \phi = \frac{C - C_0}{C_0}, \quad M = \left(\frac{\sigma}{\mu}\right)^{1/2} B_0 d_1, \quad \nu = \frac{\mu}{\rho}, \quad Re = \frac{\rho c d_1}{\mu}, \\ t &= \frac{c\bar{t}}{\lambda}, \quad u = \frac{\partial\psi}{\partial y}, \quad v = -\frac{\partial\psi}{\partial x}, \quad Br = Pr E, \quad Du = \frac{DC_0 K_T}{C_s C_p \mu T_0}, \quad Sr = \frac{\rho D K_T T_0}{\mu T_m C_0}, \\ Sc &= \frac{\mu}{\rho D}, \quad E = \frac{c^2}{C_p T_0}, \quad Pr = \frac{\mu C_p}{K}, \quad S = \frac{d_1}{\mu c} \bar{S}(\bar{x}), \quad \gamma_2 = \frac{\beta_2 c^2}{\mu a^2}, \quad \gamma_3 = \frac{\beta_3 c^2}{\mu a^2} \end{aligned} \quad (12.8)$$

we have

$$-\frac{\partial p}{\partial x} + \frac{\partial}{\partial y} S_{xy} - M^2 \left(\frac{\partial\psi}{\partial y} + 1 \right) = 0, \quad 0 = -\frac{\partial p}{\partial y}, \quad (12.9)$$

$$0 = \frac{\partial^2 \theta}{\partial y^2} + Br \zeta + Br M^2 \left(\frac{\partial\psi}{\partial y} + 1 \right)^2 + Pr Du \frac{\partial^2 \phi}{\partial y^2}, \quad (12.10)$$

$$0 = \frac{1}{Sc} \frac{\partial^2 \phi}{\partial y^2} + Sr \frac{\partial^2 \theta}{\partial y^2}, \quad (12.11)$$

$$S_{xy} = \frac{\partial^2 \psi}{\partial y^2} + 2\Gamma \left(\frac{\partial^2 \psi}{\partial y^2} \right)^3, \quad \zeta = \left(\frac{\partial^2 \psi}{\partial y^2} \right)^2 + 2\Gamma \left(\frac{\partial^2 \psi}{\partial y^2} \right)^4, \quad (12.12)$$

where p is the pressure, ψ the stream function, $\Gamma (= \gamma_2 + \gamma_3)$ the Deborah number, M the Hartman number, Re the Reynolds number, Br the Brinkman number, Du the Dufour parameter, Sr the Soret parameter, Sc the Schmidt number, E the Eckert number, Pr the Prandtl number, δ the wave number, T_0 temperature at the wall, C_0 concentration at the wall, θ the dimensionless temperature and ϕ the concentration. The boundary conditions are

$$\begin{aligned} \psi &= 0, \quad \frac{\partial^2 \psi}{\partial y^2} = 0, \quad \frac{\partial \theta}{\partial y} = 0, \quad \frac{\partial \phi}{\partial y} = 0, \quad \text{at } y = 0, \\ \psi &= F, \quad \frac{\partial \psi}{\partial y} = -1, \quad \theta = 0, \quad \phi = 0, \quad \text{at } y = h, \end{aligned} \quad (12.13)$$

$$h(x)=1 + a \cos(2\pi x), \quad F = \int_0^h \frac{\partial \psi}{\partial y} dy, \quad (12.14)$$

where F is the dimensionless volume flow rate and h is the dimensionless wave shape. Pressure rise per wavelength Δp_λ is

$$\Delta p_\lambda = \int_0^1 \frac{dp}{dx} dx. \quad (12.15)$$

We look for solutions in the series form and thus we expand the quantities in terms of small Deborah number as follows:

$$\begin{aligned} \psi &= \psi_0 + \Gamma \psi_1 + \dots \\ \theta &= \theta_0 + \Gamma \theta_1 + \dots \\ \phi &= \phi_0 + \Gamma \phi_1 + \dots \\ F &= F_0 + \Gamma F_1 + \dots \\ p &= p_0 + \Gamma p_1 + \dots \end{aligned}$$

The resulting zeroth order system is given by

$$\frac{\partial^4 \psi_0}{\partial y^4} - M^2 \frac{\partial^2 \psi_0^2}{\partial y^2} = 0, \quad (12.16)$$

$$0 = \frac{\partial^2 \theta_0}{\partial y^2} + Br \left(\frac{\partial^2 \psi_0}{\partial y^2} \right)^2 + Br M^2 \left(\frac{\partial \psi_0}{\partial y} + 1 \right)^2 + Pr Du \frac{\partial^2 \phi_0}{\partial y^2}, \quad (12.17)$$

$$0 = \frac{1}{Sc} \frac{\partial^2 \phi_0}{\partial y^2} + Sr \frac{\partial^2 \theta_0}{\partial y^2}, \quad (12.18)$$

$$\begin{aligned} \psi_0 &= 0, \quad \frac{\partial^2 \psi_0}{\partial y^2} = 0, \quad \frac{\partial \theta_0}{\partial y} = 0, \quad \frac{\partial \phi_0}{\partial y} = 0, \quad \text{at } y = 0, \\ \psi_0 &= F_0, \quad \frac{\partial \psi_0}{\partial y} = -1, \quad \theta_0 = 0, \quad \phi_0 = 0, \quad \text{at } y = h, \end{aligned} \quad (12.19)$$

and first order system becomes

$$\frac{\partial^4 \psi_1}{\partial y^4} + 2 \frac{\partial^2}{\partial y^2} \left(\frac{\partial^2 \psi_0^2}{\partial y^2} \right) - M^2 \frac{\partial^2 \psi_1^2}{\partial y^2} = 0, \quad (12.20)$$

$$0 = \frac{\partial^2 \theta_1}{\partial y^2} + Br \left(2 \frac{\partial^2 \psi_0}{\partial y^2} \frac{\partial^2 \psi_1}{\partial y^2} + \left(\frac{\partial^2 \psi_0}{\partial y^2} \right)^4 \right)^2 + Br M^2 \left(2 \frac{\partial \psi_1}{\partial y} \left(\frac{\partial \psi_0}{\partial y} + 1 \right) \right) + Pr Du \frac{\partial^2 \phi_1}{\partial y^2}, \quad (12.21)$$

$$0 = \frac{1}{Sc} \frac{\partial^2 \phi_1}{\partial y^2} + Sr \frac{\partial^2 \theta_1}{\partial y^2}, \quad (12.22)$$

$$\begin{aligned} \psi_1 &= 0, & \frac{\partial^2 \psi_1}{\partial y^2} &= 0, & \frac{\partial \theta_1}{\partial y} &= 0, & \frac{\partial \phi_1}{\partial y} &= 0, & \text{at } y &= 0, \\ \psi_1 &= F_1, & \frac{\partial \psi_1}{\partial y} &= 0, & \theta_1 &= 0, & \phi_1 &= 0, & \text{at } y &= h, \end{aligned} \quad (12.23)$$

The heat transfer coefficient at the wall can be computed by

$$Z = h_x \theta_y.$$

12.2 Solution expressions

Solving the resulting systems at zeroth and first orders we can write

$$\begin{aligned} \psi &= -\frac{l_1}{(-hM \cosh[hM] + \sinh[hM])^4} \\ &\quad + \frac{e^{-3My} (F + h)^3 M^4 \Gamma (l_2 - l_3 + l_4)}{32 (-hM \cosh[hM] + \sinh[hM])^4} \\ \theta &= \frac{Br M^2 (A_1 + 4FA_2 - A_3 \cosh[2hM] + A_4 - A_5)}{\left(8(-1 + A)(-hM \cosh[hM] + \sinh[hM])^2 \right)} \\ &\quad + \frac{-Br (F + h)^3 M^6 \Gamma}{\left(512(-1 + A)(hM \cosh[hM] - \sinh[hM])^5 \right)} \\ &\quad \times (A_6 - 16hMA_7 \cosh[hM] + A_8 + A_9 - A_{10} + A_{11} - A_{12}), \end{aligned}$$

$$\begin{aligned}
\phi = & \frac{BrM^2ScSr(B_1 + B_2 \cosh[2hM] - B_3)}{\left(8(-1 + A)(-hM \cosh[hM] + \sinh[hM])^2\right)} \\
& + \frac{Br(F + h)^3 M^6 ScSr\Gamma}{\left(512(-1 + A)(hM \cosh[hM] - \sinh[hM])^5\right)} \\
& \times (-B_4 - 16hM(B_5) \cosh[hM] + B_6 - B_7 + B_8 - B_9 - B_{10}),
\end{aligned}$$

with l_i s, A_i s and B_i s are given as follows:

$$\begin{aligned}
l_1 &= (hM \cosh[hM] - \sinh[hM])^3 (-y(FM \cosh[hM] + \sinh[hM]) + (F + h) \\
&\quad \sinh[My]), \\
l_2 &= 24e^{3My}hM^2y - hM(1 - e^{6My} + 12e^{2My}My + 12e^{4My}My) \cosh[hM], \\
l_3 &= 3e^{2My}(-1 + e^{2My})hM \cosh[3hM] + \sinh[hM] - e^{6My} \sinh[hM] \\
&\quad - 12e^{2My}h^2M^2 \sinh[hM], \\
l_4 &= 12e^{4My}h^2M^2 \sinh[hM] + 12e^{2My}My \sinh[hM] + 12e^{4My}My \sinh[hM] \\
&\quad - 16e^{3My}My \\
&\quad \sinh[2hM] - e^{2My} \sinh[3hM] + e^{4My} \sinh[3hM] + 2e^{3My}My \sinh[4hM],
\end{aligned}$$

$$\begin{aligned}
A &= \text{Pr } Du * ScSr, \\
A_1 &= 2h(4 + h + h^3 M^4) - 2(1 + h^2 M^4)y^2 + 2F^2 M^2(1 + M^2)(h - y)(h + y), \\
A_2 &= 2 + hM^2(1 + M^2)(h - y)(h + y), \\
A_3 &= F^2(1 + M^2) + 2F(4 + h + hM^2) - 2y^2 + h(8 + h(3 + M^2(1 + 2h^2 - 2y^2))), \\
A_4 &= (F + h)^2(1 + M^2) \cosh[2My] + 4hM(2F + h(2 + h) - y^2) \sinh[2hM], \\
A_5 &= 16h(F + h)M \cosh[hM](M(h - y) + \sinh[My]) + 16(F + h) \sinh[hM](M(h - y) \\
&\quad + \sinh[My]), \\
A_6 &= -288hM - 96h^3 M^3 + 288My + 96h^2 M^3 y, \\
A_7 &= -16 + 48h^2 M^2 + 12h^3(M^2 + 2M^4) + F(-5 + 3M^2(-3 + 4h^2 - 4y^2) + 24M^4 \\
&\quad (h^2 - y^2)) - h(5 + 24M^4 y^2 + 3M^2(3 + 4y^2)), \\
A_8 &= 256M(1 + 3h^2 M^2)(h - y) \cosh[2hM] - 288hM \cosh[3hM] - 33FhM \cosh[3hM] \\
&\quad - 33h^2 M \cosh[3hM] + 27FhM^3 \cosh[3hM], \\
A_9 &= 27h^2 M^3 \cosh[3hM] - 48Fh^3 M^3 \cosh[3hM] - 48h^4 M^3 \cosh[3hM] - 48Fh^3 M^5 \\
&\quad \cosh[3hM], \\
A_{10} &= 48h^4 M^5 \cosh[3hM] + 48FhM^3 y^2 \cosh[3hM] + 48h^2 M^3 y^2 \cosh[3hM] + 48FhM^5 y^2 \\
&\quad \cosh[3hM] + 48h^2 M^5 y^2 \cosh[3hM] + 32hM \cosh[4hM] + 96h^3 M^3 \cosh[4hM] \\
&\quad - 32My \cosh[4hM] - 96h^2 M^3 y \cosh[4hM] + 32My \cosh[5hM] + 7FhM \cosh[5hM], \\
A_{11} &= 7h^2 M \cosh[5hM] + 3FhM^3 \cosh[5hM] + 3h^2 M^3 \cosh[5hM] + 5FhM \\
&\quad \cosh[M(h - 4y)] + 5h^2 M \cosh[M(h - 4y)] + 9FhM^3 \cosh[M(h - 4y)] + 9h^2 M^3 \\
&\quad \cosh[M(h - 4y)] - 32hM \cosh[M(2h - 3y)] - 20FhM \cosh[M(h - 2y)] - 20h^2 M \\
&\quad \cosh[M(h - 2y)], \\
A_{12} &= 84FhM^3 \cosh[M(h - 2y)] - 84h^2 M^3 \cosh[M(h - 2y)] - 48My \cosh[M(h - 2y)] \\
&\quad (F + h) - 48M^3 y \cosh[M(h - 2y)](F + h) - 12hM \cosh[M(3h - 2y)](F + h + M^2) \\
&\quad - 32hM \cosh[M(2h - y)] + 192M \cosh[M(2h - y)](h^3 M^2 + y + h^2 M^2 y),
\end{aligned}$$

$$\begin{aligned}
B_1 &= -8F - 2h(4+h) - 2Fh^2(F+2h)M^2 - 2h^2(F+h)^2M^4 + 2B_{11}y^2, \\
B_2 &= F^2(1+M^2) + 2F(4+h+hM^2) - 2y^2 + h(8+hB_{12}), \\
B_3 &= (F+h^2)(1+M^2)\cosh[2My] - 4hM(2F+h(2+h)-y^2)\sinh[2hM] + \\
&\quad 16h(F+h)M\cosh[hM](M(h-y)+\sinh[My]) - 16(F+h)\sinh[hM] \\
&\quad (M(h-y)+\sinh[My]), \\
B_4 &= 288hM - 96h^3M^3 + 288My + 96h^2M^3y, \\
B_5 &= -16 + 48h^2M^2 + 12h^3(M^2+2M^4) + FB_{13} - h(5+24M^4y^2+3M^2(3+4y^2)), \\
B_6 &= 256M(1+3h^2M^2)(h-y)\cosh[2hM] - 288hM\cosh[3hM] - 33hM\cosh[3hM] \\
&\quad (F+h) + 27hM\cosh[3hM](FM^2+hM^2), \\
B_7 &= 48hM\cosh[3hM]B_{14} + 32M\cosh[4hM](h-y) + 96h^2M^2\cosh[4hM](hM-My), \\
B_8 &= hM\cosh[5hM](32+7F+7h+3FM^2+3hM^2) + hM\cosh[M(h-4y)] \\
&\quad (5F+5h+9FM^2+9hM^2) - 32hM\cosh[M(2h-3y)], \\
B_9 &= hM\cosh[M(h-2y)]B_{15}, \\
B_{10} &= hM\cosh[M(3h-2y)](12F+12h+12FM^2+12hM^2) - hM\cosh[M(2h-y)] \\
&\quad (32-192h^2M^2-192(y/h)-192hM^2y), \\
B_{11} &= 1+F(F+2h)M^2+(F+h)^2M^4, \quad B_{12}=3+M^2(1+2(h^2-y^2)), \\
B_{13} &= -5+3M^2(-3+4h^2-4y^2)+24M^2(h^2-y^2), \\
B_{14} &= Fh^2M^2+h^3M^2+Fh^2M^4+h^3M^4-FM^2y^2-hM^2y^2-FM^4y^2-hM^4y^2, \\
B_{15} &= 20F+20h+84FM^2+84hM^2+48Fy+48hy+48FM^2y+48hM^2y.
\end{aligned}$$

12.3 Discussion

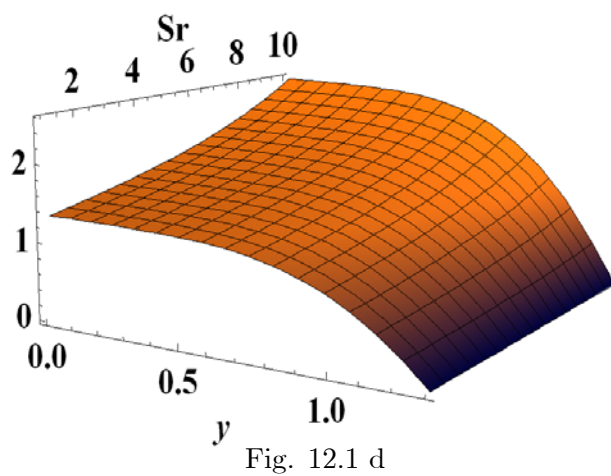
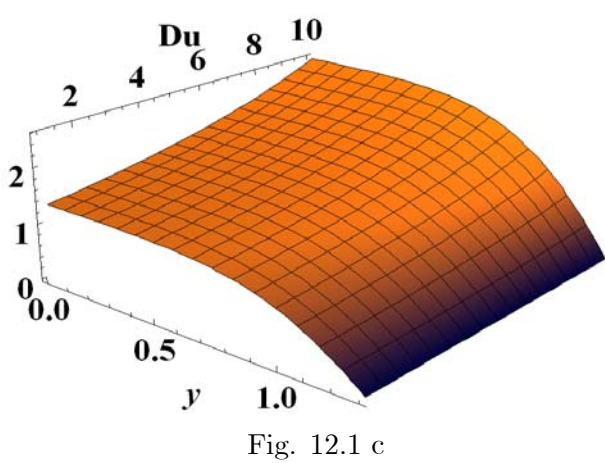
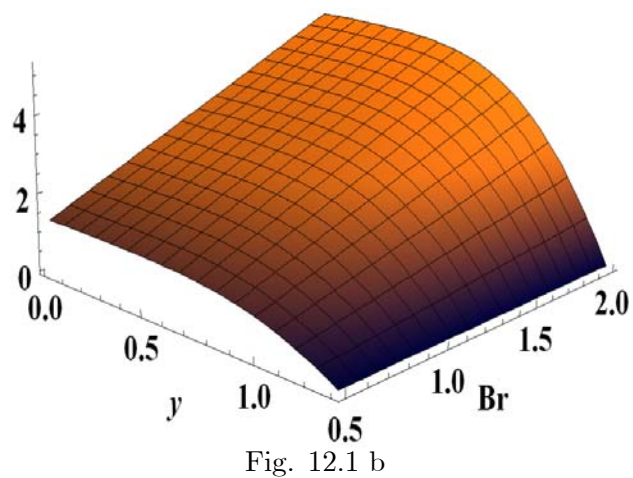
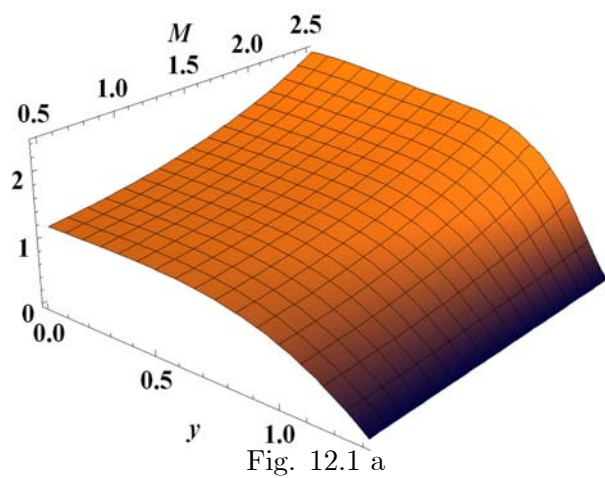
The objective of this section is to analyze the plots for temperature, concentration and heat transfer coefficient. Hence Figs. 12.1-12.3 are given in order to achieve such objective. Here Figs. 12.1(a-g) are drawn for temperature θ , Figs. 12.2(a-g) for concentration profile and Figs. 12.3(a-f) for the heat transfer coefficient Z . Explicitly 3-D graphs are plotted to analyze the behavior fully in the domain of interest.

Figs. 12.1 demonstrate that the dimensionless temperature increases with an increase in

M, Br, Du, Sr, Sc, Pr and Γ . It is also noted from Fig. 12.1a that increase in temperature with respect to M is not much for small M. However the temperature increases abruptly when M increases. Also with the increase in magnitude of applied magnetic field, the temperature increases more due to Joule heating. In Fig. 12.1b it can be seen that there is a linear relationship between Br and θ . Similar observation holds for Γ (see Fig. 12.1g). This depicts that rise in temperature is lesser for Newtonian fluid when compared with non-Newtonian fluid.

In Figs. 12.2 (a-g) it is observed that the dimensionless concentration decreases by decreasing M, Br, Du, Sr, Sc, Pr and Γ . It is found that decrease in temperature is not linear for M, linear and large for Br and Γ and smaller bit small for Du, Sr, Sc, Pr.

Figs. 12.3(a-f) explicitly see the behavior of heat transfer coefficient Z when values of different embedded parameters are altered. It is seen in all these Figs. that Z has an oscillatory behavior. It is physically acceptable in view of peristalsis. The magnitude of oscillations in Z increase most rapidly in case of Γ when compared with the other cases.



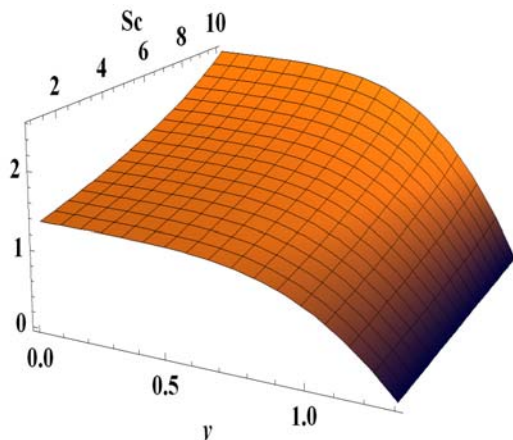


Fig. 12.1 e

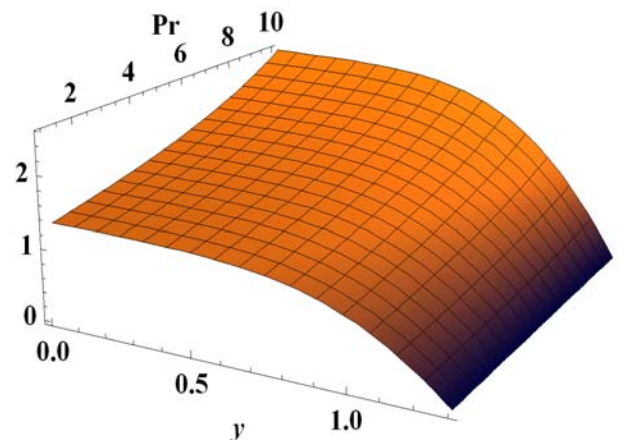


Fig. 12.1 f

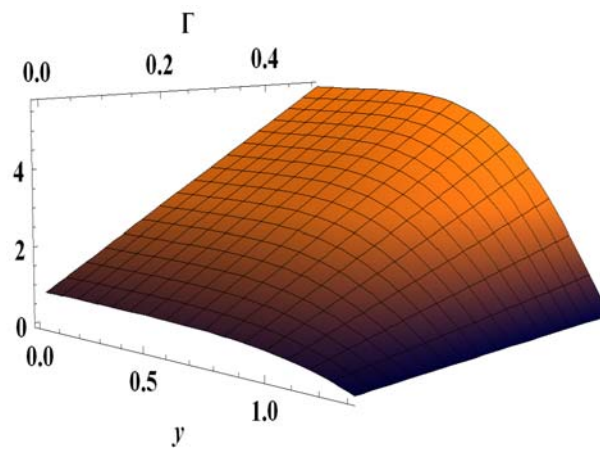


Fig. 12.1 g

Figs 12.1(a-g). Behavior of the temperature with change in values of different parameters.

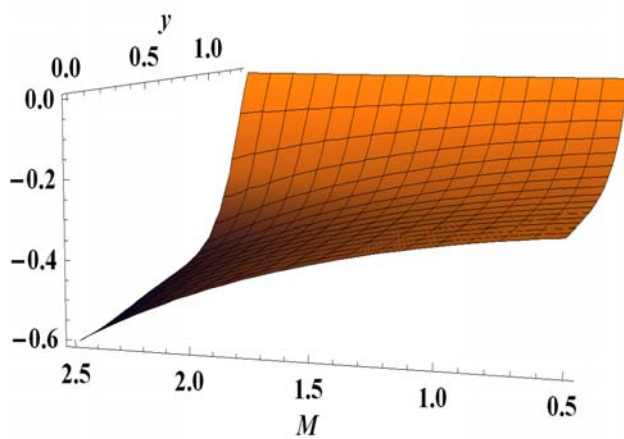


Fig. 12.2 a

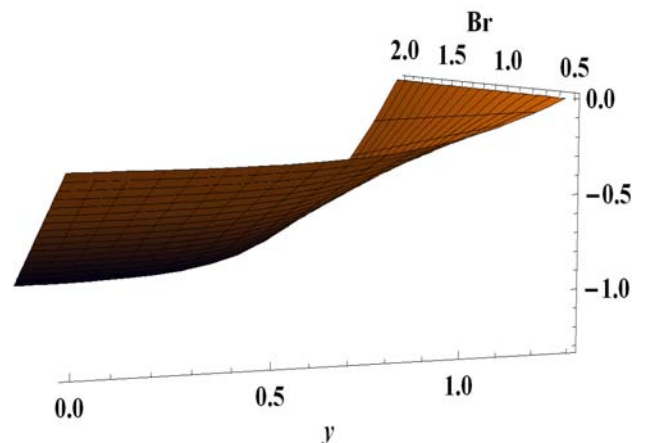


Fig. 12.2 b

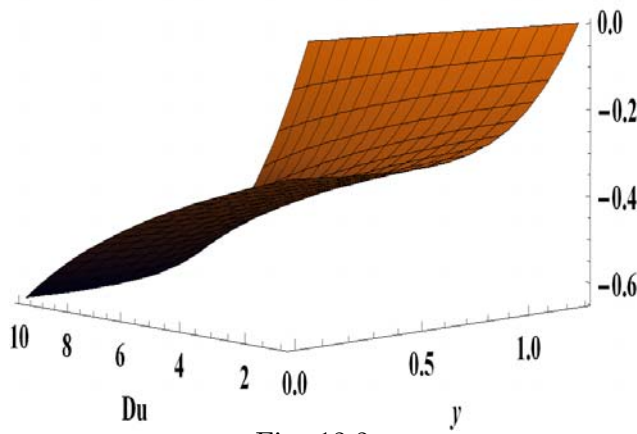


Fig. 12.2 c

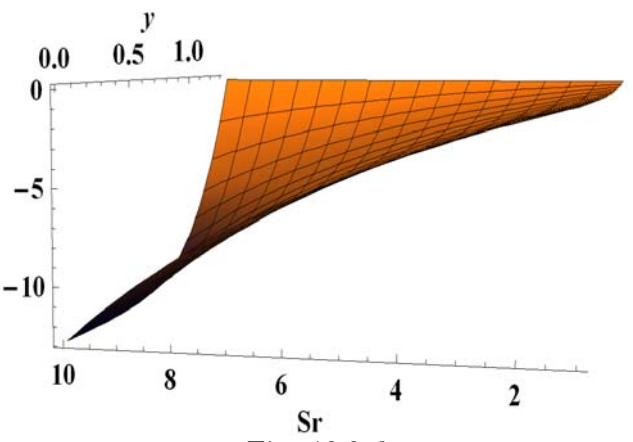


Fig. 12.2 d

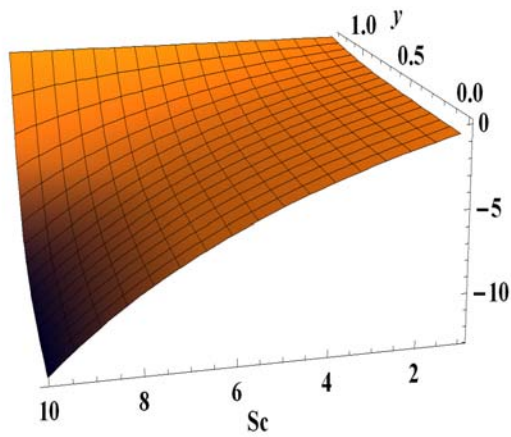


Fig. 12.2 e

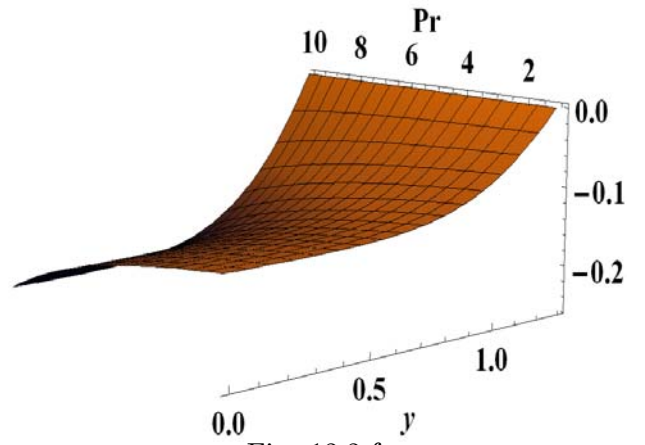


Fig. 12.2 f

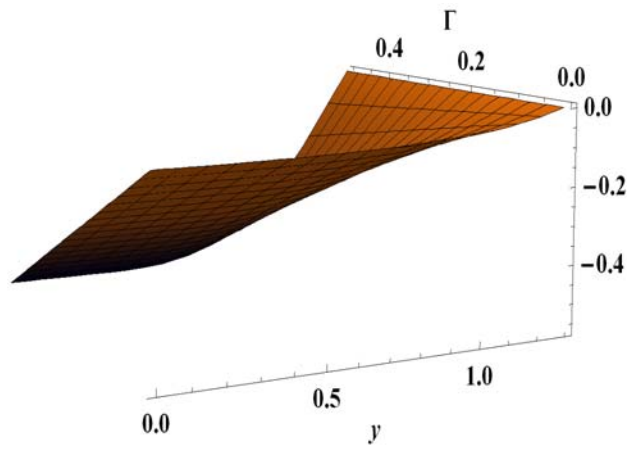


Fig. 12.2 g

Figs. 12.2(a-g). Development of concentration field with increase in values of parameters.

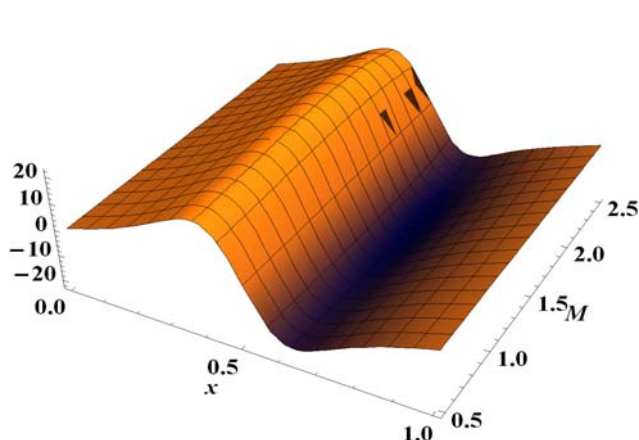


Fig. 12.3 a

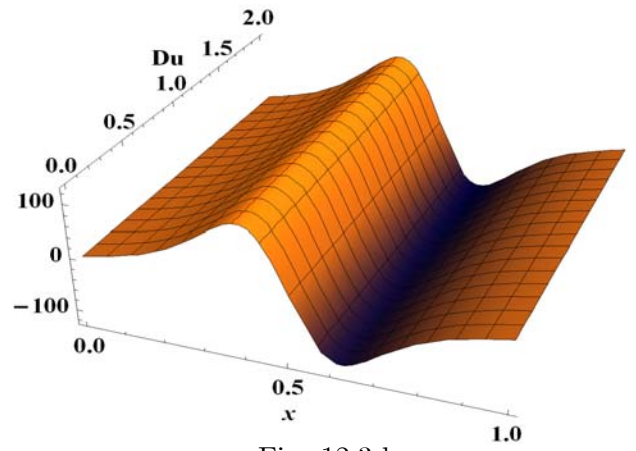


Fig. 12.3 b

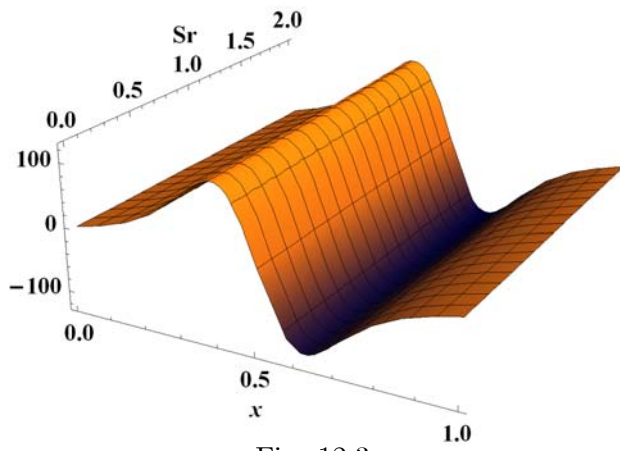


Fig. 12.3 c

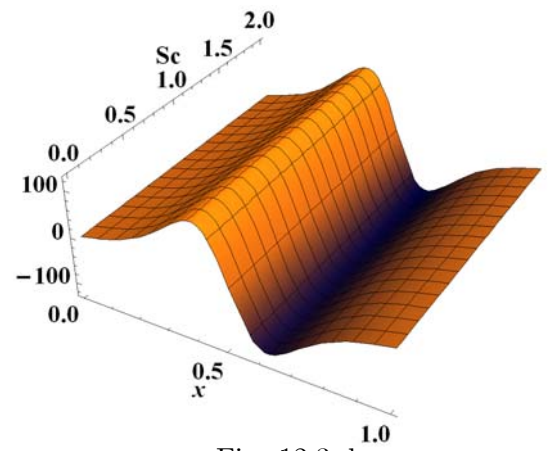


Fig. 12.3 d

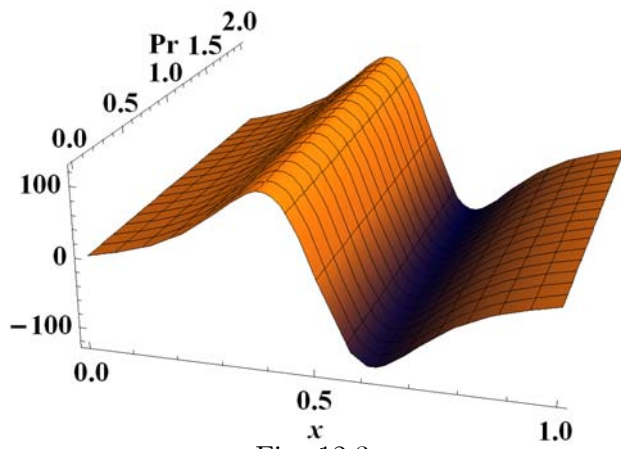


Fig. 12.3 e

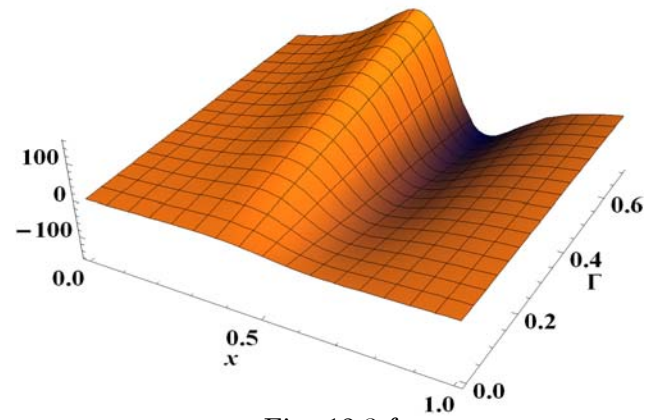


Fig. 12.3 f

Figs. 12.3(a-f). Behavior of heat transfer coefficient Z .

Bibliography

- [1] F. Kiil, The function of the ureter and the renal pelvis. Philadelphia: Saunders, (1957).
- [2] S. Boyarsky, Surgical physiology of the renal pelvis. Monogro. Surg. Sci. 1 (1964) 173.
- [3] T. W. Latham, Fluid motion in a peristaltic pump, MIT Cambridge MA, (1966).
- [4] A. H. Shapiro, Pumping and retrograde diffusion in peristaltic waves, “Proceedings. workshop on ureteral reflux in children”. National Academy of Science (Natural Research Council) (1967) 109.
- [5] P. S. Lykoudis, Peristaltic pumping; a bioengineering model. Published in Proc. Workshop Hydrodynam. Upper Urinary Tract. National Academy of Science, Wash. D. C. (1971).
- [6] S. L. Weinberg, M. Y. Jaffrin and A. H. Shapiro, A hydrodynamical model of ureteral function. Published in Proc. Workshop Hydrodynam. National Academy of Science, Wash. D. C. (1971).
- [7] C. Barton and S. Raynor, Peristaltic flow in tubes. Bull. Math. Biophys. 30 (1968) 663.
- [8] J. R. Maginniss, An analytical investigation of flow and hemolysis in peristaltic-type blood pumps. M. S. Thesis, M. I. T. Cambridge, Mass (1970).
- [9] A. H. Shapiro, M. Y. Jaffrin and S. L. Weinberg, Peristaltic pumping with long wavelength at low Reynolds number, J. Fluid Mech. 37 (1969) 799.
- [10] M. Y. Jaffrin, Inertia and streamline curvature effects in peristaltic pumping, Int. J. Eng. Sci. 11 (1973) 681.

- [11] F. Yin and Y. C. Fung, Peristaltic waves in circular cylindrical tubes, *J. Appl. Mech.* 36 (1969) 579.
- [12] Y. C. Fung and C. S. Yih, Peristaltic transport, *J. Appl. Mech.* 35 (1968) 699.
- [13] M. Y. Jaffrin and A. H. Shapiro, Peristaltic pumping, *Annual Review of Fluid Mech.* 3 (1971) 13.
- [14] T. K. Mitra and S. N. Prasad, Interaction of peristaltic motion with Poiseuille flow, *Bull. Math. Biol.* 36 (1974) 127.
- [15] D. E. Wilson and D. Perel, Interaction of Pulsatile and peristaltic induced flows. *Proc. ASME Bioengineering Symposium*, New York (1979).
- [16] T. D. Brown and T. K. Hung, Computational and experimental investigations of two dimensional nonlinear peristaltic flows, *J. Fluid Mech.* 83 (1977) 249.
- [17] L. M. Srivastava V. P. Srivastava, Interaction of peristaltic flow with pulsatile flow in a circular cylindrical tube, *J. Biomech.* 18 (1985) 247.
- [18] L. M. Srivastava and V. P. Srivastava, Peristaltic transport of blood; Casson model-II. *J. Biomech.* 17 (1984) 821.
- [19] S. Takabatake and K. Ayukawa, Numerical study of two dimensional peristaltic waves. *J. Fluid Mech.* 122 (1982) 439.
- [20] S. Takabatake, K. Ayukawa and A. Mori, Peristaltic pumping in circular cylindrical tubes: a numerical study of fluid transport and its efficiency. *J. Fluid Mech.* 193 (1988) 269.
- [21] M. Mishra and A. R. Rao, Peristaltic transport in a channel with a porous peripheral layer: model of a flow in gastrointestinal tract. *J. Biomechanics* 38 (2005) 779.
- [22] N. A. S. Afifi and N. S. Gad, Interaction of peristaltic flow with pulsatile magneto-fluid through a porous medium, *Acta Mech.* 149 (2001) 229.
- [23] E. F. Elshehawey, E. M. E. Elbarbary and N. S. Elgazery, Effect of inclined magnetic field on magneto fluid flow through porous medium between two inclined wavy porous plates (numerical study), *Appl. Math. Comput.* 135 (2003) 85.

- [24] Kh. S. Mekheimer, Peristaltic flow of blood under effect of a magnetic field in a non-uniform channel, *Appl. Math Comput.* 153 (2004) 763.
- [25] Kh. S. Mekheimer, Nonlinear peristaltic transport of magnetohydrodynamic flow in an inclined planar channel, *Arab. J. Sci. Engin.* 28 (2003) 183.
- [26] A. M. Siddiqui, T. Hayat and Masood Khan, Magnetic fluid model induced by peristaltic waves, *J. Phys. Soc. Jpn.* 73 (2004) 2142.
- [27] T. Hayat and N. Ali, Peristaltically induced motion of a MHD third grade fluid in a deformable tube, *Physica A* 367 (2006) 79.
- [28] Abd El Hakeem Abd El Naby, A. E. M. El Misery and M. F. Abd El Kareem, Effects of magnetic field on trapping through peristaltic motion for generalized Newtonian fluid in channel, *Physica A* 367 (2006) 79.
- [29] T. Hayat, M. Khan, A. M. Siddiqui and S. Asghar, Nonlinear peristaltic flow of a non-Newtonian fluid under effect of a magnetic field in a planar channel, *Comm. Nonlinear Sci. Numer. Simulat.* 12 (2007) 910.
- [30] T. Hayat and N. Ali, A mathematical description of peristaltic hydromagnetic flow in a tube, *Appl. Math. Comput.* 188 (2007) 1491.
- [31] Y. Wang, T. Hayat, N. Ali and M. Oberlack, Magnetohydrodynamic peristaltic motion of a Sisko fluid in a symmetric or asymmetric channel, *Physica A: Stat. Mech. Applications*, 387 (2008) 347.
- [32] T. Hayat, Z. Asghar, S. Asghar and S. Mesloub, Influence of inclined magnetic field on peristaltic transport of fourth grade fluid in an inclined asymmetric channel, *J. Taiwan Institute of Chemical Engineers*, 41 (2010) 553.
- [33] X. Mandviwalla and R. Archer, The influence of slip boundary conditions on the peristaltic pumping in a rectangular channel, *J. Fluids Eng.* 130 (2008) 124501.
- [34] T. Hayat, Q. Hussain and N. Ali, Influence of partial slip on the peristaltic flow in a porous medium, *Phys. Lett. A* 387 (2008) 3399.

- [35] T. Hayat, S. Hina and N. Ali, Simultaneous effects of slip and heat transfer on the peristaltic flow, *Comm. Nonlinear Sci. Numer. Simulat.* 15 (2010) 1526.
- [36] A. Yildirim and S. A. Sezer, Effects of partial slip on the peristaltic flow of a MHD Newtonian fluid in an asymmetric channel, *Math. Comp. Model.* 52 (2010) 618.
- [37] A. V. R. Kumari and G. Radhakrishnamacharya, Effect of slip on heat transfer to peristaltic transport in the presence of magnetic field with wall effects, *ARPN J. Engin. and Appl. Sci.* 6 (2011) 1819.
- [38] N. Ali, Q. Hussain, T. Hayat and S. Asghar, Slip effects on the peristaltic transport of MHD fluid with variable viscosity, *Phys. Lett. A* 372 (2008) 1477.
- [39] Abd El Hakeem Abd El Naby, A.E.M. El Misery and I.I. El Shamy, Effects of an endoscope and fluid with variable viscosity on peristaltic motion, *Appl. Math. Comput.* 158 (2004) 497.
- [40] E.F. Elshehawey and Z.M. Gharsseldien, Peristaltic transport of three-layered flow with variable viscosity, *Appl. Math. Comput.* 153 (2004) 417.
- [41] T. Hayat and N. Ali, Effect of variable viscosity on the peristaltic transport of a Newtonian fluid in an asymmetric channel, *Appl. Math. Model.* 32 (2008) 761.
- [42] A. Ebaid, A new numerical solution for the MHD peristaltic flow of a bio-fluid with variable viscosity in a circular cylindrical tube via Adomian decomposition method, *Physics Lett. A* 372 (2008) 5321.
- [43] S. Nadeem and N. S. Akbar, Effects of heat transfer on the peristaltic transport of MHD Newtonian fluid with variable viscosity: application of Adomian decomposition method, *Comm. Nonlinear Sci. Numer. Simulat.* 14 (2009) 3844.
- [44] S. Nadeem, T. Hayat, N. S. Akbar and M. Y. Malik, On the influence of heat transfer in peristalsis with variable viscosity, *Int. J. Heat Mass Transfer* 52 (2009) 4722.
- [45] S. Nadeem and N. S. Akbar, Effects of temperature dependent viscosity on peristaltic flow of a Jeffrey-six constant fluid in a non-uniform vertical tube, *Comm. Nonlinear Sci. Numer. Simulat.* 15 (2010) 3950.

- [46] S. Nadeem and N. S. Akbar, Influence of temperature dependent viscosity on peristaltic transport of a Newtonian fluid: Application of an endoscope, *Applied Mathematics and Computation* 216 (2010) 3606.
- [47] G. Radhakrishnamacharya and V. R. Murty, Heat transfer to peristaltic transport in a non-uniform channel, *Defence Sci. J.* 43 (1993) 275.
- [48] K. Vajravelu, G. Radhakrishnamacharya and V. Radhakrishnamurthy, Peristaltic flow and heat transfer in a vertical porous annulus, with long wavelength approximation, *Int. J. Nonlinear Mech.* 42 (2007) 754.
- [49] Kh. S. Mekheimer and Y. Abd Elmaboud, The influence of heat transfer and magnetic field on peristaltic transport of a Newtonian fluid in a vertical annulus: Application of an endoscope, *Phys. Lett. A* 372 (2008) 1657.
- [50] S. Srinivas and M. Kothandapani, Peristaltic transport in an asymmetric channel with heat transfer-A note, *Int. Comm. Heat Mass transfer* 34 (2008) 514.
- [51] T. Hayat, M. U. Qureshi and Q. Hussain, Effect of heat transfer on the peristaltic flow of an electrically conducting fluid in a porous space, *Appl. Math. Model.* 33 (2009) 1862.
- [52] S. Srinivas and M. Konthandapani, The influence of heat and mass transfer on MHD peristaltic flow through a porous space with compliant walls, *Appl. Math. Comput.* 213 (2009) 197.
- [53] T. Hayat and S. Hina, The influence of wall properties on the MHD peristaltic flow of a Maxwell fluid with heat and mass transfer, *Nonlinear Analysis: Real World Applications*, 11 (2010) 3155.
- [54] Kh. S. Mekheimer, S. Z. A. Husseny and Y. Abd Elmaboud, Effects of heat transfer and space porosity on peristaltic flow in a vertical channel, *Numer. Methods Partial Diff. Eqs.* 26 (2010) 747.
- [55] S. Nadeem and N. S. Akbar, Influence of radially varying MHD on the peristaltic flow in an annulus with heat and mass transfer, *J. Taiwan Institute of Chemical Engineers* 41 (2010) 286.

- [56] N. Ali, M. Sajid, T. Javed and Z. Abbas, Heat transfer analysis of peristaltic flow in a curved channel, *International Journal of Heat and Mass Transfer* 53 (2010) 3319.
- [57] T. Hayat and S. Noreen, Peristaltic transport of fourth grade fluid with heat transfer and induced magnetic field, *C. R. Mecanique* 338 (2010) 518.
- [58] S. Srinivas and R. Muthuraj, Effects of thermal radiation and space porosity on MHD mixed convection flow in a vertical channel using homotopy analysis method, *Commun Nonlinear Sci Numer Simulat.* 15 (2010) 2098.
- [59] K. Vajravelu, S. Sreenadh and P. Lakshminarayana, The influence of heat transfer on peristaltic transport of a Jeffrey fluid in a vertical porous stratum, *Comm. Nonlinear Sci. Numer. Simulat.* 16 (2011) 3107.
- [60] T. Hayat, M. Javed and A. A. Hendi, Peristaltic transport of viscous fluid in a curved channel with compliant walls, *Int. J. Heat and Mass Transfer* 54 (2011) 1615.
- [61] S. Srinivas, R. Gayathri and M. Kothandapani, Mixed convective heat and mass transfer in an asymmetric channel with peristalsis, *Comm. Nonlinear Sci. Numer. Simulat.* 16 (2011) 1845.
- [62] S. Nadeem and N. S. Akbar, Influence of heat and mass transfer on the peristaltic flow of Johnson Segalman fluid in a vertical asymmetric channel with induced MHD, *J. Taiwan Institute of Chemical Engineers* 42 (2011) 58.
- [63] D. Tripathi, A mathematical model for swallowing of food bolus through the oesophagus under the influence of heat transfer, *Int. J. Thermal Sciences* (inpress).
- [64] N. S. Akbar, S. Nadeem, T. Hayat and A. A. Hendi, Effects of heat and mass transfer on the peristaltic flow of hyperbolic tangent fluid in an annulus, *Int. J. Heat and Mass Transfer* 54 (2011) 4360.
- [65] S. Nadeem and N S. Akbar, Influence of heat and mass transfer on the peristaltic flow of a Johnson Segalman fluid in a vertical asymmetric channel with induced MHD, *J. Taiwan Institute of Chemical Engineers*, 42 (2011) 58.

- [66] T. Hayat, N. Saleem, S. Asghar, M. S. Alhothuali and A. Alhomaïdan, Influence of induced magnetic field and heat transfer on peristaltic transport of a Carreau fluid, *Comm. Nonlinear Sci. Numer. Simulat.* 16 (2011) 3559.
- [67] T. Hayat, A. Afsar, M. Khan and S. Asghar, Peristaltic transport of a third order fluid under the effect of magnetic field, *Comp. Math. Applications.* 53 (2007) 1074.
- [68] T. Hayat, M. U. Qureshi and N. Ali, The influence of slip on the peristaltic motion of a third order fluid in an asymmetric channel, *Phys. Lett. A* 372 (2008) 2653.
- [69] S. Nadeem, N. S. Akbar, N. Bibi and S. Ashiq, Influence of heat and mass transfer on peristaltic flow of a third order fluid in a diverging tube, *Comm. Nonlinear Sci. Numer. Simulat.* 15 (2010) 2916.
- [70] N. S. Akbar, T. Hayat, S. Nadeem and A. A. Hendi, Effects of slip and heat transfer on the peristaltic flow of a third order fluid in an inclined asymmetric channel, *Int. J. Heat and Mass Transfer* 54 (2011) 1654.



Turnitin Originality Report

PhD Thesis by Fahad Abbasi

From Peristaltic (8899)

Processed on 24-Dec-2013 00:32 PKT

ID: 385877909

Word Count: 30340

Similarity Index

15%

Similarity by Source

Internet Sources:	11%
Publications:	11%
Student Papers:	0%

sources:

- 1 1% match (Internet from 19-Dec-2012)
http://www.mcajournal.org/specialissue15_4/9.pdf

- 2 1% match (Internet from 27-Jan-2013)
<http://thermalscience.vinca.rs/pdfs/papers-2012/ThSci-9SWIB45368.pdf>

- 3 1% match (publications)
[Asghar, S.; Hussain, Q. and Hayat, T.. "PERISTALTIC FLOW OF REACTIVE VISCOUS FLUID WITH TEMPERATURE DEPENDENT VISCOSITY". Mathematical & Computational Applications, 2013.](#)

- 4 < 1% match (Internet from 05-Jan-2013)
<http://www.qau.edu.pk/profile.php?id=814010>

- 5 < 1% match (Internet from 08-Jan-2013)
http://www.ijens.org/Vol_12_I_05/125605-0707-IJBAS-IJENS.pdf

- 6 < 1% match (publications)
[Saravana, R.; Reddy, R. Hemadri; Sreenadh, S.; Vekataramana, S. and Kavitha, A.. "INFLUENCE OF SLIP, HEAT AND MASS TRANSFER ON THE PERISTALTIC TRANSPORT OF A THIRD ORDER FLUID IN AN INCLINED ASYMMETRIC CHANNEL". International Journal of Applied Mathematics & Mechanics, 2013.](#)

- 7 < 1% match (publications)
[Akbar, N.S.. "Effects of slip and heat transfer on the peristaltic flow of a third order fluid in an inclined asymmetric channel". International Journal of Heat and Mass Transfer, 201103](#)

- 8 < 1% match (publications)
[Md Noar, Nor\(Greenhow, M and Lawrie, JB\). "Wave impacts on rectangular structures". Brunel University, School of Information Systems, Computing and Mathematics, 2012.](#)

- 9 < 1% match (Internet from 27-Dec-2012)
http://www.arpnjournals.com/jeas/research_papers/rp_2011/jeas_0711_530.pdf

- 10 < 1% match (Internet from 04-Dec-2012)
<http://omicsgroup.org/journals/JACM/JACM-1-102.php?aid=6249>

- 11 < 1% match (publications)
[Engineering Computations, Volume 29, Issue 6 \(2012-08-18\)](#)

- 12 < 1% match (publications)
[Hayat, T.. "Peristaltic flow under the effects of an induced magnetic field and heat and mass transfer". International Journal of Heat and Mass Transfer, 20120115](#)

- 13 < 1% match (Internet from 15-Jun-2011)
<http://www.qau.edu.pk/betaqau/profile.php?id=814004>

- 14 < 1% match (publications)
[Srinivas, S.. "The influence of heat and mass transfer on MHD peristaltic flow through a porous space with compliant walls". Applied Mathematics and Computation, 20090701](#)

- 15 < 1% match (Internet from 01-Nov-2012)
<http://scihub.org/AJSIR/PDF/2010/3/AJSIR-1-3-656-666.pdf>

- 16 < 1% match (Internet from 03-Jan-2013)
<http://scik.org/index.php/imcs/article/download/209/109>

- 17 < 1% match (publications)
[Hayat, T.. "Influence of inclined magnetic field on peristaltic transport of fourth grade fluid in](#)

[an inclined asymmetric channel". Journal of the Taiwan Institute of Chemical Engineers. 201009](#)

-
- 18** < 1% match (Internet from 31-Oct-2010)
<http://www.gibonet.ch/pub/travail.pdf>
-
- 19** < 1% match (Internet from 26-Mar-2010)
http://www.epicoalition.org/valance_reports/chart_books/20060825.pdf
-
- 20** < 1% match (Internet from 29-Feb-2012)
http://www.veltechuniv.edu.in/IJMSC/current_issue/IJMSC-June2011-Paper-07.pdf
-
- 21** < 1% match (Internet from 19-Dec-2012)
http://www.mcajournal.org/specialissue15_4/10.pdf
-
- 22** < 1% match (Internet from 24-Aug-2013)
<http://njta.org/transportation/refdata/accident/00/Passaic00.txt>
-
- 23** < 1% match (publications)
[Range, Gabriel Maximilian. "Phasenverhalten und strukturelle Eigenschaften binärer dipolarer Fluide". Technische Universität Berlin. 2005.](#)
-
- 24** < 1% match (Internet from 22-Apr-2010)
<http://www.m-hikari.com/astp/astp2008/astp5-8-2008/rachidASTP5-8-2008.pdf>
-
- 25** < 1% match (Internet from 07-Feb-2012)
http://ijitce.co.uk/download/nov/IJTCE_nov2.pdf
-
- 26** < 1% match (publications)
[International Journal of Numerical Methods for Heat & Fluid Flow. Volume 22. Issue 6 \(2012-09-15\)](#)
-
- 27** < 1% match (publications)
[International Journal of Numerical Methods for Heat & Fluid Flow. Volume 22. Issue 4 \(2012-05-12\)](#)
-
- 28** < 1% match (Internet from 13-Apr-2004)
http://archive.noao.edu/ndwfs/dr1/NDWFSJ1426p3456_Bw_01_rjm.pl
-
- 29** < 1% match (Internet from 27-Jan-2013)
<http://thermalscience.vinca.rs/pdfs/papers-2012/TSCI111022143R.pdf>
-
- 30** < 1% match (Internet from 30-Jul-2012)
<http://www.chemweb.com/journals/journals?type=issue&jid=00179310&iid=00540007>
-
- 31** < 1% match (publications)
[Hayat, T.. "Peristaltic transport of fourth grade fluid with heat transfer and induced magnetic field". Comptes rendus - Mecanique. 201009](#)
-
- 32** < 1% match (publications)
[Shateyi, Stanford Motsa, Sandile Sydney. "The effects of thermal radiation, hall currents, Soret, and Dufour on MHD flow by mixed convection o". Mathematical Problems in Engineering. Annual 2010 Issue](#)
-
- 33** < 1% match (Internet from 26-Dec-2007)
<http://shatoon.ru/cartography/hgt/N48E136.hgt>
-
- 34** < 1% match (Internet from 24-Jul-2008)
<http://webserver.lemoyne.edu/courseinformation/MTH%20112/MILLERMJ/GSS2000/gss2000.por>
-
- 35** < 1% match (publications)
[Sobh, Ayman Mahmoud. "Slip flow in peristaltic transport of a Carreau fluid in an asymmetric channel.". Canadian Journal of Physics. August 2009 Issue](#)
-
- 36** < 1% match (Internet from 27-Aug-2009)
<http://www.rba.gov.au/rdp/RDP2000-05.pdf>
-
- 37** < 1% match (publications)

Kh.S. Mekheimer. "Effects of heat transfer and space porosity on peristaltic flow in a vertical asymmetric channel". Numerical Methods for Partial Differential Equations. 2009

-
- 38** < 1% match (Internet from 19-Nov-2013)
<http://dictionary.reference.com/browse/momentum>
-
- 39** < 1% match (Internet from 30-Sep-2009)
<http://www.maths.leeds.ac.uk/~charles/chainplot.pdf>
-
- 40** < 1% match (Internet from 08-Jun-2007)
<http://fraserinstitute.org/admin/books/chapterfiles/70ONEEL06DTTO.pdf>
-
- 41** < 1% match (Internet from 16-Jun-2003)
http://deposit.ddb.de/cgi-bin/dokserv?idn=964626330&dok_var=d1&dok_ext=pdf&filename=964626330.pdf
-
- 42** < 1% match (Internet from 15-Aug-2013)
http://www.abenteuerland.at/smrender/download/charts/croatia/tetra_style/KAP/Rijecki%20Zaljev_5.kap
-
- 43** < 1% match (publications)
[?????? ? ???? ??????. "?????? ?????? ? ?????? ? ?????????". Arab Group for Training & Publishing. 0000.](#)
-
- 44** < 1% match (Internet from 20-Sep-2012)
<http://www.deepdyve.com/lp/hindawi-publishing-corporation/peristaltic-flow-of-a-magneto-micropolar-fluid-effect-of-induced-VDakOLO0wh>
-
- 45** < 1% match (Internet from 18-May-2012)
<http://www.sms.edu.pk/journals/jprm/jprmvol6/05.pdf>
-
- 46** < 1% match (Internet from 19-Jan-2011)
<http://www.ecse.rpi.edu/shur/sdm2/Notes/Notespdf/18HFET.pdf>
-
- 47** < 1% match (publications)
[Chen, Cha'o-Kuang Lai, Dong-Yu. "Weakly nonlinear stability analysis of a thin magnetic fluid during spin coating.\(Research Article\)". Mathematical Problems in Engineering. Annual 2010 Issue](#)
-
- 48** < 1% match (Internet from 09-Jul-2003)
<http://cloc.isr.umich.edu/data/CLOC-BaselineOnly.por>
-
- 49** < 1% match (Internet from 29-May-2008)
http://www.epicoalition.org/valance_reports/chart_books/20061201.pdf
-
- 50** < 1% match (Internet from 18-Jun-2011)
http://www.oeb.harvard.edu/faculty/moorcroft/publications/publications/barnett_Moorcroft_2008.pdf
-
- 51** < 1% match (Internet from 22-Jun-2012)
http://www.msss.com/moc_gallery/m07_m12/img/M08/M0804963.img
-
- 52** < 1% match (Internet from 04-Dec-2012)
<http://ijamc.darbose.in/ijamc/index.php/ijamc/article/download/84/pdf2.4.8>
-
- 53** < 1% match (Internet from 03-Aug-2012)
<http://www.ssd.org/downloads/2012/Results/Saturday.pdf>
-
- 54** < 1% match (Internet from 02-Jul-2003)
http://cmd.princeton.edu/CMD_Working_Papers/cils1n2.por
-
- 55** < 1% match (Internet from 09-Jun-2012)
<http://www.internonline-science.org/upload/papers/20110915065005565.pdf>
-
- 56** < 1% match (Internet from 13-Jun-2013)
http://ijater.com/Files/741ad39f-5314-4531-badd-6f14193ef7e0_WATER_10_20.pdf
-
- 57** < 1% match (Internet from 16-Apr-2013)

<http://www.bis.org/statistics/hcsv/hanx9b.csv>

-
- 58 < 1% match (Internet from 16-Dec-2007)
<http://www.nervenet.org/papers/images/bxn/BXNRelease1InferredFull.xls>
-
- 59 < 1% match (Internet from 19-May-2012)
http://www.130th.net/pub/mirror/opera/winmobile/850b2/opera_wmppc2003_85b2.cab
-
- 60 < 1% match (Internet from 25-Jan-2007)
<http://www.pasza.ca/pdfs/PASZA%20Feb%202006.pdf>
-
- 61 < 1% match (Internet from 12-Jun-2013)
<http://www.notredame-high.org.uk/documents/exams/Exam%20Performance%20Data%202012.pdf>
-
- 62 < 1% match (Internet from 22-Apr-2009)
http://ftp.cdc.gov/pub/Health_Statistics/NCHS/Datasets/NHCHS/1998/TAB_DELIMITED/DP98PUB.TXT
-
- 63 < 1% match (Internet from 01-Nov-2010)
<http://www.m-hikari.com/ams/ams-2010/ams-29-32-2010/madiAMS29-32-2010.pdf>
-
- 64 < 1% match (Internet from 19-Apr-2012)
http://www.veltechuniv.edu.in/IJMSC/current_issue/IJMSC01-02-Paper18.pdf
-
- 65 < 1% match (Internet from 08-Jul-2013)
http://www.msss.com/moc_gallery/m07_m12/img/M09/M0901797.img
-
- 66 < 1% match (Internet from 29-Nov-2010)
http://ajse.kfupm.edu.sa/articles/301A_06P.pdf
-
- 67 < 1% match (Internet from 08-Jan-2011)
http://nuv.apnetwork.it/attach/file/Relazioni/2005/03_La_didattica_05.pdf
-
- 68 < 1% match (Internet from 26-Dec-2010)
<http://cg.tuwien.ac.at/courses/Animation/kinematics.pdf>
-
- 69 < 1% match (Internet from 04-Dec-2011)
http://www.fire01.ru/assets/files/BCH/BCH_49-86.doc
-
- 70 < 1% match (Internet from 06-Jun-2013)
<http://ijamm.bc.cityu.edu.hk/ijamm/outbox/y2011v7n21p1c66305179.pdf>
-
- 71 < 1% match (Internet from 10-Aug-2012)
<http://www.tibtcd.org.tr/2009-1/67-78.pdf>
-
- 72 < 1% match (Internet from 14-Sep-2013)
http://scholarworks.uno.edu/cgi/viewcontent.cgi?article=1046&context=honors_theses
-
- 73 < 1% match (Internet from 15-Aug-2013)
http://www.cefage.uevora.pt/en/content/download/1723/22481/version/1/file/2009_08.pdf
-
- 74 < 1% match (Internet from 23-Dec-2012)
http://audio14.archive.org/stream/SchaumsTheoryProblemsOfAbstractAlgebra/Fang-AbstractAlgebra_djvu.txt
-
- 75 < 1% match (publications)
[Landmann, Markus\(and Thomä, Reiner\). "Limitations of experimental channel characterisation". Digitale Bibliothek Thüringen. 2008.](#)
-
- 76 < 1% match (Internet from 14-Nov-2010)
<http://servicealberta.ca/pdf/vs/2005deaths.pdf>
-
- 77 < 1% match (Internet from 08-Apr-2012)
<http://146.6.139.68/users/pmueller/pap/RMR07.pdf>
-

< 1% match (Internet from 01-May-2003)

78	http://www.hendersoncountync.org/elections/nov5_by_precinct.html
79	< 1% match (publications) Abd-Alla, A. M.; Yahya, G. A. and Farhan, A. M., "Effect of Magnetic Field and Porosity on Peristaltic Flow of Micropolar Fluid", International Review of Physics, 2013.
80	< 1% match (publications) Ali, N. Wang, Y. Hayat, T. Oberlack, M., "Numerical solution of peristaltic transport of an Oldroyd 8-constant fluid in a circular cylindrical", Canadian Journal of Physics, Sept 2009 Issue
81	< 1% match (publications) Oaten, Susan Rosemary(Blitz, J), "Assessment of defects in ferromagnetic metals with eddy currents", Brunel University Institute for the Environment PhD Theses, 2011.
82	< 1% match (publications) Engineering Computations, Volume 24, Issue 4 (2007-05-27)
83	< 1% match (Internet from 15-Jun-2011) http://www.qau.edu.pk/betaqau/profile.php?id=814010
84	< 1% match (Internet from 29-Sep-2010) http://alumni.media.mit.edu/~tpminka/courses/36-350/handout/handout19.pdf
85	< 1% match (Internet from 09-May-2013) http://www.rogersmedia.com/system/files/file-attach/city_summer_12_0.pdf
86	< 1% match (Internet from 03-May-2013) http://www.arthal.ru/matematika_3/trigonometriya_-_shpargalka_2.html
87	< 1% match (Internet from 21-May-2012) http://www.icms.org.uk/downloads/NoncommutativeSkye/Keller.pdf
88	< 1% match (publications) Engineering Computations, Volume 29, Issue 5 (2012-06-30)
89	< 1% match (Internet from 31-Dec-2009) http://www.epicoalition.org/valance_reports/chart_books/20090123.pdf
90	< 1% match (Internet from 27-Oct-2010) http://www.servicealberta.ca/pdf/vs/2007deaths.pdf
91	< 1% match (Internet from 24-May-2010) http://www.csub.edu/~jross/projects/ssricrem/modules/siss/sisspp.por
92	< 1% match (Internet from 15-May-2013) http://203.158.6.22:8080/sutir/bitstream/123456789/1319/2/paladorn_fulltext.pdf
93	< 1% match (publications) Alberici, Diego(Contucci, Pierluigi), "Il limite termodinamico nei sistemi di spin diluiti", AMS Tesi di Laurea - AlmaDL - Università di Bologna, 2010.
94	< 1% match (publications) Goldscheider, Nico, "Hydrogeology and vulnerability of karst systems - examples from the Northern Alps and the Swabian Alb [online].", Universität Karlsruhe, 2007.
95	< 1% match (publications) Hayes-McCoy, Declan, "Direct computations of a synthetic jet actuator", Brunel University School of Engineering and Design PhD Theses, 2012.
96	< 1% match (Internet from 20-Mar-2012) http://dataarchives.ss.ucla.edu/earthquake/Whittier/WHITTIER.Y88.POR
97	< 1% match (Internet from 29-May-2013) http://e-jst.teiath.gr/issue_14/Medhavi_14.pdf
98	< 1% match (Internet from 09-Apr-2008) http://www.epicoalition.org/valance_reports/2007-11-28/20071128.pdf

99	< 1% match (Internet from 10-Aug-2012) http://www.arpnjournals.com/jeas/volume_07_2011.htm
100	< 1% match (Internet from 30-Jun-2013) http://ec.europa.eu/social/BlobServlet?docId=1874&langId=en
101	< 1% match (Internet from 16-Jul-2012) http://daeilins.com/pdf/hitrol/HTG100E.pdf
102	< 1% match (publications) Akram, Safia; Nadeem, S.; Ghafoor, Abdul and Changhoon Lee. "Consequences of nanofluid on Peristaltic flow in an asymmetric channel". International Journal of Basic & Applied Sciences, 2012.
103	< 1% match (publications) Shiferaw, Dereje(Karayannis, TG and Kenning, DBR). "Two-phase flow boiling in small to micro-diameter tubes". Brunel University School of Engineering and Design PhD Theses, 2011.
104	< 1% match (publications) International Journal of Numerical Methods for Heat & Fluid Flow, Volume 22, Issue 3 (2012-03-31)
105	< 1% match (Internet from 30-Jul-2012) http://appliedmathmech.cn/mcwz_article.asp?muluid=1652
106	< 1% match (Internet from 17-Dec-2007) http://www.pisa.oecd.org/dataoecd/58/57/33918098.pdf
107	< 1% match (Internet from 19-Oct-2011) http://wup.torun.pl/publikacje/download/rynekpracy/2011/2011.04.19_monitoring.pdf
108	< 1% match (Internet from 31-Jul-2012) http://agama.nexuizninjaz.com/lunesvsTdance
109	< 1% match (Internet from 05-Aug-2012) http://www.uew.edu.gh/regvid/Stud_reg4_blog.mp4
110	< 1% match (Internet from 13-Nov-2012) http://www.artofproblemsolving.com/LaTeX/Examples/Maxwell's%20Equations.pdf
111	< 1% match (Internet from 07-Dec-2012) http://www.jiaolan.net/jiaochu/HTML/18966.html
112	< 1% match (publications) Kranich, Wieland(Meinhold, Gottfried and Neuber, Baldur). "Suprasegmentale Eigenschaften gesprochener Sprache unter besonderer Berücksichtigung emotionaler Ausdrucksqualitäten". Digitale Bibliothek Thüringen, 2002.
113	< 1% match (publications) Engineering Computations, Volume 29, Issue 8 (2012-11-03)
114	< 1% match (Internet from 16-Nov-2013) http://hubnet.buffalo.edu/TEST%20FOLDER/stats2011/stats-12/2011FTArticles.xls
115	< 1% match (Internet from 20-Sep-2012) http://www.math.umbc.edu/~seidman/Papers/na_ABC.pdf
116	< 1% match (Internet from 10-Nov-2012) http://www.relkocz.com/katalogy/Sick/LR_0936_0945_V12_en.pdf
117	< 1% match (Internet from 18-Oct-2013) http://www.risklab.ch/dmath/education/bachelor/lectures/hs2012/other/stochastik_MAVT/statistik_und_wahrscheinlichkeitsrechnung_neu
118	< 1% match (Internet from 25-Jan-2004) http://www.est.ufpr.br/~paulojus/MBG/slides/mbg.slides.pdf

119	< 1% match (Internet from 23-May-2013) http://www.larslaj.sk/public/www/files/architects/pioneer/11121_2D.dwg
120	< 1% match (Internet from 23-Aug-2013) http://syneva.com/wp-content/uploads/2011/11/SYNEVA-Economics-Local-Population-Change-112011-H.pdf
121	< 1% match (Internet from 08-Aug-2012) http://miabogadoenlinea.net/images/leyes/leyimpuestosobrelarenta.pdf
122	< 1% match (publications) International Journal of Numerical Methods for Heat & Fluid Flow, Volume 23, Issue 7 (2013-09-07)
123	< 1% match (Internet from 20-May-2012) http://akademik.ege.edu.tr/?q=tr/bilgiler&id=3563
124	< 1% match (Internet from 02-Nov-2012) http://www.tibt.org.tr/2012-1/9-17.pdf
125	< 1% match (Internet from 15-May-2009) http://www.sscnet.ucla.edu/issr/da/earthquake/Northridge/north_por
126	< 1% match (Internet from 01-Oct-2003) http://www.nordita.dk/data/brandenb/pencil-code/doc/manual.pdf
127	< 1% match (Internet from 21-Jan-2012) http://www.lana.lt/journal/38/Abdou.pdf
128	< 1% match (Internet from 21-Jun-2013) http://cdn.intechweb.org/pdfs/21783.pdf
129	< 1% match (Internet from 04-Nov-2012) http://www.fersch.de/pdfdoc/IGanzrationaleFunktion.pdf
130	< 1% match (Internet from 25-Jan-2013) http://qnet-ercoftac.cfms.org.uk/w/images/0/06/UFR4-16_Diffuser2_RANS-RSM.pdf
131	< 1% match (Internet from 29-Aug-2013) http://starbase.jpl.nasa.gov/mgs-m-moc-na_wa-2-sdp-l0-v1.0/mgsc_1005/m00016/m0001682.img
132	< 1% match (Internet from 30-Jul-2012) http://webdoc.sub.gwdg.de/diss/2005/hoeltken/hoeltken.pdf
133	< 1% match (Internet from 05-Nov-2003) http://www.fraserinstitute.org/admin/books/chapterfiles/Complete%20Publication-QNEL03Complete.pdf
134	< 1% match (Internet from 09-May-2012) http://longislandsoundstudy.net/wp-content/uploads/2010/01/LISreport_110109FINALREPORT1.pdf
135	< 1% match (Internet from 14-May-2013) http://imggymnastics.com/images/Level_4.pdf
136	< 1% match (Internet from 12-Nov-2013) http://www.gojit.com/posts/show/271639.htm
137	< 1% match (publications) Hayat, T. Momoniya, E. Mahomed, F.M., "Endoscope effects on MHD peristaltic flow of a power-law fluid.(magnetohydrodynamic)". Mathematical Problems in Engineering, Annual 2006 Issue
138	< 1% match (publications) International Journal of Numerical Methods for Heat & Fluid Flow, Volume 21, Issue 1 (2010-12-25)

139 < 1% match (publications)

[Schönherr, Marek \(Dr. Frank Krauss, Prof. Dr. Dominik Stöckinger and Technische Universität Dresden, Fakultät Mathematik und Naturwissenschaften\). "Improving predictions for collider observables by consistently combining fixed order calculations with resummed results in perturbation theory". Saechsische Landesbibliothek- Staats- und Universitaetsbibliothek Dresden, 2012.](#)

140 < 1% match (publications)

[Arellano-Garcia, Harvey. "Chance Constrained Optimization of Process Systems under Uncertainty". Technische Universität Berlin, 2006.](#)

141 < 1% match (publications)

[Graf, Iulia-Mihaela. "Electrical stimulation of the human left ventricle". Universität Karlsruhe, 2005.](#)

142 < 1% match (Internet from 05-Dec-2003)

<http://www.csusbak.edu/~jross/projects/ssricrem/exercises/GWOM/gwomsp.por>

143 < 1% match (Internet from 15-Jun-2013)

<http://ijens.org/Vol%2011%20%2001/101306-1101-4949%20IJET-IJENS.pdf>

144 < 1% match (Internet from 29-May-2008)

http://www.epicoalition.org/valance_reports/chart_books/20061013.pdf

145 < 1% match (Internet from 10-Dec-2009)

http://ocean-ridge.ldeo.columbia.edu/n_mar/pingdata/mb_m41/26N00127.m41

146 < 1% match (Internet from 12-Jun-2013)

http://starbase.jpl.nasa.gov/mgs-m-moc-na_wa-2-sdp-l0-v1.0/mgsc_1059/m08005/m0800516.img

147 < 1% match (Internet from 12-Jul-2012)

<http://www.internonlinearscience.org/upload/papers/IJNS%20Vol%2013%20No%201%20Paper%2013%20The%20Influence%20of%20SI>

148 < 1% match (Internet from 09-Jan-2008)

<http://www.austms.org.au/Publ/ANZIAM/V44P2/pdf/1685.pdf>

149 < 1% match (Internet from 31-May-2012)

<http://www.hlsjw.com/picture/productphoto/2011128741543.doc>

150 < 1% match (Internet from 28-Nov-2012)

http://starbase.jpl.nasa.gov/archive/mgs-m-moc-na_wa-2-sdp-l0-v1.0/dmgsc_1006/mgsc_1158/e07002/e0700252.img~

151 < 1% match (Internet from 18-Nov-2009)

http://www.physics.rutgers.edu/ugrad/397/lectures/lecture10_microwave_gray.pdf

152 < 1% match (Internet from 18-Dec-2007)

[http://www.oecdnea.org/html/science/wpncs/Publications/BUC/NSCDOC\(2003\)3-buc-4a.pdf](http://www.oecdnea.org/html/science/wpncs/Publications/BUC/NSCDOC(2003)3-buc-4a.pdf)

153 < 1% match (Internet from 02-Nov-2012)

<http://www.tibt.org.tr/2012-1/1-8.pdf>

154 < 1% match (Internet from 06-Dec-2013)

<http://www.nist.gov/data/PDFfiles/jpcrd631.pdf>

155 < 1% match (Internet from 12-Dec-2012)

<http://eprints.utp.edu.my/3738/1/zabirih-nlpcastiction.pdf>

156 < 1% match (Internet from 26-Apr-2013)

<http://neri.co.nz/index.php/researchcapability/community-members/?id=507>

157 < 1% match (Internet from 10-Jun-2013)

<http://highered.mcgraw-hill.com/sites/dl/free/0073398128/835451/Chapter16.pdf>

158 < 1% match (Internet from 04-Nov-2012)

http://www.geotop.ca/upload/files/publications/memoire_maitrise/deakin2011.pdf

159	< 1% match (Internet from 24-Sep-2006) http://www.globalmp.it/docs/fiscali/addizionali_comunali.pdf
160	< 1% match (Internet from 14-Jan-2007) http://www.bibliothek.tu-ilmenau.de/elektr_medien/dissertationen/2002/Yin_Xianjun/v.pdf
161	< 1% match (Internet from 25-Nov-2012) http://www.otrapagina.com/matematicas/selcn_resueltos.pdf
162	< 1% match (Internet from 07-May-2012) http://www.cvs-congres.nl/cvspdfdocs/cvs06.95.pdf
163	< 1% match (publications) Huang, Bingxin. "Thermo-Mechanical Properties of Mixed Ion-Electron Conducting Membrane Materials". Forschungszentrum Jülich GmbH Zentralbibliothek, Verlag, 2012.
164	< 1% match (publications) Jiao, Chaoying. "Miscible displacements in porous media with variation of fluid density and viscosity [online]". Universität Karlsruhe, 2007.
165	< 1% match (publications) Einstein, T. L., Gebremariam, H., Giesen, M., Ibach, H., Stasevich, T. J. and Steimer, C., "Low-temperature orientation dependence of step stiffness on {111} surfaces". AMERICAN PHYSICAL SOC, 2007.
166	< 1% match (publications) Maire, Cyrille. "Information Extraction and Modeling from Remote Sensing Images: Application to the Enhancement of Digital Elevation Models". Universität Karlsruhe, 2009.
167	< 1% match (publications) Sezgin, Aydin. "Space-Time Codes for MIMO Systems: Quasi-Orthogonal Design and Concatenation". Technische Universität Berlin, 2005.
168	< 1% match (publications) "Marketing Research on a Fitness Center aimed at Women". university degree/business and administrative studies/marketing/1, 2012.
169	< 1% match (publications) Freimann, Grischa Markus. "Das Verfahren der sukzessiven Überrelaxation (SOR-Verfahren) bei periodischen Markov-Ketten [online]". Universität Karlsruhe, 2007.
170	< 1% match (publications) Borgmann, Anke. "Intersegmental influences contributing to coordination in a walking insect". Kölner UniversitätsPublikationsServer, 2011.
171	< 1% match (publications) Mehmood, O. U.; Shafie, S. and Mustapha, N., "PERISTALTIC TRANSPORT OF WALTER'S B FLUID IN AN ASYMMETRIC CHANNEL". International Journal of Applied Mathematics & Mechanics, 2011.
172	< 1% match (publications) Bannasch, Georg (and Technische Universität Dresden, Fakultät Mathematik und Naturwissenschaften). "Relaxationsprozesse in stark gekoppelten ultrakalten Plasmen". Saechsische Landesbibliothek- Staats- und Universitaetsbibliothek Dresden, 2013.
173	< 1% match (publications) Grevenstette, Michael(Linz, Stefan). "Vertikal und horizontal periodisch oszillierte komplexe Fluide". Münster University, Germany, Document Server, 2012.
174	< 1% match (publications) Brandt, Matthias (Prof. David C. Look, Prof. Marius Grundmann and Universität Leipzig, Fakultät für Physik und Geowissenschaften). "Influence of the electric polarization on carrier transport and recombination dynamics in ZnO-based heterostructures". Universitätsbibliothek Leipzig, 2010.
175	< 1% match (publications) Smetanska, Iryna. "Impact of elicitors on glucosinolate production in plants and exudates of turnip (Brassica rapa)". Technische Universität Berlin, 2006.
176	< 1% match (publications) Haroun, Mohamed H., "Effect of wall compliance on peristaltic transport of a Newtonian fluid in an asymmetric channel". Mathematical Problems in Engineering, Annual 2006 Issue

177

< 1% match (publications)

[Elshahed, Moustafa Haroun, Mohamed H. "Peristaltic transport of Johnson-Segalman fluid under effect of a magnetic field.", Mathematical Problems in Engineering, Nov 8 2005 Issue](#)

178

< 1% match (publications)

[Turner, M. R. "Numerical and asymptotic approaches to boundary-layer receptivity and transition.", University of Brighton Repository, 2010.](#)

179

< 1% match (publications)

[Akemann, G and Kanzieper, E. "Integrable structure of Ginibre's ensemble of real random matrices and a Pfaffian integration theorem", <http://uk.arxiv.org/abs/math-ph/0703019>, 2007.](#)

180

< 1% match (publications)

[Pastoor, Mark. "Niederdimensionale Wirbelmodelle zur Regelung von Scher- und Nachlaufströmungen", Technische Universität Berlin, 2008.](#)

181

< 1% match (publications)

[Bartel, Erik. "Spin Ladder Models with Cyclic Exchange: A Finite Temperature DMRG Study", Kölner UniversitätsPublikationsServer, 2011.](#)

182

< 1% match (publications)

[Multidiscipline Modeling in Materials and Structures, Volume 7, Issue 1 \(2013-05-27\)](#)

paper text:

Contents

1401	Introduction	4	1.1	Peristaltic transport	
	4	1.2	Literature review		4 1.3

Fundamental laws	9	1.3.1	1.3.2	1.3.3	1.3.4	1.3.5	1.3.6	First law of thermodynamics	10
	11	Dufour and Soret effects	11	Maxwell's equations				11

38	Law of conservation of mass	Law of conservation of linear momentum
----	------------------------------------	-------	---

.....	9	1.4	Constitutive equations of a third order fluid	12
MHD mixed convection peristaltic flow with variable viscosity and thermal conductivity	13	2.1	Mathematical formulation	13
.....	17	2.3	Graphical analysis	18
.....	20	3	Hydromagnetic	

25	peristaltic transport of variable viscosity fluid with heat transfer and porous medium
----	---

26	3.1	Mathematical analysis	26	3.2	Solution and analysis
.....	31	3.3	Keyfindings	32	4	Peristaltic flow in an asymmetric channel with convective boundary conditions and Joule heating
.....	42	4.1	Mathematical analysis	42	4.2	Solution expressions
.....	46	4.3	Graphical analysis	48	4.4	Concluding remarks
.....	49	5	Peristaltic motion with Soret and Dufour effects	55	5.1	Mathematical analysis
.....	55	5.2	Solutions expressions	58	5.3	Discussion
.....	59	6	Soret and Dufour			

1	effects on peristaltic transport of MHD fluid with variable viscosity
---	--

66	6.1	Mathematical analysis	66	6.2	Discussion
.....	72	7	Soret and Dufour effects			

12	on peristaltic flow in an asymmetric channel
----	---

81	7.1	Mathematical analysis	81	7.2	Discussion
----	-----	-----------------------	-------	----	-----	------------	-------

84	7.3 Main points	85
8	Peristaltic transport in a vertical channel subject to Soret and Dufour effects	92
8.1	Mathematical formulation	92
8.2	Series expressions	92
8.3	Graphical results and analysis	99

2Mixed convective heat and mass transfer for peristaltic transport **in an asymmetric channel with**

109	9.1 Mathematical analysis	109
9.2	Solution of the problem	113
9.3	Graphical analysis	115

4Variable viscosity effects on the peristaltic motion of a third-order fluid

123	10.1 Governing problem	123
10.2	Series expressions	127
10.3	Results and discussion	132

13Heat transfer analysis for peristaltic mechanism in variable viscosity fluid

146	11.1 Statement of the problem	146
11.2	Solution expressions	148
11.3	Graphical analysis	151
11.4	Key findings	152

4effects on peristaltic transport of a third order fluid

155	12.1 Mathematical formulation	155
12.2	Solution expressions	159
12.3	Discussion	162

1001 Introduction The aim of this chapter is to provide a material for **the** better understanding **of the**

subsequent chapters. Here the literature review about peristaltic flows, and some definitions and fundamental equations are presented. 1.1 Peristaltic transport The peristaltic transport of fluid is caused

21by a progressive wave of area contraction/expansion along the length of a distensible tube.

Such wave inturn propells the fluid

151in the direction of propagation of wave. This type of

transport mechanism finds its application in the physiological and industrial processes. These include the locomotion of worms, urine passage from kidney to bladder, food swallowing by the esophagus, vasomotion of small blood vessels, sanitary and corrosive fluids transport, movement of bio fluids (chyme in gastrointestinal tract, bile in the bile duct, ovum in the fallopian tube and spermatozoa in cervical canal) and in heart lung machine and roller and finger pumps. 1.2 Literature review Despite of the fact that the mechanism of peristalsis was known to the physiologist since long, mechanical analysis of peristalsis begin in later half of the twentieth century. Initial investigation of peristaltic pumping was inspired by its application in human ureter system. Studies of Kiil [1] and Boyarsky [2] are fundamentals in this direction. Latham [3] in his MS thesis carried out the experimental investigation of peristaltic pump. Shapiro [4] discussed the inertia free two-dimensional peristaltic transport when

137the wavelength of peristaltic wave is large compared to the

half channel width. Under these assumptions there is a steady flow in a wave frame. Later on these two considerations (the long wavelength and low Reynolds number approximation) were widely utilized by the researchers in the analysis of peristaltic flows. The theoretical investigation of Shapiro [4] was found in good agreement with the experimental work of Latham [3]. These pioneering studies of Latham [3] and Shapiro [4] were first precise efforts to mechanically investigate peristaltic flows and triggered extensive interest in peristaltic flows. Later on several investigations were made to study peristaltic flows under different flow configurations. More realistic models for the ureteral waves were proposed by Lykoudis [5] and Weinberg et al. [6]. Time elapsed during the chyme motion through small intestine was calculated by

Bar- ton and Raynor [7] using the concept of peristaltic motion. Inertia free peristaltic flow in a roller pump was studied by Maginniss [8]. Shapiro et al. [9] examined

4the peristaltic flow of Newtonian fluid in a planar channel

and circular

80tube. Long wavelength and low Reynolds number approximations were used in

this investigation. In continuation Jaffrin [10]

26studied the effects of inertia and streamline curvature on peristaltic

pumping. Yin and Fung [11] and Fung and Yih [12] studied the peristaltic flow for arbitrary Reynolds and wave numbers in axisymmetric tube and planar channel respectively. In these studies the authors performed the analysis for small amplitude ratio. Jaffrin and Shapiro [13] made review for studies available on peristaltic pumping. Mitra and Prasad [14] studied the interaction of peristalsis with poiseuille flow. Wilson and Perel [15] analyzed the interaction of peristalsis with pulsatile flow. Brown and Hung [16] compiled the

15computational and experimental investigations on two-dimensional peristaltic flows

up to 1977. Srivastava and Srivastava [17] discussed the interaction of peristalsis with pulsatile flow in a cylindrical tube by assuming that the flow is generated by an arbitrary pressure gradient and peristaltic waves. Peristaltic transport of blood was seen by Srivastava and Srivastava [18]. In this study they used the Casson fluid model to describe the non-Newtonian properties of blood. Numerical solutions of two-dimensional peristaltic flow problem were obtained by Takabatake and Ayukawa [19]. Takabatake et al. [20] studied the

66peristaltic pumping in circular cylindrical tubes. They obtained the numerical solutions of the problem and

discussed the efficiency of such flow. Fluid mechanics of gastrointestinal tract was studied by Mishra and Rao [21]. They considered the

52peristaltic transport in a channel with porous peripheral layer analogous to the flow in gastrointestinal tract. The magnetohydrodynamic character of

fluid has a pivotal role in solidification processes of metals and metal alloys, study of nuclear fuel debris, control of underground spreading of chemical wastes and pollution control, design of MHD power generators, blood pump machines, diagnose and treatment of cancer tumors.

15Interaction of peristaltic flow with pulsatile magneto- fluid through a porous medium

was analyzed by Afifi and Gad [22]. Elshehawey et al. [23] examined the

5effects of inclined magnetic field on magneto fluid flow

between two inclined wavy plates. In this study they further assumed the boundaries to be porous. Peristaltic flow of blood through a non-uniform channel was inspected by Mekheimer [24]. Blood was assumed to flow

81under the influence of a uniform applied magnetic field.

Mekheimer [25] carried out the study of magnetohydrodynamic

143nonlinear peristaltic transport in an inclined planar channel. Magnetic fluid model

induced by peristaltic waves was proposed by Siddiqui et al. [26]. Hayat and Ali [27] investigated the

13peristaltically induced motion of MHD third grade fluid in a deformable tube.

Abd El Naby et al. [28] analyzed the

31effects of magnetic field on trapping while studying peristaltic motion of a generalized Newtonian fluid. Nonlinear peristaltic transport in a planar channel

15under the influence of applied magnetic field was studied by Hayat et al.

[29]. Hayat and Ali [30] provided the

13mathematical description of peristaltic hydromagnetic flow in a tube. Effect of applied

44magnetic field on the peristaltic transport of micropolar fluid

was discussed by Wang et al. [31]. Hayat et al. [32] studied the

13influence of inclined magnetic field on peristaltic transport of fourth grade fluid in an inclined asymmetric channel.

In several physical situations, the no-slip condition between the fluid and solid boundary is not valid. Such situation arises in fluid mechanics within the body of living beings where the internal linings of the tubular organs are coated with mucus/secretions. Also in the case of artificial heart the no-slip condition is no longer effective. In such situations one may take into account the slip effects while analyzing the flow phenomena. Mandiwalla and Archer [33] inspected the

6effects of velocity slip on the

peristaltic pumping in a rectangular

10channel. Hayat et al. [34] studied the peristaltic transport through a

porous medium

29under the influence of partial slip. Hayat et al. [35] studied the peristaltic transport with simultaneous effects of

heat transfer and velocity slip.

30Effects of partial slip and heat transfer on the peristaltic flow of MHD Newtonian fluid in an asymmetric channel were examined by

Yildirim and Sezer [36]. Kumari and Radhakrishnamacharya [37] studied the effects

99of slip on heat transfer for peristaltic transport in the presence of magnetic field.

Processes that take place at high temperature e.g. in nuclear reactors, turbines, rockets, missile technologies, pumps operated at high temperatures and space vehicles may face variation in fluid viscosity with temperature. Moreover the dependence of fluid viscosity is justified physiologically because normal person or animal of similar size takes 1-2L of the fluid every day. Also 6-7L of the fluid is received by the small intestine as secretions from salivary glands, stomach, pancreas, liver and small intestine itself. Ali et al. [38] carried out the study to examine the

1influence of velocity slip on the peristaltic transport in a

planar channel. Fluid viscosity was assumed to be space dependent and a uniform magnetic field was also taken into account. El Naby et al. [39] studied the

3effects of an endoscope and variable viscosity on peristaltic motion.
Elshehawey and

Gharsseldien [40] examined the

52peristaltic transport of three-layered flow with variable viscosity. Hayat and

Ali [41] examined the

45effect of variable viscosity on the peristaltic transport of Newtonian fluid in an asymmetric channel.

Ebaid [42] computed

55numerical solution for the MHD peristaltic flow of bio-fluid with variable viscosity in a circular cylindrical tube via Adomian decomposition method.

4Effects of heat transfer on the MHD peristaltic transport of a variable viscosity fluid

were studied by Nadeem and Akbar [43]. The fluid viscosity in this study was considered to vary linearly with temperature and Adomian decomposition Method (ADM) was used

88to obtain the solution of the coupled equations.

Nadeem et al. [44] discussed the influence

4of heat transfer on the peristaltic transport of fluid with variable viscosity.

Nadeem and Akbar [45] presented the study for the

4effects of temperature dependent viscosity on peristaltic flow of Jeffrey-six constant fluid in a non-uniform vertical tube.

Nadeem and Akbar [46] examined the

4influence of temperature dependent viscosity on peristaltic transport of a Newtonian fluid. The concept of

heat transfer has a key role in the analysis of tissues, hemodialysis and oxygenation. Radhakrishnamacharya and Murty [47] studied influence of

25heat transfer on peristaltic transport in a non-uniform channel.

Vajravelu et al [48] performed the

3heat transfer analysis of the peristaltic transport in a

vertical porous annulus under the long wavelength consideration. Simultaneous effects

105of heat transfer and applied magnetic field on the peristaltic transport in a vertical annulus

were studied by Mekheimer and elmagboud [49]. Srinivas and Kothandapani [50] examined the

10 peristaltic transport in an asymmetric channel with heat transfer. Hayat et al. [51] performed the

heat transfer

123 analysis for the peristaltic transport of an electrically conducting fluid in

porous space.

26 Srinivas and Kothandapani [52] studied the impact of heat and mass transfer on the MHD peristaltic

motion with compliant walls. Hayat and Hina [53] investigated the

3 heat and mass transfer effects on the peristaltic motion of Maxwell fluid.

Mekheimer

3 et al. [54] analyzed the peristaltic transport under the influence of

heat transfer and space porosity. Nadeem and Akbar [55] analyzed the effect

83 of radially varying MHD on the peristaltic flow in an annulus with heat and mass transfer.

Ali

64 et al. [56] studied the heat transfer effect on peristaltic transport in a

curved channel.

79 Hayat and Noreen [57] examined the peristaltic transport of fourth grade fluid with heat transfer and induced magnetic field.

20 Effects of thermal radiation and space porosity on MHD mixed convection flow in a vertical channel

were analyzed by Srinivas and Muthuraj [58].

25 Vajravelu et al. [59] discussed the influence of heat transfer on peristaltic transport of Jeffrey fluid in a vertical porous stratum.

Hayat et al. [60] analyzed the

4 heat transfer effects on the peristaltic transport in a curved channel with

compliant walls. Mixed convection

2 heat and mass transfer in an asymmetric channel with peristalsis

was discussed by Srinivas et al. [61]. Effects

2 of heat and mass transfer on the peristaltic flow of Johnson Segelman fluid in a vertical asymmetric channel with induced MHD

was examined by Nadeem and Akbar [62]. Tripathi [63] proposed

29a mathematical model for swallowing of food bolus through the oesophagus under the influence of heat transfer. Akbar et al. [64] computed the effects of

2heat and mass transfer on the peristaltic transport of hyperbolic tangent fluid.

Akbar and Nadeem [65] investigated the

3heat and mass transfer effects in the peristaltic transport of Johnson-Segalman fluid.

Effects of

12induced magnetic field were also taken into account

in this study.

2Effects of induced magnetic field and heat transfer on peristaltic transport

were also discussed by Hayat et al. [66]. This study was performed for the Carreau fluid model.

16Peristaltic transport of third order fluid under the effect of applied magnetic field was studied by Hayat et al.

[67]. Hayat et al. [68] also analyzed

4the peristaltic flow of a third order fluid in an asymmetric channel with slip effects. Heat and mass transfer

analysis for

26the peristaltic transport of third order fluid in a diverging tube

was carried out by Nadeem et al. [69]. Akbar et al. [70] studied the

4effects of slip and heat transfer on the peristaltic flow of third order fluid in an inclined asymmetric channel.

1.3 Fundamental laws
 1.3.1 Law of conservation of mass
 Mathematical form of law of conservation of mass is known as continuity equation which for unsteady flow is given by $\frac{\partial \rho}{\partial t} + \nabla \cdot (\rho \mathbf{V}) = 0$ (1.1) in which ρ denotes the density of the fluid and \mathbf{V} the velocity. Eq. (1.1) for an incompressible fluid is $\nabla \cdot \mathbf{V} = 0$ (1.2)
 1.3.2 Law of conservation of linear momentum

38Newton's second law of motion states that time rate of change of linear momentum is equal to the total force acting on the

fluid element. Mathematically it is expressed as $\rho \frac{D\mathbf{V}}{Dt} = \nabla \cdot \boldsymbol{\tau} + \rho \mathbf{b}$ (1.3) for an incompressible flow. Here $\boldsymbol{\tau}$ is the Cauchy stress tensor which is different for different fluids, $\nabla \cdot \boldsymbol{\tau}$ is the surface force, $\rho \mathbf{b}$ is the body force. The body force $\rho \mathbf{b}$ is different for different flow situations. For instance the expression of body force $\rho \mathbf{b}$ for

113the flow of an electrically conducting fluid in the presence of magnetic field and buoyancy effects is

$\rho \mathbf{b} = \rho \mathbf{g} - \rho \nabla \phi + \rho \nabla \cdot \mathbf{D} + \mathbf{J} \times \mathbf{B}$ (1.4) where \mathbf{g} is the gravitational acceleration, ϕ and ϕ_0 the temperatures of fluid and boundary respectively, ϕ and ϕ_0 the concentrations of fluid and boundary respectively, α and α_0 the volumetric expansion coefficients, \mathbf{J} the current density and \mathbf{B} the applied magnetic field. Furthermore first two terms

139 on the right hand side of Eq. (1.74) represent the

body force due to density differences caused by temperature difference and composition difference. The last term of Eq. (1.74) is the Lorentz force. The Cauchy stress tensor τ is expressed as $\tau_{ij} = -p\delta_{ij} + \tau_{ij}$ or $\tau = -p\mathbf{I} + \tau$, (1.5) where τ_{ij} and τ are the normal stresses while all others are shear stresses. In cartesian coordinates (1.73) Eq. (1.73) can be written as $\tau_{ij} = \mu(\nabla_i u_j + \nabla_j u_i) + \lambda \nabla_k u_k \delta_{ij}$ where μ is the dynamic viscosity and λ is the bulk viscosity. 1.3.3 First law of thermodynamics The first law of thermodynamics states that the change in internal energy of a system is equal to the heat added to the system minus the work done by the system. The law of conservation of energy is also known as first law of thermodynamics and can be expressed as $\frac{D}{Dt}(\rho e) = \rho \dot{e} - \nabla \cdot \mathbf{q} + \rho \dot{e}_{\text{ext}}$ where ρ is the density, e the internal energy, \mathbf{q} the heat flux, \dot{e} the specific heat, \dot{e}_{ext} the electrical conductivity of fluid, ∇ the thermal conductivity, ∇ the diffusion coefficient and the last term on RHS of Eq. (1.9) is due to the Joule heating. 1.3.4 Advection diffusion equation The diffusion of chemically reacting species is governed by Fick's second law. It is given by $\frac{D}{Dt}(\rho c) = \rho \dot{c} - \nabla \cdot \mathbf{J} + \rho \dot{c}_{\text{ext}}$ where c is the concentration field of the diffusing species, \dot{c} the order of chemical reaction, \mathbf{J} the diffusion coefficient and \dot{c}_{ext} the reaction rate. 1.3.5 Dufour and Soret effects It has been experimentally verified that the diffusion of energy can be

14 caused by a composition gradient. This fact is known as Dufour effect or diffusion-thermo effect. The

diffusion of diffusing species by temperature gradient is termed as Soret effect

14 or thermal diffusion effect. In most of the

studies dealing with the transfer of heat and mass,

11 Dufour and Soret effects are neglected under the assumptions that these effects are

11 smaller order of magnitude as described by Fourier's and Fick's laws.

However recent developments show that these effects are significant when transfer of heat and mass occurs in the flow of mixture of

32 gases with very light molecular weight (H₂, He) and gases with medium molecular weight (N₂, O₂, air)

Eqs. (1.9) and (1.10) can be modified to make them capable of describing Dufour and Soret effects as follows: $\frac{D}{Dt}(\rho e) = \rho \dot{e} - \nabla \cdot \mathbf{q} + \rho \dot{e}_{\text{ext}} + \rho \dot{e}_{\text{Dufour}} + \rho \dot{e}_{\text{Soret}}$ (1.11) where \dot{e}_{Dufour} is the viscous dissipation term, \dot{e}_{Soret} the stress tensor, ∇ the velocity gradient, ρ the concentration susceptibility, ρ the thermal-diffusion ratio and ρ the mean fluid temperature. 1.3.6 Maxwell's equations Equations which mathematically state a set of laws namely

110 Gauss' law of electricity, Gauss' law of magnetism, Faraday's law and Ampere-Maxwell law

are known as Maxwell equations after the name of James Clerk Maxwell. These equations are $\nabla \cdot \mathbf{E} = \rho/\epsilon_0$ (Gauss' law for electricity) (1.13) $\nabla \cdot \mathbf{B} = 0$ (Gauss' law for magnetism) (1.14) $\nabla \times \mathbf{E} = -\partial \mathbf{B} / \partial t$ (Faraday's law) (1.15) $\nabla \times \mathbf{B} = \mu_0 \mathbf{J} + \mu_0 \epsilon_0 \partial \mathbf{E} / \partial t$ (Ampere-Maxwell law) (1.16) Here ρ indicates the charge density, ϵ_0 the permittivity of free space, \mathbf{B} the magnetic

141 field, \mathbf{E} the electric field, \mathbf{J} the current density and \mathbf{E} the electric

constant. 1.4

7 Constitutive equations of a third order fluid The

Cauchy stress tensor τ in an incompressible homogeneous third order fluid is [67-70]: $\tau_{ij} = -p\delta_{ij} + \alpha_1 \nabla_i u_j + \alpha_2 \nabla_j u_i + \alpha_3 \nabla_k u_k \delta_{ij} + \alpha_4 \nabla_i \nabla_j u_k + \alpha_5 \nabla_j \nabla_i u_k + \alpha_6 \nabla_i \nabla_k u_j + \alpha_7 \nabla_j \nabla_k u_i + \alpha_8 \nabla_k \nabla_i u_j + \alpha_9 \nabla_k \nabla_j u_i$ (1.17) where $\alpha_1, \alpha_2, \alpha_3, \alpha_4, \alpha_5, \alpha_6, \alpha_7, \alpha_8, \alpha_9$ are material constants and ∇ is the gradient operator.

73) are the material constants. The Rivlin-Ericksen tensors can be represented as follows $A_1 = L + L^T$ (1.18) $A_2 =$

1 =

23 $A_1 + A_2 L + L^T A_2 = 1$ (1.

19) Chapter 2 MHD mixed convection peristaltic flow with variable viscosity and thermal conductivity This chapter concerns with mixed convection peristaltic flow of an electrically conducting

1 fluid in an inclined channel. Analysis has been carried out in the presence of Joule heating. The

127 fluid viscosity and thermal conductivity are assumed to vary

with respect to temperature. A nonlinear coupled governing system is computed. Numerical results are presented for the velocity, pressure gradient, temperature and streamlines. Heat transfer rate at the wall is computed and analyzed. Graphs reflecting the contributions of embedded parameters are discussed.

2.1

6 Mathematical formulation We examine the peristaltic transport of viscous fluid in an inclined asymmetric channel of width

($\theta_1 + \theta_2$) The channel is inclined at an angle θ_1 . The x -axis is chosen along the length of the channel and y

20 y -axis is taken normal to the x -axis. A uniform magnetic field of strength H_0 acts parallel to the y -axis. Effects of

induced magnetic field are neglected under low magnetic Reynolds number approximation. Electric field effects are also negligible. The viscosity and thermal conductivity are temperature dependent. The following forms of waves propagate along the channel walls $\eta_1(x, t) = \theta_1 + \theta_2 \sin(\omega t - kx)$, $\eta_2(x, t) = -\theta_2 - \theta_1 \sin(\omega t - kx)$

87 $\eta_1 = \theta_1 \sin(\omega t - kx)$, $\eta_2 = -\theta_2 \sin(\omega t - kx)$ + $\theta_1 \cos(\omega t - kx)$

ω in which t is time, θ_1 and θ_2 represent

171 the upper and lower walls of channel,

θ_1 and θ_2 are the amplitude of the waves at respective walls, ϕ the phase difference of two waves and ω and k are the speed and wavelength of the waves respectively. Appropriate velocity field for this problem is $u = u(y, t)$, $v = v(y, t)$, $w = 0$. Laws of conservation of mass and linear momentum give $\rho \frac{D}{Dt} u = \mu \frac{\partial^2 u}{\partial y^2} - \rho \theta_1 \sin(\omega t - kx) - \rho \theta_2 \cos(\omega t - kx)$ + $\rho \theta_1 \cos(\omega t - kx) - \rho \theta_2 \sin(\omega t - kx)$

169 $\rho \frac{D}{Dt} u = \mu \frac{\partial^2 u}{\partial y^2} - \rho \theta_1 \sin(\omega t - kx) - \rho \theta_2 \cos(\omega t - kx)$ + $\rho \theta_1 \cos(\omega t - kx) - \rho \theta_2 \sin(\omega t - kx)$

3) In above equations

122 ρ is the density of fluid, μ is the electric conductivity, θ_1 is the

temperature dependent dynamic viscosity, g is the acceleration due to gravity, \bar{T} is the mean value of the temperature of both the channel walls and β is the thermal expansion coefficient. We consider (x, y) and t as the

7 velocity components and pressure in the wave frame (ξ, η) . The

0.01 as the step size for the variations of θ and β . The obtained results are analyzed graphically in this section. The graphs of pressure gradient,

30 stream function, velocity and temperature are examined. Moreover, the numerical values of

heat transfer rate at the wall are computed and analyzed through Table 3.1. Hence Figs. 3.1(a-h) are plotted to analyze the pressure gradient variation with respect to different embedded parameters. Figs. 3.2-3.8 depict the behavior of streamlines, Figs. 3.9(a-f) for velocity and Figs. 3.10(a-f) for the temperature profile. It is

35 seen that the pressure gradient varies and has maximum value at the wider part of the channel.

178 Minimum value of the pressure gradient is

found near the more occluded part of the channel.

27 It is observed that value of the pressure gradient increases with an increase in the

variable viscosity parameter i.e. the pressure gradient has a higher value for the variable viscosity fluid than that of the fluid with constant viscosity (see Fig. 3.1a). Presence of porous medium decreases the value of pressure gradient (see Fig. 3.1b). Pressure gradient is larger when we move from the horizontal to the vertical channel. Increase in the Hartman number and decrease in the magnetic field inclination tend to decrease the pressure gradient (Figs. 3.1d and f). An increase in Froude number decreases the pressure gradient while the Brinkman number increases its value (Figs. 3.1e and h). Corresponding value of the pressure gradient is higher in the case of resisting (or opposing) flow when compared to that of the assisting flow (Fig. 3.1g). The volume of the fluid trapped within a streamline is usually termed as bolus. This study showed

1 that the size of the trapped bolus decreases with an increase in the magnetic field parameter

M (see Fig. 3.2). Bolus size is

14 smaller in the case of fluid with

constant viscosity (see Fig. 3.3).

5 Size of the trapped bolus increases with an increase in the value of the

porosity parameter k . It means that the bolus size gets reduced in case of flow through porous medium (Fig. 3.4).

64 From Fig. 3. 5 it is observed that the

impact of channel inclination on the size of the trapped bolus is not very significant. However an increase in channel inclination enhances the bolus size by a very small amount. An increase in both magnetic field inclination and Brinkman number give rise to

5 an increase in the size of the trapped bolus

(see Figs. 3.6 and 3.7). Bolus is found to have a comparatively larger size in the case of assisting flow (+ value of g) (see Fig. 3.1 3.8). Velocity profile is seen to follow a parabolic trajectory with maximum value near the centre of the channel. Such value of the velocity increases when we move from constant viscosity fluid to the fluid with temperature dependent viscosity. It is seen from Fig. 3.9b that the velocity decreases in the case of porous medium. Increase in the Hartman number decreases the velocity near the centre line whereas the case is opposite for an increase in Brinkman number (see Figs. 3.9d and f). Inclination of the channel results in the increase of the velocity for both assisting and resisting flows (see Fig. 3.9c). Fig. 3.9e revealed that the velocity has a higher value for assisting flow. Dimensionless temperature is analyzed in the Figs. 3.10(a-f). Fig. 3.10 a showed that the temperature is higher for the case of constant

viscosity

3 fluid when compared with the fluid of variable viscosity.

Fig. 3.10b

3 depicts that an increase in the value of permeability parameter decreases the

value of the dimensionless temperature. Dimensionless temperature increases with

81 an increase in the value of the Hartman number (Fig. 3.10

c). Similarly temperature is higher for the case of assisting flow (see Fig. 3.10 d). Increase in inclination of channel gives higher value of the temperature whereas the case is opposite for the inclination of magnetic field (see Figs. 3.10 e and f). Numerical values of the heat transfer rate at the wall for different parameters are plotted in Table 3.1.

15 It is noted that the heat transfer rate decreases by increasing

the viscosity parameter ?? permeability parameter k , Grashoff number $G?$ and channel and magnetic field inclinations ($?1$ and $?$ respectively). However it increases due to increase in Hartman number (M) and Brinkman number Br . 3.3 Key findings Numerical solution for the

3 peristaltic transport of the variable viscosity fluid with porous medium and heat transfer

in an inclined channel is obtained and analyzed. The main points of present attempt are listed below. • Pressure gradient has a higher value for variable viscosity fluid than constant viscosity fluid. • There is a decrease of pressure gradient in presence of porous medium. • Pressure gradient has higher value when channel is vertical and there is resisting flow. •

1 Size of the trapped bolus increases with an increase in viscosity

and permeability parameters. • Trapped bolus has a larger size for assisting flow case. • Fluid velocity with constant viscosity is less when compared to that of variable viscosity. • Effects of porous medium on pressure gradient and velocity are qualitatively similar. • Unlike the velocity, the temperature of the fluid is higher for constant viscosity case. • Temperature is higher for the case of assisting flow. •

1 Heat transfer rate at the wall decreases with the increase in

channel and magnetic field inclinations. The used values of the parameters here are $? = 0.2$, $? = 1.0$, $? = 1.0$, $? = 0.4$, $Re = 5$, $? = 2$, $? = 0.5$, $? = 0.5$, $? = 0.5$, $? = 0.3$ and $? = 0.3$ (unless stated otherwise). 1.6 1.4 1.5 dp/dx 1.2 1.0 0.8 0

172.6 0.4 $a = 0$, 0.3, 0.

6 dp/dx 1.0 0.5 0.0 $k = 5.0$ $k = 1.5$

85 $k = 0.5$, 0.4, -0.2, 0.0, 0.2, 0.4, -0.4, -0.2, 0.0, 0.2, 0.

4 Fig. 3.1 a x Fig. 3.1 b x 2 1.6 dp/dx 1.0 -1 $a_1 = p/2$ $a_1 = p/4$ $a_1 = 0$ -0.4 -0.2 0.0 Fig. 3.1 c x 0.2 0.4 1.4 dp/dx 1.2 1.0 0.8 0.6 0.4 -0.4 $b = 0$, $p/4$, $p/6$ -0.2 0.0 0.2 Fig. 3.1 d x 0.4 7 6 $Fr = 0.5$ 1.5 5 1.0 dp/dx 4 3 0.5 $M = 0.0$ dp/dx $Fr = 1.0$ 2 1

159 $Fr = 0.5$, -0.4, -0.2, 0.0, 0.2

Fig. 3.1 e x 1.5 dp/dx 1.0 $G_t = -2$, 0, 2 0.5 -0.4 -0.2 0.0 0.2 Fig. 3.1 g

117 x 0.0 -0.5, 0.4 -0.4 1.8 1.6 1.4

dp/dx 1.2 1.0 0.8 0.6 0.4 -0.4 $M = 1.0$

76M = 2.0 -0.2 0.0 0.2

0.4 Fig. 3.1 f x

22Br = 0, 0.5, 1 .0 -0.2 0.0 0.2 0.

4 Fig. 3.1 h x Figs. 3.1 (a-h) Pressure gradient for the various parameters. Fig. 3.2 Streamlines for variation of Hartman number. Fig. 3.3 Streamlines for variation of viscosity parameter. Fig. 3.4 Streamlines for variation of porosity parameter. Fig. 3.5 Streamlines for variation of channel inclination. Fig. 3.6 Streamlines for different inclinations of magnetic field. Fig. 3.7 Streamlines for different Brinkman number. Fig. 3.8 Streamlines for different Grashoff number. 0.5 0.5

34a = 0.0, 0.3, 0.6 k = 0.4, 1, 10 0 .0 0.0

36U U -0.5 -0.5 -1.0 -1 .0 -1 .0 -0.5 0.0

y Fig. 3.9

60a 0.5 1.0 -1.0 -0.5 0.0

Fig. 3.9 b

180y 0.5 1.0 0.

5 a1 = 0, p/4, p/2 0.5 M=0,2,4 0

92.0 0.0 U U -0.5 -0.5 -1 .0 -1.0 -1.0 -0.5 0.0 0.

185 1.0 y -1.0 -0.5 0.0 0.5 1.0

Fig. 3.9 c Fig. 3.9 d y 0.5 Gt = -2, 0, 2 0.5

22Br = 0, 0.5, 1 .0 0.0 0.0

33U U -0.5 -0.5 -1 .0 -1 .0 -0.5 0.0 0.5 1 .0 -1.0 -0.5 0 .0 0.5 1.0

Fig. 3.9 e y y Fig. 3.9 f Figs. 3.9 (a-f) Velocity profile for different parameter. 1.4 1.2

175a = 0.0 1.2 k = 0.5 1.0

1.0 k = 2.0 a = 0.3 0

23.8 0.8 q a = 0.6 q 0.6 0.6

54k=10 0.4 0.4 0.2 0.2 0.0 -1 .0 -0.

5 0.0 0.5 1.0 y Fig. 3.10

114a 0.0 0.5 1 .0 -1.0 -0.5 0.0

Fig. 3.10 b y M = 2.0 1.0 Gt = -2, 0, 2 1.5 0.8 M = 1.0 q

221.0 0.6 q M = 0.0 0 .4 0.5 0.2 0.0 0.0 -1 .0 -0.5 0.0 0.5 1 .0 -1 .0 -0.5 0.0 0.

5 1.0 Fig. 3.10 c y Fig. 3.10 d y 1.4 1.0 a1 = 0, p/4, p/2 b=0 1.2 0.8 b = p/4 1.0 q 0

181.6 0.4 0.8 q 0.6 0.

4 b =

48p/2 0.2 0.2 0.0 -1 .0 -0.5 0.0 0.5 1 .0 0.0 1 .0 -0.5 0.

5 Fig. 3.10 e y -1.0 Fig. 3.10 f y 0.0 Figs. 3.10 (a-f) Temperature profile for different parameters. . ? 0?0 0?3 0?6 0?2 ? 1?0 0?5 2?0 10?0 1?0 ? 1?0 0?0 1?0 2?0 ?? 2 ?1 ? ?? ?0(?) ??4 ??4 0?5 2?32081 1? 76871 1?44276 2?24094 1?71568 1?52373 1?61917 1?91839 2?8159 1?0 -2?0 0?0 2?0 1?0 0?0 ??4 ??2 ??4 0?0 ??4 ??2 1?95425 1?93242 1?91839 1?93242 1?92427 1?92153 2?22499 1?92427 1? 62345 ??4 0?1 0?401872 0?2 0?795321 0?3 1?18027 Table 3.1. Numerical values of heat transfer rate at the wall for different parameters. Chapter 4

102Peristaltic flow in an asymmetric channel

with convective boundary conditions and Joule heating This chapter concentrates

63on the peristaltic transport of viscous fluid in an asymmetric channel. The channel

walls exhibit convective type boundary conditions. Both cases of hydrodynamic and magnetohydrodynamic (MHD) fluids are considered. Analytic solutions

70for stream function and temperature are constructed. Numerical integration is carried out for pressure rise

per wavelength. Effects of influential flow parameters are pointed out through graphs. 4.1 Mathematical analysis

5Consider the peristaltic transport of an incompressible MHD viscous fluid in an asymmetric channel of width

?1 + ?2. The

56?-axis is taken along the length of the channel whereas the ? -axis is taken normal to the ?-axis.. The

flow is due to the waves travelling on the walls of channel. A constant

32magnetic field ?0 is applied in the ? - direction. The

17fluid is electrically conducting while the channel walls are non-conducting. The upper ?1 and lower ?2 walls are maintained at the

temperature ?0 and ?1 respectively. The geometry of the walls is given as follows 2? ?1(?? ?) = ?1 + ? 1??? (? - ??) , $\mu ? \eta ?2(?? ?) = -?2 - ?1??? 2? ? (? - ??) + ? ? (4.1) \mu \eta$ where ?1 and ?1 are the amplitudes of the waves travelling

35on the upper and lower walls,

?

97is the wavelength, ? is the wave speed, ? is the phase difference and ? is the time. The

laws of mass, momentum and energy yield ?? ?? ?? ?? = 0? + (4.2) ? ? ? =- +? +? ? ? ? ? + ? +

42 $\mu ? ? ? ? ? \eta ? ? \cdot ? ? ? ? ? 2 ? ? ? ? ? ?$, - ??02? ? ? ? ? =- +? +? ? ? ? ? +? ? ? ? ? ? ? ?

(4.3) (4.4) $+? 2^3 ?? 2 + ???? + ???? + ???? + ??02?? 2^? h 2 i ??$ (4.5) $\cdot \mu^3 \cdot^3 \cdot \P^3$, where (?? ?)

?

[illegible]

$$2 + ? \mu \parallel \mu \parallel ? \text{Pr}$$

• $\mu^3 \cdot i \cdot \phi \cdot \eta^3 \cdot$, (4.7) (4.8) (4.9) (4.10) (4.11) Here η denotes the kinematic viscosity, η the Hartman

dimensionless temperature. Making use of the

have $\mu \frac{\partial T}{\partial x} = -k \frac{\partial T}{\partial x} + q$ (4.12) $\mu \frac{\partial T}{\partial x} = 0$ (4.13) $0 = k \frac{\partial T}{\partial x} + q$ (4.14) $k \frac{\partial T}{\partial x} = q$ (4.15) $k \frac{\partial T}{\partial x} = q$ (4.16) where Eq. (4.12) indicates that $T = T(x)$. Defining T and F as the dimensionless mean flows in laboratory and wave frames by $T = T(x)/T_0$ (4.15) $F = F(x)/F_0$ which after using $T = T(x)/T_0$ (4.16) give $T = T(x)/T_0$ (4.17) where $T = T(x)/T_0$ (4.18) $F = F(x)/F_0$ (4.19) The convective boundary condition for the temperature can be expressed as follows $T = T(x)/T_0$ (4.20) $F = F(x)/F_0$ (4.21) in which T

wall. Physically this condition states that the

[illegible]

9 A uniform magnetic field B_0 is applied in the z direction and induced magnetic field is neglected. The

21 is the wave amplitude, λ is the wavelength, c is the wave velocity and t is the time. The equations governing the

$$42\mu \text{ } ?? \text{ } ?? \text{ } ?? \text{ } \P \text{ } ? = -?? + ? \cdot ??? \text{ } ???, \text{ } ??? \text{ } ??? + ? \text{ } ??? + ? \text{ } ??? \text{ } ? = ? \text{ } ???2 \text{ } ?2 + ???$$

$$??? + ? \text{ } 2 \text{ } ???? + ???? + ???? + ??'?? \text{ } 2 + ?02 \text{ } ?2 + ???? \text{ } 2^3 \text{ } 2$$

$$(5.5) \quad \mu^3 \cdot \mu^3 = \mu^6$$

, + ? (5.6) where (???) are velocity components in the laboratory frame (???), ? is pressure, ? the concentration field, ? the temperature field, ? mass diffusivity, ?? thermal diffusion ratio, ?? specific heat, ?? concentration susceptibility, ?0 concentration at boundary, ?? and ?0 the fluid mean temperature and temperature at boundary respectively. If (???)

(???) then introducing $\varphi = \psi - \frac{1}{2} \ln \left(\frac{\eta + \sqrt{\eta^2 - 1}}{\eta - \sqrt{\eta^2 - 1}} \right) = \psi(\eta, \tau)$ (5.7) equations (5.2)-(5.6) in wave frame are reduced as follows:

$$65\mu \parallel \text{????} + ? \text{???222} \text{??2} \text{??2} - \text{??02} (? + 1)? + (5.9) \cdot , \text{??} \text{??} \text{??} \text{??2?} \text{??2?} \text{?} (? + 1)\text{??} + \text{???} = -?? + ? \text{???} \text{??2}$$

$$131\mu\text{T} \cdot \text{???} (2 + 1) \text{???} + ? \text{???} ? = ? \text{???} \text{???} + \text{???} \text{???} + ? \text{?} \text{???} \text{?} + \text{??}^3 \text{?}$$

$$2h_i + \dots + 2h_{i-1} + 2h_{i-2} + \dots + 2h_1 + 2h_0 = 2(h_i + h_{i-1} + h_{i-2} + \dots + h_1 + h_0) = 2(5.11) \cdot \mu_i \phi^3 \cdot \eta^3 \cdot h$$

511 **(? + 1) ?? + ? ? ? ? = ? ? ? ? ? ? + ? ? ? ? ? ?** 2 ? ? ? ? ? + **?? ? ? ?** (5.12) , , , ? ? ?
 ? ? ? + **?? ?**, Defining ? = ? = ? = ? ? ? ? = ? ? = ? ? = ? ? ? ? = **?1 ? ? = ? ? = ?**
1 ? ? = ? ? ? ? ? ?1 ? ? ? ? ?1

$$112 \text{Re} \left(\frac{1}{2} \right) + \frac{1}{2} \left(\frac{1}{2} \right) = - \frac{1}{2} + \frac{1}{2} \left(\frac{1}{2} \right) \left(\frac{1}{2} \right)$$

$$112 \text{Re}(\gamma + 1) \gamma \gamma \gamma + \gamma \gamma \gamma \gamma = -\gamma \gamma \gamma \gamma + \gamma \gamma \gamma \gamma \gamma \gamma \gamma \gamma \gamma \gamma$$

29/58

62Re (? + 1) ???? + ? ???? = ?2 ???? 2 ????2? + ?? ?2? + ?? 2 ? ? 2

¶ "Ä μ ? ? + ? 2 ? ? + ? 2 μ ¶ μ ? ? ¶ ! μ ? ? ? ? ¶ # + ???2(? + 1)2 + ? ? Pr ?2 ?2? + ?2? ? (5.17) μ ?2 ? ? 2 ¶ ? (?+1)? + ??? ? ? ? = 1 ?2?2? ?2? + ? ? ?2?2? ?2? + + ? (5.18) μ ¶ ? ? μ ?2 ?2? ¶ μ ?2 ?2? ¶ Making use of the long wavelength and low Reynolds number approximations we obtain ? ? ?3? ? ? ?3 = - ?2 ? ? + 1 ? μ ? ¶ ? ?4?4 - ? 2 ????22 = 0 ? ? ? = 0 ? (5.19) (5.20) (5.21) 0 = ????2? + ? ? ?2?2? 2 + ????2 ? (5.22) μ ? ? 2 ?2? ¶ μ ? ? + 1 + Pr ? ? ?2 ¶ 0 = ? ? ?2 + ? ? ?2 1 ?2? ?2? ? (5.23) in which ? 6 = ? (?) ? u denotes the kinematic viscosity, ? the Hartman number, Re the Reynolds number, ?? the Brinkman number, ?? the Dufour number, ?? the Soret number, ?? the Schmidt number, ? the Eckret number, ? ? the Prandtl number, ? the wave number and the dimensionless temperature and concentration are ? and ? respectively. The boundary conditions are ? = 0, ?2? ? ? ? ?2 = 0, ?? = 0? ? ? = 0? ? ? = 0, ? = ? , ?? ?? = -1, ? = 0, ? = 0, ?? ? = ?, (5.24) ?(?) = 1 + ? cos(2??), ? = ? ? ? Z0 ? ? ? ? (5.25) Pressure rise per wavelength Δ?? at this stage is 1 Δ?? = ???? ? ? (5.26) Z0 Heat transfer coefficient ? for this problem is defined as ? = ???? 5.2 Solutions expressions Solving the above equations subject to the corresponding boundary conditions one finds that ? = ? ? ? cosh (??) + ? sinh (??) - (? + ?) sinh (? ?) ?? cosh (??) - sinh (??) ? (5.27) ?? (? + ?) ? 3 cosh (??) ?? = - ?? cosh (??) - sinh (??) ? (5.28) ? = 8 (-1 + ??P?r?2? (?2? ?1? -)) (-2?c?oshc[?sh(?)? + ? + 3 + sin?h4(?)?))2 ? ? = 8 (-?1? + ?P2r????????(???) + (-??2? cosho[s(h2?(???)) - ?s3in+h (??4?)))2 ? where ?1 = ? 4 + ? + ?3?4 - 1 + ?2?4 ?2 + ?2?2 1 + ?2 (? - ?)(? + ?) + 2 2 + ? ? ?2 1 + ?2 (? - ? ? ?) ? ? ?2 = ?2 1 + ?2 + 2? ? 4 + ? + ?2 - 2?2 + ? ? 8 + ? ?3 + ?2?1 + ?2 - 2?2 ? ? ?3 = (? + ?)2 1 ? + ?2 ? cosh[2??] + ?4? ? 2 ? ? + ?(2 ? + ?) - ? ?2 sinh[2??] - ? ?1 ?6 ? (? + ?) ? cosh[??] (? - ?) + sinh[??] ? ? ?4 = 16(? + ?)sinh[? ? ?] (? - ?) + sinh[??] ? ?1 = -8? - 2?(4 + ?) - 2?2(? + 2?) ?2 - 2?2(? + ?) ?2 + 2 1 + ?(? + 2?) ?2 + (? + ?) ?2 ? 4 ? 2 ? ?2 = ?2 1 + ?2 + 2 ? 4 + ? + ? ? 2 - 2?2 + ? 8 + ? 3 + ? ? 2 1 + 2?2 ? - 2?2 ? ? ?3 ? = (? + ?)2 1 ? + ? 2 cosh[2? ? ?] ? - 4?? 2 ? ? + ? (2 + ?) ? - ? ? ?2 sinh[2??] ? ?4 = 16? (? + ?) ? cosh[??] ? (? - ?) + sinh[? ? ?] - 16 (? + ?) sinh[??] ? (? - ?) + sinh[? ? ?] ? (5.29) (5.30) 5.3 Discussion Here Figs. 5.1(a-e) are drawn for the temperature, Figs. 5.2(a-e) for concentration and Figs. 5.3(a-e) for the heat transfer coefficient. Tables 5.1 and 5.2 describe the temperature and concentration gradients. It is observed that with an increase in M the temperature increases. An increase in temperature becomes more apparent with an increase in M (see Fig. 5.1a). This fact agrees well to the expected results of Ohmic heating i.e. the temperature increases with an increase in the magnetic field strength. This fact is quite opposite to the observed results of behavior of M on temperature in the previous attempts by several other authors who considered the magnetic field but ignored the effects of Ohmic heating which in turn gives the lesser accurate prediction about the behavior of temperature for different values of M. From Figs. 5.1(b-d), the temperature increases with an increase in Schmidt, Dufour and Soret numbers but contrary to the previous case this increase is not much. Fig. 5.1(e) shows that there is rapid increase in temperature with an increase in the Brinkman number. From Figs. 5.2(a-e), we can clearly see that there is decrease in the concentration with an increase in M, Sr, Sc and Br. This decrease is more in case of Hartman number M and Brinkman number Br when compared with the other parameters. The result that concentration decreases effectively with an increase in ? is of considerable importance. This means that we can use the heating effect of applied magnetic field to develop small thermal gradients which in turn can be used to control the concentration of any particular substance in the fluid. This result has wide range of applications especially for cure of several diseases, for instance clearing several type of blockages in many arteries that exhibit peristaltic mechanism. The thermal gradients can be used more efficiently in place of radiations with lesser side effects. These thermal gradients can also be used for the transport of several minerals and medicine within the human body on the desired location. Heat transfer coefficient has its own physical significance in problems related to heat transfer. It is always helpful to examine the behavior of heat transfer coefficient (? in this case) for a given problem. Keeping this in mind the Figs. 5.3(a-e) are explicitly plotted to examine how ? develops throughout the flow field. In all the Figs. 5.3(a-e), Z has oscillatory behavior which is due to peristalsis. In all these Figs. the absolute value of heat transfer coefficient is positive. Fig. 5.3(a) shows a rapid fluctuation in Z for changing values of M. From Figs. 5.3(b-d), it is quite obvious that the Du, Sc and Sr effect the heat transfer coefficient but this effect is relatively smaller when compared with the effects of other parameters like Br, M and d. Since Soret and Dufour effects have gained reasonable interest in convective heat and mass transfer. One cannot neglect such effects when there is appreciable density difference in the flow regime. The concentration gradient in fact yields the thermal energy flux (referred as Dufour effect) whereas the temperature gradients contribute to the mass fluxes (referred as Soret effect). One can neglect Soret and Dufour effects in heat and mass transfer mechanism when such effects are small in comparison to the effects by Fourier's or Fick's laws. Motivated by this fact we computed the temperature and concentration gradients at ? = ? in the Tables 5.1 and 5.2. It is noticed from Table 1 that magnitude of temperature gradient increases when ?? Du and Br are increased. However the situation is reverse when there is an increase in a. Table 5.2 depicts that concentration gradient is an increasing function of M, Du, Br and Sr. Further the concentration gradient is decreasing function of a. ?a? Du=0.5,Sc=0.5,Sr=0.5,Br=0.5 ?b? M=1,Sc=0.5,Sr=0.5,Br=0.5 1 1.5 M= 0.5 M= 1.0 Du = 0.2 M= 1.5 Du = 0.4 Du = 0.6 1.25 M= 2.0 0.8 Du = 0.8 1 0.6 q q 0.75 0.4 0.5 0.25 0.2 0 0 0 0.2 0.4 0.6 0.8 1 1.2 y 0 0.2 0.4 0.6 0.8 1 1.2 y ?c? Du=0.5,Sc=0.5,M=1,Br=0.5 1 Sr = 0.2 Sr = 0.4 0.8 Sr = 0.6 Sr = 0.8 0.6 q 0.4 0.2 0 0 0.2 0.4 0.6 y 0.8 1 1.2 ?d? Du=0.5,Sr=0.5,M=1,Br=0.5 ?e? Du=0.5,Sc=0.5,M=1,Sr=0.5 1 Sc = 0.2 Sc = 0.4 1.4 Br = 0.2 Br = 0.4 0.8 SScc == 00..68 1.2 Br = 0.6 Br = 0.8 1 0.6 0.8 q q 0.4 0.6 0.2 0.4 0.2 0 0 0.2 0.4 0.6 0.8 1 1.2 0 0.2 0.4 0.6 0.8 1 1.2 y y Fig. 5.1(a-e) Variation of temperature when ? = 0?3? ? = 1?4? and ? = 0? ?a? Du=0.5,Sc=0.5,Sr=0.5,Br=0.5 ?b? M=1,Sc=0.5,Sr=0.5,Br=0.5 0 0 -0.1 -0.1 f -0.2 f -0.2 -0.3 -0.3 M = 0.5 M = 1.0 Du = 0.2 M = 1.5 Du = 0.4 M = 2.0 Du = 0.6 -0.4 Du = 0.8 -0.4 0 0.2 0.4 0.6 0.8 1 1.2 0 0.2 0.4 0.6 0.8 1 1.2 y y ?c? M=1,Sc=0.5,Du=0.5,Br=0.5 0 -0.25 -0.5 f -0.75 -1 -1.25 Sr = 0.2 Sr = 0.4 Sr = 0.6 -1.5 Sr = 0.8 0 0.2 0.4 0.6 0.8 1 1.2 y 0 ?d? M=1,Sr=0.5,Du=0.5,Br=0.5 0 ?e? M=1,Sr=0.5,Du=0.5,Sc=0.5 -0.05 -0.1 -0.1 f -0.2 -0.15 0.3 -0.2 -0.3 -0.4 Sc = 0.2 Sc = 0.4 Sc = 0.6 Sc = 0.8 0 0.2 0.4 0.6 0.8 1 1.2 y -0.25 -0.3 -0.35 0 0.2 0.4 0.6 y 0.8 1 Br = 0.2 Br = 0.4 Br = 0.6 Br = 0.8 1.2 Fig. 5.2(a-e) Variation of concentration when ? = 0?

3? ? = 1?4? and ? = 0? ?a? Br=0.5,Sr=0.5,Du=0.5,Sc=0.5 ?b? Br=0.5,Sr=0.5,M=1,Sc=0.5 20 M = 0.5 1.0
 10 M = 1.5 = 2.0 10 5 Du = 0.2 Du = 0.4 Du = 0.6 Du = 0.8 Z 0 Z 0 -10 -5 -20 -10 0 0.2 0.4 0.6 0.8 1 x 0
 0.2 0.4 0.6 0.8 1 x ?c? Br=0.5,Du=0.5,M=1,Sc=0.5 10 Sr = 0.2 Sr = 0.4 Sr = 0.6 Sr = 0.8 5 Z 0 -5 -10 0 0.2
 0.4 0.6 0.8 1 x ?d? Br=0.5,Du=0.5,M=1,Sr=0.5 ?e? Sc=0.5,Du=0.5,M=1,Sr=0.5 40 10 Br = 0.2 Br = 0.4 Br =
 0.6 5 20 Br = 0.8 Sc = 0.2 Sc = 0.4 Sc = 0.6 Sc = 0.8 Z 0 Z 0 -5 -20 -10 -40 0 0.2 0.4 0.6 0.8 1 0 0.2 0.4
 0.6 0.8 1 x x Fig. 5.3(a-e) Variation of Z when ? = 0?3? ? = 1?4? and ? = 0? ? ? ? ? ? ? ? 0?5 1?0 0?5 0?3 1?
 0 1?5 2?0 0?0 0?5 1?0 1?5 ?0(?) -2?8569 -3?6054 -5?0997 -7?7157 -2?7040 -3?0903 -3?6054 -4?
 3265 0?0 0?5 1?0 1?5 0?2 0?0 -3?0903 -6?1807 -9?2711 -3?3563 0?4 -2?5868 0?6 -2?11325 0?8
 -1? 81531 Table 5.1: Variation of ???? ?=? via different parameters. ? ? ? ? ? ? ?0(?) 0?5 1?0 0?5 0?3
 0?5 0?71424 1?0 0?90136 1?5 1?2749 2?0 1?9289 0?0 0?6760 0?5 0?7725 1?0 0?9013 1?5 1?0816 0?
 0 0?0 0?5 0?7725 1?0 1?5452 1?5 2?3178 0?2 0?8390 0?4 0?6467 0?6 0?5283 0?8 0?4538 0?2 0?
 2787 0?4 0?5753 0?6 0?8914 0?8 1?2291 Table 5.2: Variation of ???? ?=? via different parameters.
 Chapter 6 Soret and Dufour effects on peristaltic transport of MHD fluid with variable viscosity This chapter
 looks at the Soret and Dufour effects on the magnetohydrodynamic (MHD) peri- staltic flow of variable
 viscosity fluid in a symmetric channel. Modeling is presented in the presence of Ohmic heating.
 Mathematical analysis is carried out through large wavelength and small Reynolds number. Results for the
 stream function, temperature and concentration are developed. The variations of sundry parameters on
 the flow quantities of interest are sketched and examined. 6.1 Mathematical analysis Let us investigate the
 magnetohydrodynamic flow of an incompressible viscous fluid in a channel with width 2?1. The ?- axis is
 chosen along the walls of channel and ? - axis is taken normal to the ?- axis. A constant magnetic field of
 strength B0 is exerted in the ? - direction. Induced magnetic field is not accounted. Sinusoidal wave
 propagates along the channel walls with constant wave speed ? represented by ?(?? ?) = ?1 + ?1??? ? ?
 (? - ??) . (6.1) $\mu \parallel$ If (?? ?) and (?? ?) are the velocity components in the laboratory (?? ?) and wave (??
 ?) frames then transformations between laboratory and wave frames are ? = ? - ??? ? = ? ? ? - ?? ? =
 ? ? (?? ?) = ? (?? ? ? ? ? ?) (6.2) In above expressions ?1 is the wave amplitude, ? is the wavelength, ? is
 the time and ? and ? are the pressures in the laboratory and wave frames respectively. Introducing the
 variables in the forms ? = ? ? ? = ? ? = ? ? ? ? ? ? = ?1 ? ? = ? ? ? = ?21? ? ?1 ? ? ? ? ? ?1
 ???0 ? = ? - ?0 ? ? = ? - ?0 ? ? = ? 1?2 ? ?0?1? u = ?0 ? ?? = ???1 ? 0 ? 0 μ 0 \parallel ? ? 0 ? = ? ? ? ?
 =??????=-??? ? ?=Pr?? ??=?????0??0??0, ??=???0?????00? ?? = ?0? ? = ?2 ??? ?(??) ? ?? = ?
 ? and?(?)= ?0 ? (6.3) ??? ? the governing equations after adopting long wavelength and low Reynolds
 number approxima- tion become ???? ? ? (??)??2??2 - ?2 = ? μ ?? +1 ? \parallel μ ?? \parallel ??2 ?(?) ??2 - ? ?2 ??2
 2 ??2 = 0? μ \parallel ??2 0 = ??2??2 + ???(?) ??2??2 + ???2 2 ?? 2 ? μ ??2 +1 \parallel μ ?? \parallel + Pr ?? ??2 1 ??2 ??2
 0 = ?? ??2 + ?? ??2 ? (6.4) (6.5) (6.6) (6.7) where ? is the pressure, ? the concentration field, ? the
 temperature field, ? mass diffusivity, ?? the thermal diffusion ratio, ?? the specific heat, ?? the
 concentration susceptibility, ?(?) the variable viscosity, ?? the fluid mean temperature, u the kinematic
 viscosity, ? the Hartman number, Re the Reynolds number, ?? the Brinkman number, ?? the Dufour
 parameter, ?? the Soret parameter, ?? the Schmidt number, ? the Eckret number, ? ? the Prandtl number,
 ? the wave number, ? the stream function, ? the dimensionless temperature and ? the concentration. The
 boundary conditions are ? = 0, ?? ? ? ? ? ?2 = 0, ?? = 0? ? ? = 0? ? ? = 0, ? = ? , ?? ? ? = -1, ? = 0, ? =
 0, ?? ? = ? , (6.8) ?(?)=1 + ? cos(2??), ? = ? ? ? Z0 ? ? ??? (6.9) Pressure rise per wavelength $\Delta?$ is $\Delta? =$
 ?? ??? 1 ?? (6.10) Z0 The dimensionless expression of space dependent viscosity is ?(?) = ?-?? = 1 - ??
 ? ? 1? where "?" is the viscosity parameter. We look for solutions in the series form represented below ? =
 ?0 + ???1 + ??? ? ? = ?0 + ???1 + ??? ? ? = ?0 + ???1 + ??? Employing the procedure of perturbation
 method and retaining the results up to order ?(?) we have ? = ?1 + 8(-?? co(s?h(+???)?)?+?s2inh(??))2 ?
 (6.11) ? = -8 (-1 + Pr ?????) (?????c2o?sh1 (??) - sinh (??))2 (6.12) - 32 (-?1??+ ?Pr??2??+???
 3?+)(??4-co?s5h +(??6)---?si7n+h(??8?))3 ? ? = -8(-1+Pr???????2??)(?????[?co1s-h?(??2+?)
 -3]sinh(??))2 + ???????6[4?(-4+1?+5P+r2?(??6?+???)7(+?14?co(?sh8(+??9)---?si1n0h)- (??
 11)-3?12+?13)]? (6.13) where the involved A?(? = 1? 2)? B?(? = 1 - 8) and C?(? = 1 - 13) are ?1 = ? ?
 ? cosh(????) j+os?hs(i?n?h(?)-?si)n-h((??+?)) sinh(?? ?) ? ?2 = ??3 + (?? ? cosh (?? ?) + ?3? 2 - ? sinh
 (??))2 sinh (?? ?) ? ?3 = -1 + 2??2 2 + cosh (2??) + 2? ? cosh (?? ?) (i-?? ϕ cosh (??) + sinh (??)) - 2??
 sinh (2??) ? ?1 = -8? - 2? (4 + ?) - 2? + ??2 (?? + 2?) ? 2 - 2?? (?? + ?)2 ? 4 + 2(1 + ? (?? + 2?) ? 2 + (?? +
 ?)2 ? 4)2 + (?? 2 1 + ? 2 +2? 4 + ? + ?? 2 - 2??2 + ? 8 + ? 3 + ? 2 1 + 2?? - 2??2) cosh (2i??) - (?? + ?)2
 1 + ? ? 2 cosh (2?2?) - 4?? 2i? + ?i(2 + ?) - i ?2 sinh (2??2?) ϕ + 16? (?? + ?) ? c?osh (??2?) (?? - ?) + sinh
 (i? ?)) - 16 (?? + ?) si ϕ nh (??) ? (?? - ?) + sinh (??)?? ?2 = -8?3 (?? + ?) (?? - ?) sinh (2??) ? 4 - 12 (?? +
 ?) ?9 cosh (??) - 16?4 (?? + ?) ? 4 cosh (??) ?3 + 8?3 (?? + ?) ? 4 (?? - ?) cosh (2??) ? ?3 = 12 (?? + ?) (3 (??
 + ?) + 3 ? ? - 8?2 ? 2 + 8?4? 4) cosh (3??) + 16?2 (?? + ?) ? 4?2 cosh (??)2 cosh (?? ?) - j2? (?? + ?)2 ϕ ?
 2 1 + ? ? 2 ? cosh (??) cosh (2? ?) ? ?4 = (?? + ?) ? ?10 sinh (??) ? ?5 = 64? 1?2? 3 c?osh (??2?)2 sinh (??
) + 2?3 (?? + ?)2 ? 3 1 + ? 2

$$9\cosh(2? ?) \sinh(?? ?) + 2(?? + ?)2 ? 1 + ? 2 ? \cosh(2? ?) \sinh$$

(???) + 16 (?? + ?) ? 2?2 cosh (?? ?) sinh (??) ?2 - 8?4 (?? + ?) ?i 5 (?? - ? ϕ) sinh (2??) ? ?6 = ?? ?11 cosh
 (??) sinh (2??) ? ?7 = ?? (-4? + ? 2 - 4? + 2? ? + ?2 + (?? + ?)2 1 + ?? 2 ? 2 + ?2 (?? + ?)2 ? 4) sinh (3??))
 - 16?2 (?? + ?) ? 3? cosh (??)2 sinh (?? ?) + 1?6?3 (?? + ?) ? 3 sinh (??)2 sinh (?? ?) - 16 (?? + ?) ? ? sinh
 (??)2 sinh (?? ?) - 8?4 (?? + ?) ? 4 sinh (2??) sinh (?? ?) ? ?8 = 16? (?? + ?) ? 2? sinh (2??) sinh (?? ?) + (??
 + ?)2 1 + ? 2 - 3 + 2? 2?2 sinh (??) sinh (2? ?) - ? (?? + ?) ? cosh (??) ?12? ?9 = i ? 1 + ϕ ? ? 2 (3 + 4??
 ϕ 2(-3? +2?3? 2 + 2? - 2? 2?3)) + ?(3 + ? 2(3 + 4?(? -3 + ? 2 -j3 + 2? ϕ 1 + ? + ?? 2 +2 (-3 + ?) + 2? 2?
 - 2? 2 1 + ? 2 ?3)))? ?10i = -3? (4 + i ? + ?) + i ?(-3 + 5 ϕ ?2 ϕ + ? (-3 + ? (16 + 5?)))? 2 + i?3 (?? + ϕ ?) 5 +
 4?2 ? 4 + 4?5 (?? + ?) ? 6 + 4i (?? + ?) ϕ 1 + ? 2 ? - 4?3 (?? + ?) ? 4 1 + ? 2 ?i2 - 4 (?? + ?) ? 2 1 + ? 2 ?3?
 ?11 = -3 (?? + ?)2 + i -3? 2 ϕ - 6? ? + 32? 1? + (-j3 + 2? (ϕ 8 + ?)) ?2 + 4 (4 + ?i) ?3 + 2 ϕ ?4 ? 2 + 2?2 (?? +
 ?)2 ?i4? ?12 = 16? 2?2 sinh (?? (?? - ?)) + (?? + ?) 1 + ? 2 -3 + 2? 2?2 ϕ sinh (2? ?) + 16 ? 2?2 sinh (?? (?? +
 ?)) ? ?1 = 2?14 - 16? (?? + ?i) ? 2 (??-i ?) cosh (??) ϕ - (?? 2 1 + ? 2 +2? 4 + ? + ?? 2 - 2?2 + ? 8 + ? 3 +
 ? 2 1 + 2?2 - 2?2) cosh (2??) ?i?2 = 8? ϕ cosh (i? (?? - ?)) - ϕ 8? cosh (?? (i? - ?)i) + ? 2 cojsh (2? ?) +

$$2\epsilon^2 \cosh(2\epsilon) + 2 \cosh(2\epsilon) + 2\epsilon^2$$

$$9 \cosh(2\tau) + 2\tau^2 \cosh(2\tau) + \tau^2 \cosh(2\tau) + 8(\tau + \tau) \cosh(2\tau)$$

$$\begin{aligned} & (2 \sinh(x) + 16 \sinh(2x) - 16 \sinh(3x) - 16 \sinh(4x) + 8 \sinh(5x)) \\ & \sinh(2x) + 8 \sinh(3x) \end{aligned}$$

$$9 \sinh(2??) + 4?^3 \sinh(2??) - 4??^2 \sinh(2??) + 8?^? \sinh$$

$(? \, (? \, - ?)) + 8?2? \sinh (? \, (? \, - ?)) - 8? \, (? \, + ?) ? \sinh (? \, (? \, + ?)) ? \, ?4 = (3 \, (? \, + ?)2 + 3? \, 2 + 6? \, (1 - 4?) ? + ? \, (64? \, 1 + 3 \, (1 - 8?) ?) ? \, 2) \cosh (3??) ? \, ?5 = 2? \cosh (??) ?2 \, ?15? \, ?6 = -8?3 \, (? \, + ?) ? \, 4 \, (? \, - ?) + 2 \, (? \, + ?)2 ? \, 1 + ? \, 2 \, ?3? \, 2 + ? \cosh (? \, ?) ? \, ?7 = 2? ? \sinh (??) + 16 \, (? \, + ?) ? \, ?22 \cosh (? \, ?) \sinh ? \, (??) ?2 \, ?? ? ? ?8 = 64? \, 1? ? ? \cosh (??) + 32?3 \, (? \, + ?) ? \, 3 \, (? \, - ?) \cosh (2??) - 64? \, 1? ? \cosh (3??) ? \, ?9 = ?16 \sinh (??) ? \, ?10 = 32?4 \, (? \, + ?) ? \, 4 \, (? \, - ?) \sinh (2??) + (-? \, (? \, + ?) - 8 + 5? + 5? + (5? + (5 - 16?) ?) ? \, 2 + 8? \, 1 \, 4 + ? \, + ? \, + ? \, - 4?2 \, ? \, 2) \sinh (3?? ? \, ?) ? \, ?11 = 4? ? \, 1 \, 4 - 4?2? \, 2 + 4? \, (? ? + ?) - ?3? + ?2? \, 2 \, (3? ? + ?) + 4? ? (? \, 1 \, ? \, 4 - 4?2? \, 2 +$

$$434? \left(? + ?_j \right) ? + ??? 2\phi(-? + ?) \cosh_j(???) + 4? 2? \left(? + \phi? \right) ? \left(?3? 2 - j2? \right)$$

$$\sinh(2\theta) \sinh(\theta) + \frac{1}{2} 4\theta^2 (1 + \theta^2) - 2\theta^2 \sinh(\theta) \sinh(2\theta) + \frac{1}{2} 12 = \cosh(\theta) (\theta + \theta^2 + \theta^3 + \frac{1}{2} 4\theta^2 - \cosh(\theta) + 2\theta^2 - 2\theta^2 \cosh(\theta) + \cosh(\theta) (\theta + \theta^2 + \theta^3 + \frac{1}{2} 4\theta^2 - \cosh(\theta) + 2\theta^2 - 2\theta^2 \cosh(\theta))) + \frac{1}{2} 64\theta^2 \cos$$

$$119j\hbar(???) + 4?c(?? + ?)2?21 + ?2? \cosh(???) + j2??-3?c2?1??2 \sinh(???)$$

(+ ? + ?) ?18 ? ?14 = ? 4 + ? + ?3 ?4 ? - 1 + ?2 ? 4 ?2 + ? j ?2 ? 1 + ? 2 (? - ?) (? + ?) + ?2 (2 + ? ? ? 2 ? 1 + ? j ? 2 (? - ?) (? ? + ?)) , ?15 = 16 ?2 (? ? + ?) ? 3 ?2 c josh (? ? ?) - (? (? + ?) -8 + 5 ? + 5 ? + i(5 ? + (5 ? - 16 ?) ?) ? 2 + 8 ? 1 4 + ? + ? + ? + ? + 4 ?2 ? 2) sinh (??i) - 8((4 ? 1 - 1 + ?2 ? 2 + (? + ?) (? + ? ?2 ? 2 (-j ? + ?))) sinh j(? ?) ? ?16 = ?8 ? 1 ?4 + ? + ? + ? + ? - j 4 ?2 ? 2 + ? (? + ?) ?17 ? ?17 = ?(-56 + ? 1 + ? 2 -13 + 24 ?j ?2 ? 2 + 16 ?4 ?j 4 + ?(-13 ? + ? 2 ?(-13 + 8 ?(10 + ? 1 + ? 2 3 + 2 ?2 j ? 2))) ? + j 16 (? + ?) 1 + ? 2 ? - 1 ?6 ?3 (? + ?) ? 4 1 + ? 2 ?2 - 16 (j ? + ?) ? ?j 2 1 + ? 2 ? ?3 ? ?18 = 16 ? ?2 ? sinh (? (? ? - ?)) + (? + ?) 1 + ? j ? 2 - ?3 + 2 ? ?2 ?2 sinh (2 ? ?) + j 16 ? ?2 ?2 sinh (? (? + ?)) ? j ? j ? Heat transfer coefficient is defined as follows: $\eta = \frac{\mu}{k} \frac{du}{dy}$ 6.2 Discussion This section describes the impacts of pertinent parameters on the temperature and concentration. We recall that theme of this study is to point out the influences of Soret and Dufour. Therefore, the results of various parameters associated with velocity are not included. In order to achieve the desired objective, we present the plots in such a way that the left panels are for constant viscosity (i.e. for $\eta = 0$) and the right ones are for variable viscosity ($\eta = 0.4$). It is observed in all the graphs related to temperature that the rise in temperature for variable viscosity fluid is relatively slower when compared with fluid having constant viscosity. Here Figs. 6.1-6.5 are drawn for temperature whereas the Figs. 6.6-6.10 show variation of concentration. Temperature increases with an increase in M (Fig. 6.1). Further an increase in temperature is abrupt in view of Ohmic heating. The variations of Du, Sr, Sc and Br on the temperature are displayed in the Figs. 6.2-6.5. These Figs. indicate that there is an increase in temperature by increasing Du, Sr, Sc and Br. It is also found that an increase in temperature is more for Br when compared with the other parameters. Figs. 6.6-6.10 are presented to examine the behavior of embedded parameters on the concentration. Increase in concentration is observed when M and Du are increased (see Figs. 6.6 & 6.7). Concentration also increases when Sr, Sc and Br are increased (Figs. 6.8-6.10). Behavior of heat transfer coefficient Z for various parameters is shown in the Figs. 6.11-6.15. As expected Z shows an oscillatory behavior which is because of peristalsis. It is also noted that there is no variation in Z for amplitude ratio (γ) between 0 and 0.3. It is observed from Fig. 6.11 that Z increases when M is increased. The absolute values of Z in variable viscosity fluid are more than the constant viscosity fluid. Figs 6.12-6.15 show that Z increases with the increase in Du, Sr, Sc and Br. Effects of Du, Sr, Sc and Br on Z are opposite to that of M. Fig. 6.1 Effect of M on θ when $\eta = 0.5$? $\eta = 0.5$? $\eta = 0.5$? $\eta = 0.3$? $\eta = 1.4$, $\eta = 0.5$ and $\eta = 0$? Fig. 6.2 Effect of Du on θ when $\eta = 0.5$? $\eta = 0.5$? $\eta = 0.5$? $\eta = 0.3$? $\eta = 1.4$, $\eta = 0.5$ and $\eta = 0$? Fig. 6.3 Effect of Sr on θ when $\eta = 0.5$? $\eta = 0.5$? $\eta = 0.5$? $\eta = 0.3$? $\eta = 1.4$, $\eta = 0.5$ and $\eta = 0$? Fig. 6.4 Effect of Sc on θ when $\eta = 0.5$? $\eta = 0.5$? $\eta = 0.5$? $\eta = 0.3$? $\eta = 1.4$, $\eta = 0.5$ and $\eta = 0$? Fig. 6.5 Effect of Br on θ when $\eta = 0.5$? $\eta = 0.5$? $\eta = 0.5$? $\eta = 0.3$? $\eta = 1.4$, $\eta = 0.5$ and $\eta = 0$? Fig. 6.6 Effect of M on ϕ when Du=0.5, Sr=0.5, Sc=0.5, $\gamma = 0.3$? $\gamma = 1.4$, Br=0.5 and x=0. Fig. 6.7 Effect of Du on ϕ when $\eta = 0.5$? $\eta = 0.5$? $\eta = 0.5$? $\eta = 0.3$? $\eta = 1.4$, $\eta = 0.5$ and $\eta = 0$? Fig. 6.8 Effect of Sr on ϕ when $\eta = 0.5$? $\eta = 0.5$? $\eta = 0.5$? $\eta = 0.3$? $\eta = 1.4$, $\eta = 0.5$ and x=0. Fig. 6.9 Effect of Sc on ϕ when $\eta = 0.5$? $\eta = 0.5$? $\eta = 0.5$? $\eta = 0.3$? $\eta = 1.4$? $\eta = 0.5$ and $\eta = 0$? Fig. 6.10 Effect of Br on ϕ when $\eta = 0.5$? $\eta = 0.5$? $\eta = 0.5$? $\eta = 0.3$? $\eta = 1.4$, $\eta = 0.5$ and $\eta = 0$? Fig. 6.11 Effect of M on Z when $\eta = 0.5$? $\eta = 0.5$? $\eta = 0.5$? $\eta = 0.3$? $\eta = 1.4$ and $\eta = 0.5$ and $\eta = 0$? Fig. 6.12 Effect of Du on Z when $\eta = 0.5$? $\eta = 0.5$? $\eta = 0.5$? $\eta = 0.3$? $\eta = 1.4$ and $\eta = 0.5$? Fig. 6.13 Effect of Sr on Z when $\eta = 0.5$? $\eta = 0.5$? $\eta = 0.5$? $\eta = 0.3$? $\eta = 1.4$ and $\eta = 0.5$? Fig. 6.14 Effect of Sc on Z when $\eta = 0.5$? $\eta = 0.5$? $\eta = 0.5$? $\eta = 0.3$? $\eta = 1.4$ and $\eta = 0.5$? Fig. 6.15 Effect of Br on Z when $\eta = 0.5$? $\eta = 0.5$? $\eta = 0.5$? $\eta = 0.3$? $\eta = 1.4$ and $\eta = 0.5$? Chapter 7 Soret and Dufour effects

102on peristaltic flow in an asymmetric channel

This chapter studies the combined

2effects of heat and mass transfer on the peristaltic flow of magnetohydrodynamic (MHD) fluid in an asymmetric channel. Asymmetry in channel is induced because of

the wave amplitude and phases. Analysis

1has been performed in the presence of slip condition.

Attention has been given to the Soret and Dufour effects. The obtained results are plotted and discussed.

7.1 Mathematical analysis

We consider MHD

63flow of incompressible fluid in an asymmetric channel. The

η -axis is selected along the channel walls and η -axis perpendicular to the η -axis. The flow is due to the sinusoidal wave trains travelling

6 on the walls of the channel with speed

?? The geometry of the waves is given below

$$r_1 \cos(\theta_1 - \theta_2) = r_1 \cos(\theta_1) \cos(\theta_2) + r_1 \sin(\theta_1) \sin(\theta_2)$$

¶ (7.1) (7.2) in which a_1 and b_1 are the amplitudes of the waves travelling

153on the upper and lower walls respectively, ? is the

phase difference of two waves and $\phi_1 + \phi_2$ is the

176width of the channel. The phase difference

? ranges $0 \leq ? \leq ??$ Here $? = 0$

37 corresponds to the symmetric channel with waves out of phase and for $\theta = \pi$ the waves are in phase. Moreover a_1, b_1 and a_2, b_2 satisfy the

$$\text{condition } r_1^2 + r_2^2 + 2r_1r_2 \cos(\theta) \leq (r_1 + r_2)^2$$

16 A uniform magnetic field B_0 is applied in the transverse direction to the flow. Effects of induced magnetic

field are not considered by choosing low magnetic Reynolds number. However, Joule heating and

¹⁰⁴Soret and Dufour effects are taken into account. The

equations

104of mass, momentum, energy and concentration in the

laboratory frame (?? ?) are ?? ?? ?? = 0? + (7.3) ? + ?? + ? ?? + ? ?? = -?? ?? 2??? ? ? ? ?? + ?
?? + ? μ ?? μ ?? $\cdot \mu$????? ?? \mathbb{I}_μ - ??02?? (7.4) ? ? + ? ? ? ?? + ? ? ? ?? μ ?? ? ? ?
 $\mathbb{I} = -?? ? ? \cdot \mu ? ? ? ? \mathbb{I} \cdot (7.5) ? ?$

42μ ?? ¶ ??? ??? + ? ??? + ? ??? ? = ? ???2? 2 + ???2?2 +? 2 ???? + ???? +
 ???? + ????' 2 + ?02 ?2 + ???? 2³ 2 h i · ½³ · 3³ · ¾³ · h ???

Sc and Pr whereas it increases by increasing γ_1 and γ_2 . Here decrease in γ is much for M, γ_3 ? Sr, Sc, Pr and small for Du. Moreover the concentration remains invariant for thermal slip parameter γ_2 ? Figs. 7.4(a-e) are plotted to see

1 the behavior of heat transfer coefficient Z_1 at the upper wall?

Because of peristalsis it is found that, Z_1 has an oscillatory behavior. Moreover Z_1 has maximum value near the upper wall. It increases with the increase in M and γ_2 . Further Z_1 decreases with increase in d and γ_1 ? An interesting and noteworthy fact is that the thermal slip parameter γ_2 has no meaningful variation on Z_1 ? 7.3 Main points Simultaneous

2 effects of heat and mass transfer on the peristaltic transport of viscous fluid in an asymmetric channel with slip effects are

analyzed. Their main observations are summarized as follows: • The trapped bolus gets elongated as the value of viscosity parameter is increased. •

17 Effects of Hartman number M, Dufour number Du and

temperature slip parameter γ_2 on the temperature are opposite to that of velocity slip parameter γ_1 . • Increase in temperature subject to an increase in Hartman number M is rapid when compared to that of other parameters. • Increase in applied magnetic field results in decrease of concentration. • Thermal slip parameter has no effect on the fluid concentration. •

29 Absolute value of the heat transfer coefficient increases with increase in

the Hartman number M. Fig. 7.1. Effect of velocity slip parameter γ_1 on stream lines. 5 20

77 $b_2 = 0.1, 0.2, 0.3, 0.4$

15

19 $M = 0.5, 1.0, 1.5, 2.0$

144 $0 < q < 10$ $q = -5, -10, -1.5, -1, 0$

-0.5 y 0.0 Fig. 7.2

34 $a = 0.5, 1.0, 1.5, 2.0$

2 Fig. 7.2 b y 4.0 Du = 0.5, 1.0, 1.5, 2.0 4.0 Sr = 0.5, 1.0, 1.5, 2.0 3.5 3.5 3.0 3.0 2.5 2.5

49 $q = 2.0, 2.5, 3.0, 3.5, 4.0$ $q = 1.5, 1.0, 0.5, 0.0, -0.5, -1.0$

-1.0 -0.5 0.0 0.5 1.0 -1.5 -1.0 0.5 1.0 -0.5 0.0 Fig. 7.2 c y Fig. 7.2 d y 4.0 40 Pr = 2.0 Sc = 0.5, 1.0, 1.5, 2.0 3.5 Pr = 1.5 3.0 30 q 2.5 q 20 Pr = 1.0 2.0 1.5 Pr = 0.5 10 1.0 0.5 -1.5 -1.0 -0.5 0.0 0

93 $5.1, 0.0, y = -1.5, -1.0, -0.5, 0.0, 0.5, 1.0$

Fig. 7.2 e Fig. 7.2 f y 4 4 g =

86 $p/6, p/4, p/3, p/2$

69 $d = 0.3, 0.6, 0.9, 1.2$

3 3 q

48q 2 2 1 1 0 -0.5 0.0 0.5 1 .0

-1.0 -0.5 0.0 0.5 1.0 Fig. 7.2 g y y Fig. 7.2 h 3 2 q 1

8b1 = 0.1, 0.2, 0.3, 0.4 0 -1 -1 .5 -1.0 -0.5 0.0 0.

5 1.0 1.5 y Fig. 7.2 i Figs. 7.2(a-i). Effects of various parameters on temperature ?? 1.5 1.0 1.0 0.8 f 0.5 0.0 -0.5

49M = 2.0, 1.5, 1.0, 0.5 f 0.6 0.4 0.

2

8b1 = 0.1, 0.2, 0.3, 0.4 -1.0 0.0 -1.5 -0.2

-1.5 -1.0 -0.5 0.0 0.5 1.0 -1.5 -1.0 y Fig. 7.3 a -0.5 0.0 Fig. 7.3 b

18y 0.5 1.0 1.5 1.0 0.8 1 .0 0.

6

125f 0.4 0.2 0.0 b2 = 0.1, 0.2, 0.3, 0.

4

28f 0.5 0.0 b3 = 0.4, 0.3, 0.2, 0.

1 -1.5 -1.0 -0.5 0.0 Fig. 7.3 c

18y 0.5 1.0 -1.5 -1.0 -0.5 0.0 0.5

y Fig. 7.3

135d 1.0 1.5 1.0 1.0

f 0.8 0.6 0.4 Du = 2.0, 1.5, 1.0, 0.5 0.5 f 0.0 Sr = 2.0, 1.5, 1.0, 0.5 0.2 -0.5 0.0 -1.0 -0.2 -1.5 -1.0 -0.5 0.0 Fig. 7.3 e

84y 0.5 1.0 -1.5 -1.0 -0.5 0.0 0.5 1.0

Fig. 7.3 f y 1

162.0 1.0 Pr = 2.0, 1.5,

1.0, 0.5 0.5 0.5 Sc = 2.0, 1.5, 1.0, 0.5 f 0.0

90f 0.0 -0.5 -0.5 -1.0 -1.0 -1.5 -1.5 -1.0 -0.5 0.0 0.

5 1.0 -1.5

98y -1.5 -1.0 -0.5 0.0 0.5 1.0

Fig. 7.3 g Fig. 7.3 h y Figs. 7.3(a-h). Effects of various parameters on concentration. 20 15 15 10 10 Z1 Z1

19M = 2.0, 1.5, 1.0, 0.5 5 0

+ 16?2 (? + ?) ? 4?2 cosh (??)2 cosh (? ?) ??(sinh (? ?) - 16 (? ? + ?) ? ? sinh (? ?)2 sinh (? ?))? ?5 = 2? 4 + ? + ?? 2 - 2?2 + ??(? 8 + ? 3 + ? 2 1 + 2?2 - 2?2)) cosh (2??) ? ?6 = 2?2i(? + ?)(2? 4 ? + ? ? 2 - ?i?2?2 + i ? 8 + ?i 3 + ? 2 1 + ?2?2?2 - 2?2)? ?7 = (? + 2?3)? 2 coish (2? ?) + 2? ? 2 cosh (2?i ?) + ?i2? 2 cosh (2? ?) + 8 (? ? ? + ? ?) ? ?8 = ?()?+2??? (16 (? + ?) sinh (? ?) (? (? - ?) + sinh (? ?)))? ?9 = 16? 2?2 sinh (? (? - ?)) + (? + ?) 1 + ? 2 2 - 3 + 2? 2?2 sinh (2? ?) + 16?? + ? 2?2 sinh (? (? + ?)) ? i ? i ? 10 = 1 + ? 2 ? - 4?3 (? + ?) ? 4 1 + ? 2 2 - 4 (? + ?) ? 2 1 + ? 2 2 ?3? ?1 = ?i1(-8? 2? - 2? (4 + ? + 3?) - 2i ? ? + 2?2(? + 2?) ? 2 - 2?2 i(? + ?)2?2 4) + 2(1 + ? (? + 2?) ? 2 + (? + ?)2 ? 4)?2 + (? 2 1 + ? 2 + 2? 4 + ? + ?? 2 - 2?2 + ? 8 + ? 3 + ? 2 1 + 2?2 - 2?2) cosh i(2??) - ? (? + i ?)2 1 + ? 2 cosh (2? ?) ? ?2 = 16? i(? + ?i) ? ???3(i + ? 2?) cosh ? ? (? ?) (? (? - ?) + sinh (?i ?)) - 16 ? (? + ?) ? sinh (? ?) (? (? - ?) ? sinh (? ?))? ?3 = 12 (? + ?) ?9 cosh (??) - 16?4 (? + ?) ?3 + 8?3 (? + ?) ? 4 (? - ?) cosh (2??) ? ?4 = 128? 1?3? 4 cosh (??)2 sinh (??) + 2?3 (? + ?)2 ? 3 1 + ? 2 cosh (2? ?) + 8?3 (? + ?)?4(? - ?)?5? i ? ?5 = ?4? ?(-4? ? + ? 2 - 4? + 2?2? ? + ?2 + (? + ?)2 1 + ?2 ? 2 + ?2 (? + ?)2 ? 4)? ?1 = 16? (? + ?) ? 2 (? - ?) cosh (??) ??? - (? 2 1 + ?i 2 + 2?2 4 + ? + ?? 2 - 2?2 + ? 8 + ? 3 + ? 2 1 + 2?2 - 2?2) cosh (2i ??) ? ? i ? ?2 = ? 2?i 2

9cosh(2? ?) + i 2? ?? 2 cosh (?2? ?) + ?? 2 cosh (2? ?) + 8 (? + ?) ? 2 cosh (2?

?) + 2? ? cosh (2? ?) ? ?3 = 32?2 (? + ?) ? 3?2 cosh (? ?) ?2 - (? (? + ?) - 8 + 5? + 5? + (5? + (5 - 16?) ?) ? 2 ? ?4=8? 4+?+?+ ?+?+4?2 2)sinh(??i)-8((4? -1+?2?2 +(??)? ? ?5 = ?(-i64 + ? ? 1 + i ? 2 ?6 -13?+ 24?2? 2 + 16?4? 4 + i??3(-13 + ? ? 2(-13 + 8?(10 + ?)))? i ? i ? 8.3 Graphical results and analysis This section emphasizes the impact of embedding flow parameters in the solution expressions. Here plots are prepared in the two and three dimensions. Arrangement of the graphs is made in such a way that Figs. 8.1 (a-d) show the pressure gradient, Figs. 8.2 (a-d) the pressure rise per wavelength, Figs. 8.3 (a-d) the 3-D plots for velocity profile, Figs. 8.4-8.9 the stream lines and Figs. 8.10 and 8.11 the 3D plots for temperature and concentration fields respectively. Figs. 8.1 (a-d) reveal that pressure gradient decreases by increasing ? and ??? However, the

26pressure gradient increases with an increase in Φ and Du . It is further noticed that

the change in dp/dx is larger in the cases of Φ and M when compared with Du and Sr . Pressure rise per wavelength via mean flow rate ? is displayed in the Figs. 8.2 (a-d). These Figs. show that the pressure rise decreases when flow rate increases. For a given constant value of the mean flow rate, the

5pressure rise increases with an increase in Φ and ?? but it

decreases with increase in ?? (see Figs. 8.2 a,c and d). Behavior of pressure rise for M is however different. The pressure rise increases for negative value of mean flow rate when ? increases. However, the behavior is opposite for positive values of mean flow rate (Fig. 8.2b). We displayed the 3D plots for velocity, temperature and concentration. Here

5it is observed from Fig. 8.3 that the velocity decreases

when ? is increased. Such decrease largely depends upon the values of ?? Physically the decrease in velocity is due to the reason that the Lorentz force has a role of retarding force. Consequently it increases the friction resistance which opposes the motion of fluid. Figs. 8.3 (b-d) depict

31that the velocity is increasing function of

Φ and ??? However reverse situation is observed for ?? i.e. the velocity decreases when ?? increases. Trapping is considered interesting feature of the peristaltic transport. The volume of fluid that gets trapped in a stream line during peristaltic motion is known as bolus. Figs. 8.4-8.9 depict

5that the size of trapped bolus decreases when ?, ?? and

?? are larger. It is also found that the results are opposite for the cases of ??? Φ and ?? . The variations of temperature and concentration fields

3can be seen through Figs. 8.10 and 8.

11. These Figs show that the temperature increases when ?, ??, Φ and Du are increased. Clearly the rise in temperature with an increase in M and Du is more than Φ and ?? . Effects of ?? on the temperature are not significant. 99 Figs. 8.11 plot the influences of ?? Φ ??, ?? and ?? on the concentration field. Here concentration field decreases when there is an increase in ?, Φ and ?? . Further, the variations of concentration field for ?? and ?? are insignificant. It is also concluded that temperature increases and concentration decreases when ? increases. 0 0 $M = 1.0 - 1$

129 **F = 2.0** -5 **F = 1.0** **M = 2.0** -2 -10 -3 **F = 0.**

0 dp?dx **M = 3.0** dp?dx -4 -15 -5 **F = -2.0** -20 **M = 4.0** -6 -7 -0.4 -0.2 Fig.

508.1 a **x 0.0 0.2 0.4 -0.4 -0.2 Fig.**

718.1 b **x 0.0 0.2 0.4**

-2 0 **Du = 6.0** **Sr = 0.0** **Sr = 1.0** -1 **Du = 4.0** -3 **Sr = 2.0** **Du = -2** -4 **Du = 0.0** **Sr = 3.0** dp?dx -3 dp?dx -5 -4 -6 -5 -6 -7 -7 -0.4 -0.2 Fig.

508.1 c **x 0.0 0.2 0.4 -0.4 -0.2 Fig.**

718.1 d **x 0.0 0.2 0.4**

Figs. 8.1 (a-d) Behavior of pressure gradient for variations in M , Φ , Du and Sr . 30 20 10 0 Dpl $M =$

1011.0 -10 **M = 2.0** **M = 3.0** -20 **M = 4.0** -30

-1 0 1 2 3 Fig. 8.2 a Fig. 8.2 b h 10 10 5 5 0 $Gt = 1.0$ Dpl -5 $Gt = 2.0$ $Gt = 3.0$ -10 $Gt = 4.0$ -15 0 $Gc = 1.0$ Dpl -5 $Gc = 2.0$ $Gc = 3.0$ -10 $Gc = 4.0$ -15 -20 -20 -25 -1 0 1 2 3 -1 0 h 1 2 3 h Fig. 8.2 c Fig. 8.2 d Fig. 8.2 (a-d) Pressure rise per wavelength. Fig. 3 a Fig. 8.3 c Fig. 8.3 d Fig. 8.3(a-d) Velocity profile with variations of Φ , Φ ? and Φ ?. Fig. 8.4 Effect of Hartman number (Φ) on stream lines when $\Phi = 1$? $\Phi = 0$? 5, $\Phi = 0.75$? $\Phi = 0.25$? $\Phi = 2$ and $\Phi = 1$? Fig. 8.5 Effect of Φ on stream lines for $\Phi = 1$? $\Phi = 0.75$, $\Phi = 0.25$? $\Phi = 0.25$? $\Phi = 2$ and $\Phi = 1$? Fig. 8.6 Effect of Φ on stream lines when $\Phi = 1$? $\Phi = 0.75$, $\Phi = 0.25$? $\Phi = 0.25$? $\Phi = 2$ and $\Phi = 1$? Fig. 8.7 Effect of Φ on stream lines when $\Phi = 2$? $\Phi = 0.75$, $\Phi = 0.25$? $\Phi = 0.25$? $\Phi = 2$ and $\Phi = 1$? Fig. 8.8 Effect of Φ on stream lines for $\Phi = 1$? $\Phi = 2$? $\Phi = 0.75$, $\Phi = 0.25$? $\Phi = 0.25$? $\Phi = 2$ and $\Phi = 1$? Fig. 8.9 Effect of Φ on stream lines when $\Phi = 1$? $\Phi = 2$? $\Phi = 0.75$, $\Phi = 0.25$? $\Phi = 0.25$? $\Phi = 2$ and $\Phi = 1$?

75 Fig. 8. 10 a Fig. 8. 10 b

75 Fig. 8. 10 c Fig. 8. 10 d

Fig. 8.10 e Figs. 8.10 (a-e) Variation of Φ , Φ ?, Φ and Φ on temperature.

166 Fig. 8.11 a Fig. 8.11 b

75 Fig. 8. 11 c Fig. 8. 11 d

Fig. 8.11 e Figs. 8.11 (a-e) Diagrams analyzing the development of concentration field when Φ , Φ ?, Φ and Φ are varied. Chapter 9

2 **Mixed convective heat and mass transfer** for peristaltic transport **in an asymmetric channel with**

32 **Soret and Dufour effects** The aim of

present chapter is to address the

12 **simultaneous effects of heat and mass transfer** in the mixed convection **peristaltic flow of viscous fluid in an asymmetric channel. The**

channel walls exhibit the convective boundary conditions. In addition the effects due to Soret and Dufour are taken in to consideration. Resulting problems are solved for the series solutions. Numerical values of heat and mass transfer rates are displayed and studied. 9.1 Mathematical analysis We consider an

asymmetric channel of width $\eta_1 + \eta_2$ with flexible walls. An incompressible viscous fluid is considered. Cartesian coordinate system is adopted such

9that the η -axis is along the length of the channel and the η -axis is normal to the η -axis. The flow is

generated due to peristaltic

1waves propagating on the channel walls with speed c .

Moreover, the channel walls possess the characteristics of convective type boundary condition. We intend to study the flow

32in the presence of Soret and Dufour effects. The

channel walls are described by the following expressions $\eta_1(\eta, \eta) = \eta_1 + \eta_1$, left wall and $\eta_2(\eta, \eta) = -(\eta_2 + \eta_2)$ right wall where η_1 and η_2 are the disturbances produced

2due to propagation of peristaltic waves at the left and right walls respectively. The

values of η_1 and η_2 can be written in the forms $\eta_1 = \eta_1 \cos(\eta - \eta)$ and $\eta_2 = \eta_2 \cos(\eta - \eta) + \eta$ where η is time, η is the phase difference and η_1 and η_2 are the amplitudes of the waves travelling on the left and right walls with speed c respectively. Temperature and concentration at the walls are assumed to be η and η ($\eta = 0$ for left wall and $\eta = 1$ for right one) respectively. Velocity field for this problem is $\eta = \eta(\eta, \eta, \eta)$ where $\eta = 0$ at $\eta = 0$

10Fundamental equations governing the flow of an incompressible viscous fluid

are $\nabla \cdot \eta = 0$ (9.1) $\eta = -\nabla \cdot \eta + \eta \nabla \cdot \eta + \eta \nabla \cdot \eta$ ($\eta = 0$) + $\eta \nabla \cdot \eta$ ($\eta = 0$) (9.2) $\eta = \eta$ in which η

66is the density of fluid, η is the pressure, η is the dynamic viscosity, η is the

acceleration due to gravity and η and η are the thermal and concentration expansion coefficients respectively. The energy and concentration equations can be expressed as $\eta \nabla \cdot \eta = \eta \nabla \cdot \eta + \eta \nabla \cdot \eta$ (9.3) $\eta \nabla \cdot \eta = \eta \nabla \cdot \eta + \eta \nabla \cdot \eta$ (9.4) Here η is the specific heat, η is the

6thermal conductivity, η is the mass diffusivity, η is the $\eta \nabla \cdot \eta$ thermal diffusion ratio, η is the concentration susceptibility, η is the

mean temperature, η and η are respectively the

14temperature and concentration of the fluid.

We consider (η, η) and η as the

7velocity components and pressure in the wave frame (η, η) . The

7transformations between laboratory and wave frames are

$\eta = \eta - \eta \eta = \eta - \eta \eta = \eta - \eta \eta$ ($\eta = \eta$) ($\eta = \eta$) (9

24.5) where (η, η) and η are the velocity components and pressure in the laboratory frame.

The fundamental

$\cosh(2\eta) + 2\eta\phi_1\eta^2 \cosh(2\eta) + \phi_2\eta^2\eta^2 \cosh(2\eta) + 8(\eta + \eta^2) + \eta(\eta + 2\eta^2 + \eta^3)\eta(16(\eta + \eta^2 + 4\eta^3) \sinh(\eta\eta) (\eta(\eta - \eta) + \sinh(\eta\eta))) + (\eta + \eta^2 + 4\eta^3)1 + \eta^2\eta^2 - 3 + 2\eta^2\eta^2 \sinh(2\eta\eta) + 16\eta\eta + (\eta^3 + 4\eta^2)\eta^2 \sinh(\eta(\eta + 2\eta))\eta\phi_1\eta^3 = 1 + \eta^2\phi_1\eta - 4\eta^3(2(\eta + \eta^3)1 + \eta^2\eta^2 - 4(\eta + \eta^2)\eta^2 1 + \eta^2\eta^3(\eta^3 - \eta^2\eta^2)(-8\eta^2\phi_1 - 2\eta^2(4 + \eta^3 + 3\eta) - \eta^2\eta^2 + \eta^2\eta^2(\eta + \eta^3)\eta^2 - 2\eta^3\eta^2(\eta + \eta^2\phi_1)\eta^2\eta^2\eta^4) + 2(1 + \eta(\eta + \eta^3)\eta^2 + (\eta + \eta^2 + 4\eta^3)\eta^2\eta^4)\eta^2 + (\eta^2 1 + \eta^2\eta^3) \eta^3$

9.3 Graphical analysis η In order to provide a comparative study of the results by the two methods, we have plotted graphs for both solutions. Left panel depicts the perturbation solution whereas right panel for the numerical solution. Graphical analysis is carried out for the dimensionless temperature, concentration and velocity fields. Numerical values for the rates of

20heat and mass transfer at the left wall are given in the Tables

9.1 and 9.2 respectively. The values of different parameters in all the graphs are taken as follows: $\eta = 1\eta\eta = \eta\eta^4\eta\eta = 0\eta^5\eta\eta = 0\eta^7\eta\eta = 0\eta^8\eta\eta = 0\eta\eta\eta = 1\eta\eta\eta = 2\eta\eta\eta = 0\eta^5\eta\eta = 0\eta^5\eta\eta\eta = 1\eta\eta\eta = 0\eta^25\eta\eta\eta = 0\eta^5\eta\eta\eta = 0\eta^7\eta\eta$ The graphs of temperature profile showed

15that the temperature decreases with an increase in the values of

Bi and it increases by increasing Mi . The decrease in the temperature with increase in the heat transfer Biot-number is very rapid for $\eta\eta \leq 1$ It is noted that for $\eta\eta \geq 1$ corresponding decrease in temperature becomes very slow (see Fig. 9.1). This fact is totally opposite to the case of increase in Mi in which temperature not only increases by increasing $\eta\eta$ but also such increase is constant and very slow (Fig. 9.2). Fig. 9.3 showed that the temperature increases when $\eta\eta$ is increased? Increase in the temperature is smaller for small values of $G\eta$ but this increase becomes much for higher values of $G\eta$. However this increase in temperature is observed throughout the channel. Unlike the case of $\eta\eta\eta$ small increase in temperature is observed when $G\eta$ increases but this increase is not uniform throughout the channel. Near the right wall the temperature tends to decrease very slowly by increasing $\eta\eta$ (see Fig. 9.4) Figs. 9.5-9.7 are plotted to analyze the concentration profile in detail. It is found that the concentration increases when $\eta\eta$ is increased? This increase is large for $\eta\eta \leq 1$ and very slow for large values of Mi (see Fig. 9.5). It is noticed from Figs. 9.6 and 9.7

5that the concentration generally decreases with an increase in $\eta\eta$ and $\eta\eta$. This decrease is

much and constant for $\eta\eta$ and $\eta\eta$ respectively. However concentration profile showed different behavior near the right wall. The concentration here increases which is quite different for its behavior at all other parts of the channel. Figs. 9.8 and 9.9 depict that the value of velocity increases by increasing $\eta\eta$ but it remains constant with variation in $\eta\eta\eta$ The velocity in both cases is increased for increasing $\eta\eta$ and $\eta\eta$ in the region where "y" is negative and decreased for positive y. Tables 9.1 and 9.2 are plotted for the numerical values of rates of heat and mass transfer. It is seen that solution up to first order perturbation gives an agreement with the numerical results up to second decimal place. Table 9.1 shows that heat transfer rate is increasing function of Biot-number. However the Grashoff numbers and mass transfer Biot number reduce the heat transfer rate (see Table 9.1). Table 9.2 illustrates that the mass transfer rate at the wall tends to decrease when $\eta\eta$, $\eta\eta$, $\eta\eta$ and $\eta\eta$ are increased. 3.0 3.0 Bi = 0.5 Bi = 0.5 2.5 2.5 2.0 q 2.0 q Bi = 1.0 1.5 Bi = 1.5 1.5 1.0 1.0 Bi = 2.0 Bi = 1.0 Bi = 1.5 Bi = 2.0 -1.0 -0.5 0.0 0.5 1.0 1.5 0.5 -1.0 -0.5 0.0 0.5 1.0 y y Fig. 9.1 Effect of $\eta\eta$ on the temperature profile. 3.2 $Mi = 0.5, 1.0, 1.5, 2.0$ 3.2 $q = 0.0, 1.0, 1.5, 2.0$ 3.0 3.0 q 2.8

40q 2.8 2.6 2.6 2.4 2.

4 -1.0 -0.5 0.0 0.5 1.0 1.5 -1.0 -0.5 0.0 0.5 1.0 y y Fig. 9.2 Effect of $\eta\eta$ on the temperature profile. 3.2 $G\eta = 0.0, 1.0, 2.0, 3.0$ 3.2

57 $G\eta = 0.0, 1.0, 2.0, 3.0$ 3.0 3.0 3.0

q 2.8

40q 2.8 2.6 2.6 2.4 2.

4 -1.0 -0.5 0.0 0.5 1.0 1.5 -1.0 -0.5 0.0 0.5 1.0 y y Fig. 9.3 Effect of $\eta\eta$ on the temperature profile. 3.2

46 $Gc = 0.0, 2.0, 4.0, 6.0$

3.2

46 $Gc = 0.0, 2.0, 4.0, 6.0$

3.0 3.0 q

40q 2.8 2.8 2.6 2.6 2.4 2.4

-1.0 -0.5 0.0 0.5 1.0 1.5 1.0 -1.0 -0.5 0.0 0.5 y

173y 0.6 0.6 0.4 Mi = 2.

0 0

155.4 0.2 f 0.0 -0.2

Mi = 2.0

82Mi = 1.5 0.2 Mi = 1.5 Δ 0.0

82Mi = 1.0 Mi = 1.0 -0.2 Mi = 0.5 -0.

4

120Mi = 0.5 -1.0 -0.5 0.0 0.5 1.0 1.5 -0.

4 y -1.0 -0

118.5 0.0 y 0.5 1.0 1.5

Fig. 9.5

11Effect of ?? on the concentration profile. 0.0 -0.1 -0.1 -0.

2

133-0.2 f -0.3 f -0.3 -0.4 Gt = 0.

0, 1.0, 2.0, 3.0 -0.4

57Gt = 0.0, 1.0, 2.0, 3.0 -1.0 -0.5 0.0 0.5 1.0 1.5 -0.

5 y -1.0 -0

128.5 0.0 y 0.5 1.0 Fig.

9.6

11Effect of ?? on the concentration profile. 0.0 -0.1 -0.1 -0.

762 -0.2 f Δ -0.3 -0.3 -0.4 Gc = 0.0,

2.0, 4.0, -0.4

46Gc=0.0,2.0,4.0,6.0

-0.5 -1.0 -0.5 0.0 0.5 1.0 1.5 -0.5

39y -1.0 -0.5 0.0 0.5 1.0 y

Fig. 9.7

11 **Effect of ?? on the concentration** profile. 1.0 1 .0

0.5 0.5

28 **U 0.0 U 0.0** $Gt = 0.0, 2 .0, 4 .0, 6 .0$ $Gt = 0.0, 2 .0, 4 .0, 6 .0$ -0.5 -0.

5 -1.0 -1.0 -1.0 -0.5 0.0 0

36.5 1.0 1.5 **y -1.0 -0.5 0.0 0.5 1.0** $y 1.0 1.0 0.5 0.5 0 .0$ $Gc=0 .0, 2.0, 4 .0,$

6.0

121 **U 0.0 U** $Gc = 0.0, 2 .0, 4 .0, 6 .0$ -0.5 -0.

5 -1.0 -1.0 -1.0 -0.5 0.0 0

18.5 1.0 1.5 **y -1.0 -0.5 0.0 0.5 1.0**

y Fig. 9.9 Effect of ?? on the Velocity profile. ?? ?? ?? ?? $-?0(?1) - ?0 * (?1)$ 0?5 1?0 2?0 0?5 1?1935
j 1?1?927 1?0 1?2343 1?2343 1?5 1?2550 1?2560 2?0 1?2674 1?2693 0?0 1?2988 1?3018 1?0 1?2674
1?2693 2?0 1?2411 1?2402 3?0 1?2197 1?2176 0?0 1?2439 1?2349 1?0 1?2310 1?2254 2?0 1?2197
1?2176 3?0 1?2100 1?2110 0?5 1?2100 1?2110 1?0 1?1999 1?2006 1?5 1?1955 1?1967 2?0 1?1930
1?1951 Table 9.1. Numerical values of heat transfer rate

161 **at ?1. ?? ?? ?? ?? ?0(?1)** $?0 * (?1)$ 0?5 1 **?0 2? 0 0?**

5 0?2190 j 0?2187 1?0 0?2179 0?2179 1?5 0?2174 0?2176 2?0 0?2171 0?2173 0?0 0?2219 0?2225
1?0 0?2171 0?2173 2?0 0?2139 0?2141 3?0 0?2125 0?2139 0?0 0?2142 0?2146 1?0 0?2131 0?2141
2?0 0?2125 0?2139 3?0 0?2125 0?2140 0?5 0?2125 0?2140 1?0 0?1346 0?1360 1?5 0?0903 0?0914
2?0 0?0618 0?0625 Table 9.2. Numerical values of mass transfer rate at ?1. Chapter 10

4 **Variable viscosity effects on the peristaltic motion of a third-order fluid**

The

45 **effect of variable viscosity on the peristaltic motion of MHD non -Newtonian fluid in a channel**

is studied. Constitutive relations of third order fluid are employed in the development of flow. Mathematical analysis is presented when no-slip condition is no longer valid. The

17 **series solutions for stream function, longitudinal velocity and pressure gradient are**

first derived and then discussed in detail. The

6 **pressure rise and frictional forces are** monitored through **numerical integration.**

Physical interpretation is also made. 10.1 Governing problem We

12 **consider an incompressible magnetohydrodynamic (MHD) third order fluid with variable viscosity in a uniform channel of**

width 2?1.

16 A uniform magnetic field B_0 is applied in the z -direction. The induced magnetic

and electric fields are not considered. Wave shapes are written as $\psi(x, y, z, t) = \psi_1 + \psi_2 + \dots + \psi_n$, (10.1), where

c is the velocity of propagation of the

wave, ?1

9 is the wave amplitude, λ is the wavelength, T is the time, \vec{v} is the direction of wave

propagation and η is transverse to \mathbf{B} . The constitutive equations for the third order fluid are given through Eqs. (1.17-1.19). Hence we directly write the following governing equations for two dimensional flow of MHD third order fluid as

$$\rho \frac{D\mathbf{v}}{Dt} = \nabla \cdot \mathbf{T} + \mathbf{J} \times \mathbf{B} \quad (10.2)$$

$$\mu \nabla^2 \mathbf{v} = -\nabla \pi \quad (10.3)$$

$$\nabla \cdot \mathbf{v} = 0 \quad (10.4)$$

51 $\mu \text{ } ?? \text{ } ?? \text{ } ? = - \text{ } ?? \text{ } ???? \text{ } ???? \text{ } ?? \text{ } \P \text{ } ?? \text{ } ?? \text{ } ?? \text{ } ?^- \text{ } ?^- = ?(2?^- \text{ } ?^-) + ? \mid (2?^- \text{ } ?^- \text{ } ?^- \text{ } ?^- \text{ } ?^- + 2?^- \text{ } ?^- \text{ } ?^- \text{ } ?^- + 4 \text{ } ?^- \text{ } ?2^- + 2?^- \text{ } ?^- \text{ } ?^- \text{ } ?^- + 2?^- \text{ } ?^- \text{ } 2) + ?2 \text{ } (4 \text{ } ?^- \text{ } ?2^- \text{ } + ?^- \text{ } ?2^- \text{ } + ?^- \text{ } ?2^- \text{ } + 2?^- \text{ } ?^- \text{ } ?^- \text{ } ?^-) + ?1(2?^- \text{ } ?^- \text{ } ?^- \text{ } ?^- +$

[illegible]

3 are the velocity components and pressure in the fixed frame (???) and the

subscripts denote the partial derivatives f_{ij} and δ indicate the

17velocity components and pressure in the wave frame then defining

? = ? - ??? ? = ? ? ? = ? - ?? ? = ? ? ?(?? ?) = ? (? ? ? ? ?) (10.5) and using ? = ? = ? ? ? ? = ? ? = ?
? = ? ? ? 2? ? ? ? ? = ? 1 ? ? = ? ? = ? 1 ? ? = ? ? ? ? 1 ? 1 ? 1 ???0 ?(?) μ ?0 ¶1?2 ?0?1? ?0 = ?0 ? ?? =
????01 ? ? ?0? ?0 ? 1 ? (?) ? ?(?) = ? ? = ?? ? ? ? = ????? ? = -???????2 = ??02???221?73 = ??03??
221? (10.6) we obtain

3 under the long wavelength and low Reynolds number approximation the

[illegible]

ψ is the stream function, ν is the constant kinematic viscosity, λ is the Hartman

$\cosh [2\eta] + \cosh [4\eta] - 8 \sinh [2\eta] + \sinh [4\eta] \eta \approx 10$

163.3 Results and discussion In this section the

main objective is

24 to study the influence of various parameters of interest on the

flow quantities. In particular the variations of Hartman number (H) Deborah number (Γ) amplitude ratio (η) slip parameter (β) and viscosity parameter (μ)

21 on the longitudinal velocity, pressure gradient, pressure rise (Δp) and frictional

force (F) per wavelength have been examined. Figs. 10.1-10.3 show the effects of H , β and Γ on the longitudinal velocity u . The plots show that velocity at the center of the channel and near the walls has opposite behavior. Further the velocity at the center of the channel decreases with an increase in H and β but it increases by increasing Γ .

10 The variation of pressure gradient for certain values of H , β and Γ

are depicted in the Figs 10.4-10.6

2 It is anticipated that the absolute value of pressure gradient increases with an increase in H and β but it

decreases when Γ is increased. The

6 pressure rise and frictional force per wavelength have been computed numerically. The

pressure rise versus flow rate has been plotted in the Figs 10.7-10.11.

5 It is noticed from Fig. 10.7 that the pressure rise decreases with an increase in β . It is

found that magnitude of pressure rise per wavelength increases by increasing H (see Fig. 10.8). Fig. 10.9 depicts an important phenomenon that is the graph for pressure rise for $\Gamma = 0$ is linear whereas in the case of non zero Γ it is non linear. Fig 10.11 shows

10 that the pressure rise increases with an increase in the amplitude ratio

η . The

3 free pumping flux increases by increasing

η (see Fig. 10.10). Figs. 10.12-10.16 monitor the features of frictional force (F)

3 It is clear that there exists a critical value

of η below which η resists the flow and above which it assists the flow. This critical value of η decreases by increasing β and H (see Figs. 10.12 and 10.13). Contrary to this the critical value of η increases with an increase in Γ and μ (see Figs 10.14 and 10.15). It is revealed from Fig. 16 that the effect of Γ on frictional force is quite opposite to that of pressure rise. Another important fact of interest here is a comparison between the viscous and non-Newtonian fluids (see Figs. 10.3, 10.6, 10.9 and 10.14). In all these Figs. the case of viscous fluid is given by putting $\Gamma = 0$. Fig. 10.3 shows that velocity at the centre of the channel in non-Newtonian fluid is larger when compared with a viscous fluid. Fig. 10.6 shows that the 132 non-Newtonian fluid exhibits larger pressure gradient than the viscous fluid. Figs. 10.17-10.20 examine the trapping phenomenon.

27 It is observed that the size of the trapped bolus decreases with an increase

in η and Γ ? The size of trapped bolus also increases by increasing the viscosity parameter

η (see Figs. 10.17 and 10.18). It is noted

167 that by increasing the Deborah number Γ the size of the

bolus decreases whereas it increases by increasing η 0.6 0.6

19 $M = 0.5, 1.0, 1.5, 2.$

116 $M = 0.5, 1.0, 1.5, 2.0$

0.4 0.4

33 $U = 0.2, 0.2, 0.0, 0.0, -1.0, -0.5, 0.0, 0.5, 1.0, -1.0, -0.5, 0.0, 0.5, 1.0$

y y Fig. 10.1. Effect of η on velocity U when $\eta = 0.2$? $\Gamma = 0.04$? $\eta = 1$? $\eta = 1$

8 η and $\eta = 0.3$? Left panel is for

$\eta = 0$ and right panel is

8 for $\eta = 0.4$? 0.8 0.6 0.

5 0.4 $b_1 = 0.0, 0.2, 0$

130.4, 0.6 $U_{b1} = 0.0, 0.2, 0.4, 0.$

6

61 $U = 0.2, 0.0, 0.0, -0.2, -0.5, -0.4, -1.0, -0.5, 0.0, 0.5, 1.0, y = -1.0, -0.5, 0.0, 0.5, 1.0$

y Fig. 10.2. Effect of η on velocity U when $\eta = 1$? $\Gamma = 0.04$? $\eta = 1$? $\eta = 1.3$ and $\eta = 0.3$? Left panel is for $\eta = 0$ and right panel is for $\eta = 0.4$ 0.6

134 $G = 0.08, 0.06, 0.04, 0.0, 0.$

4

28 $U = 0.2, 0.0, -1.0, -0.5, 0.0, y = 0.5, 1.0$

Fig. 10.3. Effect of Γ on velocity U when $\eta = 1$? $\eta = 0.04$? $\eta = 1$? $\eta = 1.3$ and $\eta = 0.3$? 3 3 2 2 1 1 dp/dx

19 $M = 2.5, 2.0, 1.5, 1.0, 0$

dp/dx

91 $M = 2.5, 2.0, 1.5, 1.0, 0, -1, -2, -2, 0.0, 0.2, 0.4, 0.6, 0.$

398 $1.0 \times 0.0, 0.2, 0.4, 0.6, 0.8, 1.0 \times$ Fig.

10.4. Effect of η on pressure gradient when $\eta = 0.2$? $\Gamma = 0.001$? $\eta = 0.1$ and $\eta = 0.3$? Left panel is for $\eta = 0$ and right panel is for $\eta = 0.4$ 2.0 1.5 1.0 dp/dx 0.5 0.0 2.0 1.5

67 $b_1 = 0.0, 0.1, 0.2, 0.3$

dp?dx 1.0 0.5 0.0

8b1 = 0.0, 0.1, 0.2, 0.3 -0.5 -0.5 -1.0 0.0 0.2 0.4 0.6 0.8 1.0 0.0 0.2 0.4 0.6 0.

8 1.0 x x Fig. 10.5. Effect of Γ on pressure gradient when $\Gamma = 0$? $\Gamma = 0.001$? $\Gamma = 0.01$ and $\Gamma = 0.03$? Left panel is for $\Gamma = 0$ and right panel is for $\Gamma = 0.04$? 1.5 1.5 1.0 1.0 dp?dx 0.5

132G = 0.03, 0.02, 0.01, 0.0

dp?dx 0.5

53G = 0.03, 0.02, 0.01, 0.0 0.0 0.0 -0.5 -0.5 0.0 0.2 0.4 0.6 0.8 1.0 0.0 0.2 0.4 0.6 0.

4 0.6 0.8 1.0 x x Fig. 10.6. Effect of Γ on pressure gradient when $\Gamma = 0$? $\Gamma = 0.02$? $\Gamma = 0.01$ and $\Gamma = 0.03$? Left panel is for $\Gamma = 0$ and right panel is for $\Gamma = 0.04$? 10 5 Dpl 0 -5

41b1 = 0.3, 0.2, 0.1, 0.0 -10 -1.0 -0.5 0.0

0.5 1.0 1.5 h Fig. 10.7. Variation of Γ on $\Delta\Gamma$ when $\Gamma = 0$? $\Gamma = 1$? $\Gamma = 0.03$ and $\Gamma = 0.02$? 10 5 Dpl 0 -5

89M = 0.5, 1.0, 1.5, 2.0 -10 -15 -1.0 -0.5 0.0 0.5 1.0 1.5

h 20 10 Dpl 0 -10

28G = 0.00, 0.01, 0.02, 0.03 -20 -1.0 -0.5 0.0 0.0

5 1.0 1.5 h Fig. 10.9. Variation of Γ on $\Delta\Gamma$ when $\Gamma = 0$? $\Gamma = 1$? $\Gamma = 0.03$ and $\Gamma = 0.02$? 6 4 2 Dpl -2 0 -4 -6

96a = 0.0, 0.3, 0.6, 0.9 -1.0 -0.5 0.0 0.5 1.0

1.5 h 5 Dpl 0 -5

54a = 0.2, 0.3, 0.4, 0.5 -1.0 -0.5 0.0 0.5 1.0

0 1.5 h Fig. 10.11. Variation of Γ on $\Delta\Gamma$ when $\Gamma = 0$? $\Gamma = 1$? $\Gamma = 0.02$ and $\Gamma = 0.01$? 10 5 b1 = 0.3, 0.2, 0

78.1, 0.0 Fl 0 -5 -1.0 -0.

5 0.0 0.5 1.0 1.5 h 10

19M = 0.5, 1.0, 1.5, 2.0

5 Fl 0 -5 -10 -1.0 -0.5 0.0 0.5 1.0 1.5 h Fig. 10.13 Variation of Γ on $\Delta\Gamma$ when $\Gamma = 0$? $\Gamma = 0.03$? $\Gamma = 0.02$? $\Gamma = 0.01$? 20 15 10

154G = 0.0, 0.1, 0.2, 0.3 5 Fl 0

-5 -10 -15 -1.0 -0.5 0.0 0.5 1.0 1.5 h 6

34a = 0.0, 0.3, 0.6, 0.9 4 2

Fl 0 -2 -4 -1.0 -0.5 0.0 0.5 1.0 1.5 h Fig. 10.15. Variation of Γ on $\Delta\Gamma$ when $\Gamma = 0$? $\Gamma = 1$? $\Gamma = 0.01$ and $\Gamma = 0.02$? 6 4

23a = 0.5, 0.4, 0.3, 0.2 2 Fl 0 -2 -4 -1.0 -0.5 0.0 0.5 1.0

58 $h \begin{bmatrix} 1.2 & 1.2 & 1.1 & 0.8 & 0.8 \end{bmatrix} ? = \begin{bmatrix} 0.5 & 0.6 & 0.6 & 0.4 & 0.4 & 0.2 & 0.2 & 0.0 & -0.4 & -0.2 & 0.0 & 0.2 & 0.4 \\ -0.4 & -0. \end{bmatrix}$

23 $\Gamma = 0? \ 1 \ 0.6 \ 0.6 \ 0.4 \ 0.4 \ 0.$

23 $\Gamma = 0?$ 2 0.6 0.6 0.4 0.4 0.

$$23 \Gamma = 0? \quad 3 \quad 0.6 \quad 0.6 \quad 0.4 \quad 0.4 \quad 0.$$

13Heat transfer analysis for peristaltic mechanism in variable viscosity fluid

30 **an incompressible magnetohydrodynamic (MHD) third order fluid** with
variable viscosity **in** a uniform **channel**

138 fluid is electrically conducting under an applied magnetic field B_0 in the z -direction.

47 kinematic viscosity, ν the Hartman number, Re the Reynolds number, τ the

51/58

i) Temperature in constant viscosity fluid is greater than variable viscosity situation. ii) Temperature is decreasing function of thermal slip parameter γ_2 . iii) The qualitative effects of γ_2 and γ_1 on the temperature are opposite. iv) Behavior of γ_1

103 on the heat transfer coefficient is

opposite to that of γ_2 0.15 0.15 0.10 0.10 q 0.05 q

19 $M = 0.5, 1.0, 1.5, 2.0$

0.05 0.00

106 $M = 0.5, 1.0, 1.5, 2.0$ -0.05 0.00 0.0 0.2 0.4 0.6 0.

8 1.0 1.2 0.0 0.2 0.4 0.6 0.8 1.0 1.2 y y

60 (a) $\gamma = 0.2$ (b) $\gamma = 0.2$ 0.35 0.4 0.30 0.3 0.25 0.

20 q 0.2 q 0.15 0.1

67 $b_1 = 0.0, 0.1, 0.2, 0.3$ 0.

10

8 $b_1 = 0.0, 0.1, 0.2, 0.3$ 0.05 0.0 0.00 0.0 0.2 0.4 0.6 0.8 1.0 1.2 0.0 0.2 0.4 0.6 0.

8 1.0 1.2 y y (c) $\gamma = 0.2$ (d) $\gamma = 0.2$ Fig. 11.1 (a-d): Variation of γ for $\Gamma = 0.04$ $\gamma = 0.3$ $\gamma = 1.1$ $\gamma = 0.7$ 1 and $Br = 0.5$ 0.25 0.25 0.20 0.20 0.15 0.10 0.15 q 0

158.10 0.05 0.05 $Br = 0.8, 0.6, 0.4, 0.$

2

22 $Br = 0.8, 0.6, 0.4, 0.2$ 0.00 0.00 0.0 0.2 0.4 0.6 0.

738 1.0 1.2 y 0.0 0.2 0.4 0.6 0.8 1.0 1.2 y (a) γ_2

= 0.2

107 (b) $\gamma_2 = 0.2$ 0.2 0.2 0.1 0.1 0.0 0.0

q q -0.1

77 $b_2 = 0.1, 0.2, 0.3, 0.$

414 $b_2 = 0.1, 0.2, 0.3, 0.4$ -0.1 -0.2 -0.2 -0.3 -0.3 0.0 0.2 0.4 0.6 0.

8 1.0 1.2 1.4 0.0 0.2 0.4 0.6 0.8 1.0 1.2 1.4 y y (c) $\gamma = 0.5$ (d) $\gamma = 0.5$ Fig. 11.2 (a-d): Variation of γ for $\gamma = 1$ $\Gamma = 0.04$ $\gamma = 0.3$ $\gamma = 1.1$ and $\gamma = 0.2$ 150 150 100 100 50 50

126 $Z_0 Z_0$ -50 $b_1 = 0.0, 0.1, 0.15, 0.$

2 -50

8 $b_1 = 0.0, 0.1, 0.15, 0.$

2 -100 -100 -150 0.0 0.2 0.4 0.6 0

72.8 1.0 -150 x 0.0 0.2 0.4 0.6 0.8 1.0 (a) ?? = 0? 5 (b) ?? = 0?

5 x 40 40 20 20 Z 0 Z 0 Br = 2.0, 1.5, 1.0, 0.5 Br = 2.0, 1.5, 1.0, 0.5 -20 -20 -40 -40 0.0 0.2 0.4 0.6 0.8 1.0
0.0 0.2 0.4 0.6 0.8 1.0 (c) ?1 = 0?2 x (d) ?1 = 0?2 x Fig. 11.3 (a-d): Variation of Z when $\Gamma = 0?04? ? = 0?$
3? ? = 1?1? and ? = 1? Chapter 12 Soret and Dufour

4effects on peristaltic transport of a third order fluid

Soret and Dufour effects

44on peristaltic transport of third order fluid in a symmetric channel have been reported in

this chapter. Joule heating effect is also taken in to account. The

37governing nonlinear problem is solved using perturbation

approach. Graphical

177results are reported and discussed for various parameters of

interest entering into the problem 12.1

6Mathematical formulation We consider the magnetohydrodynamic (MHD) flow of third order fluid in a channel of width

2?1? The ?- axis is chosen along the walls of channel and ? -

20axis is taken normal to the ?- axis. A constant magnetic field of strength B_0 is applied in the

? - direction. Induced magnetic field is not accounted. Sinusoidal wave propagating on channel walls with constant wave speed ? is represented by $2? ?(?? ?) = ?1 + ?1??? ? (? - ??)$, (12.1) $\mu \parallel$ where ?1

44is the wave amplitude, ? is the wavelength and ? is the

time . The continuity, momentum, energy and concentration equations of the problem may be written as follows: $?? ? ? ? ? = 0? + ? ? + ? ? ? + \mu ? ? ? ? \parallel ? = -???? ? ? ? ? ? - ? ? 02?? ? ? + ? ? ? ? = - ? ? ? ? ? ? ? + \mu ? ? ? ? ? \parallel ? ? ? ? ? ? ? ? + ? ? ? ? + ? ? ? ? = ? ? ? ? 2?2 + ? ? ? 2?2$ (12.2) (12.3) (12.4) $^3 + ?? + ? ? ? 20?2 + ? ? ' ? ? ? ? ? ? ? 2$

145??³+ ? ? ? ? ? ' 2 (12.5) $^3 ? + ? ? ? + ? ? ? = ? \mu ? ? ? 2 \parallel ? ? ? ? ? ? ? ?$

?? ? + + ? (12.6) $\mu ? ? ? ? \parallel ? ? \mu ? ? ? 2 \parallel$ In the above equations, ? and ? are the velocity components along ? and ? directions re- spectively

5in fixed (laboratory frame), ? is the density, ? is the pressure, ? is the kinematic viscosity, ? is the electrical conductivity, ? is the

thermal conductivity, ?0 is the applied mag- netic field, ? is the temperature field, ??

7is the specific heat, ?? is the viscous dissipation,

? is mass diffusivity, ??

11is the thermal diffusion ratio, ?? is the concentration susceptibility, ? is the

147 **Extra stress tensor S in third order fluid is**

are the material constants. The Rivlin-Ericksen tensors can be represented as follows $A_1 = L + L^T$ $A_2 = L \cdot L + L^T \cdot L^T$

179 $A?L + L? A? ? = 1? 2?$ where L

31 are the velocity components in the laboratory (???) and wave (???) frames respectively

1 the Hartman number, Re the Reynolds number, ?? the Brinkman number, ?? the

2we expand the quantities in terms of small Deborah number as

$$68 \Gamma ? 1 + ? ? ? ? ? = ? 0 + \Gamma ? 1 + ? ? ? ? ? = ? 0 + \Gamma ? 1 + ? ? ? ? ? = ? 0 + \Gamma ? 1 + ? ? ? ? ? = ? 0 + \Gamma ? 1$$

103 heat transfer coefficient at the wall can be computed by

12 Solving the resulting systems at zeroth and first orders

55/58

2 f Fig. 12.2 g Figs. 12.2(a-g). Development of concentration field with increase in values of parameters. Fig. 12.3 a Fig. 12.3 b Fig. 12.3 c Fig. 12.3 d Fig. 12.3 e Fig. 12.3 f Figs. 12.3(a-f). Behavior of heat transfer coefficient Z. Bibliography [1] F. Kiil, The function of the ureter and the renal pelvis. Philadelphia: Saunders, (1957). [2] S. Boyarsky, Surgical physiology of the renal pelvis. Monogro. Surg. Sci. 1 (1964) 173. [3] T. W. Latham, Fluid motion in a peristaltic pump, MIT Cambridge MA, (1966). [4] A. H. Shapiro, Pumping and retrograde diffusion in peristaltic waves, "Proceedings. work- shop on ureteral reflux in children". National Academy of Science (Natural Research Coun- cil) (1967) 109. [5] P. S. Lykoudis, Peristaltic pumping; a bioengineering model. Published in Proc. Workshop Hydrodynam. Upper Urinary Tract. National Academy of Science, Wash. D. C. (1971). [6] S. L. Weinberg, M. Y. Jaffrin and A. H. Shapiro, A hydrodynamical model of ureteral function. Published in Proc. Workshop Hydrodynam. National Academy of Science, Wash. D. C. (1971). [7] C. Barton and S. Raynor, Peristaltic flow in tubes. Bull. Math. Biophys. 30 (1968) 663. [8] J. R. Maginniss, An analytical investigation of flow and hemolysis in peristaltic-type blood pumps. M. S. Thesis, M. I. T. Cambridge, Mass (1970). [9] A. H. Shapiro, M. Y. Jaffrin and S. L. Weinberg, Peristaltic pumping with long wavelength at low Reynolds number, J. Fluid Mech. 37 (1969) 799. [10] M. Y. Jaffrin, Inertia and streamline curvature effects in peristaltic pumping, Int. J. Eng. Sci. 11 (1973) 681. [11] F. Yin and Y. C. Fung, Peristaltic waves in circular cylindrical tubes, J. Appl. Mech. 36 (1969) 579. [12] Y. C. Fung and C. S. Yih, Peristaltic transport, J. Appl. Mech. 35 (1968) 699. [13] M. Y. Jaffrin and A. H. Shapiro, Peristaltic pumping, Annual Review of Fluid Mech. 3 (1971) 13. [14] T. K. Mitra and S. N. Prasad, Interaction of peristaltic motion with Poiseuille flow, Bull. Math. Biol. 36 (1974) 127. [15] D. E. Wilson and D. Perel, Interaction of Pulsatile and peristaltic induced flows. Proc. ASME Bioengineering Symposium, New York (1979). [16] T. D. Brown and T. K. Hung, Computational and experimental investigations of two dimensional nonlinear peristaltic flows, J. Fluid Mech. 83 (1977) 249. [17] L. M. Srivastava V. P. Srivastava, Interaction of peristaltic flow with pulsatile flow in a circular cylindrical tube, J. Biomech. 18 (1985) 247. [18] L. M. Srivastava and V. P. Srivastava, Peristaltic transport of blood; Casson model-II. J. Biomech. 17 (1984) 821. [19] S. Takabatake and K. Ayukawa, Numerical study of two dimensional peristaltic waves. J. Fluid Mech. 122 (1982) 439. [20] S. Takabatake, K. Ayukawa and A. Mori, Peristaltic pumping in circular cylindrical tubes: a numerical study of fluid transport and its efficiency. J. Fluid Mech. 193 (1988) 269. [21] M. Mishra and A. R. Rao, Peristaltic transport in a channel with a porous peripheral layer: model of a flow in gastrointestinal tract. J. Biomechanics 38 (2005) 779. [22] N. A. S. Affi and N. S. Gad, Interaction of peristaltic flow with pulsatile magneto-fluid through a porous medium, Acta Mech. 149 (2001) 229. [23] E. F. Elshehawey, E. M. E. Elbarbary and N. S. Elgazery, Effect of inclined magnetic field on magneto fluid flow through porous medium between two inclined wavy porous plates (numerical study), Appl. Math. Comput. 135 (2003) 85. 169 [24] Kh. S. Mekheimer, Peristaltic flow of blood under effect of a magnetic field in a non-uniform channel, Appl. Math Comput. 153 (2004) 763. [25] Kh. S. Mekheimer, Nonlinear peristaltic transport of magnetohydrodynamic flow in an inclined planar channel, Arab. J. Sci. Engin. 28 (2003) 183. [26] A. M. Siddiqui, T. Hayat and Masood Khan, Magnetic fluid model induced by peristaltic waves, J. Phys. Soc. Jpn. 73 (2004) 2142. [27] T. Hayat and N. Ali, Peristaltically induced motion of a MHD third grade fluid in a deformable tube, Physica A 367 (2006) 79. [28] Abd El Hakeem Abd El Naby, A. E. M. El Misery and M. F. Abd El Kareem, Effects of magnetic field on trapping through peristaltic motion for generalized Newtonian fluid in channel, Physica A 367 (2006) 79. [29] T. Hayat, M. Khan, A. M. Siddiqui and S. Asghar, Nonlinear peristaltic flow of a non-Newtonian fluid under effect of a magnetic field in a planar channel, Comm. Nonlinear Sci. Numer. Simulat. 12 (2007) 910. [30] T. Hayat and N. Ali, A mathematical description of peristaltic hydromagnetic flow in a tube, Appl. Math. Comput. 188 (2007) 1491. [31] Y. Wang, T. Hayat, N. Ali and M. Oberlack, Magnetohydrodynamic peristaltic motion of a Sisko fluid in a symmetric or asymmetric channel, Physica A: Stat. Mech. Applications, 387 (2008) 347. [32] T. Hayat, Z. Asghar, S. Asghar and S. Mesloub, Influence of inclined magnetic field on peristaltic transport of fourth grade fluid in an inclined asymmetric channel, J. Taiwan Institute of Chemical Engineers, 41 (2010) 553. [33] X. Mandviwalla and R. Archer, The influence of slip boundary conditions on the peristaltic pumping in a rectangular channel, J. Fluids Eng. 130 (2008) 124501. [34] T. Hayat, Q. Hussain and N. Ali, Influence of partial slip on the peristaltic flow in a porous medium, Phys. Lett. A 387 (2008) 3399. 170 [35] T. Hayat, S. Hina and N. Ali, Simultaneous effects of slip and heat transfer on the peristaltic flow, Comm. Nonlinear Sci. Numer. Simulat. 15 (2010) 1526. [36] A. Yildirim and S. A. Sezer, Effects of partial slip on the peristaltic flow of a MHD Newtonian fluid in an asymmetric channel, Math. Comp. Model. 52 (2010) 618. [37] A. V. R. Kumari and G. Radhakrishnamacharya, Effect of slip on heat transfer to peristaltic transport in the presence of magnetic field with wall effects, ARPN J. Engin. and Appl. Sci. 6 (2011) 1819. [38] N. Ali, Q. Hussain, T. Hayat and S. Asghar, Slip effects on the peristaltic transport of MHD fluid with variable viscosity, Phys. Lett. A 372 (2008) 1477. [39] Abd El Hakeem Abd El Naby, A.E.M. El Misery and I.I. El Shamy, Effects of an endoscope and fluid with variable viscosity on peristaltic motion, Appl. Math. Comput. 158 (2004) 497. [40] E.F. Elshehawey and Z.M. Gharsseldien, Peristaltic transport of three-layered flow with variable viscosity, Appl. Math. Comput. 153 (2004) 417. [41] T. Hayat and N. Ali, Effect of variable viscosity on the peristaltic transport of a Newtonian fluid in an asymmetric channel, Appl. Math. Model. 32 (2008) 761. [42] A. Ebaid, A new numerical solution for the MHD peristaltic flow of a bio-fluid with variable viscosity in a circular cylindrical tube via Adomian decomposition method, Physics Lett. A 372 (2008) 5321. [43] S. Nadeem and N. S. Akbar, Effects of heat transfer on the peristaltic transport of MHD Newtonian fluid with variable viscosity: application of Adomian decomposition method, Comm. Nonlinear Sci. Numer. Simulat. 14 (2009) 3844. [44] S. Nadeem, T. Hayat, N. S. Akbar and M. Y. Malik, On the influence of heat transfer in peristalsis with variable viscosity, Int. J. Heat Mass Transfer 52 (2009) 4722. [45] S. Nadeem and N. S. Akbar, Effects of temperature dependent viscosity on peristaltic flow of a Jeffrey-six constant fluid in a non-uniform vertical tube, Comm. Nonlinear Sci. Numer. Simulat. 15 (2010) 3950. 171 [46] S. Nadeem and N. S. Akbar, Influence of temperature dependent viscosity on peristaltic transport of a Newtonian fluid: Application of an endoscope, Applied Mathematics and Computation 216 (2010) 3606. [47] G. Radhakrishnamacharya and V. R. Murty, Heat transfer to peristaltic transport in a non-uniform channel, Defence Sci. J. 43 (1993) 275. [48] K. Vajravelu, G. Radhakrishnamacharya and V. Radhakrishnamurthy, Peristaltic flow and heat transfer in a vertical porous

annulus, with long wavelength approximation, *Int. J. Nonlinear Mech.* 42 (2007) 754. [49] Kh. S. Mekheimer and Y. Abd Elmaboud, The influence of heat transfer and magnetic field on peristaltic transport of a Newtonian fluid in a vertical annulus: Application of an endoscope, *Phys. Lett. A* 372 (2008) 1657. [50] S. Srinivas and M. Kothandapani, Peristaltic transport in an asymmetric channel with heat transfer-A note, *Int. Comm. Heat Mass transfer* 34 (2008) 514. [51] T. Hayat, M. U. Qureshi and Q. Hussain, Effect of heat transfer on the peristaltic flow of an electrically conducting fluid in a porous space, *Appl. Math. Model.* 33 (2009) 1862. [52] S. Srinivas and M. Konthandapani, The influence of heat and mass transfer on MHD peristaltic flow through a porous space with compliant walls, *Appl. Math. Comput.* 213 (2009) 197. [53] T. Hayat and S. Hina, The influence of wall properties on the MHD peristaltic flow of a Maxwell fluid with heat and mass transfer, *Nonlinear Analysis: Real World Applications*, 11 (2010) 3155. [54] Kh. S. Mekheimer, S. Z. A. Husseny and Y. Abd Elmaboud, Effects of heat transfer and space porosity on peristaltic flow in a vertical channel, *Numer. Methods Partial Diff. Eqs.* 26 (2010) 747. [55] S. Nadeem and N. S. Akbar, Influence of radially varying MHD on the peristaltic flow in an annulus with heat and mass transfer, *J. Taiwan Institute of Chemical Engineers* 41 (2010) 286. 172 [56] N. Ali, M. Sajid, T. Javed and Z. Abbas, Heat transfer analysis of peristaltic flow in a curved channel, *International Journal of Heat and Mass Transfer* 53 (2010) 3319. [57] T. Hayat and S. Noreen, Peristaltic transport of fourth grade fluid with heat transfer and induced magnetic field, *C. R. Mecanique* 338 (2010) 518. [58] S. Srinivas and R. Muthuraj, Effects of thermal radiation and space porosity on MHD mixed convection flow in a vertical channel using homotopy analysis method, *Commun Nonlinear Sci Numer Simulat.* 15 (2010) 2098. [59] K. Vajravelu, S. Sreenadh and P. Lakshminarayana, The influence of heat transfer on peristaltic transport of a Jeffrey fluid in a vertical porous stratum, *Comm. Nonlinear Sci. Numer. Simulat.* 16 (2011) 3107. [60] T. Hayat, M. Javed and A. A. Hendi, Peristaltic transport of viscous fluid in a curved channel with compliant walls, *Int. J. Heat and Mass Transfer* 54 (2011) 1615. [61] S. Srinivas, R. Gayathri and M. Kothandapani, Mixed convective heat and mass transfer in an asymmetric channel with peristalsis, *Comm. Nonlinear Sci. Numer. Simulat.* 16 (2011) 1845. [62] S. Nadeem and N. S. Akbar, Influence of heat and mass transfer on the peristaltic flow of Johnson Segalman fluid in a vertical asymmetric channel with induced MHD, *J. Taiwan Institute of Chemical Engineers* 42 (2011) 58. [63] D. Tripathi, A mathematical model for swallowing of food bolus through the oesophagus under the influence of heat transfer, *Int. J. Thermal Sciences* (inpress). [64] N. S. Akbar, S. Nadeem, T. Hayat and A. A. Hendi, Effects of heat and mass transfer on the peristaltic flow of hyperbolic tangent fluid in an annulus, *Int. J. Heat and Mass Transfer* 54 (2011) 4360. [65] S. Nadeem and N. S. Akbar, Influence of heat and mass transfer on the peristaltic flow of a Johnson Segalman fluid in a vertical asymmetric channel with induced MHD, *J. Taiwan Institute of Chemical Engineers*, 42 (2011) 58. 173 [66] T. Hayat, N. Saleem, S. Asghar, M. S. Alhothuali and A. Alhomaidan, Influence of induced magnetic field and heat transfer on peristaltic transport of a Carreau fluid, *Comm. Nonlinear Sci. Numer. Simulat.* 16 (2011) 3559. [67] T. Hayat, A. Afsar, M. Khan and S. Asghar, Peristaltic transport of a third order fluid under the effect of magnetic field, *Comp. Math. Applications*. 53 (2007) 1074. [68] T. Hayat, M. U. Qureshi and N. Ali, The influence of slip on the peristaltic motion of a third order fluid in an asymmetric channel, *Phys. Lett. A* 372 (2008) 2653. [69] S. Nadeem, N. S. Akbar, N. Bibi and S. Ashiq, Influence of heat and mass transfer on peristaltic flow of a third order fluid in a diverging tube, *Comm. Nonlinear Sci. Numer. Simulat.* 15 (2010) 2916. [70] N. S. Akbar, T. Hayat, S. Nadeem and A. A. Hendi, Effects of slip and heat transfer on the peristaltic flow of a third order fluid in an inclined asymmetric channel, *Int. J. Heat and Mass Transfer* 54 (2011) 1654. 174 Fig. 9.4 Effect of ?? on the temperature profile. Fig. 9.8 Effect of ?? on the velocity profile. Fig. 10.8. Variation of ? on $\Delta??$ when $\Gamma = 0.01$? $\gamma_1 = 0.02$? $\gamma = 0.3$ and $\gamma = 0.22$? Fig. 10.10. Variation of ? on $\Delta??$ when $\gamma_1 = 0.02$? $\gamma = 1.5$? $\gamma = 0.3$ and $\Gamma = 0.01$? Fig. 10.12. Variation of γ_1 on ?? when $\gamma = 0.3$? $\gamma = 1.5$? $\gamma = 0.2$ and $\Gamma = 0.01$? Fig. 10.14. Variation of Γ on ?? when $\gamma = 0.3$? $\gamma = 1.5$? $\gamma = 0.2$ and $\gamma_1 = 0.02$? Fig. 10.16. Variation of ? on ?? when $\gamma = 0.22$? $\gamma = 1.5$? $\Gamma = 0.01$ and $\gamma_1 = 0.02$? panels are for $\gamma = 0$ and right panels are for $\gamma = 0.4$?() panels are for $\gamma = 0$ and right panels are for $\gamma = 0.4$? panels are for $\gamma = 0$ and right panels are for $\gamma = 0.4$? Left panels are for $\gamma = 0$ and right panels are for $\gamma = 0.4$? 1 2 3 4 5 6 7 8 9 10 11 12 13 14 15 16 17 18 19 20 21 22 23 24 25 26 27 28 29 30 32 33 34 35 36 37 38 39 40 41 42 43 44 45 46 47 48 49 50 51 52 53 54 55 56 57 58 59 60 61 62 63 64 65 66 67 68 69 70 71 72 73 74 75 76 77 78 79 80 81 82 83 84 85 86 87 88 89 90 91 92 93 94 95 96 97 98 100 101 102 103 104 105 106 107 108 109 110 111 112 113 114 115 116 117 118 119 120 121 122 123 124 125 126 127 128 129 130 131 133 134 135 136 137 138 139 140 141 142 143 144 145 146 147 148 149 150 151 152 153 154 155 156 157 158 159 160 161 162 163 164 165 166 167 168 1.5 1.5 1.5 1. 1.5 1.5 1.5 1.5 0.4 0.4 0.4 0.4 0.4 0.4